



HAL
open science

Origin and fate of hepatic macrophages during liver regeneration

Yeni Ait Ahmed

► **To cite this version:**

Yeni Ait Ahmed. Origin and fate of hepatic macrophages during liver regeneration. Human health and pathology. Université Paris-Est Créteil Val-de-Marne - Paris 12, 2021. English. NNT : 2021PA120007 . tel-04011237

HAL Id: tel-04011237

<https://theses.hal.science/tel-04011237>

Submitted on 2 Mar 2023

HAL is a multi-disciplinary open access archive for the deposit and dissemination of scientific research documents, whether they are published or not. The documents may come from teaching and research institutions in France or abroad, or from public or private research centers.

L'archive ouverte pluridisciplinaire **HAL**, est destinée au dépôt et à la diffusion de documents scientifiques de niveau recherche, publiés ou non, émanant des établissements d'enseignement et de recherche français ou étrangers, des laboratoires publics ou privés.

UNIVERSITY OF PARIS-EST CRETEIL
ECOLE DOCTORALE SCIENCES DE LA VIE ET DE LA SANTE
Thesis realized in partnership with
THE NATIONAL INSTITUTE ON ALCOHOL ABUSE AND
ALCOHOLISM

PhD Specialty: Cellular and Molecular Biology

AIT AHMED Yeni

ORIGIN AND FATE OF HEPATIC MACROPHAGES
DURING LIVER REGENERATION

July 8th, 2021

Jury members:

Dr TORDJMANN Thierry, Directeur de Recherche	Rapporteur
Dr JULIEN Boris, Maître de conférence	Rapporteur
Dr PILON Caroline, Ingénieure de Recherche	Examinatrice
Pr ALBANESE Patricia, Professeure des Universités	Examinatrice (Présidente du jury)
Pr LAFDIL Fouad, Professeur des Universités	Directeur de Thèse
Dr GAO Bin, Principal Investigator	Co-directeur de Thèse

Acknowledgments

I would like to start by expressing my gratitude toward my two mentors Pr Fouad Lafdil and Dr Bin Gao who made this partnership possible and created a very stimulating environment to realize my PhD work. They provided all the scientific guidance and advice to help me evolve throughout my PhD. It is without a doubt thanks to their patience and continuous supervision that my work could achieve this extent form. For me it was a privilege to get to work with two amazing researchers that will for sure inspire me for the rest of my career.

I would also like to thank each member of the Laboratory of Liver Diseases for their warm welcome and positive interactions that fostered great relationships and an enjoyable work environment. I would also deeply thank Adrien Guillot and Robim Rodrigues for their support and their European energy whenever I needed it, while away from family and friends.

Lastly, I would like to thank all the members of the National Institute on Alcohol Abuse and Alcoholism who I interacted with and who helped me in my research work.

Table of Content

ACKNOWLEDGMENTS	2
PREFACE	3
LIST OF ABBREVIATIONS	5
LIST OF FIGURES	6
1. ANATOMY, STRUCTURE AND FUNCTIONS OF THE LIVER	7
1.1. ANATOMY AND STRUCTURE	7
1.2. LIVER CELL POPULATIONS	8
1.2.1. HEPATOCYTES	9
1.2.2. LIVER SINUSOIDAL ENDOTHELIAL CELLS	10
1.2.3. BILIARY EPITHELIAL CELLS.....	11
1.2.4. LIVER PROGENITOR CELLS	12
1.2.5. HEPATIC STELLATE CELLS	13
1.2.6. IMMUNE CELLS.....	14
1.3. LIVER FUNCTIONS	15
1.3.1. GLUCOSE METABOLISM	15
1.3.2. LIPID AND CHOLESTEROL METABOLISM.....	16
1.3.3. VITAMIN AND MINERAL STORAGE.....	18
1.3.4. BILE PRODUCTION.....	20
1.3.5. PROTEIN SYNTHESIS.....	21
1.3.6. DETOXIFICATION OF THE ORGANISM.....	21
1.3.7. INTERACTION OF THE LIVER WITH OTHER ORGANS	23
2. LIVER REGENERATION	25
2.1. LIVER REGENERATION FROM HEPATOCYTES	25
2.1.1. MECHANISMS OF REGENERATION FOLLOWING MECHANICAL STRESS	26
2.1.2. MECHANISMS OF REGENERATION FOLLOWING ACUTE DRUG-INDUCED-LIVER INJURY.....	30
2.2. LIVER REGENERATION FROM LIVER PROGENITOR CELLS	31
2.2.1. CONTRIBUTION OF LPC TO LIVER REGENERATION IN SEVERE AND CHRONIC INJURY	31
2.2.2. DELETERIOUS EFFECTS OF SUSTAINED LPC ACTIVATION IN THE LIVER.....	34
3. ROLE OF THE IMMUNE RESPONSE IN REGENERATING LIVERS	36
3.1. NATURAL KILLER CELLS.....	36
3.2. B AND T LYMPHOCYTES	37
3.3. GRANULOCYTES.....	38
3.4. DENDRITIC CELLS.....	39

3.5.	HEPATIC MACROPHAGES	39
4.	PHD PUBLICATIONS.....	43
4.1.	KUPFFER CELL RESTORATION AFTER PARTIAL HEPATECTOMY IS DRIVEN BY THEIR LOCAL CELL PROLIFERATION IN AUTOCRINE AND PARACRINE IL-6-DEPENDENT MANNERS.....	43
4.2.	INTERLEUKINS-17 AND 27 PROMOTE LIVER REGENERATION BY SEQUENTIALLY INDUCING PROGENITOR CELL EXPANSION AND DIFFERENTIATION.....	45
4.3.	BILE ACID-ACTIVATED MACROPHAGES PROMOTE BILIARY EPITHELIAL CELL PROLIFERATION THROUGH INTEGRIN AVB6 UPREGULATION FOLLOWING LIVER INJURY	47
5.	DISCUSSION	49
	REFERENCES.....	57

List of Abbreviations

BDL	Bile duct ligation
BEC	Biliary epithelial cell
CCl ₄	Carbon tetrachloride
CD	Cluster of differentiation
DAMP	Danger-associated molecular pattern
HSC	Hepatic stellate cell
IFN γ	Interferon γ
KC	Kupffer cell
LPC	Liver progenitor cell
LPS	Lipopolysaccharides
LSEC	Liver sinusoidal cell
NF- κ B	Nuclear factor kappa-light-chain-enhancer of activated B cells
PAMP	Pathogen-associated molecular pattern
PD-L1	Programmed death-ligand 1
PHx	Partial hepatectomy
PRR	Pathogen recognition receptor
TLR	Toll-like receptor
TNF α	Tumor necrosis factor α
VEGF	Vascular endothelial growth factor

List of Figures

- Figure 1 Architecture of a hepatic lobule
- Figure 2 Liver progenitor cell bipotential differentiation into hepatocyte and biliary cells
- Figure 3 Anatomy of the liver before and after 2/3 PHx in the mouse
- Figure 4 Mechanisms of liver regeneration depending on the volume of resected liver
- Figure 5 Pathways of liver regeneration depending on the stimulus
- Figure 6 Dynamic of hepatic macrophage populations during liver regeneration
- Figure 7 Dynamic of hepatic macrophage populations during liver regeneration
- Figure 8 IL-17 induces liver progenitor cell proliferation while IL-27 favors their
differentiation toward a hepatocytic phenotype
- Figure 9 Monocyte-driven BEC proliferation in a context of biliary injury

1. Anatomy, structure and functions of the liver

1.1. Anatomy and structure

The human liver is a vital organ located in the rib cage under the diaphragm in the right upper quadrant of the abdominal cavity. It is composed of two large lobes and represents the largest solid organ of the human body. Its weight varies from 0.97 to 1.8 kg for men and 0.6 to 1.77 for women making up 2 to 2.5% of total body weight. Liver weight is significantly correlated to body weight and body mass index (Gholamzadeh *et al.*, 2017; Mubbunu *et al.*, 2018). The liver to body weight ratio depends on many parameters such as the age, the gender and is finely regulated to maintain homeostasis. The liver mass tends to rise in pathological contexts and therefore can constitute a marker of hepatic injury, especially in the case of steatosis characterized by an accumulation of fat in the liver (Simon *et al.*, 2020). Anatomically, the liver is strategically connected to the intestines via the portal circulation. Through this blood network the liver represents the entry point of every nutrient and drug absorbed in the gut and functions as a biochemical defense against toxic chemicals entering through the food. In fact, unlike most other organs, the liver has two major sources of blood. It is connected to both systemic and portal circulation with 80 % of the blood is provided through the portal vein while the other 20 % arrive from the hepatic artery (Jenne and Kubes, 2013). The portal vein brings nutrient-rich blood from the intestines and the hepatic artery that supplies oxygenated blood from the heart. The hepatic lobule represents the functional unit of the liver. It is characterized by its hexagonal shape and consists of layers of hepatocytes (**Figure 1**). Alongside hepatocytes which represent the main hepatic parenchymal cell, the liver hosts biliary cells involved in bile production and many other non-parenchymal cells such as hepatic stellate cells involved in tissue repair and vitamin storage, or immune cells, which will be described in the following section.

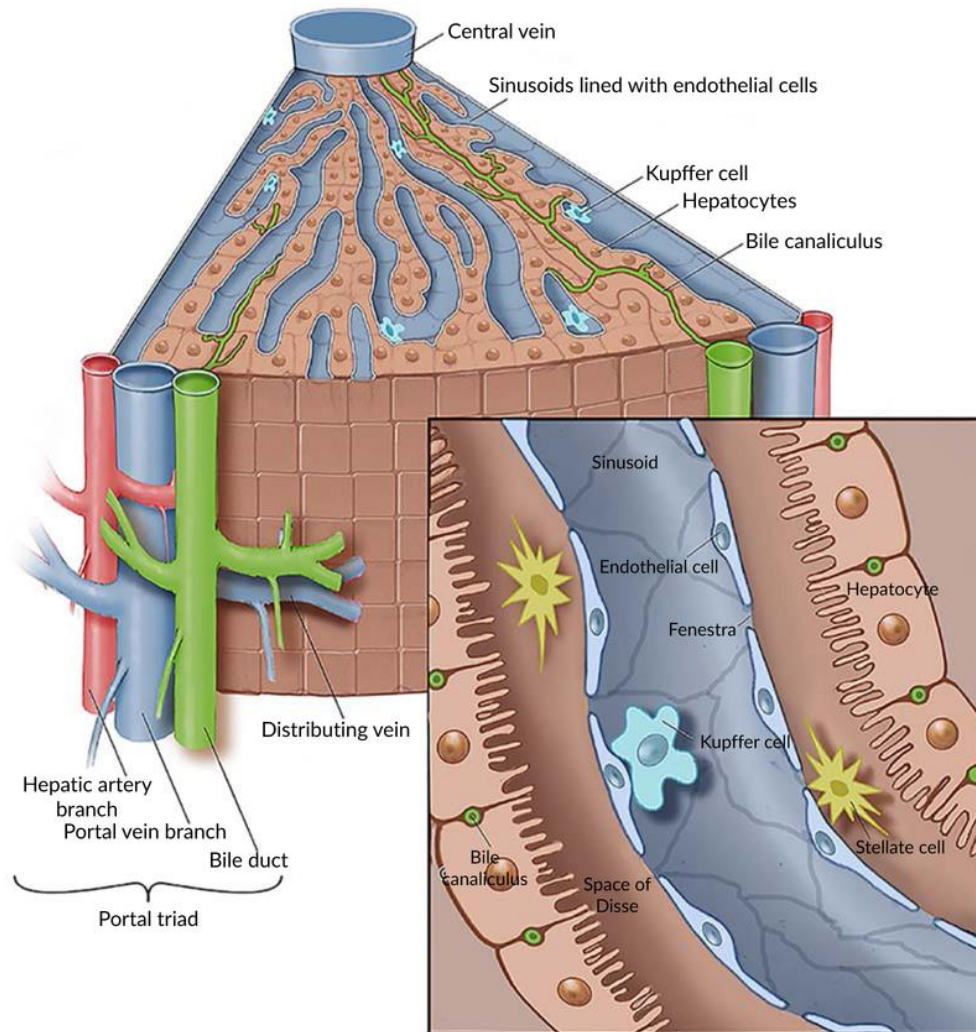


Figure 1: Architecture of a hepatic lobule. *The lobule is considered as a functional unit of the liver characterized by a central vein and portal triads in periphery composed of a branch of the hepatic artery, the portal vein and a bile duct (Abu Rmilah et al., 2019)*

1.2. Liver cell populations

Liver cell populations can be grouped in two categories mainly, parenchymal and non-parenchymal cells. Parenchymal cells comprise hepatocytes, the main hepatic cell type and biliary epithelial cells. These two populations are responsible for the essential metabolic functions of the liver. Additionally, the liver hosts several other populations of non-parenchymal cells that can be further sorted in two categories: non-immune cells including liver sinusoidal endothelial cells, and hepatic stellate cells, and immune cells such as macrophages, natural killer cells, B and T lymphocytes.

1.2.1. Hepatocytes

Hepatocytes represents more than 80% of liver mass and about 60% of the total liver cell populations. They are highly specialized epithelial cells with a polarity that enables their functions of protein trafficking. Indeed, hepatocytes are characterized by a basal (sinusoidal) membrane facing liver sinusoidal endothelial cells and an apical (canalicular) pole characterized by distinct sets of surface proteins, receptors and channels (Schulze *et al.*, 2019). The sinusoidal domain contains various receptor tyrosine kinases like EGF receptor, lipid and iron scavenging receptors.

Hepatocytes are further organized in rows and are connected to both highly oxygenated arterial blood from the aorta via the hepatic artery (about 25% of the incoming blood supply) and partially deoxygenated but nutrient dense venous blood from the portal vein (representing the remaining 75% inbound blood) (Vollmar and Menger, 2009). Hepatocytes are further organized in hexagonal lobules identified by 6 peripheral triads composed of a bile duct, a hepatic artery and a portal vein converging to a central vein. This specific architecture makes hepatocytes the first cells to be exposed to all substances absorbed through the gut, whether they are nutrients or toxins. It allows degraded proteins, lipids and salts that are secreted from the apical membrane of hepatocytes to be drained into the bile via small canaliculi of ramified ductular network. Those specific features allow hepatocytes to perform essential hematological filtering functions (Schulze *et al.*, 2019). Indeed, hepatocytes uptake many molecules such as lipids, growth factors and also responsible for the production of most blood plasma proteins. In addition, hepatocytes are major producers of serum proteins. Indeed, hepatocytes release into the circulation numerous key proteins involved in the transport of other proteins and cations like albumin, transferrin, plasminogen, fibrinogen, clotting factors, serum albumin which is the most abundant secreted protein (Franko *et al.*, 2019), and α -fetoprotein during tumorigenesis. However, these properties can also put the liver at risk as it makes it more vulnerable to injury mediated by an exposure to high levels of fat, gut-derived toxins, drugs and alcohol.

Therefore, as highly specialized cells involved in metabolic functions, hepatocytes need complementary help from other non-parenchymal hepatic cells to ensure non-metabolic functions. These include liver sinusoidal endothelial cells.

1.2.2. Liver sinusoidal endothelial cells

Liver sinusoidal endothelial cells (LSEC) line hepatic sinusoids and constitute a unique interface between blood, coming from both the hepatic artery and the portal vein, and the hepatic parenchyma. These sinusoids are highly fenestrated vessels due to the loose cell junctions between LSEC (Géraud *et al.*, 2012) and the absence of basal membrane, unlike the fenestrated glomerular endothelial cells for example (Poisson *et al.*, 2017). As LSEC represent the interface between hepatocytes and the blood flow, they line the space of Disse and contribute to lymphatic drainage within this interstice. This other feature may explain why LSEC and lymphatic cells share characteristic surface markers and functional properties (Knolle and Wöhlleber, 2016).

LSEC are further organized in sieve plates making them permeable. Many factors like vascular endothelial growth factor (VEGF) but also exogenous agents such as alcohol, diet and fasting are known to induce dynamic changes in the size of hepatic fenestration (Shetty, Lalor and Adams, 2018). This fenestrated organization of LSEC represent an interface that enables bidirectional exchanges and the recycling of all kinds of proteins and lipids but also gut-derived antigens coming from food or pathogens entering through the portal vein. It is therefore critical for the liver to ensure that no damaging immune response is triggered against harmless antigens while at the same time performing the clearance of invading pathogens. In this context, LSEC play a critical role balancing tolerance and immune response. Indeed, in collaboration with Kupffer cells, the liver resident macrophages which are tightly associated to LSEC, they constitute the most efficient scavenger cellular system in the body (Sørensen *et al.*, 2015). The first crucial step involves pathogen recognition receptors (PRR) which include the Toll-like receptors (TLR) expressed on the surface of LSEC and that recognize antigens, damage and pathogen-associated molecular patterns (DAMP and PAMP respectively) (Knolle and Wöhlleber, 2016). However, LSEC are also able to regulate inflammatory and immune responses when they are chronically exposed to antigens like LPS for instance. Studies have shown that LSEC chronically exposed to LPS had reduced nuclear translocation of NF- κ B and eventually lower leukocyte adhesion (Uhrig *et al.*, 2005). It has also been shown that LSEC have developed unique TLR signaling pathway different from classical antigen presenting cells. This kind of regulatory mechanism avoid a constant activation of an inflamed state in the liver in response to the permanent flow of antigens coming from the gut (Shetty, Lalor and Adams, 2018).

Alongside scavenger receptors, LSEC also express C-type lectin receptors such as L-SIGN (Bashirova *et al.*, 2001) and LSECtin (Liu *et al.*, 2004). Interestingly, studies have identified CD44 expressed on activated T-cells as a ligand for LSECtin and showed that CD44-LSECtin bond inhibits T-cell activation, proliferation and functions. In fact, LSECtin knockout mice displayed exacerbated T-cell immunity and liver damage (Tang *et al.*, 2009). This highlights the ability of LSEC to modulate inflammation and might in part explain the unique immunological status of the liver and its tolerogenic environment (Wu *et al.*, 2010).

1.2.3. Biliary epithelial cells

Biliary epithelial cells (BEC), also known as cholangiocytes, are the second major cell population. They originally derived from bipotent hepatoblasts that differentiate into hepatocytes and cholangiocytes around embryonic day 13. BEC are highly specialized epithelial cells lining bile ducts and are mainly involved in bile production. They form a complex network of interconnected and ramified tubes, often referred to as the “biliary tree”, extending from the canals of Hering to the duodenum. This biliary network is estimated to be as long as 2 km, in humans (Banales *et al.*, 2019).

Along the biliary tree, BEC have been shown to be a heterogeneous population. Indeed, BEC residing around to the canals of Hering tend to be immature and display progenitor cell features as they contribute to the renewal of the epithelium and hepatic regeneration (Han *et al.*, 2013). Conversely, around larger bile ducts, BEC progressively show higher levels of differentiation with a more distinct polarity, and expression of cellular receptor involved in hormone response, namely.

In fact, biliary cells are polarized with basolateral and apical membrane domains that enable key functions in molecule trafficking and bile production. This cellular organization allow BEC to regulate the composition, pH and fluidity canalicular bile coming from hepatic canaliculi to bile ducts through the canals of Hering. Indeed, BEC are involved in the absorption of bile acids, glucose and amino acids, and the secretion of bicarbonate (HCO_3^-) and water. During postprandial periods, secretin is released by the S cells of the duodenum and stimulates BEC via its G protein-coupled receptor expressed on their basolateral membrane. Secretin will stimulate intracellular vesicle trafficking from the basal to the apical pole of the cell of $\text{Cl}^-/\text{HCO}_3^-$ anion exchange protein 2 (AE2) and water channel aquaporin 1 (AQP1) involved

in the release of HCO_3^- and water in the bile duct lumen which contribute to the alkalization and fluidization of the bile (Trampert *et al.*, 2021).

Beyond necessary components like biliary acids, amino acids and minerals, the bile can carry pathogens coming from the gut and the blood circulation and a wide variety of chemokines released by immune cells in response to PAMP and DAMP. In this context BEC, which constitutively express TLR (Fabris *et al.*, 2017), play an important immunological role. Indeed, they form a barrier through their tight junctions and produce immunoglobulins such as secretory immunoglobulin A (IgA) which have been shown to contribute to the antimicrobial defense within the bile ducts and intestine, and the clearance of systemic antigens. Indeed, impaired hepatobiliary IgA secretion has been reported in chronic liver diseases (Banales *et al.*, 2019). However, in some cases of infection, intoxication, cholestasis or ischemia (O'Hara *et al.*, 2013), BEC can be activated which can lead to proliferation, fibrosis, inflammation and the recruitment of other immune cells (Pinto *et al.*, 2018).

1.2.4. Liver progenitor cells

Liver progenitor cells (LPC), also known as oval cells in rodents and characterized by their oval shape and high nucleus to cytoplasm ratio, are located in canals of Hering. They originate from hepatoblasts during fetal liver development. LPC are bipotent cells and are able to differentiate into hepatocytes and biliary cells (**Figure 2**) (Tsuchiya and Lu, 2019). Their activation and expansion called ductular reaction is part of the liver's response to severe injury upon impaired hepatocyte proliferation. However, some controversy remains about the exact origins of these cells during ductular reaction as studies have shown that BEC and hepatocytes could express LPC markers such as Sox9 (Ko *et al.*, 2020). Additionally, evidence indicate that mature and differentiated hepatocytes and BEC could undergoing metaplasia into a progenitor state (Rodrigo-Torres *et al.*, 2014; Tarlow *et al.*, 2014). This has contributed to the emergence of the hypothesis that there might be no LPC independent population in the liver but rather a plasticity of hepatocytes and BEC that behave as facultative stem cells and can potentially transdifferentiate into one another under certain circumstances (Michalopoulos and Khan, 2015). Ductular reaction is usually associated with the induction of infiltrating inflammatory cells, activation of myofibroblasts and extracellular matrix accumulation (Sato *et al.*, 2019).

However, it is a very complex response that differs according to the injury context and the origins of ductular cells still remain unclear.

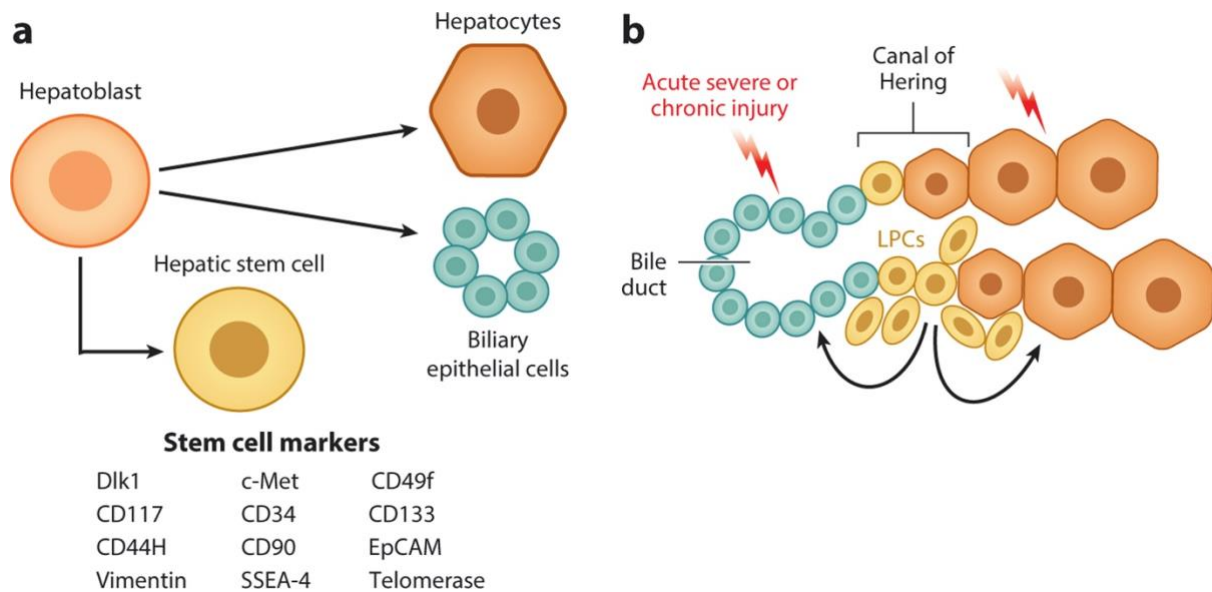


Figure 2: Liver progenitor cell bipotential differentiation into hepatocyte and biliary cells. (a) Origin of LPC during fetal liver development from hepatoblast. (b) Activation of LPC located in the canal of Hering after severe injury and differentiation into hepatocytes and BEC, contributing to liver repair (Ko *et al.*, 2020)

1.2.5. Hepatic stellate cells

Hepatic stellate cells (HSC), also known as Ito cells, are important cells involved in tissue repair and inflammatory responses (Tsuchida and Friedman, 2017). They represent the hepatic fibroblasts and are located in the space of Disse, the tiny area between hepatocytes and LSEC (**Figure 1**). Their embryonic origin is still debated as they display marker genes of various germ layers (Shang *et al.*, 2018). They are described as fat storing pericytes represent 5 to 8% of total liver cells. Although their exact role in normal liver is still being debated, HSC are known to be responsible for collagen synthesis and vitamin storage. Eighty percent of all vitamin A (retinol) contained in the body are stored within HSC lipid droplets (Senoo, Mezaki and Fujiwara, 2017).

Lately, studies have revealed that HSC functions were more diverse. Indeed, HSC are sensitive to inflammatory stimuli as they express complement receptor C5aR (Xu *et al.*, 2013) and PRR,

and can even act as antigen presenting cells (Weiskirchen and Tacke, 2014). For instance, exposure to LPS induces NF- κ B in HSC leading to their activation. Upon liver injury, HSC can contribute to inflammation by producing reactive oxygen species and pro-inflammatory cytokines (Fujita and Narumiya, 2016). Interestingly, HSC have also been shown to be key regulators of the adaptive immune response as they express high levels of programmed death-ligand 1 (PD-L1), also known as CD274 and B7-H1, which suppresses lymphocyte-mediated immune responses. Conversely, quiescent HSC do not express PD-L1 that seem to be upregulated after activation by IFN- γ or contact with activated T cells (Yu *et al.*, 2004; Li *et al.*, 2016).

Additionally, Activated HSC have been shown to be involved in liver regeneration by producing angiogenic factors and remodeling the extracellular matrix, which support endothelial cell and hepatocyte proliferation in liver regeneration (Jin *et al.*, 2018; Kitto and Henderson, 2021). This is further supported by murine knockout models inhibiting activated stellate cells. When those mice undergo severe liver injury, regenerative responses of both hepatocytes and oval cells are significantly impaired and more severe necrosis (Kalinichenko *et al.*, 2003; Pintilie *et al.*, 2010; Shen *et al.*, 2011).

However, when overly activated they can contribute to the development of fibrotic tissue and cause liver fibrosis. Indeed, HSC have been shown to be major contributors to the development of fibrosis (Hoffmann *et al.*, 2020). However, several negative feedback pathways of liver fibrosis have been described. For example, tissue inhibitor of metalloproteinase 1 TIMP-1, mainly produced by HSC and KC during liver injury, protected hepatocytes against CCl₄-mediated liver injury. In different contexts of liver injury characterized by sustained inflammation and fibrosis, CB2 receptors, have also been identified as a novel negative regulator of profibrogenic functions of IL-17, a key cytokine in the profibrogenic response (Guillot *et al.*, 2014). These findings bring interesting new opportunities to the care of liver fibrosis.

1.2.6. Immune cells

The liver shelters a variety of immune cells from both the innate and adaptive immune systems. Indeed, the liver holds the largest population of macrophages in the body (Ju and Tacke, 2016). These hepatic macrophages, called Kupffer cells, reside in the lumen of sinusoids closely tied

to endothelial cells (**Figure 1**). They play a role of sentinels as they are critical for systemic response to gut-derived pathogens.

In addition, the liver harbors many cell types of the adaptive immune system including B and T lymphocytes, natural killer T cells and $\gamma\delta$ T cells. The features and functions of these immune cells will be described with more details in the third part.

This abundance of immune cells in the liver has led to propose the liver as an immunological organ (Gao, 2016). Alongside its immunological properties, the liver also performs vital tasks to maintain homeostasis by regulating metabolism and inflammation.

1.3. Liver functions

The liver is a vital organ that shelters a wide variety of cells. This translates into a large spectrum of hepatic functions in metabolism, storage of nutrients, protein synthesis and homeostasis monitored by the liver.

1.3.1. Glucose metabolism

Dietary carbohydrates are metabolized in the digestive tract by glucosidase chain reactions into glucose and absorbed to be transported to tissues to be used as energy in the form of ATP (Han *et al.*, 2016).

Glucose is transported from the intestines to the hepatocytes by glucose transporters. GLUT2 is the predominant glucose transport in the human liver (Adeva-Andany *et al.*, 2016) and enables bidirectional fluxes of glucose in and out hepatocytes. Beyond utilizing glucose, the liver can release it into the blood stream, from stored glycogen (glycogenolysis) or by synthesizing glucose from precursors including alanine, lactate and glycerol (gluconeogenesis). This unique ability to store and release glucose is essential to provide energy to all organs through periods of fasting. During postprandial windows, the liver switches from a net output to a net intake of glucose which is operated by a decrease of glucagon levels and an increase of insulin in the blood. This translates to glycogen accumulation and an

activation of glycolysis in hepatocytes. Glucose uptake by the liver is not dependent on insulin, rather, hyperglycemia is the main factor inducing glucose transportation inside hepatocytes (Chadt and Al-Hasani, 2020). Conversely, further away from the feeding windows, the liver shifts from a glucose storage mode to a net glucose release. The pancreas starts releasing glucagon, which in turns triggers a cascade of kinases leading to the breakdown of stored glycogen into glucose, known as glycogenolysis (Han *et al.*, 2016). Additionally, new molecules of glucose are generated from carbon substrates to meet energy needs of all organs, referred to as gluconeogenesis (Trefts, Gannon and Wasserman, 2017).

Within the cells, glucose is metabolized into glucose-6-phosphate by glucokinase enzyme (Adeva-Andany *et al.*, 2016). From this step, glucose-6-phosphate can follow different paths: it can be transformed into uridine 5' diphosphate (UDP)-glucose to be further utilized for glycogen synthesis, and also UDP-galactose for protein glycosylation or UDP-glucuronate (Egger *et al.*, 2010) involved in the formation of glycosaminoglycans. On average, 50% of the absorbed glucose is converted and stored as glycogen, representing the direct pathway of glycogen synthesis. More than 70% of glycogen is formed via this direct pathway, alternatively 27% of the glycogen formation results from glucose derived from gluconeogenesis (indirect pathway) (Rito *et al.*, 2018). The capacity of the liver to store glycogen is limited, therefore excess dietary glucose is converted into fat by *de novo* lipogenesis in the liver, but represents an energetically expensive pathway (Adeva-Andany *et al.*, 2016).

Altogether, these features make the liver a central organ in glucose metabolism. In addition, lipid metabolism is another important hepatic function, processed either from excess glucose intake or from ingested lipids.

1.3.2. Lipid and cholesterol metabolism

The liver also plays a major role in the production of cholesterol and proteins that carry fatty acids to other tissues throughout the body.

Lipid metabolism in hepatocytes mainly comprises three major pathways: first, lipid and fatty acid uptake, along with fatty acid synthesis (referred to as *de novo* lipogenesis); second, lipid storage, involving triglyceride synthesis and lipid droplet formation; and lastly, lipid consumption, implicating fatty acid degradation (lipolysis), β -oxidation, and the synthesis of lipoproteins.

The hepatic bile secretion and lipoprotein synthesis facilitate the absorption of lipids assembled in chylomicrons in the gut. Fatty acids will eventually be hydrolyzed into non-esterified fatty acids (NEFA) by lipoprotein lipases or thioesterases and delivered to hepatocytes thanks to transport proteins namely fatty acid transport protein, fatty acid translocase and CD36, or by diffusion (Ruiz-Palacios *et al.*, 2017). Inside hepatocytes, NEFA and fatty acyl-CoA are bound to fatty acid binding protein and acyl CoA binding protein that carry them to either intracellular compartments for metabolism or to the nucleus to further regulate the activity and nuclear abundance of transcription factors.

After feeding, the liver also converts NEFA into triglycerides by assembling fatty acids and glycerol with very low-density lipoproteins, released by hepatocytes into the bloodstream to provide lipids to the whole body. Those glycerolipids also include phospholipids and glycolipids. Glycerophospholipids represent the most abundant type of phospholipids. They are mostly found in cell membranes where they constitute anchors for proteins in cell membranes. They are also a source of physiologically active compounds such as eicosanoids.

The liver is also a key metabolic hub for energy homeostasis by performing *de novo* synthesis of fatty acid (referred to as lipogenesis) from carbohydrates and acetyl-CoA. This pathway is sensitive to insulin concentration and tissue sensitivity to insulin (Song, Xiaoli and Yang, 2018). In the body two tissues have the capacity to produce fatty acids: the liver and the adipose tissue. While *de novo* lipogenesis in adipose tissue is directly involved in *in situ* fat accumulation and energy storage, fatty acids in the liver are carried by lipoproteins and provide energy and structural elements for membrane building. Additionally, the liver is the main site of cholesterol biosynthesis. It is an essential component of cell membranes that maintains their integrity and fluidity and serve as a precursor for the synthesis of bile acids, steroid hormones, and vitamin D (Zampelas and Magriplis, 2019). Cholesterol is formed from acetyl-CoA via a multistep metabolic process involving 3-hydroxy-methylglutaryl-CoA reductase (HMG-CoA-R) which mediates the rate-limiting step that catalyzes the conversion of HMG-CoA into mevalonic acid. However, excess of lipid accumulation in the form of triglycerides or cholesterol inside hepatocytes results in fatty liver disease (also known as hepatic steatosis) and atherosclerosis (Kim *et al.*, 2014). Statins which are inhibitors of 3-hydroxy-methylglutaryl CoA reductase represent the mainstay hypercholesterolemia and cardiovascular disease treatment (Oliveira *et al.*, 2016).

Conversely, in periods of fasting, the liver produces ketone bodies (including acetoacetate and β -hydroxybutyrate) through the breakdown of fatty acids, in a process called ketogenesis.

Ketogenesis occurs in conditions of low glucose levels in the blood, after exhaustion of stores of glycogen and carbohydrate.

1.3.3. Vitamin and mineral storage

The liver stores vitamins A, D, E, K, and B12 and keeps significant amounts of these vitamins stored in some cases several years as a backup. Unlike vitamin B12 which is a water-soluble vitamin, vitamins A, D, E and K are liposoluble vitamins, their absorption in the form of micelles is dependent on bile acids and dietary fats. Vitamin A is a family that comprises retinol, retinal and pro-vitamin A carotenoids (such as beta-carotene). They have key roles in the vision, maintenance of epithelial integrity, immune competence, reproduction.

Once in the intestine, enterocytes absorb them and combine them with triglycerides, cholesterol, phospholipids and proteins, into chylomicrons formed in the Golgi and excreted via exocytotic vesicles in the form of retinyl esters or directly as retinol (Hussain, 2014). Chylomicrons then deliver the nutrients to the tissues and the excess is internalized by hepatocytes. Several proteins such as low-density lipoprotein receptors and syndecan-1 (a heparin sulfate proteoglycan) and apolipoprotein E, which facilitate chylomicron binding (Stanford *et al.*, 2009; Mondal *et al.*, 2016; Saeed *et al.*, 2017). Inside hepatocytes, retinyl ester hydrolase will further hydrolyzed retinyl esters into retinol (Linke, Dawson and Harrison, 2005). Retinol is then delivered to hepatic stellate cells where it is esterified into retinyl esters for storage inside lipid droplets (Saeed *et al.*, 2017). This suggests that retinol constitutes the active form of vitamin A and retinyl ester, the storage form.

Vitamin D is a secosteroid hormone involved in calcium homeostasis and bone structure. It can be absorbed from dietary sources in the form of vitamin D₂ (ergocalciferol) and D₃ (cholecalciferol) or synthesized within the skin. Vitamin D from both sources is biologically inactive. It is activated by two hydroxylation steps, the first one occurs in the liver and the second in the kidney. Endogenous synthesis of vitamin D involves ultraviolet B light exposure that catalyzes the stereoisomeric conversion of 7-dehydrocholesterol into pre-vitamin D₃. Pre-vitamin D₃ will be further converted to vitamin D₃ (Elangovan, Chahal and Gunton, 2017). Subsequently, vitamin D₃ will be hydroxylated into 25-hydroxyvitamin D (25D) by CYP2R1 in the liver, that will in turn be converted to 1,25 dihydroxyvitamin D (1,25D) by CYP27B1 in the kidney, which represents the active form (Keane *et al.*, 2018). Interestingly, the levels of

hepatic vitamin D receptors (VDR) VDL are low in normal liver and the distribution has been shown to be in favor of BEC, KC and other non-parenchymal cells. Indeed, their VDR expression is higher than that of hepatocytes indicating that non parenchymal cells might be the main responders to vitamin D in the liver (Elangovan, Chahal and Gunton, 2017).

Vitamin E is another fat-soluble vitamin group essential for human health, involved in the protection against reactive oxygen species, that includes 4 tocopherol and 4 tocotrienol members. As a fat-soluble vitamin, the absorption, hepatic metabolism and cellular uptake are similar to those of other lipids. After feeding, most vitamin E is carried by lipoproteins (namely LDL and HDL) within chylomicrons to the liver. These vitamin E-rich vesicles will be stored within LSEC, HSC and KC. Outside feeding windows, vitamin E will be transferred from cytoplasm of liver cells to the plasma (in the form of α -tocopherol) via α -tocopherol transfer protein (α -TTP) and transported through blood circulation by LDL and HDL transport proteins (Schmölz *et al.*, 2016).

Lastly, vitamin K is a family that comprises two members, vitamin K1 (phylloquinone) synthesized in plants and vitamin K2 (menaquinone) derived from animals and bacteria (Schubert *et al.*, 2018). The metabolism of vitamin K occurs in the liver and follows that of vitamin E, which include the uptake of chylomicrons by enterocytes, the packaging with dietary lipids and the exocytosis into the lymphatic system (Shearer, Fu and Booth, 2012).

Alongside those vitamins, the liver also stores essential minerals including iron from hemoglobin in the form of ferritin involved in the creation of new red blood cells, and copper. Indeed, dietary iron is absorbed in enterocytes then loaded on transferrin (Tf) to circulate throughout the body. Subsequently, iron is delivered to the liver which performs essential function in maintaining systemic iron homeostasis. Indeed, the liver is an important site for the storage of iron and the production of iron-related proteins including Tf, copper-dependent serum ferroxidase (Cp) involved in the iron export into the circulation and ferritin that stores and releases iron in a regulated fashion (Winn, Volk and Hasty, 2020). Iron enters liver cells via transferrin receptor (Tfr). Tfr1 transcript stability is regulated by the IRP/IRE system. When iron levels are low, more Tfr1 is translated allowing for increased iron uptake through Tf. When iron levels are high, IRP are inactivated that leading to a reduction of Tfr1 mRNA stability and iron uptake. This mechanism allows a fine regulation of iron levels (Anderson and Shah, 2013). Iron is then released into the blood stream via Cp in a copper-dependent manner (Doguer, Ha and Collins, 2018).

In fact, the liver is also a key organ in the supply, storage and excretion of copper. Copper is an important mineral for the action of diverse enzymes involved in a wide variety of physiologic functions (Bost *et al.*, 2016). Seventy-five percent of the copper coming from the portal vein is taken up by the liver where it enters hepatocytes by the human copper transporter hCTR1 (Linder, 2020). The remainder reaches the peripheral circulation, bound to albumin (Bost *et al.*, 2016).

1.3.4. Bile production

In addition to its role in the metabolism of nutrients and the storage of essential vitamins and minerals, the liver is the site of production of bile which is vital to the survival of the organism. The bile is a complex fluid secreted aqueous liquid by hepatocytes that acts as a surfactant to extract lipids and lipophilic nutrients from the food and helps break down proteins for digestion. The main function of bile are to facilitate the absorption of dietary fats in the intestines, excrete cholesterol, harmful lipophilic xenobiotics and endogenous metabolites (including bilirubin and bile salts) with a molecular weight superior to 300 Daltons that are not excreted by the kidneys and finally to protect against enteric infections by carrying immunoglobulin A (IgA), inflammatory cytokines that stimulate the gut immune system (Chiang and Ferrell, 2020). Bile also carries vitamins; As detailed previously, vitamin D metabolite (25-hydroxyvitamin D is secreted in the bile by hepatocytes and contributes to calcium homeostasis (Gil, Plaza-Diaz and Mesa, 2018). Bile flows through bile ducts where it is enriched by cholangiocytes and is stored in the gallbladder or directly delivered to the intestinal lumen. Initially, hepatocyte secrete bile formed by water bile salts, electrolytes, bilirubin and lipids like phospholipids and cholesterol (Chiang and Ferrell, 2020). Bile salts have a hydrophobic and a hydrophilic part which help promote lipid emulsion in the blood by forming micelles. Primary bile acids (cholic, chenodeoxycholic) are synthesized by hepatocytes from cholesterol catabolism. They are further dehydroxylated by gut bacteria in leading to the formation of secondary bile acids (deoxycholic acid and lithocholic acid). Both primary and secondary bile acids are further conjugated with glycine and taurine by the liver to form bile salts (Suga *et al.*, 2017). At the cellular level, The sodium-potassium ATPase localized on the basolateral membrane of the hepatocyte regulates sodium and potassium

gradients (Boyer, 2013). Additionally, ion exchangers like the sodium-hydrogen exchanger maintain a stable pH.

1.3.5. Protein synthesis

Protein synthesis and breakdown are essential to all cellular and organ functions. We saw earlier that the liver plays a major role in lipid-related protein synthesis, but it is also an organ responsible for the production of many plasma proteins such as albumin which is a crucial oncotic pressure regulator and proteins of the complement system involved in the innate immunity.

In fact, 80 to 90% of all circulating innate immunity proteins, namely proteins of the acute phase, complement system and secreted PRR, are produced within the liver by hepatocytes. Liver-specific expression of these proteins results from the liver-specific transcription factors that regulate the gene expression of these proteins (Gao, Jeong and Tian, 2008). In the context of an inflammation or acute phase response, these inflammatory cytokines including IL-6, TNF α and IFN γ stimulate hepatocyte to produce high amounts of these innate immunity proteins.

In addition, the liver has the capacity to break down proteins and metabolize their amino acids. Metabolizing amino acid provides energy for hepatocytes but leads to nitrogenous wastes. One of the mechanisms the liver uses to dispose of these damaging reactive nitrogenous molecules is the urea cycle. Some specific amino acids can also serve as gluconeogenic substrates. This enables the conversion of amino acids from tissues including skeletal muscle and intestines into glucose, which is particularly pertinent to provide stable and sustained energy to glucose-dependent organs in times of extended fasting (Trefts, Gannon and Wasserman, 2017).

1.3.6. Detoxification of the organism

The strategic location of the liver at the intersection between the portal system and general circulation is one of the key features of this organ. In fact, the liver is known to play a key role in processing and metabolizing all gut-derived substances and nutrients before releasing them into the blood stream. The liver which hosts a high number of neutrophils is essential for the clearance of bacteria and related toxins like endotoxin from the blood (Strnad *et al.*, 2017).

Hepatic neutrophils provide immune protection through their phagocytic properties and the release of antimicrobial granule proteins (Protzer, Maini and Knolle, 2012; Heymann and Tacke, 2016). Moreover, neutrophils have the capacity to form extracellular webs, known as neutrophil extracellular traps (NET), of nuclear DNA associated with histones and proteases that trap and kill bacteria (McDonald *et al.*, 2012).

Liver macrophages perform erythrophagocytosis leading to hemolysis which contribute to the renewal of the red blood cell pool.

Additionally, the liver produces key enzymes involved in the detoxification of the organism. Indeed, through the portal flow the body is exposed to a variety of chemicals of many sorts (including pharmaceutical drugs, household chemicals, food-derived antigens, environmental contaminants) that can be toxic. These metabolic pathways in the liver can be mainly centered around two phases of enzyme systems of drug metabolizing enzymes (DME) aiming to target xenobiotics and lead to their excretion. DME are primarily produced by the liver, and in a much lower extent in the kidney and intestine (Hodges and Minich, 2015). Among those DME, cytochrome P450 superfamily of enzymes (CYP450) represents the first defense (phase I) used to process all kinds of xenobiotics, steroid hormones and pharmaceuticals (Danielson, 2002). CYP450 enzyme are involved in the oxidation of nearly 90% currently used drugs (Chen, Zhang and Wei, 2011). The mechanism of action of CYP450 enzymes involves adding a reactive group (namely hydroxyl, carboxyl, amino group) via oxidation, reduction, and hydrolysis reactions (Guengerich, 2018). Variability in the expression of CYP450 enzymes can have consequences on the organism's response to a toxin or a drug. In fact, CYP450 genes are subject to genetic polymorphisms that can lead to impaired expression and function of the enzymes in the individuals. Clinical application of this knowledge about CYP450 enzymes translates in the pharmacological understanding of drug interactions, side effects, and interindividual variability in drug metabolism (Guengerich, 2018). In addition, many foods (such as cruciferous vegetables, tea, curcumin, soybeans, garlic) have been shown to have inhibitory or stimulatory properties over CYP450 enzymes (Hodges and Minich, 2015). CYP450 family is composed of a variety of enzymes involved in specific metabolism pathways. For instance, CYP1 family metabolizes procarcinogens, hormones, and pharmaceuticals. CYP2 enzymes process drugs, xenobiotics, hormones, along with other endogenous compounds including ketones, glycerol, and fatty acids. In this cytochrome family, CYP2E1 has been the center of many studies as it involved in the metabolism of ethanol (Danielson, 2002). CYP3 substrate comprise caffeine, testosterone, progesterone, and androstenedione procarcinogens including aflatoxin B1. Lastly, the CYP4 family seems to

have an extrahepatic expression and is involved in the metabolism of medium chain triglycerides and toxicants like phthalates (Hodges and Minich, 2015).

Once a xenobiotic has been processed by enzymes of phase I, it becomes hydrophilic and can be conjugated. This second phase also called “detoxification phase” consists in the transfer of hydrophilic compounds by their respective enzymes such as glucuronic acid (by glucuronyl transferases), sulfate (by sulfotransferases), glutathione (by glutathione transferases), amino acids (by amino acid transferases), an acetyl group (by N-acetyl transferases), and a methyl group (by N- and O-methyltransferases) (Xu, Li and Kong, 2005). These phase II reactions aim at making the metabolites more hydrophilic to enhance their excretion in the bile and the urine.

1.3.7. Interaction of the liver with other organs

The liver is also crucial for the homeostasis and functions of other organs. Indeed, the liver contributes to optimal brain functions as loss of liver functions leads to chronic hepatic encephalopathy and eventually coma. Hepatic encephalopathy also known as portosystemic encephalopathy is a syndrome characterized by impaired brain function in patients with advanced liver diseases. The mechanisms by which liver failure leads to brain dysfunction are still unclear but several hypotheses have been proposed in the last few years.

First, ammonia is the best described neurotoxin linked to hepatic encephalopathy. In healthy livers, ammonia produced by enterocytes or gut bacteria and released in the portal vein is converted into glutamine, preventing its entry in the systemic circulation (Sawhney and Jalan, 2015). However, in advanced liver diseases, impaired hepatic functions lead to a buildup of ammonia and is often associated with muscle wasting, as muscle represents an important extrahepatic site for ammonia removal. This increase in ammonia blood levels is responsible for astrocyte swelling mediated by the water channel protein aquaporin-4 (Wright *et al.*, 2010). As a consequence of hyperammonia, astrocytes start metabolizing ammonia into glutamine leading to an increase in intracellular osmolarity, eventually resulting in brain edema (Jover *et al.*, 2006). In fact, glutamine levels are significantly higher in acute liver disease patients (Görg, Schliess and Häussinger, 2013). Ammonia has also been shown to disturb neuronal electric activity through the inhibition of excitatory and inhibitory postsynaptic potentials (Ferenci, 2017).

Other hypotheses of the link between the liver and brain dysfunction include alterations of blood flow and the role of inflammatory mediators released in the blood stream, without being associated with brain tissue infection necessarily (Ferenci, 2017). Cirrhotic patients are characterized by weakened immune capacities and more prone to developing infections. Although the underlying mechanisms are still not fully understood, infection is a risk factor of hepatic encephalopathy (Merli *et al.*, 2013). In addition, further investigations are needed to determine whether the systemic release inflammatory mediators or infections on their own contribute to hepatic encephalopathy.

Cirrhotic patients also have a higher risk to develop cirrhotic cardiomyopathy, highlighting the importance of a healthy liver to maintain proper heart functions (Chayanupatkul and Liangpunsakul, 2014). Indeed, cirrhotic cardiomyopathy is characterized by chronic cardiac dysfunction that translates into hyperdynamic circulation with a higher splanchnic arterial vasodilatation and lower systemic vascular resistance. Cirrhotic patients displayed lower elevation of cardiac output and ejection fraction in response to exercise compared to controls.

Recently, new approaches to study organ interactions between the liver and the brain or the lungs have recently been engineered (Skardal *et al.*, 2017). These multi tissue-on-a-chip platforms aim at predicting more accurately effects of drugs, chemicals, and proteins in the body and reducing the costs of drug development as 90% of drugs that enter phase I clinical trials eventually fail (Seruga *et al.*, 2015).

This wide variety of liver functions and their major impact on the other organs and overall homeostasis have been safeguarded by the evolution by imparting to the liver the remarkable capacity to regenerate. This unique advantage allows the liver to recover any lost mass and prevents jeopardizing survival of the organism globally.

2. Liver regeneration

Strategically located as a hub between the portal system coming from the gut and the general circulation, the liver is exposed to many kinds of harmful substances such as gut-derived toxins, excess of fat and alcohol that can lead to severe liver injury. The proper execution of liver function is crucial for body homeostasis (Michalopoulos and Bhushan, 2021). Therefore, it is essential for the liver to regenerate in order to maintain its mass and functions. Liver regeneration results from the ability of the liver to adjust its mass to the whole-body weight. Indeed, after severe weight loss or weight gain and pregnancy, the liver size decreases and increases respectively (Michalopoulos, 2013). It is defined as a process by which the liver replaces lost tissue by the differentiation and/or proliferation of remaining cells. Unlike in species like fish (Chu and Sadler, 2009), the liver of humans and rodents regenerate following a compensatory growth mechanism that only recovers the mass but not the shape of the liver. Indeed, following liver resection in humans and rodents, for instance, the remaining liver lobes will undergo hyperplasia to compensate for tissue loss, but the resected lobes will not grow back.

On the cellular level, there are mainly two regenerative pathways in the liver. First, the classical liver regeneration is driven by healthy hepatocyte hyperplasia and proliferation. In fact, unlike most somatic cells, a few cell types including megakaryocytes, cardiac myocytes, skeletal muscle cells, and hepatocytes are polyploid cells which enables multipolar divisions into diploid daughter cells (Wilkinson *et al.*, 2019). Alternatively, when hepatocyte proliferation is compromised following severe liver injury or massive tissue loss, hepatic regeneration involves liver progenitor cells. They are characterized by stem-cell like features and are able to differentiate into both hepatocytes and biliary cells.

2.1. Liver regeneration from hepatocytes

Following loss of liver mass or acute injury, the liver has the ability to trigger regenerative processes through the hypertrophy and proliferation of hepatocytes. Liver regeneration is a unique feature of the liver. It is observed in all vertebrates including rodents (Michalopoulos and Bhushan, 2021). This complex process is triggered by many parameters such as liver to

body weight ratio when livers of small individuals are transplanted into larger ones but also after a loss of tissue or function. Liver regeneration involves a myriad of cellular actors and is finely regulated. In normal liver, hepatocytes are quiescent and less than 1–2% of hepatocytes are in the cell cycle in homeostasis state. Following acute hepatic stress, hepatocyte proliferation represents the default regenerative pathway in response to liver mass loss (Michalopoulos, 2017). Hepatocyte polyploidy is a key factor that allows hepatocytes to undergo division and self-renew to maintain hepatocyte pool (Wang *et al.*, 2017). A key endpoint of liver regeneration is the restoration of total number and mass of hepatocytes, the main functional cells of the liver responsible for delivering most of the hepatic functions and maintaining homeostasis (Walesky *et al.*, 2020).

Liver regeneration is triggered by a wide variety of signals which can be classified into two main categories: mechanical stimuli on the one hand and chemical stimuli on the other hand.

2.1.1. Mechanisms of regeneration following mechanical stress

In humans, liver resection which consists in the surgical removal of a portion of the liver, is commonly performed to treat multiple hepatic injuries.

Knowledge about the underlying mechanisms of liver regeneration has significantly grown thanks to the model of PHx. In 1932, the first PHx in rats was reported. It was first performed on humans only 20 years later (Kruepunga *et al.*, 2019). This delay can be explained by the fact that human liver is not lobated. Indeed, in rodents, the liver is composed of several lobes that are easily removable after ligation (**Figure 3**). The most common PHx model is the 2/3 hepatectomy.

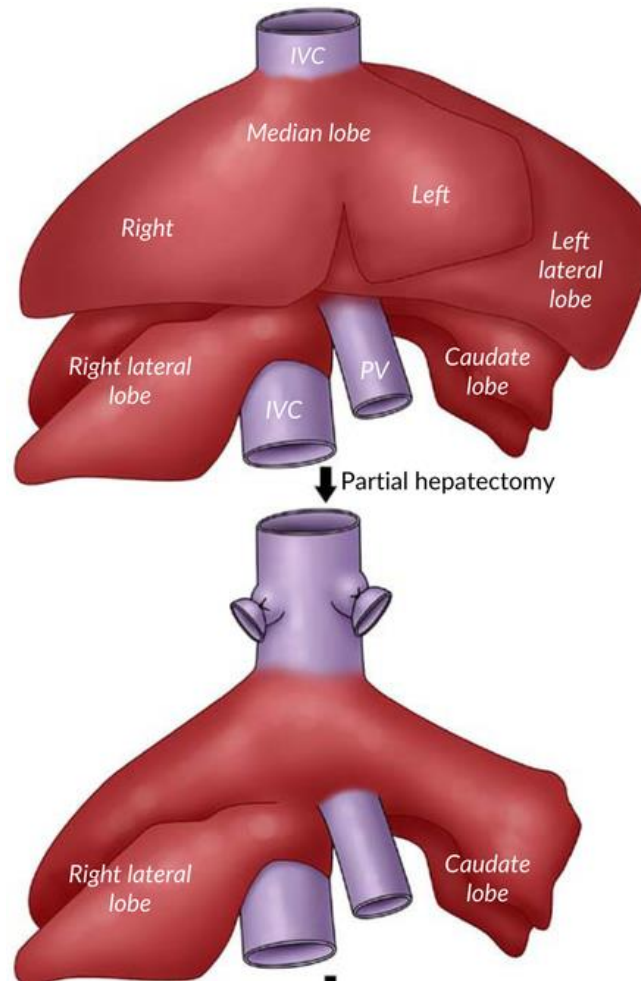


Figure 3: Anatomy of the liver before and after 2/3 PHx in the mouse. *The 2/3 hepatectomy model in the mouse consists in the removal of the two biggest (median and left lateral) lobes (Abu Rmilah et al., 2019)*

Depending on the proportion of the liver mass resected, different types of hepatocyte responses are induced (Gilgenkrantz and Collin de l'Hortet, 2018): for example, 1/3 PHx stimulates hepatocyte hypertrophy while 2/3 PHx triggers division and proliferation of remaining polyploid hepatocytes (**Figure 4**) (Miyaoaka *et al.*, 2012).

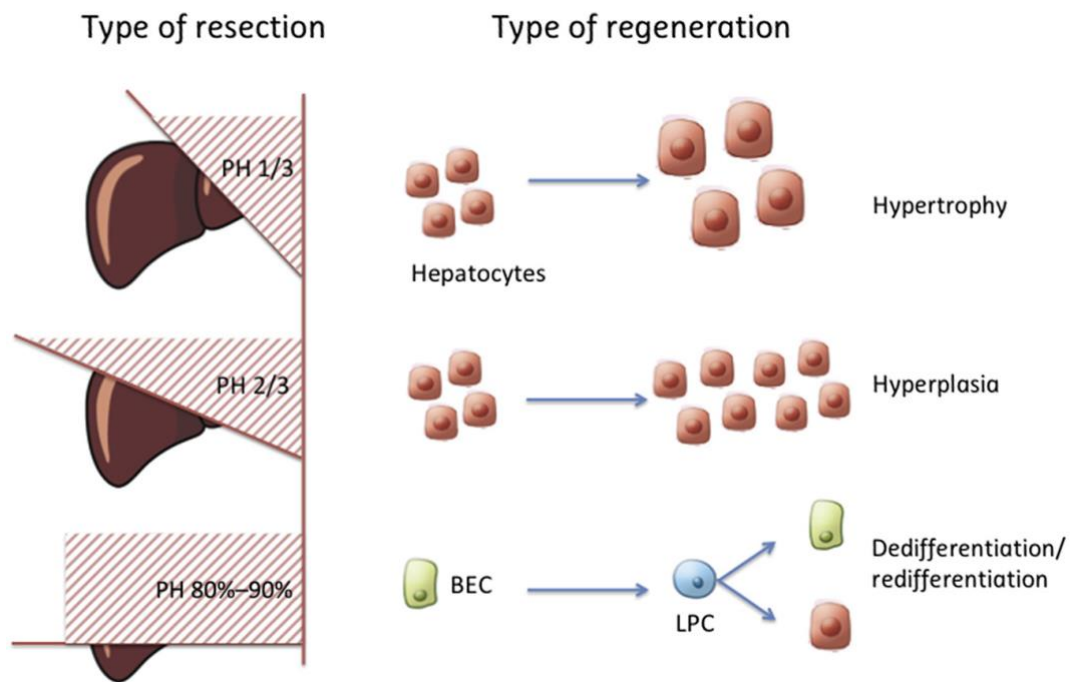


Figure 4: Mechanisms of liver regeneration depending on the volume of resected liver. Liver mass is restored through hepatocyte-driven regeneration when remaining cells are sufficient: by hypertrophy or hyperplasia of remaining hepatocytes following 1/3 and 2/3 hepatectomy respectively. Alternatively, liver mass recovery requires the activation of the LPC compartment following 80% hepatectomy or above by triggering LPC expansion and differentiation into hepatocytes and biliary cells (Gilgenkrantz and Collin de l'Hortet, 2018)

A common characteristic of partial hepatectomy models is the transient accumulation of fat in residual hepatocytes, known as steatosis (Rao *et al.*, 2001; Kachaylo *et al.*, 2017). Within the few hours following PHx, lipid accumulation occurs in the liver and has been shown to be required for a proper liver regeneration. In fact, those lipids have been shown to provide fuel for regenerating cells. Studies described that blockade of fat accumulation either by drugs or in KO mice was associated with impaired liver regeneration (Yamauchi *et al.*, 2003; Shteyer *et al.*, 2004). Although the underlying mechanisms regulating those lipid changes after PHx still remain to be elucidated, lipid metabolism and liver regeneration are very sensitive to the circadian rhythm (Atwood *et al.*, 2011; Gooley, 2016). Indeed, the initiation of liver regeneration is dependent on polyamine synthesis, which is required for the cell proliferation. This includes several enzymes whose transcripts follow circadian oscillations revealing hepatocytes' autonomous internal clock that orchestrate liver regeneration (Atwood *et al.*, 2011). Additionally, histone deacetylase SIRT1 which is a central actor in many liver processes such as glucose and lipid metabolism, but also cell proliferation, has been shown to be tightly associated with circadian oscillations and responsible for regulating deacetylation of histone

H3 in the promoter region of clock-controlled genes in a circadian pattern within hepatocytes during liver regeneration in mice (Bellet *et al.*, 2016).

The complexity of the regulation of liver regeneration translates into a large diversity of molecular factors and mitogenic signals involved in this process.

One of the earliest biochemical changes following PHx is the induction of the activity of urokinase plasminogen activator (uPA) that converts plasminogen to plasmin which activates metalloproteinases (Mangnall *et al.*, 2004). This occurs widely across the tissue in remnant lobes as early as 5 min after PHx. Although uPA was initially described in the conversion of plasminogen to plasmin, it has been now shown to have a wider role in tumor metastasis and liver regeneration by contributing to extracellular matrix remodeling and angiogenesis (Drixler *et al.*, 2003). In hepatocytes, beta catenin and notch-1 intracellular domain (NICD) are induced inside the nucleus within the first half hour that follows PHx. The use of RNA interference to block their expression impairs the regenerative response (Köhler *et al.*, 2004). Within 1h after PHx, it has been reported that Stat3 and NFκB are activated. However, the blockage of these molecules does not seem to disturb the regenerative response. This can likely be due to the presence of redundant signaling pathways that balance the loss of proteins such as STAT1 assuming the function of STAT3). STAT3 and NF-κB are crucial signaling molecules involved in the cell cycle of many cells. Their activation in hepatocytes early after PHx contributes tremendously to the signaling pathways inducing their proliferation. At 6h after PHx cyclin D1 activity is induced. TOR functions as a regulator of this activation (Nelsen *et al.*, 2003). The first signs of DNA synthesis are observed 12h after PHx in the rat, and peak at 24h. In the mouse, the kinetic is shifted later by 6–12 h.

The early steps occurring within the first 5h following PHx are often being referred to as “priming” (Fausto, 2000). In fact, this word describes both preparatory events for the entry into the cell cycle and mechanisms orchestrating modifications of gene expression patterns within hepatocytes allowing them to keep assuring their homeostatic functions. Among mitogens, HGF and ligands of the EGFR represent the main direct mitogens inducing hepatocyte proliferation, as they induce a strong mitogenic response in hepatocytes in primary culture. HGF, EGF, and TGFα also induce hepatocyte proliferation and liver enlargement when injected alone into intact normal mice and rats. In addition to these proteins, however, there are other substances which, although not directly mitogenic to hepatocytes, enhance the effect of the direct mitogens such as TNF. IL-6 family cytokines have been shown to be key players in

both triggering and resolving the tissue damage and to promote liver regeneration (Schmidt-Arras and Rose-John, 2016). In the partial hepatectomy (PHx) model, hepatocytes contribute to IL-6 production, which is dependent on the HGF/cMET signaling pathway, thereby promoting liver repair. IL-6 promotes liver regeneration by activating STAT3 via the classic signaling pathway, but a recent study suggests that IL-6 trans-signaling through sIL-6ra also controls liver regeneration after PHx.

2.1.2. Mechanisms of regeneration following acute drug-induced-liver injury

As opposed to PHx, where tissue loss results from the surgical removal of a large portion of the liver, xenobiotic hepatotoxicity induces necrosis of liver tissue. Therefore, the underlying cellular and molecular mechanisms driving liver regeneration significantly differ.

The CCl₄ model represents one of the most common models to study drug-induced liver injury (DILI). Similarly to liver regeneration following PHx, CCl₄ triggers a hepatocyte response with a minor input from LPC as shown in a model of osteopontin-linked Cre to label LPC (Español-Suñer *et al.*, 2012). Although CCl₄ is not a drug, it is a hepatotoxic compound cleaved by cytochromes P450. The resulting products trigger oxidative damage to DNA, proteins, lipids, and carbohydrates within hepatocytes leading to tissue necrosis. In fact, it is associated with lipid peroxidation and cross links between lipids and proteins resulting in cell dysfunction and membrane damage (Clemens, McGill and Apte, 2019). This cell damage is accompanied by a production of cytokines such as IL-6 and TNF- α that amplify tissue injury (Sudo *et al.*, 2005). In fact, TNF- α is a proinflammatory mediator rapidly produced by macrophages in response to tissue injury. TNFR1 deficient mice exhibit significantly less CCl₄-mediated liver fibrosis than the control mice. In addition, following CCl₄ injection, TNFR1 deficient mice display no increase of TGF- β 2, a pro-fibrogenic factor involved in the activation of fibroblasts and the production of extracellular matrix molecules, unlike the wild type group (Sudo *et al.*, 2005).

However, these cytokines and growth factors, also found increased following PHx, are double-edged swords as they have been shown to be beneficial for hepatocyte survival and liver regeneration. Indeed, these pro-inflammatory mediators promote regeneration and tissue

repair, however in case of chronic insult, sustained establishment of a pro-inflammatory environment can lead to tissue damage (Cordero-Espinoza and Huch, 2018).

Gao et al. recently provided evidence suggesting that hypoxia-inducible factor 2 α reprograms hepatic macrophages to produce the hepatoprotective cytokine IL-6, thereby ameliorating DILI in mice (Gao *et al.*, 2020). Additionally, IL-6 has been shown to have hepatoprotective properties by reducing MMP-2 expression involved in DILI-mediated tissue injury (Bansal *et al.*, 2005). In hepatocytes, IL-6 activates Stat3 signaling pathways. Studies showed that following CCl₄ exposure, TNFR1-deficient mice display reduced Stat3 signaling leading to a delayed regeneration compared to the wild-type group. Similarly, as in the PHx model, hepatocyte growth factor (HGF) is also upregulated after CCl₄ exposure. HGF is produced by hepatic non-parenchymal cells and is involved in regeneration following CCl₄ injury. Indeed, administration of antibodies against HGF resulted in dramatically reduced DNA synthesis in mice injected with CCl₄.

2.2. Liver regeneration from liver progenitor cells

By contrast to surgical loss of liver mass or acute injury, upon severe or chronic tissue damage characterized by a massive destruction of hepatocytes and chronic inflammation, the proliferation of remaining hepatocytes is altered. Therefore, the classic regenerative pathway through hepatocyte is compromised as proliferation of remaining and healthy hepatocytes is not sufficient to restore the initial liver mass and hepatic functions. In these cases, liver progenitor cells (LPC) activate to help restore liver tissue mass and functions.

2.2.1. Contribution of LPC to liver regeneration in severe and chronic injury

LPC have been shown to have beneficial properties during liver regeneration by differentiating into hepatocytes and biliary cells. Activation of LPC have been described in various liver diseases such as NAFLD, ALD, viral hepatitis and cholestatic hepatitis (So *et al.*, 2020), all characterized by an important loss of hepatocytes. In addition, following large tissue resection,

when remaining hepatocytes cannot sustain a proper restoration of the liver mass, regeneration is conducted from the conversion of biliary cells into progenitor cells (**Figure 5**) (Choi *et al.*, 2014; He *et al.*, 2014).

This activation and expansion of the LPC compartment in the periportal areas of the liver is usually referred to as ductular reaction and leads to the development of bile ductules and a remodeling of the extracellular matrix as it is accompanied by the activation of myofibroblasts and the infiltration of macrophages (Jakubowski *et al.*, 2005; Boulter *et al.*, 2012). Suppression of LPC differentiation leads to impaired liver regeneration and recovery (Choi *et al.*, 2017; Ko *et al.*, 2019) hence the importance of this LPC-mediated regenerative pathways.

Indeed, the role of LPC have been described in many contexts of liver injury such as acute intoxication, hepatitis, cirrhosis, where hepatocyte regeneration is compromised, thanks to the development of several murine models allowing to study these liver injuries and the impact of LPC on liver regeneration. These models include drug-induced intoxication with 2-acetylaminofluoren and retrorsine which are chemicals with strong inhibitory properties on hepatocyte proliferation that lead to the induction of a robust LPC response and ductular reaction. The murine model of choline-deficient ethionine-supplemented (CDE) diet also recapitulates this chronic liver injury and leads to stimulation of liver progenitor cell accumulation and proliferation. In this model, IL-27 has recently been shown to play a pivotal role in liver regeneration by promoting progenitor cell differentiation into hepatocytes (Guillot *et al.*, 2018). In fact, IL-27 displayed a direct role on LPC *in vitro* by promoting their differentiation into a hepatocyte-like phenotype. Alternatively, disruption of WSX-1 signaling prevented LPC accumulation and further led to a significant reduction of macrophage recruitment which are known to be central actors in the expansion of LPC. Those properties highlight the essential role of IL-27 in liver regeneration by promoting the activation and expansion of the LPC compartment.

LPC expansion has also been described in many contexts of hepatotoxin-derived necrotic injury in centrilobular (like acetaminophen) or periportal (like allyl alcohol) areas (Dollé *et al.*, 2010). Carbon tetrachloride (CCl₄) triggers liver injury by the breakdown of its metabolites from cytochrome P450. The highly reactive metabolite triggers lipid peroxidation in the hepatocytes which damages these (centrilobular) cells and induces necrosis. Under normal circumstances, acetaminophen (AAF) and paracetamol (APAP) undergo biotransformation by cytochrome P450 (glucuronidation and sulphation) and are excreted by the kidneys. After an overdose, the toxic metabolites accumulate and create adducts with DNA and protein leading to necrosis of the hepatocytes.

In a model of mice fed a DDC diet that recapitulates human cholestatic disease, liver-specific c-Met knockout mice showed a significantly reduced number of A6⁺/EpCAM⁻ hepatocyte-like cells compared to c-Met wild-type mice, indicating that HGF/c-Met pathway may regulate LPC differentiation into hepatocytes during liver regeneration (Ishikawa *et al.*, 2012).

Notch and Wnt/ β -catenin signaling have also been shown to play a role in LPC differentiation (Gao *et al.*, 2021). Indeed, macrophage-derived-Wnt3a increases Numb expression leading to an inhibition of Notch signaling in LPC, which eventually promote their differentiation into hepatocytes. Contrastingly, Jag1 expression in myofibroblasts induces Notch signaling in LPC and promote LPC differentiation into BEC (Boulter *et al.*, 2012).

Recently, studies highlighted the interaction between LPC and the extracellular matrix as matrix remodeling is required for the proliferation of LPC (Lukacs-Kornek and Lammert, 2017). These new insights represent interesting and promising therapeutic options to promote LPC-mediated liver regeneration (Williams, Clouston and Forbes, 2014). Indeed, transgenic mice expressing a mutated version of collagen I and fed a CDE diet displayed lower LPC numbers and laminin deposition, another key component of the extracellular matrix (Kallis *et al.*, 2011). Interestingly, data suggest that the differentiation of LPC into hepatocytes is associated with a disappearance of the basement membrane accompanied with changes in adhesion molecule profile including the replacement of the biliary cell-specific alpha6 integrin and connexin 43 with the hepatocyte-specific alpha1 integrin and connexin 32 (Paku *et al.*, 2004). Laminin have also been shown to be required for LPC to maintain their stem cell like features. As shown in an *in vitro* study, LPC cultured without laminin for 7 days lost the expression of pan-cytokeratin as opposed to the control cells cultured on laminin (Lorenzini *et al.*, 2010). In addition, the glycoprotein CD44, receptor of hyaluronic acid, has been reported to be involved in LPC invasion and related to the maintenance of an undifferentiated phenotype (Williams, Clouston and Forbes, 2014).

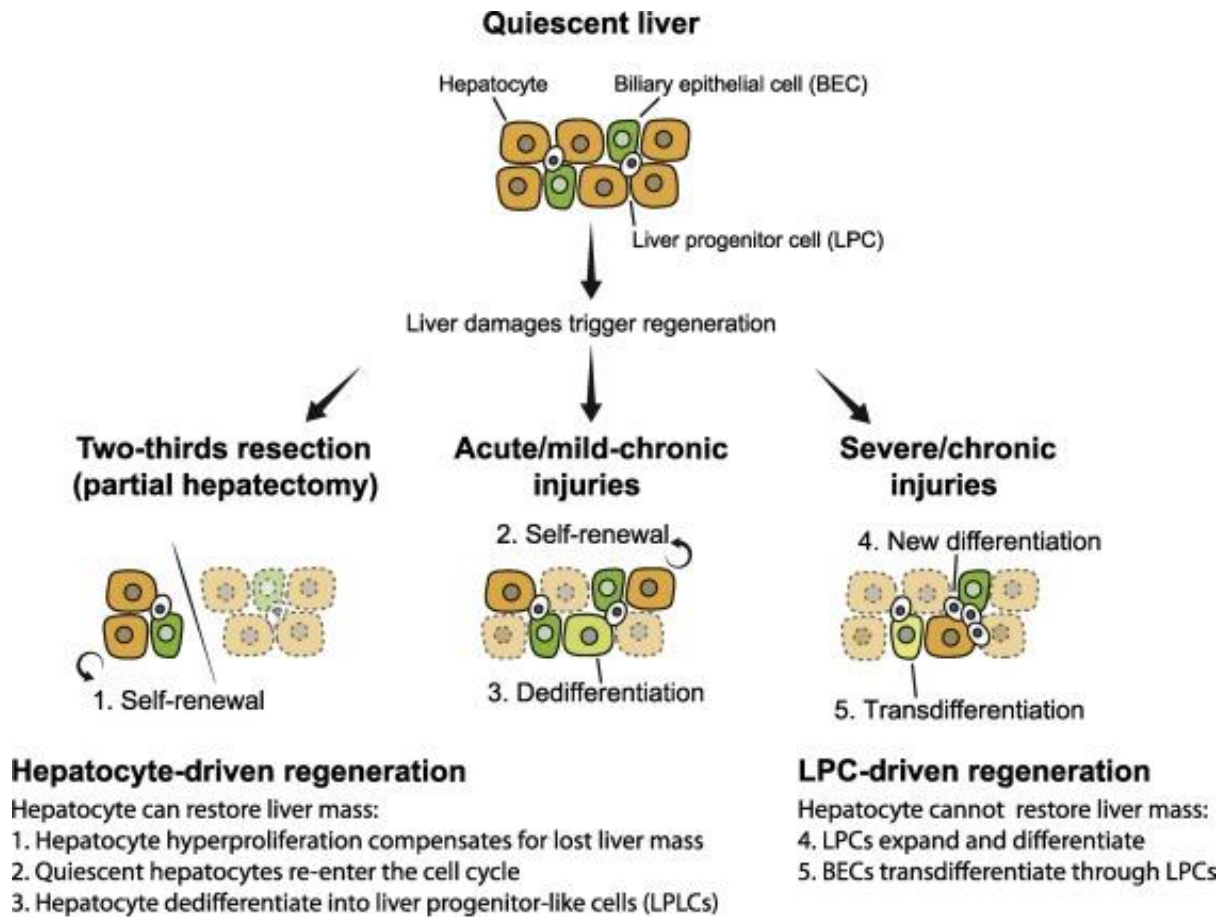


Figure 5: Pathways of liver regeneration depending on the stimulus. *Quiescent liver hosts liver progenitor cells that can differentiate into hepatocytes and biliary cells. Following two-third hepatectomy, liver mass recovery is mainly mediated by hepatocyte proliferation. Alternatively, in case of acute or mild injury, biliary cells can dedifferentiate to restore liver mass along with hepatocyte proliferation. Lastly, when the liver suffers from severe and chronic injury and hepatocyte self-renewal is compromised, LPC expand to restore a proper liver mass (Macchi and Sadler, 2020)*

2.2.2. Deleterious effects of sustained LPC activation in the liver

Although LPC activation and expansion is a necessary alternative pathway to restore liver mass when hepatocyte regeneration is compromised, this compensatory mechanism of regeneration is slow and not very efficient. Additionally, LPC proliferation can also be detrimental and lead to liver injury, promote fibrosis and contribute to liver cancer (So *et al.*, 2020).

Implication of LPC in liver fibrosis. In a context of liver injury, amid significant hepatocyte damage, LPC face the challenge of restoring lost or damaged liver tissue, as cellular and

molecular mechanisms controlling homeostatic replacement of healthy tissue are disturbed. In response to liver injury, LPC activation is associated with the activation of quiescent HSC into profibrogenic fibroblast (So *et al.*, 2020). Studies have shown a correlation between the number of LPC and the severity of fibrosis in chronic liver diseases (Clouston *et al.*, 2005; Richardson *et al.*, 2007). Indeed, the interaction of T helper type 1 (Th1) cells and LPC contributes to liver fibrosis: Th1 cells produce IFN γ , which regulates LPC proliferation (Weng *et al.*, 2013). BALB/c mice deficient in Th1 signaling fed a CDE diet exhibited reduced LPC proliferation and fibrosis compared to C57Bl/6 mice, which have normal Th1 signaling. Supplementation of IFN γ increased both LPC number and fibrosis in the CDE model (Knight *et al.*, 2007). Recently, LPC regulation by a treatment with an angiotensin II type 1 receptor blocker leading to a blockage of NOTCH signaling in LPC has shown improved fibrosis and better regeneration by redirecting LPC differentiation toward hepatocytes (Kitade *et al.*, 2019).

Implication of LPC in liver cancer. Liver cancer is the third most common cause of cancer related death worldwide responsible for approximately 830,180 deaths annually and 905,667 new cases per year (Globocan 2020). Among primary liver cancers, hepatocellular carcinoma represents about 70% and cholangiocarcinoma 15% (Massarweh and El-Serag, 2017). LPC have been associated with liver cancer development (Libbrecht, 2006). Indeed, LPC markers such as KRT7, KRT19, OV6, and EpCAM have been described in HCC (Liu, Yeh and Lin, 2020). Additionally, inhibition of LPC proliferation in chronically injured mouse livers reduced tumor development (So *et al.*, 2020).

Furthermore, the development of cancer recurrence, metastasis, and chemo/radioresistance has been associated with the presence of cancer stem cells (CSC) The transformation of LPC has been proposed as one possible origin of liver CSC (Nio, Yamashita and Kaneko, 2017). Data indicate that LPC can generate lesions from regenerating nodules giving rise to aggressive HCC. The expression of Sox9, a marker of LPC, correlates with degrees of liver injury and fibrosis, and Sox9-positive cells have been reported to expand in early stages of human hepatocarcinogenesis (Tummala *et al.*, 2017).

These cellular processes are the site of complex immunological activity mediated by different kinds of immune cells. Several cytokines produced by innate and adaptive immune cells regulate the activation of hepatocytes and the LPC compartment.

3. Role of the immune response in regenerating livers

The liver is known to be an organ with essential immunological functions and has been proposed as an immunological organ (Racanelli and Rehermann, 2006). Although the primary role of the liver is not thought to be related to immunity, the liver also performs major immunological tasks as the host of a wide variety of immune cells from the innate and adaptive immunity including macrophages, natural killer, natural killer T, and $\gamma\delta$ T cells (Gao, Jeong and Tian, 2008; Robinson, Harmon and O'Farrelly, 2016).

Among those immune cells, hepatic macrophages, also known as Kupffer cells, account for about 30% of total non-parenchymal cells in the liver (Nguyen-Lefebvre and Horuzsko, 2015) and are known as the largest population of resident macrophages as they represent 80% of all macrophages in the body (Merlin *et al.*, 2016). At steady state, they perform essential tasks for the liver and the entire organism including the control of LPS and endotoxins coming from the intestinal tract through the portal vein, the phagocytosis of cellular debris and the overall homeostasis of the liver.

3.1. Natural killer cells

Natural killer cells represent the major sinusoidal lymphocyte population in the liver (Mikulak *et al.*, 2019). NK cells are capable of recognizing abnormal cells, infected by viruses, transformed into tumor cells or cells in a state of stress, without excessively responding to the permanent flow of gut-derived antigens (Zheng, Sun and Tian, 2018). There are mainly two types of NK in the liver, conventional NK cells derived from the bone marrow and liver resident NK cells derived from liver hematopoietic progenitor cells.

Recently, a classification of hepatic NK cells has been proposed on the basis of CD56 (NCAM-1) expression, discriminating between CD56^{bright} and CD56^{dim} NK cell subsets (Scoville, Freud and Caligiuri, 2017). CD56^{bright} NK cells referred to as liver-resident NK cells are characterized by the expression of transcription factors Eomes and Hobit (Peng and Tian, 2017). They produce low amounts of intracellular cytotoxic granules (such as perforin and granzymes A-B) and are also not capable of antibody-dependent cellular cytotoxicity in line with

the absence of CD16 expression. However, they exert important regulatory functions through secretion of chemokines and pro-inflammatory cytokines such as IFN- γ , TNF- α in response to different stimuli including IL-1 β , IL-2, IL-12, IL-15, and IL-18 delivered by surrounding immune cells like macrophages, DC, and T lymphocytes. NK's main mechanisms of action are finely regulated by a dynamic balance between activation and inhibitory receptors, respectively aNKR and iNKR. The latter receptors bind to major histocompatibility complex class I (MHC-I) on autologous cells that ensure tolerance towards own cells (Abel *et al.*, 2018).

In a context of liver regeneration after PHx, NK cells have been shown to promote liver regeneration and hepatocellular expansion (Hosoya *et al.*, 2012). Following PHx, ATP is released rapidly in the liver (Gonzales *et al.*, 2010). The extracellular ATP has been shown to inhibit NK cells' cytotoxic capacities through P2 receptors to prevent tissue damage (Graubardt *et al.*, 2013). Clearance of extracellular ATP stimulates NK cells' cytotoxic capacities which in turn enhances liver regeneration and tissue repair. Contrastingly with these beneficial properties in regenerating livers following PHx, NK cells have been associated with a less efficient hepatic regeneration in models of infectious-type stimuli. Indeed, in a context of infection by the murine cytomegalovirus, depletion of NK cells has been associated with enhanced regenerative capacities due to the reduction of IFN- γ production known to induce hepatocyte death and inhibit their proliferation (Li and Hua, 2017). Similarly, in an HBV transgenic model, HBV has been shown to trigger NKT cell accumulation associated with increased production of IFN- γ and impairment of liver generation. The impairment of liver regeneration was ameliorated in NKT cell depleted mice which also displayed reduced IFN- γ levels (Dong *et al.*, 2007).

NK cells are also important actors in the crosstalk between the immune system and liver stem cells. Their local secretion of cytokines stimulates oval cell expansion and has been proven to promote tissue regeneration following acute liver damage. Indeed, mice lacking NK cells and fed a CDE diet to trigger LPC expansion, display reduced ductular reaction (Strick-Marchand *et al.*, 2008).

3.2. B and T lymphocytes

The concept of "heptoimmunology" was first proposed in 2002 by Mackay to acknowledge the liver as a lymphoid organ (Mackay, 2002). In the context of liver regeneration after PHx,

lymphocytes have been described as key players in stimulating hepatic cell proliferation and promoting regeneration (Li and Hua, 2017). Indeed, following PHx, TNF is rapidly produced and TNFR1 signaling is essential for a proper induction of liver regeneration. RAG1^{-/-} mice show increased mortality and extensive hepatic injury, indicating that adaptive immune cells are critical in regulating liver regeneration (Markose *et al.*, 2018). Indeed, lymphotoxin expression by T cells promotes liver regeneration through direct hepatocyte contact and via the IL-6 pathway (Tumanov *et al.*, 2009).

PHx characterized is characterized by tolerogenic immune cell activation and is also followed by an increase in anti-inflammatory cytokines production such as IL-10 that controls hepatocyte proliferation (Yin *et al.*, 2011) and limits inflammation in the liver.

Interestingly, CD4 T lymphocytes colocalize with LPC in CDE fed mice. Consistently, T cell deficient animals exhibited lower LPC numbers. The oval cell response in T cell-deficient mice under CDE diet is associated with an activation and increased number of NK cells, showing that T lymphocytes have a positive impact on liver regeneration in a non-infectious context, by stimulating LPC expansion through their local cytokine production, namely IFN- γ and TNF- α (Strick-Marchand *et al.*, 2008).

3.3. Granulocytes

At steady state there are relatively low numbers of neutrophils in the liver (Williams *et al.*, 2010). After PHx, neutrophils numbers increase. They have been shown to be required for a proper liver regeneration after PHx as ICAM-1^{-/-} (a chemokine required for neutrophil infiltration) display a delayed liver regeneration (Selzner *et al.*, 2003). In addition, mice injected with APAP display a substantial infiltration of neutrophils in the liver. Interestingly, genetic depletion of neutrophils or administration of specific anti-Ly6G antibodies both resulted in exacerbated liver injury and impaired liver regeneration (Yang *et al.*, 2019).

Significant infiltration of eosinophil has also been reported in patients with APAP overdose (Markose *et al.*, 2018). Although very low inflammation is observed following PHx, some cytokines necessary to trigger liver regeneration and described as pro-inflammatory are upregulated like IL-4 which is secreted by eosinophils and has been shown to be important for hepatocyte proliferation as mice lacking eosinophils display reduced hepatocyte proliferative capabilities (Goh *et al.*, 2013).

3.4. Dendritic cells

Dendritic cells (DC) are professional antigen presenting cells. They represent approximately 1% of total non-parenchymal cells in the liver. They are mostly located in the periportal areas (Freitas-Lopes *et al.*, 2017). In the liver, DC can be classified into two subsets, classical DCs (cDCs) and plasmacytoid DCs (pDCs). The latter is characterized by reduced expression of MHCII which explain their limited ability to process antigens, whereas cDCs express higher levels of MHCII and are very professional antigen-presenting cells (Li and Hua, 2017). Dendritic cells, alongside KC, are known to play an important role in maintaining a tolerogenic environment in the liver (Elchaninov *et al.*, 2018). In a context of liver regeneration, DC have been reported to expand within 6 hours following PHx and return to pre-PHx levels by 24 hours. Interestingly this expansion seems to be specific to liver dendritic cells since no difference in DC number has been observed in the spleen following PHx (Castellaneta *et al.*, 2006). Estrogen is upregulated after PHx and is associated with an upregulation of estrogen receptor on dendritic cells and contribute to their tolerogenicity and expansion (Castellaneta *et al.*, 2006). Interestingly, administration of Flt3L which increases liver DC numbers accelerated liver regeneration.

3.5. Hepatic macrophages

Macrophages represent the largest immune cell population in the liver. Within the liver, KC are located along the sinusoids tightly attached to endothelial cells. Thanks to this strategic location, they represent the first cell population meeting gut-derived substances brought through the portal vein. Every 10 hepatocytes is accompanied by about 3 macrophages (Lopez *et al.*, 2011). Therefore, it has long been assumed that macrophages play a crucial role in liver functions and whole-body homeostasis. Indeed, in response to the microenvironment, KC can produce a wide variety of cytokines and polarize into two main phenotypes: M1 pro-inflammatory macrophages characterized by a great ability to present antigens, significant production of IL-12, IL-23 cytokines and nitric oxide, and M2 anti-inflammatory macrophages characterized by high production of IL-10 and low production of IL-12, IL-6 and TNF- α .

Liver macrophage populations. Macrophages were initially described as phagocytic cells capable of recognizing, engulfing and degrading pathogens and cellular debris. Since then, distinct resident macrophage populations have been described in many tissues of the body including the liver, in addition to bone marrow-derived circulating monocytes. Alongside resident KC which originate from yolk sac-derived CSF1R⁺ erythromyeloid progenitors, bone-marrow derived monocytes circulate through the hepatic vascular network at steady state as patrolling cells and infiltrate the liver tissue upon injury (Krenkel and Tacke, 2017; Cai, Zhang and Li, 2019; Wen *et al.*, 2021). Recently, several markers have been identified to discriminate between KC and infiltrating macrophages. The ionized calcium-binding adapter molecule 1 (IBA1) has been described to be a common marker of both monocytes and KC as well as monocyte and macrophage populations found in other organs of the body such as microglia (Guillot, Buch and Jourdan, 2020). However, C-type lectin domain family 4 member F (CLEC4F) has been identified as the most specific KC marker to date as it is not expressed by monocytes. KC are commonly described as CD45⁺F4/80⁺CD11b^{intermediate}CLEC4F⁺ cells (Hsieh and Yang, 2009; Yang *et al.*, 2013).

Contrastingly, CX3CR1, the G-protein coupled fractalkine receptor, is known to be expressed by monocytes and capsular macrophages and absent from KC (Yona *et al.*, 2013).

Recently, single-cell RNA-sequencing brought new insights to complex heterogeneity of macrophages that reside in the liver. Liver resident KC are composed of two populations: CD68⁺MARCO⁺ KC characterized by a profile of genes contributing to the maintenance of immune tolerance and regulation of inflammation while CD68⁺MARCO⁻ KC display similar transcriptional profile as recruited pro-inflammatory macrophages. Interestingly, both populations seem to trigger weaker pro-inflammatory responses than CD14⁺ circulating monocytes (Zhao *et al.*, 2020).

The identification of these markers has led to a better characterization of hepatic macrophage populations and emerging evidence suggests that while at steady state most macrophages present in the liver are identified as KC, following tissue damage and inflammation, which causes loss of KC, circulating monocytes infiltrate the hepatic parenchyma. For example, a loss and decrease of liver KC has been reported in several contexts fulminant hepatitis including infection with murine cytomegalovirus (Borst *et al.*, 2018), or the bacterium *Listeria monocytogenes* (Blériot *et al.*, 2015), and in models of methionine/choline-deficient (MCD) diet-induced nonalcoholic steatohepatitis (NASH) (Devisscher *et al.*, 2017) and hepatocellular carcinoma (HCC) (Lefere *et al.*, 2019). Several studies suggest that such KC loss is partially

replaced by circulating monocytes (Nishiyama *et al.*, 2015; Reid *et al.*, 2016; Tran *et al.*, 2020). However, whether local KC proliferation or circulating monocytes restore liver macrophages after partial hepatectomy (PHx) remains unclear (**Figure 6**).

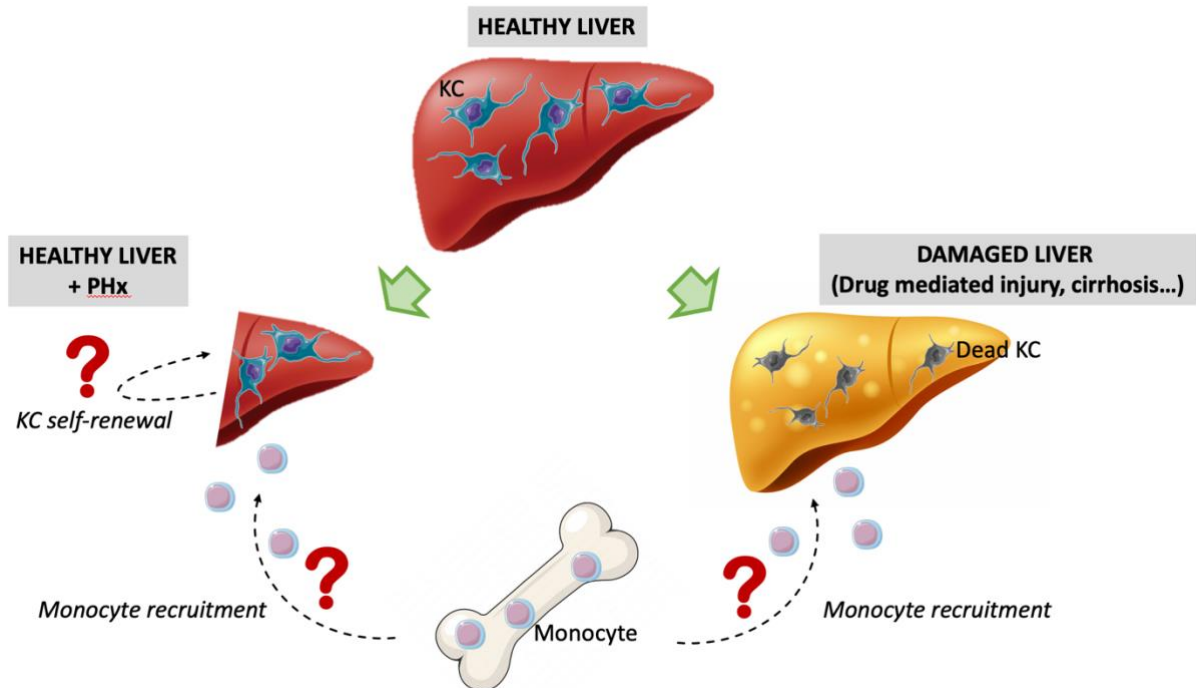


Figure 6: Potential sources of macrophages in different contexts of liver regeneration. In the healthy liver at steady state, hepatic macrophages mostly comprise KC. Following a stress either mechanic or induced by a hepatotoxic compound, the liver undergoes a process of regeneration and tissue repair to recover lost tissue mass. Although the underlying mechanisms driving hepatocytes and LPC have been well described using different models of liver regeneration, the origins of repopulating macrophages remain to be elucidated.

Role of KC in regenerating livers from hepatocytes. Although their origin during hepatic regeneration remains to be elucidated, KC are known to be a major source of cytokines in the liver. Therefore, they are key players in regulating liver homeostasis and immune responses. Impaired liver regeneration when KC are depleted. Indeed, pretreatment of mice with either liposomal clodronate or gadolinium chloride to deplete or inhibit macrophages respectively, resulted in impaired liver regeneration following PHx. Indeed, it has been reported in the murine models of bile-duct ligation (BDL) and alcohol-induced liver injury that KC depletion by liposome-entrapped clodronate leads to an impairment of DNA synthesis in the proliferating hepatocytes (Osawa *et al.*, 2010; Owumi *et al.*, 2014). In addition, both TNF- α and IL-6 are crucial to trigger hepatocyte proliferation (Schmidt-Arras and Rose-John, 2016) and KC-depleted mice display lower levels those cytokines. Transfer of wild-type bone-marrow to IL-6-deficient mice restores hepatocyte proliferation following PHx (Wen *et al.*, 2021).

Additionally, the absence of KC was associated with decreased NF- κ B activation, which in turn resulted in retarded liver regeneration (Abshagen *et al.*, 2007). Of note, specific inhibition of NF- κ B in hepatocytes in a transgenic mouse model did not affect DNA synthesis (Chaisson *et al.*, 2002), indicating that KC-derived NF- κ B has a greater impact on liver than hepatocellular NF- κ B activation.

Role of KC in regenerating livers from LPC. In toxic injuries, liver regeneration is a dose dependent process, increasing with the extent of hepatic injury until a certain threshold where hepatic injury leads to acute liver failure (Bhushan *et al.*, 2014). Indeed, upon liver injury, necrotic hepatocytes are phagocytized by macrophages that stimulate liver regeneration through Wnt signaling in nearby LPC (Boulter *et al.*, 2012). In a context of liver injury induced by the CDE diet, Kupffer cells have been shown to be key actors in LPC expansion. Indeed, KC depletion reduced LPC proliferation and an adoptive transfer of monocytes led to a restoration of LPC expansion in KC depleted mice (Elsegood *et al.*, 2015). Interestingly, macrophage therapy using bone-marrow transplant is associated with upregulated MMP-9 and MMP-13 along with increased number of LPC and liver regeneration (Thomas *et al.*, 2011). Acute liver failure (studied through the APAP model) is characterized by heavy hepatocyte necrosis: dying hepatocytes trigger inflammation by releasing “DAMP” signals (high-mobility group box 1 protein and heat shock protein-70) which will be recognized by TLR on non-parenchymal cells (Guicciardi *et al.*, 2018). In chronically injured livers following a CDE diet, invading macrophages have been associated with LPC expansion through the persistent secretion of TNF- α . In such contexts, following hepatocytes deaths, KC are essential for the engulfment and removal of debris. They start producing (TNF)-like weak inducer of apoptosis (TWEAK) which binds to its receptor FGF-inducible 14 (Fn14), expressed on LPC leading to their activation and expansion (So *et al.*, 2020). Recently, WSX-1 deficiency, the IL-27 receptor, has been associated with a reduction of macrophages and less LPC leading to a less efficient LPC-driven regeneration (Guillot *et al.*, 2018).

Although the importance of KC is widely known in liver regeneration, their origin and the underlying mechanisms involved in their proliferation during liver regeneration remain unclear. Additionally, their role on alternative pathways of regeneration from LPC and the underlying mechanisms of the cytokines they produce are yet to be elucidated.

4. PhD Publications

4.1. PUBLICATION 1: Kupffer cell restoration after partial hepatectomy is driven by their local cell proliferation in autocrine and paracrine IL-6-dependent manners

In this first publication, we brought new insights shedding lights on the origin of hepatic macrophages during liver regeneration after PHx and uncovered the underlying mechanisms driving their restoration. By using 10 different strains of genetically modified mice and performing immunohistochemistry analyses, we proposed to address the question whether, in regenerating livers post partial hepatectomy (PHx), liver macrophage restoration results from circulating monocyte infiltration or local KC proliferation, and to uncover the involved underlying mechanisms. By performing immunohistochemistry analyses, we demonstrated that local KC proliferation and not circulating monocytes, restored liver macrophages after PHx. This KC proliferation was impaired in *Il6* KO mice, which was restored after administration of IL-6 protein, whereas KC proliferation was not affected in *Il4* KO and *Csf2* KO mice. The source of IL-6 was identified using hepatocyte- and myeloid-specific *Il6* knockout mice, which revealed both hepatocytes and myeloid cells contribute to IL-6 production after PHx. Moreover, KC proliferation was also impaired in myeloid-specific *Il6* receptor knockout mice after PHx, suggesting that IL-6 signaling directly promotes KC proliferation. Studies using several inhibitors that blocked IL-6 signaling pathways revealed that sirtuin 1 (SIRT1) contributed to IL-6-mediated KC proliferation *in vitro*. Genetic deletion of the *Sirt1* gene in myeloid cells including KC impaired KC proliferation after PHx. In conclusion, our data suggested that KC repopulation after PHx is driven by local KC proliferation independently of circulating monocytes, which was dependent on IL-6 and SIRT1 activation in KC (**Figure 7**). Although macrophages clearly play a role in sustaining and orchestrating hepatocyte-mediated regeneration in a context characterized with very low and controlled inflammation and no associated fibrosis or tissue injury, little is known about the involvement of macrophages in alternative pathways of hepatic regeneration mediated by LPC often associated with an inflammatory environment.

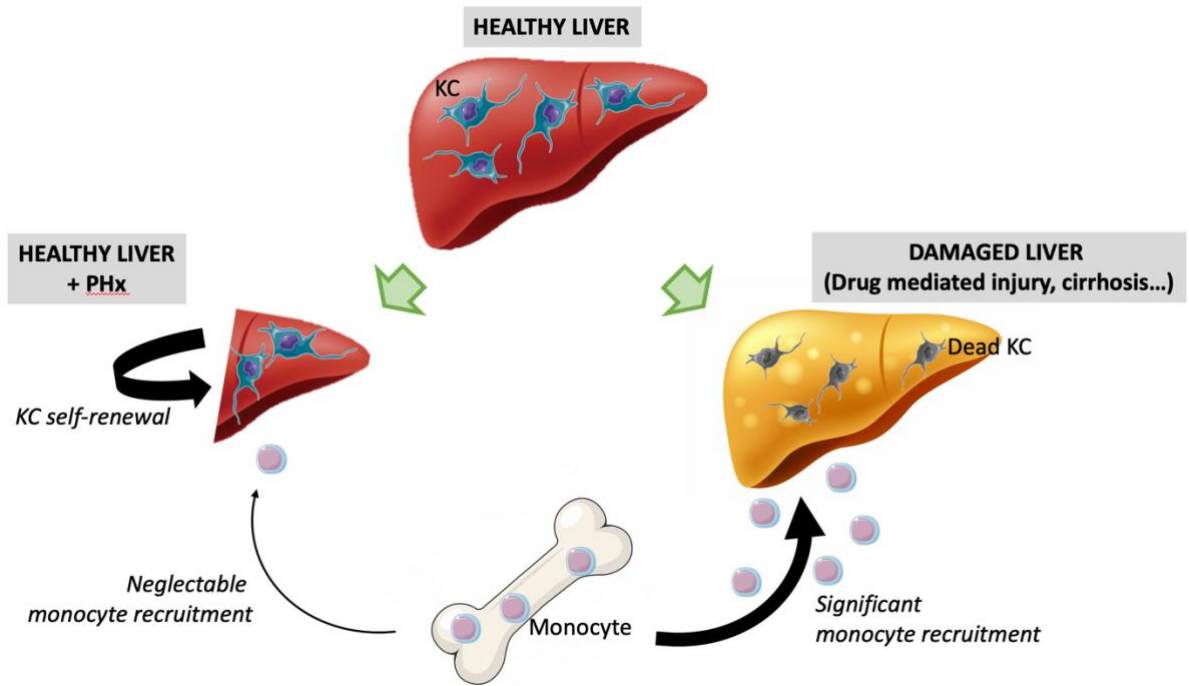


Figure 7: Dynamic of hepatic macrophage populations during liver regeneration. *Repopulation of hepatic KC is mainly driven by local KC proliferation in a PHx context where remaining KC are healthy. Contrastingly, following liver damage resulting in KC death, circulating monocytes infiltrate the liver to repopulate lost macrophages.*

4.2. PUBLICATION 2: Interleukins-17 and 27 promote liver regeneration by sequentially inducing progenitor cell expansion and differentiation

LPC accumulation is associated with inflammation and implicated in the pathogenesis of chronic liver diseases. However, how inflammation regulates LPC/DR remains largely unknown. Identification of inflammatory processes that involve LPC activation and expansion represent a key step in understanding the pathogenesis of liver diseases. In the current study, we found that diverse types of chronic liver diseases are associated with elevation of infiltrated IL-17⁺ cells and cytokeratin 19 (CK19)⁺ LPC, and both cell types colocalized and their numbers positively correlated with each other. The role of IL-17 in the induction of LPC was examined in a mouse model fed a choline-deficient and ethionine-supplemented (CDE) diet. Feeding of wild-type mice with the CDE diet markedly elevated CK19⁺Ki67⁺proliferating LPC and hepatic inflammation. Disruption of the IL-17 gene or IL-27 receptor, alpha subunit (WSX-1) gene abolished CDE diet-induced LPC expansion and inflammation. *In vitro* treatment with IL-17 promoted proliferation of bipotential murine oval liver cells (a liver progenitor cell line) and markedly up-regulated IL-27 expression in macrophages. Treatment with IL-27 favored the differentiation of bipotential murine oval liver cells and freshly isolated LPC into hepatocytes. This study provided evidence for a collaborative role between IL-17 and IL-27 in promoting LPC expansion and differentiation, respectively, thereby contributing to liver regeneration (**Figure 8**).

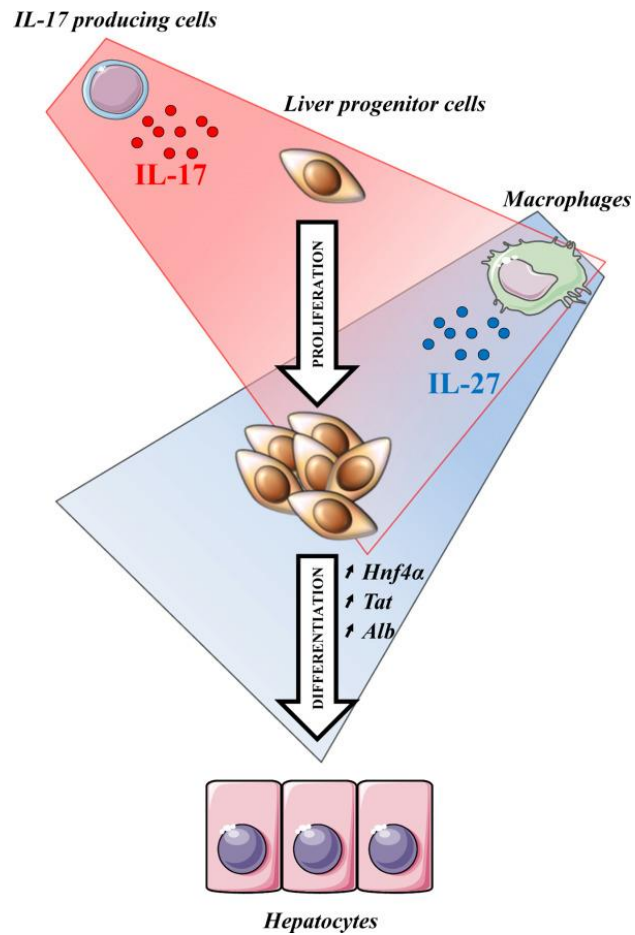


Figure 8: IL-17 induces liver progenitor cell proliferation while IL-27 favors their differentiation toward a hepatocytic phenotype. Taken together, these data provide evidence of a collaborative role of IL-17 and IL-27 in promoting liver regeneration. IL-17 directly acts on LPCs to favor their proliferation. IL-17 also induces macrophage IL-27 production, which enhances LPC differentiation toward hepatocytes (Guillot et al., 2018)

4.3. PUBLICATION 3: Bile acid-activated macrophages promote biliary epithelial cell proliferation through integrin $\alpha\text{v}\beta\text{6}$ upregulation following liver injury

Cholangiopathies caused by biliary epithelial cell (BEC) injury represent a leading cause of liver failure. No effective pharmacologic therapies exist, and the underlying mechanisms remain obscure. We aimed to explore the mechanisms of bile duct repair after targeted BEC injury. Injection of intermedilysin into BEC-specific human CD59 (hCD59) transgenic mice induced acute and specific BEC death, representing a model to study the early signals that drive bile duct repair. Acute BEC injury induced cholestasis followed by CCR2⁺ monocyte recruitment and BEC proliferation. By using microdissection and next generation RNA sequencing, we identified five genes that were most upregulated in proliferating BECs after acute injury including *Mapk8ip2*, *Cdkn1a*, *Itgb6*, *Rgs4*, and *Ccl2*. Immunohistochemistry analyses confirmed robust upregulation of integrin $\alpha\text{v}\beta\text{6}$ (ITG β6) expression in this BEC injury model, after BDL, and in patients with chronic cholangiopathies. Deletion of *Itgb6* gene attenuated BEC proliferation post-acute bile duct injury. Macrophage depletion or *Ccr2*-deficiency impaired ITG β6 expression and BEC proliferation. *In vitro* experiments revealed that bile-acid activated monocytes promoted BEC proliferation through ITG β6 . Our data suggest that BEC injury induces cholestasis, monocyte recruitment, and induction of ITG β6 , which work together to promote BEC proliferation, and that therefore represent potential therapeutic targets for cholangiopathies (**Figure 9**).

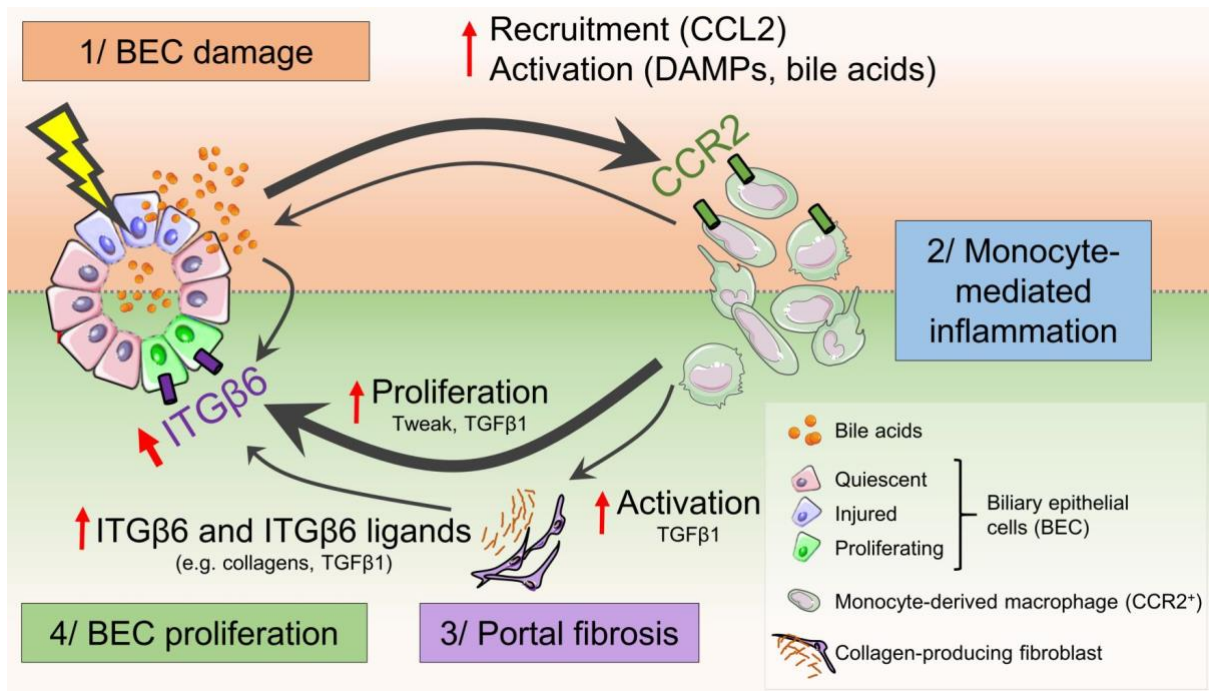


Figure 9: Monocyte-driven BEC proliferation in a context of biliary injury. *BEC injury induces cholestasis, monocyte recruitment, and induction of ITGβ6, which work together to promote BEC proliferation and therefore represent potential therapeutic targets for cholangiopathies (Guillot et al., 2021)*

5. Discussion

Collectively, this PhD work aimed at investigating macrophages' contribution to liver regeneration and unveiling the underlying mechanisms of their repopulation in regenerating livers to restore their initial pool. In fact, liver macrophages represent one of the largest macrophage population in the body and an important source of cytokines in the liver. However, their number is significantly reduced after liver resection or liver transplantation. Therefore, it is vital to restore their initial pool to maintain proper liver functions and overall homeostasis. Our first study aimed at elucidating the origin of proliferating macrophages during liver regeneration after PHx.

Origin of proliferating macrophages following PHx. Indeed, we first showed that liver KC restoration after PHx is predominantly driven by local KC proliferation with minor contribution from circulating macrophages. Our immunofluorescence analysis has shown that macrophage proliferation peaked at 48h post-PHx, a few hours after that of hepatocytes occurring at 40h. However, whether new macrophages are derived from circulating monocytes or resident KC after PHx was not clear. In fact, the origin of repopulating hepatic macrophages has remained controversial as recent studies have provided conflicting data about the capacity of monocytes and KC to give rise to a fully regenerated pool of liver macrophages during liver injury (Krenkel and Tacke, 2017; Wen *et al.*, 2021). These conflicting findings might result from the different models used to investigate the origin of hepatic macrophages. In a study where KC were completely depleted in a healthy liver without PHx, KC restoration was achieved from bone-marrow derived monocyte recruitment and differentiation into the liver (Scott *et al.*, 2016). In another study where all immune cells including KC in mice were depleted before PHx by non-lethal 5 Gy irradiation, the authors suggest that monocytes were recruited into partially hepatectomized livers and play a pivotal role in accelerating liver regeneration (Nishiyama *et al.*, 2015). However, under conditions where residual KC are preserved in the remaining part of the liver after PHx, we provided several lines of evidence suggesting that circulating monocytes are minor components contributing to restore the initial pool of KC. First, using mice expressing GFP under the control of CX3CR1 promotor (a gene expressed on monocytes and absent from KC) we observed that few CX3CR1 labelled monocytes were recruited into regenerating livers after PHx. Second, *Ccr2* deficiency in mice, which is a key chemokine receptor for monocyte recruitment, had normal KC repopulation after PHx. Third,

we assessed the phenotype of proliferating macrophages in our PHx model, focusing on IBA1 a pan-macrophage marker and CLEC4F a C-type lectin expressed on KC but not on monocytes. Most macrophages found in the liver 48h post-PHx, at the peak of liver macrophage proliferation, were IBA⁺CLEC4F⁺ KC, and few IBA⁺CLEC4F⁻ infiltrating monocytes were detected in regenerating liver after PHx. Lastly, CLEC4F⁺ KC were capable of self-proliferation following PHx.

Role of IL-6 in KC proliferation after PHx. Once the origin of the macrophages was elucidated, we further investigated the underlying cytokines involved in their proliferation. Although PHx is not characterized by a strong inflammatory response, several cytokines that are involved in macrophage proliferation such as IL-6, IL-4 and CSF-2 are elevated post PHx (Vassiliou *et al.*, 2010; Markose *et al.*, 2018). In the current study, we demonstrated that after PHx, KC proliferation was impaired in *Il6* KO mice but not in *Il4* KO and *Csf2* KO mice. Administration of rIL-6 injection partially increased hepatocyte proliferation and interestingly, fully restored KC proliferation in *Il6* KO mice after PHx. Collectively, our data suggested that IL-6 but not IL-4 nor CSF-2 plays a critical role in promoting KC proliferation after PHx. Although the elevation of IL-6 after PHx has been well documented, the source of this cytokine during liver regeneration remains obscure. Previous studies suggest that PHx induces an increase of gut derived LPS in the blood (Liu *et al.*, 2015), which likely contributes to IL-6 elevation after PHx because LPS is well known to stimulate macrophages to produce IL-6. In addition, one study suggests that LPS can also stimulate hepatocytes to produce IL-6 (Norris *et al.*, 2014). However, the exact sources of IL-6 after PHx remain unclear. In the current study, we demonstrated that serum levels of IL-6 were reduced by approximately 50% in myeloid- and hepatocyte-specific *Il6* KO mice, respectively, compared to WT mice after PHx. Thus, our data suggest that after PHx not only hepatocytes represent a significant source of IL-6 as a paracrine manner to promote KC proliferation, but KC could also be considered as an important autocrine source of IL-6.

IL-6-mediated KC proliferation after PHx through SIRT1. Whatever the potential source of IL-6 production, its deficiency significantly reduced KC proliferation after PHx as demonstrated in the current study, suggesting that IL-6 is essential for KC repopulation after PHx. Our further studies demonstrated that IL-6 signaling directly contributes to KC proliferation because when IL-6 signaling pathway is abrogated only in myeloid cells, including KC, in *Il6^{r^{Myc}}* KO mice, KC proliferation is partially impaired. Additional flow

cytometry experiments could be performed to confirm the role of IL-6 on KC proliferation that we show here; we have several lines of evidence that strongly support a stimulatory effect of IL-6 on KC proliferation, such as IL-6 stimulation of KC proliferation *in vitro* and *in vivo*, suppressed KC proliferation in IL6 KO, hepatocyte- or myeloid-specific Il-6 KO mice, myeloid-specific Il-6R KO.

To explore the molecular mechanisms by which IL-6 stimulates KC proliferation, we used several inhibitors to block IL-6 downstream signaling pathways. Interestingly, among these inhibitors, the SIRT1 inhibitor showed the strongest inhibition to block IL-6 stimulation of KC proliferation *in vitro*. Furthermore, we demonstrated that genetic deletion of *Sirt1* in myeloid cells including KC markedly reduced KC proliferation *in vivo* after PHx, and impaired liver regeneration, as shown by the reduction of liver weight to body weight ratio and hepatocyte proliferation in *Sirt1* deficient mice. In addition, IL-6 treatment directly increased SIRT1 activity in macrophages, suggesting that SIRT1 contributes to IL-6 promotion of KC proliferation during liver regeneration after PHx. A recent study also reported that SIRT1 plays a role in stimulating macrophage proliferation as demonstrated by the findings that SIRT1 overexpression via transfection of *Sirt1* into bone-marrow derived macrophages was associated with an increased macrophage proliferation *in vitro*; whereas SIRT1 blockade by CRISPR/Cas9 gene editing or by nicotinamide injection in mice impaired respectively alveolar and peritoneal macrophage self-renewal capacities (Imperatore *et al.*, 2017). Interestingly, previous studies have reported in the PHx model that age-related SIRT1 reduction and SIRT1 inhibition by short-interfering RNA (siRNA) were associated with a less efficient liver regeneration (hepatocyte proliferation) after PHx (Jin *et al.*, 2011). Collectively, SIRT1 not only promotes KC renewal but also stimulates hepatocyte proliferation after PHx. In addition to promoting macrophage proliferation, IL-6 signaling also plays an important role in enhancing macrophage survival (Hunter and Jones, 2015). However, in the current study, no enhanced KC apoptosis was observed in myeloid cell-specific *Il6r* knockout mice compared to WT mice, suggesting that IL-6 is not required for KC survival after PHx or, alternatively, that IL-6 trans-signaling might be contributing. Interestingly, our recent studies demonstrated that IL-6 signaling is required for infiltrating macrophage survival but not KC survival in the liver of high-fat diet-fed mice (Hou *et al.*, 2020). Taken together, IL-6 is required for KC proliferation but not for KC survival after PHx, which is probably because long-lived KC do not need IL-6 signaling for survival.

In conclusion, our findings brought new insight on the origin of KC in regenerating liver after PHx, showing local proliferation of remaining KC independently of circulating monocytes. In

this process, KC proliferation is partly controlled by IL-6 produced by both hepatocytes and KC, in regenerating livers, and IL-6 stimulates KC proliferation by increasing SIRT1 activity. Additional studies regarding the interaction of IL-6 and other cytokines and growth factors such as HGF which is known to be involved in hepatocyte proliferation after PHx could be interesting insights to KC proliferation.

Upon chronic or severe injury, liver progenitor cells or activated cholangiocytes proliferate and accumulate in the liver. This phenomenon, known as the ductular reaction, coincides with intense and localized inflammation and fibrogenesis as part of the tissue response to chronic or severe injury, in an attempt to repair or regenerate the bile ducts and liver architecture. Repair mechanism dysregulation and exacerbation may lead to chronic inflammation, fibrosis, and cirrhosis and may ultimately serve as a soil for liver cancer and organ failure. Although the ductular reaction is widespread in virtually any chronic liver disease, and BECs represent a crucial cell type implicated in liver function and architecture, there is a paucity of data on their regeneration and interaction with other cell populations in liver disease, given the lack of targeted BEC injury models.

Recruitment of monocytes to the injured area upon acute BEC injury. Inflammatory monocytes are among the first responders after injury, clearing pathogens and cell debris and initiating tissue regeneration. A recent study reported that macrophages play a crucial role in inducing the ductular reaction, portal area fibrosis, and monocyte-driven inflammation in a chronic (*Mdr2*^{-/-} mice) mouse model of sclerosing cholangitis (Guicciardi *et al.*, 2018). An interesting finding in the current study was that monocytes were rapidly recruited in response to sudden BEC death, as early as 3 hours after injury, and this recruitment may have been induced by a number of factors, including the release of damage-associated molecular patterns (DAMPs) and/or the production of chemokines (e.g., CCL2) by surrounding cells including BECs and Kupffer cells (Tacke, 2017). Notably, we observed that recruited monocytes expressed CCR2 (CCL2 receptor) and the chemokine receptor CX3CR1. However, an additional deletion of either *Ccr2* or *Cx3cr1* did not dramatically affect monocyte recruitment in ILY-treated *ihCD59*^{BEC-TG} mice (data not shown), suggesting that monocyte recruitment after acute BEC injury may be dependent on additional factors. Another possibility that we have not excluded is that because of the redundancy of both receptors, deletion of 1 of them was insufficient to affect monocyte recruitment. Despite this, *Ccr2*-deficient mice displayed

reduced BEC proliferation, suggesting that CCL2 signaling polarized recruited monocytes toward a regenerative phenotype.

Another important finding from the current study was that the recruited monocytes after BEC injury were intimately interacting with collagen-producing cells in ILY-treated ihCD59^{BEC-TG} mice *in vivo*. First, liver macrophages isolated from ihCD59^{BEC-TG} mice during BEC regeneration tended to have increased *Tgfb1* gene expression. Second, by performing immunohistochemical analyses in 2 strains of ihCD59^{BEC-TG}Cx3cr1^{GFP} and ihCD59^{BEC-TG}Coll1^{GFP} double-mutant mice, we demonstrated that IBA⁺ macrophages near damaged bile ducts were in close contact with α -SMA⁺ and collagen-expressing fibroblasts. Macrophages and fibrogenic cells were so intimately colocalized that confocal microscopy led to a partial staining overlap, raising doubts about the possibility that some cells may coexpress IBA1 and α -SMA or GFP (collagen I). Intriguingly, flow cytometric analyses revealed that numerous collagen-producing cells expressed macrophage markers such as CD45, CD11b, and F4/80 in ILY-treated ihCD59^{BEC-TG} Coll1^{GFP} double-mutant mice.

Monocyte-derived CCR2⁺ macrophages enhance BEC repair through ITG β 6: a potential role of bile acid. In the current study, we demonstrated that macrophage depletion or *Ccr2* deficiency reduced BEC proliferation in ihCD59^{BEC-TG} mice, indicating that the recruited monocyte-derived CCR2⁺ macrophages promote bile duct repair. Macrophages are known partners of tissue regeneration through their extensive production of mitogens. Indeed, our data showed that liver macrophages isolated at the peak of BEC proliferation overexpressed *Tweak*, a known mitogen for BEC and liver progenitor cells (Jakubowski *et al.*, 2005; Tirnitz-Parker *et al.*, 2010; Karaca *et al.*, 2014). Although fibrogenesis may lead to fibrosis, it provides crucial signals for bile ducts to regenerate and should thus be regarded as a part of normal bile duct regeneration, if it does not become excessive. This could partly explain why our data indicated that macrophage depletion, which reduced both inflammation and fibrogenesis, also impaired BEC proliferation, although the initial cell injury was identical. Furthermore, by performing next-generation transcriptome sequencing specifically on regenerating BECs and identified 5 genes, namely *Mapk8ip2*, *Cdkn1a*, *Itgb6*, *Rgs4*, and *Ccl2*, that were most upregulated in proliferating BECs after acute injury. Given the small proportion of BECs in the liver, these important gene expression changes would not have been detectable using whole-tissue transcriptomics. Among these, ITG β 6 has been implicated in promoting BEC- and liver progenitor-mediated liver regeneration (Patsenker *et al.*, 2008; Peng *et al.*, 2016). Furthermore, it was previously proposed in a chronic mouse model of congenital hepatic

fibrosis that macrophages are implicated in ITG β 6 induction in chronically injured BEC (Locatelli *et al.*, 2016). Macrophage depletion or CCR2 deficiency impaired ITG β 6 expression and BEC regeneration. In addition, incubation with an ITG β 6-blocking antibody reduced the BEC proliferation in vitro that was induced by conditioned media from TLCA-treated macrophages. Together, these in vivo and in vitro findings highlight an important role of macrophages in promoting BEC regeneration through ITG β 6. In addition, in our model, hepatic expression of fibronectin 1, a potent ITG β 6 agonist (Patsenker *et al.*, 2008) that is mainly produced by hepatocytes and activated macrophages, was upregulated after acute BEC injury. Thus, it is likely that activated macrophages promote BEC regeneration by expressing fibronectin, which interacts with ITG β 6 on BEC.

A hallmark of bile duct injury is cholestasis, which leads to accumulation of bile acids. In the current study, we demonstrated that TLCA treatment directly upregulated ITG β 6 expression on BECs without affecting BEC proliferation, whereas conditioned media from TLCA-treated macrophages enhanced BEC proliferation in an ITG β 6-dependent manner. These data suggest that bile acids can direct monocytes toward a regenerative phenotype, which stimulates BEC proliferation via ITG β 6. However, how bile acid-activated macrophages promote BEC proliferation via ITG β 6 remains unclear.

Upon severe or chronic liver injury, hepatocyte and BEC-driven regeneration is often compromised. In these cases, an alternative regenerative process involving the LPC compartment is engaged (Williams, Clouston and Forbes, 2014). The induction and progression of this LPC-driven regenerative pathway is highly influenced by the microenvironment and the cytokines released by immune cells during inflammation (Knight *et al.*, 2005; Gadd *et al.*, 2014). In this inflammatory environment, Th17 lymphocytes have been implicated in several types of liver diseases through the effects of IL-17 (Lafdil *et al.*, 2010). Findings from our lab reported direct and indirect profibrogenic and proinflammatory effects of IL-17 by stimulating both myofibroblasts and macrophages (Guillot *et al.*, 2014). It has been further shown that IL-17-producing $\gamma\delta$ T lymphocytes were recruited during hepatocyte-driven liver regeneration induced by PHx (Rao *et al.*, 2014).

Interestingly, macrophages have been identified as key players modulating liver inflammation by producing IL-27, a cytokine shown to directly favor stem/progenitor cell differentiation in different organs (Tanaka *et al.*, 2015; Xu *et al.*, 2015; Furusawa *et al.*, 2016). Although the importance of macrophage during liver regeneration has been well documented, especially

using macrophage depleted mice, the mechanisms involved in macrophage driven LPC activation remain unclear.

In this context, the other goal of this PhD work was to study the role of liver macrophages on LPC-mediated liver regeneration through the IL-27/WSX-1 axis, in a pro-inflammatory context characterized by increased levels of IL-17.

In this third paper, we reported a correlation between IL-17-producing cell recruitment and the severity of the DR, and we identified IL-17 as a cytokine with a central role in triggering LPC compartment activation and proliferation. We also reveal that IL-17 is responsible for macrophage-induced IL-27 expression that favors LPC differentiation into hepatocytes. We therefore highlighted the collaborative work between IL-17 and IL-27 that is required to properly achieve liver regeneration from LPC.

Role of macrophages in LPC expansion. We previously reported a role of IL-17 in polarizing macrophages toward a proinflammatory M1 phenotype (Guillot *et al.*, 2014). In this study, we show that IL-17 deficiency causes impairment of macrophage cell recruitment in CDE-diet-induced liver regeneration, resulting in reduced hepatic inflammation. This reduced inflammatory response may explain the reduced liver injury observed at later time points in IL-17^{-/-} animals. These results are consistent with previous reports showing that macrophage depletion by clodronate injections abrogates LPC accumulation and subsequent liver regeneration during a CDE diet (Van Hul *et al.*, 2011). The results obtained *in vivo* clearly provide evidence that IL-17 deficiency alters LPC expansion, which fits with *in vitro* data. However, neither IL-17 deficiency nor macrophage depletion (Elsegood *et al.*, 2015) were sufficient to completely abolish DR. This suggests that IL-17 could contribute to LPC expansion by i) directly promoting LPC proliferation and ii) indirectly through M1-macrophage-induced production of required factors, e.g., TNF- α and IL-6, which support LPC accumulation (Jakubowski *et al.*, 2005; Knight *et al.*, 2005).

Role of macrophages in LPC-mediated differentiation through the IL-27/WSX-1 axis. In addition to its function in triggering LPC activation in regenerating livers, we demonstrated that IL-17 also induced IL-27 cytokine production by macrophages. Here, we showed a direct role of IL-27 on LPC by favoring their differentiation into a hepatocytic phenotype *in vitro* without a direct mitogenic effect. Additional experiments, such as lineage tracing in several models, including CDE, or hepatocyte-specific MDM2 proto-oncogene (Mdm2)-deficient

mice, are required to conclude on the role of IL-27 effects on LPC differentiation *in vivo*. Reduced LPC accumulation in WSX-1^{-/-} mice was associated with a significant decrease in recruitment of macrophages, which have been reported as essential actors in supporting LPC expansion (Elsegood *et al.*, 2015).

In conclusion, this PhD work and related publications have revealed new concepts on the origins of hepatic macrophages during liver regeneration. It also shed light on the role of the macrophage-mediated immune response during liver regeneration from hepatocytes and LPC and different contexts of hepatic stress.

Our studies demonstrated that, despite their highly differentiated state, KC were able to proliferate in regenerating livers following PHx. Additionally, we elucidated the underlying mechanisms driving their proliferation by revealing the role of IL-6 and Sirt1 interaction in the stimulation of KC repopulation. Contrastingly, we showed in a model of BEC injury that monocytes were recruited to promote BEC repair.

Alternatively, we demonstrated that hepatic macrophages were crucial for LPC-driver liver regeneration by favoring their proliferation and differentiation into hepatocytes.

These interesting findings open new areas of investigation on the use of macrophage modulation to improve liver regeneration.

References

- Abel, A. M. *et al.* (2018) 'Natural Killer Cells: Development, Maturation, and Clinical Utilization', *Frontiers in Immunology*, p. 1869.
- Abshagen, K. *et al.* (2007) 'Loss of NF- κ B activation in Kupffer cell-depleted mice impairs liver regeneration after partial hepatectomy', *American Journal of Physiology-Gastrointestinal and Liver Physiology*, 292(6), pp. 1570–1577. doi: 10.1152/ajpgi.00399.2006.
- Abu Rmilah, A. *et al.* (2019) 'Understanding the marvels behind liver regeneration', *Wiley interdisciplinary reviews. Developmental biology*. 2019/03/28, 8(3), pp. e340–e340. doi: 10.1002/wdev.340.
- Adeva-Andany, M. M. *et al.* (2016) 'Liver glucose metabolism in humans', *Bioscience reports*, 36(6), p. e00416. doi: 10.1042/BSR20160385.
- Anderson, E. R. and Shah, Y. M. (2013) 'Iron homeostasis in the liver', *Comprehensive Physiology*, 3(1), pp. 315–330. doi: 10.1002/cphy.c120016.
- Atwood, A. *et al.* (2011) 'Cell-autonomous circadian clock of hepatocytes drives rhythms in transcription and polyamine synthesis', *Proceedings of the National Academy of Sciences*, 108(45), pp. 18560 LP – 18565. doi: 10.1073/pnas.1115753108.
- Banales, J. M. *et al.* (2019) 'Cholangiocyte pathobiology', *Nature Reviews Gastroenterology & Hepatology*, 16(5), pp. 269–281. doi: 10.1038/s41575-019-0125-y.
- Bansal, M. B. *et al.* (2005) 'Interleukin-6 protects hepatocytes from CCl₄-mediated necrosis and apoptosis in mice by reducing MMP-2 expression', *Journal of Hepatology*, 42(4), pp. 548–556. doi: 10.1016/j.jhep.2004.11.043.
- Bashirova, A. A. *et al.* (2001) 'A Dendritic Cell-Specific Intercellular Adhesion Molecule 3-Grabbing Nonintegrin (Dc-Sign)-Related Protein Is Highly Expressed on Human Liver Sinusoidal Endothelial Cells and Promotes HIV-1 Infection', *Journal of Experimental Medicine*, 193(6), pp. 671–678. doi: 10.1084/jem.193.6.671.
- Bellet, M. M. *et al.* (2016) 'Histone Deacetylase SIRT1 Controls Proliferation, Circadian Rhythm, and Lipid Metabolism during Liver Regeneration in Mice', *The Journal of biological chemistry*. 2016/09/15, 291(44), pp. 23318–23329. doi: 10.1074/jbc.M116.737114.
- Bhushan, B. *et al.* (2014) 'Pro-Regenerative Signaling after Acetaminophen-Induced Acute Liver Injury in Mice Identified Using a Novel Incremental Dose Model', *The American Journal of Pathology*, 184(11), pp. 3013–3025. doi: 10.1016/j.ajpath.2014.07.019.
- Blériot, C. *et al.* (2015) 'Liver-Resident Macrophage Necroptosis Orchestrates Type 1 Microbicidal Inflammation and Type-2-Mediated Tissue Repair during Bacterial Infection', *Immunity*, 42(1), pp. 145–158. doi: <https://doi.org/10.1016/j.immuni.2014.12.020>.
- Borst, K. *et al.* (2018) 'Type I interferon receptor signaling delays Kupffer cell replenishment during acute fulminant viral hepatitis', *Journal of Hepatology*, 68(4), pp. 682–690. doi: 10.1016/j.jhep.2017.11.029.
- Bost, M. *et al.* (2016) 'Dietary copper and human health: Current evidence and unresolved issues', *Journal of Trace Elements in Medicine and Biology*, 35, pp. 107–115. doi: <https://doi.org/10.1016/j.jtemb.2016.02.006>.
- Boulter, L. *et al.* (2012) 'Macrophage-derived Wnt opposes Notch signaling to specify hepatic progenitor cell fate in chronic liver disease', *Nature medicine*, 18(4), pp. 572–579. doi: 10.1038/nm.2667.
- Boyer, J. L. (2013) 'Bile formation and secretion', *Comprehensive Physiology*, 3(3), pp. 1035–1078. doi: 10.1002/cphy.c120027.
- Cai, J., Zhang, X.-J. and Li, H. (2019) 'The Role of Innate Immune Cells in Nonalcoholic Steatohepatitis', *Hepatology*, 70(3), pp. 1026–1037. doi: <https://doi.org/10.1002/hep.30506>.
- Castellaneta, A. *et al.* (2006) 'Functional modification of CD11c+ liver dendritic cells during liver regeneration after partial hepatectomy in mice', *Hepatology*, 43(4), pp. 807–816. doi: <https://doi.org/10.1002/hep.21098>.
- Chadt, A. and Al-Hasani, H. (2020) 'Glucose transporters in adipose tissue, liver, and skeletal muscle in metabolic health and disease', *Pflügers Archiv - European Journal of Physiology*, 472(9), pp. 1273–1298. doi: 10.1007/s00424-020-02417-x.
- Chaisson, M. L. *et al.* (2002) 'Hepatocyte-specific inhibition of NF- κ B leads to apoptosis after TNF treatment, but not after partial hepatectomy', *The Journal of Clinical Investigation*, 110(2), pp. 193–202. doi: 10.1172/JCI15295.
- Chayanupatkul, M. and Liangpunsakul, S. (2014) 'Cirrhotic cardiomyopathy: review of pathophysiology and treatment', *Hepatology international*, 8(3), pp. 308–315. doi: 10.1007/s12072-014-9531-y.
- Chen, Q., Zhang, T. and Wei, J.-F. W. and D.-Q. (2011) 'Advances in Human Cytochrome P450 and Personalized Medicine', *Current Drug Metabolism*, pp. 436–444. doi: <http://dx.doi.org/10.2174/138920011795495259>.

- Chiang, J. Y. L. and Ferrell, J. M. (2020) 'Bile Acid Biology, Pathophysiology, and Therapeutics', *Clinical Liver Disease*, 15(3), pp. 91–94. doi: <https://doi.org/10.1002/cld.861>.
- Choi, T.-Y. *et al.* (2017) 'Bone morphogenetic protein signaling governs biliary-driven liver regeneration in zebrafish through *tbx2b* and *id2a*', *Hepatology (Baltimore, Md.)*. 2017/09/29, 66(5), pp. 1616–1630. doi: [10.1002/hep.29309](https://doi.org/10.1002/hep.29309).
- Choi, T. *et al.* (2014) 'Extensive Conversion of Hepatic Biliary Epithelial Cells to Hepatocytes After Near Total Loss of Hepatocytes in Zebrafish', *Gastroenterology*, 146(3), pp. 776–788. doi: <https://doi.org/10.1053/j.gastro.2013.10.019>.
- Chu, J. and Sadler, K. C. (2009) 'New school in liver development: Lessons from zebrafish', *Hepatology*, 50(5), pp. 1656–1663. doi: <https://doi.org/10.1002/hep.23157>.
- Clemens, M. M., McGill, M. R. and Apte, U. (2019) 'Mechanisms and biomarkers of liver regeneration after drug-induced liver injury', *Advances in pharmacology (San Diego, Calif.)*. 2019/03/21, 85, pp. 241–262. doi: [10.1016/bs.apha.2019.03.001](https://doi.org/10.1016/bs.apha.2019.03.001).
- Clouston, A. D. *et al.* (2005) 'Fibrosis correlates with a ductular reaction in hepatitis C: Roles of impaired replication, progenitor cells and steatosis', *Hepatology*, 41(4), pp. 809–818. doi: <https://doi.org/10.1002/hep.20650>.
- Cordero-Espinoza, L. and Huch, M. (2018) 'The balancing act of the liver: tissue regeneration versus fibrosis', *The Journal of Clinical Investigation*, 128(1), pp. 85–96. doi: [10.1172/JCI93562](https://doi.org/10.1172/JCI93562).
- Danielson, P. B. (2002) 'The Cytochrome P450 Superfamily: Biochemistry, Evolution and Drug Metabolism in Humans', *Current Drug Metabolism*, pp. 561–597. doi: <http://dx.doi.org/10.2174/1389200023337054>.
- Devischer, L. *et al.* (2017) 'Non-alcoholic steatohepatitis induces transient changes within the liver macrophage pool', *Cellular Immunology*, 322, pp. 74–83. doi: <https://doi.org/10.1016/j.cellimm.2017.10.006>.
- Doguer, C., Ha, J.-H. and Collins, J. F. (2018) 'Intersection of Iron and Copper Metabolism in the Mammalian Intestine and Liver', *Comprehensive Physiology*, 8(4), pp. 1433–1461. doi: [10.1002/cphy.c170045](https://doi.org/10.1002/cphy.c170045).
- Dollé, L. *et al.* (2010) 'The quest for liver progenitor cells: A practical point of view', *Journal of Hepatology*, 52(1), pp. 117–129. doi: <https://doi.org/10.1016/j.jhep.2009.10.009>.
- Dong, Z. *et al.* (2007) 'Impairment of liver regeneration correlates with activated hepatic NKT cells in HBV transgenic mice', *Hepatology*, 45(6), pp. 1400–1412. doi: <https://doi.org/10.1002/hep.21597>.
- Drixler, T. A. *et al.* (2003) 'Plasminogen mediates liver regeneration and angiogenesis after experimental partial hepatectomy', *BJS (British Journal of Surgery)*, 90(11), pp. 1384–1390. doi: <https://doi.org/10.1002/bjs.4275>.
- Egger, S. *et al.* (2010) 'UDP-glucose dehydrogenase: structure and function of a potential drug target', *Biochemical Society Transactions*, 38(5), pp. 1378–1385. doi: [10.1042/BST0381378](https://doi.org/10.1042/BST0381378).
- Elangovan, H., Chahal, S. and Gunton, J. E. (2017) 'Vitamin D in liver disease: Current evidence and potential directions', *Biochimica et Biophysica Acta (BBA) - Molecular Basis of Disease*, 1863(4), pp. 907–916. doi: <https://doi.org/10.1016/j.bbadis.2017.01.001>.
- Elchaninov, A. V. *et al.* (2018) 'Dynamics of macrophage populations of the liver after subtotal hepatectomy in rats', *BMC Immunology*, 19(1), p. 23. doi: [10.1186/s12865-018-0260-1](https://doi.org/10.1186/s12865-018-0260-1).
- Elsegood, C. L. *et al.* (2015) 'Kupffer cell–monocyte communication is essential for initiating murine liver progenitor cell–mediated liver regeneration', *Hepatology*, 62(4), pp. 1272–1284. doi: [10.1002/hep.27977](https://doi.org/10.1002/hep.27977).
- Español-Suñer, R. *et al.* (2012) 'Liver Progenitor Cells Yield Functional Hepatocytes in Response to Chronic Liver Injury in Mice', *Gastroenterology*, 143(6), pp. 1564–1575.e7. doi: [10.1053/j.gastro.2012.08.024](https://doi.org/10.1053/j.gastro.2012.08.024).
- Fabris, L. *et al.* (2017) 'Emerging concepts in biliary repair and fibrosis', *American Journal of Physiology-Gastrointestinal and Liver Physiology*, 313(2), pp. G102–G116. doi: [10.1152/ajpgi.00452.2016](https://doi.org/10.1152/ajpgi.00452.2016).
- Fausto, N. (2000) 'Liver regeneration', *Journal of Hepatology*, 32, pp. 19–31. doi: [10.1016/S0168-8278\(00\)80412-2](https://doi.org/10.1016/S0168-8278(00)80412-2).
- Ferenci, P. (2017) 'Hepatic encephalopathy', *Gastroenterology report*. 2017/04/18, 5(2), pp. 138–147. doi: [10.1093/gastro/gox013](https://doi.org/10.1093/gastro/gox013).
- Franko, A. *et al.* (2019) 'Identification of the Secreted Proteins Originated from Primary Human Hepatocytes and HepG2 Cells', *Nutrients*, 11(8), p. 1795. doi: [10.3390/nu11081795](https://doi.org/10.3390/nu11081795).
- Freitas-Lopes, M. A. *et al.* (2017) 'Differential Location and Distribution of Hepatic Immune Cells', *Cells*, 6(4), p. 48. doi: [10.3390/cells6040048](https://doi.org/10.3390/cells6040048).
- Fujita, T. and Narumiya, S. (2016) 'Roles of hepatic stellate cells in liver inflammation: a new perspective', *Inflammation and regeneration*, 36, p. 1. doi: [10.1186/s41232-016-0005-6](https://doi.org/10.1186/s41232-016-0005-6).
- Furusawa, J. *et al.* (2016) 'Promotion of Expansion and Differentiation of Hematopoietic Stem Cells by Interleukin-27 into Myeloid Progenitors to Control Infection in Emergency Myelopoiesis', *PLOS Pathogens*, 12(3), p. e1005507.
- Gadd, V. L. *et al.* (2014) 'The portal inflammatory infiltrate and ductular reaction in human nonalcoholic fatty liver disease', *Hepatology*, 59(4), pp. 1393–1405. doi: <https://doi.org/10.1002/hep.26937>.

- Gao, B. (2016) 'Basic liver immunology', *Cellular & molecular immunology*. 2016/04/04, 13(3), pp. 265–266. doi: 10.1038/cmi.2016.09.
- Gao, B., Jeong, W.-I. and Tian, Z. (2008) 'Liver: An organ with predominant innate immunity', *Hepatology*, 47(2), pp. 729–736. doi: <https://doi.org/10.1002/hep.22034>.
- Gao, J. *et al.* (2021) 'The interaction of Notch and Wnt signaling pathways in vertebrate regeneration', *Cell Regeneration*, 10(1), p. 11. doi: 10.1186/s13619-020-00072-2.
- Gao, R. Y. *et al.* (2020) 'Hypoxia-Inducible Factor-2 α Reprograms Liver Macrophages to Protect Against Acute Liver Injury Through the Production of Interleukin-6', *Hepatology*, 71(6), pp. 2105–2117. doi: 10.1002/hep.30954.
- Géraud, C. *et al.* (2012) 'Unique cell type-specific junctional complexes in vascular endothelium of human and rat liver sinusoids', *PLoS one*. 2012/04/03, 7(4), pp. e34206–e34206. doi: 10.1371/journal.pone.0034206.
- Gholamzadeh, S. *et al.* (2017) 'Statistical Analysis of Organ Morphometric Parameters and Weights in South Iranian Adult Autopsies', *Medicine*, 96(21).
- Gil, A., Plaza-Diaz, J. and Mesa, M. D. (2018) 'Vitamin D: Classic and Novel Actions', *Annals of Nutrition and Metabolism*, 72(2), pp. 87–95. doi: 10.1159/000486536.
- Gilgenkrantz, H. and Collin de l'Hortet, A. (2018) 'Understanding Liver Regeneration: From Mechanisms to Regenerative Medicine', *The American Journal of Pathology*, 188(6), pp. 1316–1327. doi: <https://doi.org/10.1016/j.ajpath.2018.03.008>.
- Goh, Y. P. S. *et al.* (2013) 'Eosinophils secrete IL-4 to facilitate liver regeneration', *Proceedings of the National Academy of Sciences*, 110(24), pp. 9914 LP – 9919. doi: 10.1073/pnas.1304046110.
- Gonzales, E. *et al.* (2010) 'ATP release after partial hepatectomy regulates liver regeneration in the rat', *Journal of Hepatology*, 52(1), pp. 54–62. doi: 10.1016/j.jhep.2009.10.005.
- Gooley, J. J. (2016) 'Circadian regulation of lipid metabolism', *Proceedings of the Nutrition Society*. 2016/05/26, 75(4), pp. 440–450. doi: DOI: 10.1017/S0029665116000288.
- Görg, B., Schliess, F. and Häussinger, D. (2013) 'Osmotic and oxidative/nitrosative stress in ammonia toxicity and hepatic encephalopathy', *Archives of Biochemistry and Biophysics*, 536(2), pp. 158–163. doi: <https://doi.org/10.1016/j.abb.2013.03.010>.
- Graubardt, N. *et al.* (2013) 'Promotion of liver regeneration by natural killer cells in a murine model is dependent on extracellular adenosine triphosphate phosphohydrolysis', *Hepatology*, 57(5), pp. 1969–1979. doi: <https://doi.org/10.1002/hep.26008>.
- Guengerich, F. P. (2018) 'Mechanisms of Cytochrome P450-Catalyzed Oxidations', *ACS catalysis*. 2018/10/18, 8(12), pp. 10964–10976. doi: 10.1021/acscatal.8b03401.
- Guicciardi, M. E. *et al.* (2018) 'Macrophages contribute to the pathogenesis of sclerosing cholangitis in mice', *Journal of Hepatology*, 69(3), pp. 676–686. doi: 10.1016/j.jhep.2018.05.018.
- Guillot, A. *et al.* (2014) 'Cannabinoid receptor 2 counteracts interleukin-17-induced immune and fibrogenic responses in mouse liver', *Hepatology*, 59(1), pp. 296–306. doi: <https://doi.org/10.1002/hep.26598>.
- Guillot, A. *et al.* (2018) 'Interleukins-17 and 27 promote liver regeneration by sequentially inducing progenitor cell expansion and differentiation', *Hepatology Communications*, 2(3), pp. 329–343. doi: 10.1002/hep4.1145.
- Guillot, A. *et al.* (2021) 'Bile acid-activated macrophages promote biliary epithelial cell proliferation through integrin $\alpha\beta 6$ upregulation following liver injury', *The Journal of Clinical Investigation*, 131(9). doi: 10.1172/JCI132305.
- Guillot, A., Buch, C. and Jourdan, T. (2020) 'Kupffer Cell and Monocyte-Derived Macrophage Identification by Immunofluorescence on Formalin-Fixed, Paraffin-Embedded (FFPE) Mouse Liver Sections', in Aouadi, M. and Azzimato, V. (eds) *Kupffer Cells: Methods and Protocols*. New York, NY: Springer US, pp. 45–53. doi: 10.1007/978-1-0716-0704-6_6.
- Han, H.-S. *et al.* (2016) 'Regulation of glucose metabolism from a liver-centric perspective', *Experimental & Molecular Medicine*, 48(3), pp. e218–e218. doi: 10.1038/emm.2015.122.
- Han, Y. *et al.* (2013) 'Recent advances in the morphological and functional heterogeneity of the biliary epithelium', *Experimental biology and medicine (Maywood, N.J.)*, 238(5), pp. 549–565. doi: 10.1177/1535370213489926.
- He, J. *et al.* (2014) 'Regeneration of Liver After Extreme Hepatocyte Loss Occurs Mainly via Biliary Transdifferentiation in Zebrafish', *Gastroenterology*, 146(3), pp. 789–800.e8. doi: <https://doi.org/10.1053/j.gastro.2013.11.045>.
- Heymann, F. and Tacke, F. (2016) 'Immunology in the liver — from homeostasis to disease', *Nature Reviews Gastroenterology & Hepatology*, 13(2), pp. 88–110. doi: 10.1038/nrgastro.2015.200.
- Hodges, R. E. and Minich, D. M. (2015) 'Modulation of Metabolic Detoxification Pathways Using Foods and Food-Derived Components: A Scientific Review with Clinical Application', *Journal of nutrition and metabolism*. 2015/06/16, 2015, p. 760689. doi: 10.1155/2015/760689.

- Hoffmann, C. *et al.* (2020) ‘Hepatic stellate cell hypertrophy is associated with metabolic liver fibrosis’, *Scientific Reports*, 10(1), p. 3850. doi: 10.1038/s41598-020-60615-0.
- Hosoya, S. *et al.* (2012) ‘Innate immune responses involving natural killer and natural killer T cells promote liver regeneration after partial hepatectomy in mice’, *American Journal of Physiology-Gastrointestinal and Liver Physiology*, 304(3), pp. G293–G299. doi: 10.1152/ajpgi.00083.2012.
- Hou, X. *et al.* (2020) ‘Myeloid cell-specific IL-6 signaling promotes miR-223-enriched exosome production to attenuate NAFLD-associated fibrosis’, *Hepatology*, n/a(n/a). doi: <https://doi.org/10.1002/hep.31658>.
- Hsieh, S.-L. E. and Yang, C.-Y. (2009) ‘CLEC4F, A Kupffer Cells Specific Marker, Is Critical for Presentation of Alfa-Galactoceromide to NKT Cells’, *The Journal of Immunology*, 182(1 Supplement), p. 78.
- Van Hul, N. *et al.* (2011) ‘Kupffer Cells Influence Parenchymal Invasion and Phenotypic Orientation, but Not the Proliferation, of Liver Progenitor Cells in a Murine Model of Liver Injury’, *The American Journal of Pathology*, 179(4), pp. 1839–1850. doi: <https://doi.org/10.1016/j.ajpath.2011.06.042>.
- Hunter, C. A. and Jones, S. A. (2015) ‘IL-6 as a keystone cytokine in health and disease’, *Nature Immunology*, 16(5), pp. 448–457. doi: 10.1038/ni.3153.
- Hussain, M. M. (2014) ‘Intestinal lipid absorption and lipoprotein formation’, *Current opinion in lipidology*, 25(3), pp. 200–206. doi: 10.1097/MOL.0000000000000084.
- Imperatore, F. *et al.* (2017) ‘SIRT1 regulates macrophage self-renewal’, *The EMBO journal*. 2017/07/12, 36(16), pp. 2353–2372. doi: 10.15252/embj.201695737.
- Ishikawa, T. *et al.* (2012) ‘Hepatocyte growth factor/c-met signaling is required for stem-cell-mediated liver regeneration in mice’, *Hepatology (Baltimore, Md.)*, 55(4), pp. 1215–1226. doi: 10.1002/hep.24796.
- Jakubowski, A. *et al.* (2005) ‘TWEAK induces liver progenitor cell proliferation’, *The Journal of Clinical Investigation*, 115(9), pp. 2330–2340. doi: 10.1172/JCI23486.
- Jenne, C. N. and Kubes, P. (2013) ‘Immune surveillance by the liver’, *Nature Immunology*, 14(10), pp. 996–1006. doi: 10.1038/ni.2691.
- Jin, J. *et al.* (2011) ‘The reduction of SIRT1 in livers of old mice leads to impaired body homeostasis and to inhibition of liver proliferation’, *Hepatology (Baltimore, Md.)*. 2011/07/27, 54(3), pp. 989–998. doi: 10.1002/hep.24471.
- Jin, X. *et al.* (2018) ‘Hepatic stellate cells promote angiogenesis via the TGF- β 1-Jagged1/VEGFA axis’, *Experimental Cell Research*, 373(1), pp. 34–43. doi: <https://doi.org/10.1016/j.yexcr.2018.07.045>.
- Jover, R. *et al.* (2006) ‘Brain edema and inflammatory activation in bile duct ligated rats with diet-induced hyperammonemia: A model of hepatic encephalopathy in cirrhosis’, *Hepatology*, 43(6), pp. 1257–1266. doi: <https://doi.org/10.1002/hep.21180>.
- Ju, C. and Tacke, F. (2016) ‘Hepatic macrophages in homeostasis and liver diseases: from pathogenesis to novel therapeutic strategies’, *Cellular & Molecular Immunology*, 13(3), pp. 316–327. doi: 10.1038/cmi.2015.104.
- Kachaylo, E. *et al.* (2017) ‘PTEN Down-Regulation Promotes β -Oxidation to Fuel Hypertrophic Liver Growth After Hepatectomy in Mice’, *Hepatology (Baltimore, Md.)*, 66(3), p. 908–921. doi: 10.1002/hep.29226.
- Kalinichenko, V. V *et al.* (2003) ‘Foxf1 +/- mice exhibit defective stellate cell activation and abnormal liver regeneration following CCl4 injury’, *Hepatology*, 37(1), pp. 107–117. doi: <https://doi.org/10.1053/jhep.2003.50005>.
- Kallis, Y. N. *et al.* (2011) ‘Remodelling of extracellular matrix is a requirement for the hepatic progenitor cell response’, *Gut*, 60(4), pp. 525 LP – 533. doi: 10.1136/gut.2010.224436.
- Karaca, G. *et al.* (2014) ‘TWEAK/Fn14 Signaling Is Required for Liver Regeneration after Partial Hepatectomy in Mice’, *PLOS ONE*, 9(1), p. e83987.
- Keane, J. T. *et al.* (2018) ‘Vitamin D and the Liver-Correlation or Cause?’, *Nutrients*, 10(4), p. 496. doi: 10.3390/nu10040496.
- Kim, E. J. *et al.* (2014) ‘Cholesterol-Induced Non-Alcoholic Fatty Liver Disease and Atherosclerosis Aggravated by Systemic Inflammation’, *PLOS ONE*, 9(6), p. e97841.
- Kitade, M. *et al.* (2019) ‘Blocking development of liver fibrosis augments hepatic progenitor cell-derived liver regeneration in a mouse chronic liver injury model’, *Hepatology Research*, 49(9), pp. 1034–1045. doi: <https://doi.org/10.1111/hepr.13351>.
- Kitto, L. J. and Henderson, N. C. (2021) ‘Hepatic Stellate Cell Regulation of Liver Regeneration and Repair’, *Hepatology Communications*, 5(3), pp. 358–370. doi: <https://doi.org/10.1002/hep4.1628>.
- Knight, B. *et al.* (2005) ‘Liver inflammation and cytokine production, but not acute phase protein synthesis, accompany the adult liver progenitor (oval) cell response to chronic liver injury’, *Immunology & Cell Biology*, 83(4), pp. 364–374. doi: <https://doi.org/10.1111/j.1440-1711.2005.01346.x>.
- Knight, B. *et al.* (2007) ‘Interferon- γ ; exacerbates liver damage, the hepatic progenitor cell response and fibrosis in a mouse model of chronic liver injury’, *Journal of Hepatology*, 47(6), pp. 826–833. doi: 10.1016/j.jhep.2007.06.022.

- Knolle, P. A. and Wohlleber, D. (2016) 'Immunological functions of liver sinusoidal endothelial cells', *Cellular & Molecular Immunology*, 13(3), pp. 347–353. doi: 10.1038/cmi.2016.5.
- Ko, S. *et al.* (2019) 'Hdac1 Regulates Differentiation of Bipotent Liver Progenitor Cells During Regeneration via Sox9b and Cdk8', *Gastroenterology*. 2018/09/26, 156(1), pp. 187–202.e14. doi: 10.1053/j.gastro.2018.09.039.
- Ko, S. *et al.* (2020) 'Liver Progenitors and Adult Cell Plasticity in Hepatic Injury and Repair: Knowns and Unknowns', *Annual Review of Pathology: Mechanisms of Disease*, 15(1), pp. 23–50. doi: 10.1146/annurev-pathmechdis-012419-032824.
- Köhler, C. *et al.* (2004) 'Expression of Notch-1 and its ligand Jagged-1 in rat liver during liver regeneration', *Hepatology*, 39(4), pp. 1056–1065. doi: <https://doi.org/10.1002/hep.20156>.
- Krenkel, O. and Tacke, F. (2017) 'Liver macrophages in tissue homeostasis and disease', *Nature Reviews Immunology*, 17(5), pp. 306–321. doi: 10.1038/nri.2017.11.
- Kruepunga, N. *et al.* (2019) 'Anatomy of rodent and human livers: What are the differences?', *Biochimica et Biophysica Acta (BBA) - Molecular Basis of Disease*, 1865(5), pp. 869–878. doi: <https://doi.org/10.1016/j.bbadis.2018.05.019>.
- Lafdil, F. *et al.* (2010) 'Th17 cells and their associated cytokines in liver diseases', *Cellular & Molecular Immunology*, 7(4), pp. 250–254. doi: 10.1038/cmi.2010.5.
- Lefere, S. *et al.* (2019) 'Unveiling the depletion of Kupffer cells in experimental hepatocarcinogenesis through liver macrophage subtype-specific markers', *Journal of Hepatology*, 71(3), pp. 631–633. doi: 10.1016/j.jhep.2019.03.016.
- Li, N. and Hua, J. (2017) 'Immune cells in liver regeneration', *Oncotarget*, 8(2), pp. 3628–3639. doi: 10.18632/oncotarget.12275.
- Li, Y. *et al.* (2016) 'Hepatic Stellate Cells Directly Inhibit B Cells via Programmed Death-Ligand 1', *Journal of immunology (Baltimore, Md. : 1950)*. 2016/01/11, 196(4), pp. 1617–1625. doi: 10.4049/jimmunol.1501737.
- Libbrecht, L. (2006) 'Hepatic progenitor cells in human liver tumor development', *World journal of gastroenterology*, 12(39), pp. 6261–6265. doi: 10.3748/wjg.v12.i39.6261.
- Linder, M. C. (2020) 'Copper Homeostasis in Mammals, with Emphasis on Secretion and Excretion. A Review', *International journal of molecular sciences*, 21(14), p. 4932. doi: 10.3390/ijms21144932.
- Linke, T., Dawson, H. and Harrison, E. H. (2005) 'Isolation and Characterization of a Microsomal Acid Retinyl Ester Hydrolase *', *Journal of Biological Chemistry*, 280(24), pp. 23287–23294. doi: 10.1074/jbc.M413585200.
- Liu, H.-X. *et al.* (2015) 'Implications of microbiota and bile acid in liver injury and regeneration', *Journal of Hepatology*, 63(6), pp. 1502–1510. doi: <https://doi.org/10.1016/j.jhep.2015.08.001>.
- Liu, W. *et al.* (2004) 'Characterization of a Novel C-type Lectin-like Gene, LSECTin: DEMONSTRATION OF CARBOHYDRATE BINDING AND EXPRESSION IN SINUSOIDAL ENDOTHELIAL CELLS OF LIVER AND LYMPH NODE *', *Journal of Biological Chemistry*, 279(18), pp. 18748–18758. doi: 10.1074/jbc.M311227200.
- Liu, Y.-C., Yeh, C.-T. and Lin, K.-H. (2020) 'Cancer Stem Cell Functions in Hepatocellular Carcinoma and Comprehensive Therapeutic Strategies', *Cells*. doi: 10.3390/cells9061331.
- Locatelli, L. *et al.* (2016) 'Macrophage recruitment by fibrocystin-defective biliary epithelial cells promotes portal fibrosis in congenital hepatic fibrosis', *Hepatology*, 63(3), pp. 965–982. doi: <https://doi.org/10.1002/hep.28382>.
- Lopez, B. G. *et al.* (2011) 'Characterization of Kupffer cells in livers of developing mice', *Comparative Hepatology*, 10(1), p. 2. doi: 10.1186/1476-5926-10-2.
- Lorenzini, S. *et al.* (2010) 'Characterisation of a stereotypical cellular and extracellular adult liver progenitor cell niche in rodents and diseased human liver', *Gut*, 59(5), pp. 645–654. doi: 10.1136/gut.2009.182345.
- Lukacs-Kornek, V. and Lammert, F. (2017) 'The progenitor cell dilemma: Cellular and functional heterogeneity in assistance or escalation of liver injury', *Journal of Hepatology*, 66(3), pp. 619–630. doi: <https://doi.org/10.1016/j.jhep.2016.10.033>.
- Macchi, F. and Sadler, K. C. (2020) 'Unraveling the Epigenetic Basis of Liver Development, Regeneration and Disease', *Trends in Genetics*, 36(8), pp. 587–597. doi: 10.1016/j.tig.2020.05.002.
- Mackay, I. R. (2002) 'Hepatoimmunology: A perspective', *Immunology & Cell Biology*, 80(1), pp. 36–44. doi: <https://doi.org/10.1046/j.1440-1711.2002.01063.x>.
- Mangnall, D. *et al.* (2004) 'Early increases in plasminogen activator activity following partial hepatectomy in humans', *Comparative hepatology*, 3(1), p. 11. doi: 10.1186/1476-5926-3-11.
- Markose, D. *et al.* (2018) 'Immune cell regulation of liver regeneration and repair', *Journal of Immunology and Regenerative Medicine*, 2, pp. 1–10. doi: <https://doi.org/10.1016/j.regen.2018.03.003>.
- Massarweh, N. N. and El-Serag, H. B. (2017) 'Epidemiology of Hepatocellular Carcinoma and

- Intrahepatic Cholangiocarcinoma', *Cancer control: journal of the Moffitt Cancer Center*, 24(3), pp. 1073274817729245–1073274817729245. doi: 10.1177/1073274817729245.
- McDonald, B. *et al.* (2012) 'Intravascular Neutrophil Extracellular Traps Capture Bacteria from the Bloodstream during Sepsis', *Cell Host & Microbe*, 12(3), pp. 324–333. doi: 10.1016/j.chom.2012.06.011.
- Merli, M. *et al.* (2013) 'Increased risk of cognitive impairment in cirrhotic patients with bacterial infections', *Journal of Hepatology*, 59(2), pp. 243–250. doi: 10.1016/j.jhep.2013.03.012.
- Merlin, S. *et al.* (2016) 'Kupffer Cell Transplantation in Mice for Elucidating Monocyte/Macrophage Biology and for Potential in Cell or Gene Therapy', *The American journal of pathology*. 2016/01/07, 186(3), pp. 539–551. doi: 10.1016/j.ajpath.2015.11.002.
- Michalopoulos, G. K. (2013) 'Principles of Liver Regeneration and Growth Homeostasis', *Comprehensive Physiology*. (Major Reference Works), pp. 485–513. doi: <https://doi.org/10.1002/cphy.c120014>.
- Michalopoulos, G. K. (2017) 'Hepatostat: Liver regeneration and normal liver tissue maintenance', *Hepatology*, 65(4), pp. 1384–1392. doi: <https://doi.org/10.1002/hep.28988>.
- Michalopoulos, G. K. and Bhushan, B. (2021) 'Liver regeneration: biological and pathological mechanisms and implications', *Nature Reviews Gastroenterology & Hepatology*, 18(1), pp. 40–55. doi: 10.1038/s41575-020-0342-4.
- Michalopoulos, G. K. and Khan, Z. (2015) 'Liver Stem Cells: Experimental Findings and Implications for Human Liver Disease', *Gastroenterology*, 149(4), pp. 876–882. doi: <https://doi.org/10.1053/j.gastro.2015.08.004>.
- Mikulak, J. *et al.* (2019) 'Hepatic Natural Killer Cells: Organ-Specific Sentinels of Liver Immune Homeostasis and Physiopathology', *Frontiers in Immunology*, p. 946.
- Miyaoka, Y. *et al.* (2012) 'Hypertrophy and Unconventional Cell Division of Hepatocytes Underlie Liver Regeneration', *Current Biology*, 22(13), pp. 1166–1175. doi: <https://doi.org/10.1016/j.cub.2012.05.016>.
- Mondal, T. *et al.* (2016) 'ApoE: In Vitro Studies of a Small Molecule Effector', *Biochemistry*, 55(18), pp. 2613–2621. doi: 10.1021/acs.biochem.6b00324.
- Mubbunu, L. *et al.* (2018) 'Correlation of Internal Organ Weights with Body Weight and Body Height in Normal Adult Zambians: A Case Study of Ndola Teaching Hospital', *Anatomy Research International*. Edited by F. Sinowatz, 2018, p. 4687538. doi: 10.1155/2018/4687538.
- Nelsen, C. J. *et al.* (2003) 'Evidence That Cyclin D1 Mediates Both Growth and Proliferation Downstream of TOR in Hepatocytes *', *Journal of Biological Chemistry*, 278(6), pp. 3656–3663. doi: 10.1074/jbc.M209374200.
- Nguyen-Lefebvre, A. T. and Horuzsko, A. (2015) 'Kupffer Cell Metabolism and Function', *Journal of enzymology and metabolism*. 2015/08/14, 1(1), p. 101.
- Nio, K., Yamashita, T. and Kaneko, S. (2017) 'The evolving concept of liver cancer stem cells', *Molecular Cancer*, 16(1), p. 4. doi: 10.1186/s12943-016-0572-9.
- Nishiyama, K. *et al.* (2015) 'Mouse CD11b+Kupffer Cells Recruited from Bone Marrow Accelerate Liver Regeneration after Partial Hepatectomy', *PLOS ONE*, 10(9), p. e0136774.
- Norris, C. A. *et al.* (2014) 'Synthesis of IL-6 by Hepatocytes Is a Normal Response to Common Hepatic Stimuli', *PLOS ONE*, 9(4), p. e96053.
- O'Hara, S. P. *et al.* (2013) 'The dynamic biliary epithelia: Molecules, pathways, and disease', *Journal of Hepatology*, 58(3), pp. 575–582. doi: <https://doi.org/10.1016/j.jhep.2012.10.011>.
- Oliveira, E. F. *et al.* (2016) 'HMG-CoA Reductase inhibitors: an updated review of patents of novel compounds and formulations (2011-2015)', *Expert Opinion on Therapeutic Patents*, 26(11), pp. 1257–1272. doi: 10.1080/13543776.2016.1216977.
- Osawa, Y. *et al.* (2010) 'Role of acid sphingomyelinase of Kupffer cells in cholestatic liver injury in mice', *Hepatology*, 51(1), pp. 237–245. doi: 10.1002/hep.23262.
- Owumi, S. E. *et al.* (2014) 'Depletion of Kupffer cells modulates ethanol-induced hepatocyte DNA synthesis in C57Bl/6 mice', *Environmental Toxicology*, 29(8), pp. 867–875. doi: <https://doi.org/10.1002/tox.21814>.
- Paku, S. *et al.* (2004) '2-acetylaminofluorene dose-dependent differentiation of rat oval cells into hepatocytes: Confocal and electron microscopic studies', *Hepatology*, 39(5), pp. 1353–1361. doi: <https://doi.org/10.1002/hep.20178>.
- Patsenker, E. *et al.* (2008) 'Inhibition of Integrin $\alpha 5 \beta 1$ and $\alpha 5 \beta 2$ on Cholangiocytes Blocks Transforming Growth Factor- $\beta 2$ Activation and Retards Biliary Fibrosis Progression', *Gastroenterology*, 135(2), pp. 660–670. doi: 10.1053/j.gastro.2008.04.009.
- Peng, H. and Tian, Z. (2017) 'Diversity of tissue-resident NK cells', *Seminars in Immunology*, 31, pp. 3–10. doi: <https://doi.org/10.1016/j.smim.2017.07.006>.
- Peng, Z.-W. *et al.* (2016) 'Integrin $\alpha \beta 6$ critically regulates hepatic progenitor cell function and promotes ductular reaction, fibrosis, and tumorigenesis', *Hepatology*, 63(1), pp. 217–232. doi: <https://doi.org/10.1002/hep.28274>.

- Pintilie, D. G. *et al.* (2010) 'Hepatic stellate cells' involvement in progenitor-mediated liver regeneration', *Laboratory investigation; a journal of technical methods and pathology*. 2010/05/03, 90(8), pp. 1199–1208. doi: 10.1038/labinvest.2010.88.
- Pinto, C. *et al.* (2018) 'Role of inflammation and proinflammatory cytokines in cholangiocyte pathophysiology', *Biochimica et Biophysica Acta (BBA) - Molecular Basis of Disease*, 1864(4, Part B), pp. 1270–1278. doi: <https://doi.org/10.1016/j.bbadis.2017.07.024>.
- Poisson, J. *et al.* (2017) 'Liver sinusoidal endothelial cells: Physiology and role in liver diseases', *Journal of Hepatology*, 66(1), pp. 212–227. doi: 10.1016/j.jhep.2016.07.009.
- Protzer, U., Maini, M. K. and Knolle, P. A. (2012) 'Living in the liver: hepatic infections', *Nature Reviews Immunology*, 12(3), pp. 201–213. doi: 10.1038/nri3169.
- Racanelli, V. and Rehermann, B. (2006) 'The liver as an immunological organ', *Hepatology*, 43(S1), pp. S54–S62. doi: <https://doi.org/10.1002/hep.21060>.
- Rao, M. S. *et al.* (2001) 'Regeneration of Liver with Marked Fatty Change Following Partial Hepatectomy in Rats', *Digestive Diseases and Sciences*, 46(9), pp. 1821–1826. doi: 10.1023/A:1010654908938.
- Rao, R. *et al.* (2014) 'Interleukin 17–Producing $\gamma\delta$ T Cells Promote Hepatic Regeneration in Mice', *Gastroenterology*, 147(2), pp. 473–484.e2. doi: <https://doi.org/10.1053/j.gastro.2014.04.042>.
- Reid, D. T. *et al.* (2016) 'Kupffer Cells Undergo Fundamental Changes during the Development of Experimental NASH and Are Critical in Initiating Liver Damage and Inflammation', *PLOS ONE*, 11(7), p. e0159524.
- Richardson, M. M. *et al.* (2007) 'Progressive Fibrosis in Nonalcoholic Steatohepatitis: Association With Altered Regeneration and a Ductular Reaction', *Gastroenterology*, 133(1), pp. 80–90. doi: 10.1053/j.gastro.2007.05.012.
- Rito, J. *et al.* (2018) 'Disposition of a Glucose Load into Hepatic Glycogen by Direct and Indirect Pathways in Juvenile Seabass and Seabream', *Scientific Reports*, 8(1), p. 464. doi: 10.1038/s41598-017-19087-y.
- Robinson, M. W., Harmon, C. and O'Farrelly, C. (2016) 'Liver immunology and its role in inflammation and homeostasis', *Cellular & Molecular Immunology*, 13(3), pp. 267–276. doi: 10.1038/cmi.2016.3.
- Rodrigo-Torres, D. *et al.* (2014) 'The biliary epithelium gives rise to liver progenitor cells', *Hepatology*, 60(4), pp. 1367–1377. doi: <https://doi.org/10.1002/hep.27078>.
- Ruiz-Palacios, M. *et al.* (2017) 'Insulin Treatment May Alter Fatty Acid Carriers in Placentas from Gestational Diabetes Subjects', *International Journal of Molecular Sciences*. doi: 10.3390/ijms18061203.
- Saeed, A. *et al.* (2017) 'The interrelationship between bile acid and vitamin A homeostasis', *Biochimica et Biophysica Acta (BBA) - Molecular and Cell Biology of Lipids*, 1862(5), pp. 496–512. doi: <https://doi.org/10.1016/j.bbalip.2017.01.007>.
- Sato, K. *et al.* (2019) 'Ductular Reaction in Liver Diseases: Pathological Mechanisms and Translational Significances', *Hepatology*, 69(1), pp. 420–430. doi: <https://doi.org/10.1002/hep.30150>.
- Sawhney, R. and Jalan, R. (2015) 'The gut is a key target of therapy in hepatic encephalopathy', *Nature Reviews Gastroenterology & Hepatology*, 12(1), pp. 7–8. doi: 10.1038/nrgastro.2014.185.
- Schmidt-Arras, D. and Rose-John, S. (2016) 'IL-6 pathway in the liver: From physiopathology to therapy', *Journal of Hepatology*, 64(6), pp. 1403–1415. doi: 10.1016/j.jhep.2016.02.004.
- Schmölz, L. *et al.* (2016) 'Complexity of vitamin E metabolism', *World journal of biological chemistry*, 7(1), pp. 14–43. doi: 10.4331/wjbc.v7.i1.14.
- Schubert, M. *et al.* (2018) 'Long-Chain Metabolites of Vitamin E: Metabolic Activation as a General Concept for Lipid-Soluble Vitamins?', *Antioxidants*. doi: 10.3390/antiox7010010.
- Schulze, R. J. *et al.* (2019) 'The cell biology of the hepatocyte: A membrane trafficking machine', *The Journal of cell biology*. 2019/06/14, 218(7), pp. 2096–2112. doi: 10.1083/jcb.201903090.
- Scott, C. L. *et al.* (2016) 'Bone marrow-derived monocytes give rise to self-renewing and fully differentiated Kupffer cells', *Nature Communications*, 7(1), p. 10321. doi: 10.1038/ncomms10321.
- Scoville, S. D., Freud, A. G. and Caligiuri, M. A. (2017) 'Modeling Human Natural Killer Cell Development in the Era of Innate Lymphoid Cells', *Frontiers in Immunology*, p. 360.
- Selzner, N. *et al.* (2003) 'ICAM-1 triggers liver regeneration through leukocyte recruitment and Kupffer cell-dependent release of TNF- α /IL-6 in mice', *Gastroenterology*, 124(3), pp. 692–700. doi: <https://doi.org/10.1053/gast.2003.50098>.
- Senoo, H., Mezaki, Y. and Fujiwara, M. (2017) 'The stellate cell system (vitamin A-storing cell system)', *Anatomical Science International*, 92(4), pp. 387–455. doi: 10.1007/s12565-017-0395-9.
- Seruga, B. *et al.* (2015) 'Failures in Phase III: Causes and Consequences', *Clinical Cancer Research*, 21(20), pp. 4552 LP – 4560. doi: 10.1158/1078-0432.CCR-15-0124.
- Shang, L. *et al.* (2018) 'Human hepatic stellate cell isolation and characterization', *Journal of Gastroenterology*, 53(1), pp. 6–17. doi: 10.1007/s00535-017-1404-4.
- Shearer, M. J., Fu, X. and Booth, S. L. (2012) 'Vitamin K nutrition, metabolism, and requirements: current concepts and future research', *Advances in nutrition (Bethesda, Md.)*, 3(2), pp. 182–195. doi:

10.3945/an.111.001800.

Shen, K. *et al.* (2011) 'Depletion of activated hepatic stellate cell correlates with severe liver damage and abnormal liver regeneration in acetaminophen-induced liver injury', *Acta Biochimica et Biophysica Sinica*, 43(4), pp. 307–315. doi: 10.1093/abbs/gmr005.

Shetty, S., Lalor, P. F. and Adams, D. H. (2018) 'Liver sinusoidal endothelial cells — gatekeepers of hepatic immunity', *Nature Reviews Gastroenterology & Hepatology*, 15(9), pp. 555–567. doi: 10.1038/s41575-018-0020-y.

Shteyer, E. *et al.* (2004) 'Disruption of hepatic adipogenesis is associated with impaired liver regeneration in mice', *Hepatology*, 40(6), pp. 1322–1332. doi: <https://doi.org/10.1002/hep.20462>.

Simon, G. *et al.* (2020) 'The effect of hepatic steatosis and fibrosis on liver weight and dimensions', *Legal Medicine*, 47, p. 101781. doi: <https://doi.org/10.1016/j.legalmed.2020.101781>.

Skardal, A. *et al.* (2017) 'Multi-tissue interactions in an integrated three-tissue organ-on-a-chip platform', *Scientific reports*, 7(1), p. 8837. doi: 10.1038/s41598-017-08879-x.

So, J. *et al.* (2020) 'Liver progenitor cell-driven liver regeneration', *Experimental & Molecular Medicine*, 52(8), pp. 1230–1238. doi: 10.1038/s12276-020-0483-0.

Song, Z., Xiaoli, A. M. and Yang, F. (2018) 'Regulation and Metabolic Significance of De Novo Lipogenesis in Adipose Tissues', *Nutrients*. doi: 10.3390/nu10101383.

Sørensen, K. K. *et al.* (2015) 'Liver Sinusoidal Endothelial Cells', *Comprehensive Physiology*. (Major Reference Works), pp. 1751–1774. doi: <https://doi.org/10.1002/cphy.c140078>.

Stanford, K. I. *et al.* (2009) 'Syndecan-1 is the primary heparan sulfate proteoglycan mediating hepatic clearance of triglyceride-rich lipoproteins in mice', *The Journal of Clinical Investigation*, 119(11), pp. 3236–3245. doi: 10.1172/JCI38251.

Strick-Marchand, H. *et al.* (2008) 'Lymphocytes Support Oval Cell-Dependent Liver Regeneration', *The Journal of Immunology*, 181(4), pp. 2764 LP – 2771. doi: 10.4049/jimmunol.181.4.2764.

Strnad, P. *et al.* (2017) 'Liver — guardian, modifier and target of sepsis', *Nature Reviews Gastroenterology & Hepatology*, 14(1), pp. 55–66. doi: 10.1038/nrgastro.2016.168.

Sudo, K. *et al.* (2005) 'Lack of tumor necrosis factor receptor type 1 inhibits liver fibrosis induced by carbon tetrachloride in mice', *Cytokine*, 29(5), pp. 236–244. doi: <https://doi.org/10.1016/j.cyto.2004.11.001>.

Suga, T. *et al.* (2017) 'Preference of Conjugated Bile Acids over Unconjugated Bile Acids as Substrates for OATP1B1 and OATP1B3', *PloS one*, 12(1), pp. e0169719–e0169719. doi: 10.1371/journal.pone.0169719.

Tacke, F. (2017) 'Targeting hepatic macrophages to treat liver diseases', *Journal of Hepatology*, 66(6), pp. 1300–1312. doi: 10.1016/j.jhep.2017.02.026.

Tanaka, T. *et al.* (2015) 'Interleukin-27 induces the endothelial differentiation in Sca-1+ cardiac resident stem cells', *Cytokine*, 75(2), pp. 365–372. doi: <https://doi.org/10.1016/j.cyto.2015.06.009>.

Tang, L. *et al.* (2009) 'Liver Sinusoidal Endothelial Cell Lectin, LSECtin, Negatively Regulates Hepatic T-Cell Immune Response', *Gastroenterology*, 137(4), pp. 1498–1508.e5. doi: 10.1053/j.gastro.2009.07.051.

Tarlow, B. D. *et al.* (2014) 'Bipotential adult liver progenitors are derived from chronically injured mature hepatocytes', *Cell stem cell*. 2014/10/09, 15(5), pp. 605–618. doi: 10.1016/j.stem.2014.09.008.

Thomas, J. A. *et al.* (2011) 'Macrophage therapy for murine liver fibrosis recruits host effector cells improving fibrosis, regeneration, and function', *Hepatology*, 53(6), pp. 2003–2015. doi: <https://doi.org/10.1002/hep.24315>.

Tirnitz-Parker, J. E. E. *et al.* (2010) 'Tumor necrosis factor-like weak inducer of apoptosis is a mitogen for liver progenitor cells', *Hepatology*, 52(1), pp. 291–302. doi: <https://doi.org/10.1002/hep.23663>.

Trampert, D. C. *et al.* (2021) 'Hepatobiliary acid-base homeostasis: Insights from analogous secretory epithelia', *Journal of Hepatology*, 74(2), pp. 428–441. doi: <https://doi.org/10.1016/j.jhep.2020.10.010>.

Tran, S. *et al.* (2020) 'Impaired Kupffer Cell Self-Renewal Alters the Liver Response to Lipid Overload during Non-alcoholic Steatohepatitis', *Immunity*, 53(3), pp. 627–640. doi: 10.1016/j.immuni.2020.06.003.

Trefts, E., Gannon, M. and Wasserman, D. H. (2017) 'The liver', *Current biology: CB*, 27(21), pp. R1147–R1151. doi: 10.1016/j.cub.2017.09.019.

Tsuchida, T. and Friedman, S. L. (2017) 'Mechanisms of hepatic stellate cell activation', *Nature Reviews Gastroenterology & Hepatology*, 14(7), pp. 397–411. doi: 10.1038/nrgastro.2017.38.

Tsuchiya, A. and Lu, W.-Y. (2019) 'Liver stem cells: Plasticity of the liver epithelium', *World journal of gastroenterology*, 25(9), pp. 1037–1049. doi: 10.3748/wjg.v25.i9.1037.

Tumanov, A. V. *et al.* (2009) 'T Cell-Derived Lymphotoxin Regulates Liver Regeneration', *Gastroenterology*, 136(2), pp. 694–704.e4. doi: 10.1053/j.gastro.2008.09.015.

Tummala, K. S. *et al.* (2017) 'Hepatocellular Carcinomas Originate Predominantly from Hepatocytes and Benign Lesions from Hepatic Progenitor Cells', *Cell Reports*, 19(3), pp. 584–600. doi: 10.1016/j.celrep.2017.03.059.

Uhrig, A. *et al.* (2005) 'Development and functional consequences of LPS tolerance in sinusoidal endothelial cells of the liver', *Journal of Leukocyte Biology*, 77(5), pp. 626–633. doi:

<https://doi.org/10.1189/jlb.0604332>.

Vassiliou, I. *et al.* (2010) 'The combined effect of erythropoietin and granulocyte macrophage colony stimulating factor on liver regeneration after major hepatectomy in rats', *World Journal of Surgical Oncology*, 8(1), p. 57. doi: 10.1186/1477-7819-8-57.

Vollmar, B. and Menger, M. D. (2009) 'The Hepatic Microcirculation: Mechanistic Contributions and Therapeutic Targets in Liver Injury and Repair', *Physiological Reviews*, 89(4), pp. 1269–1339. doi: 10.1152/physrev.00027.2008.

Walesky, C. M. *et al.* (2020) 'Functional compensation precedes recovery of tissue mass following acute liver injury', *Nature Communications*, 11(1), p. 5785. doi: 10.1038/s41467-020-19558-3.

Wang, M.-J. *et al.* (2017) 'Hepatocyte polyploidization and its association with pathophysiological processes', *Cell Death & Disease*, 8(5), pp. e2805–e2805. doi: 10.1038/cddis.2017.167.

Weiskirchen, R. and Tacke, F. (2014) 'Cellular and molecular functions of hepatic stellate cells in inflammatory responses and liver immunology', *Hepatobiliary Surgery and Nutrition; Vol 3, No 6 (December 2014): Hepatobiliary Surgery and Nutrition (Special Focus on Liver Immunology: Part I)*.

Wen, Y. *et al.* (2021) 'Hepatic macrophages in liver homeostasis and diseases-diversity, plasticity and therapeutic opportunities', *Cellular & Molecular Immunology*, 18(1), pp. 45–56. doi: 10.1038/s41423-020-00558-8.

Weng, H. *et al.* (2013) 'IFN- γ inhibits liver progenitor cell proliferation in HBV-infected patients and in 3,5-diethoxycarbonyl-1,4-dihydrocollidine diet-fed mice', *Journal of hepatology*. 2013/06/04, 59(4), pp. 738–745. doi: 10.1016/j.jhep.2013.05.041.

Wilkinson, P. D. *et al.* (2019) 'The Polyploid State Restricts Hepatocyte Proliferation and Liver Regeneration in Mice', *Hepatology*, 69(3), pp. 1242–1258. doi: <https://doi.org/10.1002/hep.30286>.

Williams, C. D. *et al.* (2010) 'Acetaminophen-induced hepatic neutrophil accumulation and inflammatory liver injury in CD18-deficient mice', *Liver International*, 30(9), pp. 1280–1292. doi: <https://doi.org/10.1111/j.1478-3231.2010.02284.x>.

Williams, M. J., Clouston, A. D. and Forbes, S. J. (2014) 'Links Between Hepatic Fibrosis, Ductular Reaction, and Progenitor Cell Expansion', *Gastroenterology*, 146(2), pp. 349–356. doi: <https://doi.org/10.1053/j.gastro.2013.11.034>.

Winn, N. C., Volk, K. M. and Hasty, A. H. (2020) 'Regulation of tissue iron homeostasis: the macrophage “ferrostat”', *JCI Insight*, 5(2). doi: 10.1172/jci.insight.132964.

Wright, G. *et al.* (2010) 'Role of aquaporin-4 in the development of brain oedema in liver failure', *Journal of Hepatology*, 53(1), pp. 91–97. doi: 10.1016/j.jhep.2010.02.020.

Wu, J. *et al.* (2010) 'Toll-like receptor-induced innate immune responses in non-parenchymal liver cells are cell type-specific', *Immunology*, 129(3), pp. 363–374. doi: <https://doi.org/10.1111/j.1365-2567.2009.03179.x>.

Xu, C., Li, C. Y.-T. and Kong, A.-N. T. (2005) 'Induction of phase I, II and III drug metabolism/transport by xenobiotics', *Archives of Pharmacal Research*, 28(3), p. 249. doi: 10.1007/BF02977789.

Xu, R. *et al.* (2013) 'Complement 5a stimulates hepatic stellate cells in vitro, and is increased in the plasma of patients with chronic hepatitis B', *Immunology*, 138(3), pp. 228–234. doi: <https://doi.org/10.1111/imm.12024>.

Xu, Y. *et al.* (2015) 'Activated adult microglia influence retinal progenitor cell proliferation and differentiation toward recoverin-expressing neuron-like cells in a co-culture model', *Graefe's Archive for Clinical and Experimental Ophthalmology*, 253(7), pp. 1085–1096. doi: 10.1007/s00417-015-2961-y.

Yamauchi, H. *et al.* (2003) 'Impaired liver regeneration after partial hepatectomy in db/db mice', *Experimental and Toxicologic Pathology*, 54(4), pp. 281–286. doi: <https://doi.org/10.1078/0940-2993-00265>.

Yang, C.-Y. *et al.* (2013) 'CLEC4F is an inducible C-type lectin in F4/80-positive cells and is involved in alpha-galactosylceramide presentation in liver', *PloS one*, 8(6), pp. e65070–e65070. doi: 10.1371/journal.pone.0065070.

Yang, W. *et al.* (2019) 'Neutrophils promote the development of reparative macrophages mediated by ROS to orchestrate liver repair', *Nature Communications*, 10(1), p. 1076. doi: 10.1038/s41467-019-09046-8.

Yin, S. *et al.* (2011) 'Enhanced liver regeneration in IL-10-deficient mice after partial hepatectomy via stimulating inflammatory response and activating hepatocyte STAT3', *The American journal of pathology*, 178(4), pp. 1614–1621. doi: 10.1016/j.ajpath.2011.01.001.

Yona, S. *et al.* (2013) 'Fate Mapping Reveals Origins and Dynamics of Monocytes and Tissue Macrophages under Homeostasis', *Immunity*, 38(1), pp. 79–91. doi: 10.1016/j.immuni.2012.12.001.

Yu, M.-C. *et al.* (2004) 'Inhibition of T-cell responses by hepatic stellate cells via B7-H1-mediated T-cell apoptosis in mice', *Hepatology*, 40(6), pp. 1312–1321. doi: <https://doi.org/10.1002/hep.20488>.

Zampelas, A. and Magriplis, E. (2019) 'New Insights into Cholesterol Functions: A Friend or an Enemy?', *Nutrients*, 11(7), p. 1645. doi: 10.3390/nu11071645.

Zhao, J. *et al.* (2020) 'Single-cell RNA sequencing reveals the heterogeneity of liver-resident immune cells in human', *Cell Discovery*, 6(1), p. 22. doi: 10.1038/s41421-020-0157-z.

Zheng, M., Sun, H. and Tian, Z. (2018) 'Natural killer cells in liver diseases', *Frontiers of Medicine*, 12(3), pp. 269–279. doi: 10.1007/s11684-018-0621-4.

ANNEXES
PhD Publications

PUBLICATION 1

**Kupffer cell restoration after partial
hepatectomy is driven by their local cell
proliferation in autocrine and paracrine IL-6-
dependent manners**

1 **Kupffer cell restoration after partial hepatectomy is mainly driven by their**
2 **local cell proliferation in autocrine and paracrine IL-6-dependent manners**

3
4
5 Yeni Ait Ahmed^{1,2}, Yaojie Fu¹, Robim M Rodrigues¹, Yong He¹, Yukun Guan¹, Adrien Guillot¹,
6 Ruixue Ren¹, Dechun Feng¹, Juan Hidalgo³, Cynthia Ju⁴, Fouad Lafdil^{2,5,6}✉, Bin Gao¹✉
7

8 ¹Laboratory of Liver Diseases, National Institute on Alcohol Abuse and Alcoholism, National
9 Institutes of Health, Bethesda, MD, USA; ²Université Paris-Est-Créteil, Créteil, France;
10 ³Universitat Autònoma de Barcelona, Barcelona, Spain; ⁴Department of Anesthesiology,
11 McGovern Medical School, University of Texas Health Science Center at Houston, Houston,
12 TX, USA ; ⁵INSERM U955, Institut Mondor de Recherche Biomédicale, Créteil, France;
13 ⁶Institut Universitaire de France (IUF), Paris, France.
14

15 **Running title: Kupffer cell repopulation after partial hepatectomy via IL-6**

16
17 Yeni Ait Ahmed was a participant in the NIH Graduate Partnerships Program and a graduate
18 student in the Université Paris-Est-Créteil, France, and is affiliated with the Université Paris-Est-
19 Créteil (UPEC) and the NIH Graduate Partnerships Program.
20

21 ✉ **Corresponding authors:**

22 Fouad Lafdil, Ph.D., Université Paris-Est-Créteil, UMR-S955, UPEC; INSERM, U955, F-94000,
23 Créteil, France; Tel: +33 1 49 81 35 38. Email: fouad.lafdil@inserm.fr

24 Bin Gao, M.D., Ph.D., Laboratory of Liver Diseases, NIAAA/NIH, 5625 Fishers Lane,
25 Bethesda, MD 20892, USA; Tel: 301-443-3998. E-mail: bgao@mail.nih.gov
26

27 **ABSTRACT**

28

29 Kupffer cells (KC), the liver resident macrophages, originate from the fetal yolk sac and
30 represent one of the largest macrophage populations in the body. However, the current data on
31 the origin of the cells that restore macrophages during liver injury and regeneration remain
32 controversial. Here, we propose to address the question whether, in regenerating livers post
33 partial hepatectomy (PHx), liver macrophage restoration results from circulating monocyte
34 infiltration or local KC proliferation, and uncover the underlying mechanisms. By using several
35 strains of genetically modified mice and performing immunohistochemistry analyses, we
36 demonstrated that local KC proliferation mainly contributed to the restoration of liver
37 macrophages after PHx. The peak of KC proliferation was impaired in *Il6* knockout (KO) mice
38 and restored after administration of IL-6 protein, whereas KC proliferation was not affected in
39 *Il4* KO and *Csf2* KO mice. The source of IL-6 was identified using hepatocyte- and myeloid-
40 specific *Il6* KO mice, which revealed both hepatocytes and myeloid cells contribute to IL-6
41 production after PHx. Moreover, KC proliferation peak was also impaired in myeloid-specific *Il6*
42 receptor KO mice after PHx, suggesting that IL-6 signaling directly promotes KC proliferation.
43 Studies using several inhibitors that blocked IL-6 signaling pathways revealed that sirtuin 1
44 (SIRT1) contributed to IL-6-mediated KC proliferation *in vitro*. Genetic deletion of the *Sirt1*
45 gene in myeloid cells including KC impaired KC proliferation after PHx. In conclusion, our data
46 suggest that KC repopulation after PHx is mainly driven by local KC proliferation, which is
47 dependent on IL-6 and SIRT1 activation in KC.

48

49 **Keywords: IL-6, Sirtuin 1, liver regeneration, Kupffer cells, myeloid cells**

50 **INTRODUCTION**

51

52 The liver has unique capabilities to regenerate after injury or partial resection. These regenerative
53 functions are orchestrated by a variety of immune cells and mediators produced by these cells.^{1,2}
54 The liver is considered as an immunological organ as it concentrates a high density of immune
55 cells such as resident macrophages called Kupffer cells (KC), innate immune cells (eg. NK and
56 NKT cells), and lymphoid immune cells including T and B lymphocytes.^{3,4} Among those cells,
57 KC represent one of the largest macrophage populations in the human body,⁵ and represent about
58 30% of hepatic non-parenchymal cells.⁶ Because KC play a wide variety of roles in metabolism,
59 toxin clearance, immunity, and inflammation, their quick restoration is critical in the clinical care
60 of liver diseases including injury mediated by alcohol, lipids, drugs, toxins, viruses, bacteria, and
61 ischemia, to ensure hepatic regeneration.⁷⁻¹⁰ However, their origin and the underlying
62 mechanisms leading to their restoration remain largely unclear or controversial.

63

64 Alongside resident KC which derive from the fetal yolk-sac, bone-marrow derived monocytes
65 circulate through the hepatic vascular network at steady state as patrolling cells and infiltrate the
66 liver tissue upon injury.^{7,8,11} Recently, several markers have been identified to discriminate
67 between KC and infiltrating macrophages. The ionized calcium-binding adapter molecule 1
68 (IBA1) has been described to be a common marker of both monocytes and KC as well as
69 monocyte and macrophage populations found in other organs of the body such as microglia.¹²
70 However, C-type lectin domain family 4 member F (CLEC4F) has been identified as the most
71 specific KC marker to date as it is not expressed by monocytes. KC are commonly described as
72 CD45⁺F4/80⁺CD11b^{intermediate}CLEC4F⁺ cells.^{13,14} Contrastingly, CX3CR1, the G-protein coupled

73 fractalkine receptor, is known to be expressed by monocytes and capsular macrophages and
74 absent from KC.¹⁵ The identification of these markers has led to better characterization of
75 hepatic macrophage populations and emerging evidence suggests that while at steady state most
76 macrophages present in the liver are identified as KC, following tissue damage and
77 inflammation, which causes loss of KC, circulating monocytes infiltrate the hepatic parenchyma.
78 For example, a loss and decrease of liver KC has been reported in several contexts fulminant
79 hepatitis including infection with murine cytomegalovirus¹⁶ or the bacterium *Listeria*
80 *monocytogenes*,¹⁷ and in models of methionine/choline-deficient (MCD) diet-induced
81 nonalcoholic steatohepatitis (NASH)¹⁸ and hepatocellular carcinoma (HCC).¹⁹ Several studies
82 suggest that such KC loss is partially replaced by circulating monocytes.^{17,20-23} However,
83 whether local KC proliferation or circulating monocytes restore liver macrophages after partial
84 hepatectomy (PHx) remains unclear.

85

86 The liver has remarkable ability to regenerate after tissue loss (such as PHx) or injury.^{24,25}
87 Previous studies suggest that PHx triggers the activation of KC which in turn start producing
88 cytokines such as tumor necrosis factor α (TNF- α) and interleukin 6 (IL-6) that stimulate
89 hepatocyte proliferation^{24,25} and finely regulate liver regeneration to reach a stable liver mass.²⁶
90 Although the mechanisms of hepatocyte proliferation have been well described,²⁷ the underlying
91 mechanisms involved in macrophage replenishment remain unclear. As macrophages orchestrate
92 liver regeneration and interact with other hepatic cells in regenerating livers through the
93 production of cytokines,²⁸⁻³⁰ it is crucial to restore their pool to sustain the regenerative process.
94 In fact, studies have shown that liver regeneration is severely impaired when macrophages are
95 depleted.^{31,32} Among several cytokines produced by the liver during regenerative processes, IL-6

96 is known to be a key regulator of the hepatic parenchyma restoration.^{29,33} Indeed, deletion of the
97 *Il6* gene has been shown to cause liver failure in mice after PHx.³⁴ Interestingly, IL-6 is a
98 cytokine that targets several types of hepatic cells in addition to hepatocytes during
99 regeneration.^{35,36} IL-6 receptor is composed of two subunits, IL-6R α and gp130. While gp130 is
100 ubiquitously expressed in the body, IL-6R α is only expressed by a few cell types including
101 hepatocytes, KC, hepatic stellate cells, and biliary cells.^{35,36} In addition, IL-6 can also bind to
102 soluble IL-6R α to form a more stable IL-6/IL-6R α complex which can in turn bind to gp130
103 expressed on the cell membrane. This alternative pathway is called IL-6 trans-signaling and is
104 particularly important for IL-6 signaling in cells that do not express transmembrane IL-6R α .
105 This trans-signaling pathway has been associated with better liver regenerative capacities.^{37,38}
106 However little information is available about the potential impact of IL-6 on KC during liver
107 regeneration following PHx.

108

109 In the current study, we demonstrated that no apoptosis was observed in KC in the remnant liver
110 after PHx and that restoration of KC during liver regeneration in this model mainly originates
111 from local proliferation of remaining KC, which occurred in an IL-6-dependent manner through
112 the activation of SIRT1. Finally, both hepatocytes and myeloid cells contribute to IL-6
113 production after PHx.

114

115

116

117 **MATERIALS AND METHODS**

118

119 *Animals*

120 *Il6* KO, *Il4* KO, *Csf2* KO, *Ccr2* KO mice on a C57BL6/J background and their wild-type

121 C57BL6J mice were purchased from the Jackson Laboratory (Maine, ME). *Lyz^{Cre/Cre}*, *Alb^{Cre/Cre}*,

122 and *Cx3cr1^{GFP}* knock-in/knock-out mice were also purchased from Jackson Laboratory.

123 Homozygous *Cx3cr1^{GFP/GFP}* mice were bred with C57BL/6J mice to obtain heterozygous

124 *Cx3cr1^{GFP/-}* mice. Mice with specific deletion of the *Il6r* gene in myeloid cells (*Il6r^{Mye}* KO) were

125 generated via the several steps of crossing *Il6r^{f/f}* with *Lyz^{Cre/Cre}* mice as described previously.³⁹

126 *Il6^{f/f}* mice were generated as previously described.⁴⁰ Mice with specific deletion of the *Il6* gene

127 in myeloid cells (*Il6^{Mye}* KO) and hepatocytes (*Il6^{Hep}* KO) were generated via several steps of

128 crossing *Il6^{f/f}* with *Lyz^{Cre/Cre}* and *Alb^{Cre/Cre}* mice respectively. AlbCre line has been widely used to

129 delete genes of interest in hepatocytes, and we have previously demonstrated *Il6* in hepatocytes

130 is effectively deleted in *Il6^{Hep}* KO mice.⁴¹ Effective deletion of *Il-6* in KC from *Il6^{Mye}* KO mice

131 was confirmed in the current study (see result section). Myeloid-specific *Sirt1* knockout mice

132 (*Sirt1^{Mye}* KO) were kindly provided by Dr. Xiaoling Li (NIEHS, NIH) as described previously.⁴²

133

134 Eight- to 12-week-old mice were used for PHx. Free access to food and water was offered to the

135 animals and bacon softies were added on the floor to all animals after surgeries. PHx was

136 performed between 8 am and 1 pm, under sterile conditions. The animals were anesthetized with

137 isoflurane and buprenorphine (0.6 g/g) was injected subcutaneously on the left side of the

138 abdomen. Alcohol and betadine were applied on the abdominal skin of the animals prior to the

139 midline laparotomy. The left and middle lobes of the liver along with the gall bladder were

140 consecutively ligated at the base and resected. The abdominal wall and the skin were sutured
141 separately. BrdU (Sigma-Aldrich, St. Louis, MO) was injected intraperitoneally (50 g/g) 2
142 hours before sacrifice. When indicated, recombinant IL-6 (2 g/g) was injected intraperitoneally.
143 Recombinant human IL-6 was produced through recombinant DNA technology and purified as
144 described previously.⁴³

145
146 All animals received humane care in accordance with the Guide for the Care and Use of
147 Laboratory Animals published by the National Institutes of Health, and all animal experiments
148 were approved by the NIAAA Animal Care and Use Committee.

149

150 ***KC isolation***

151 KC were isolated from mouse livers as described by Marcela Aparicio-Vergara et al.⁴⁴ The liver
152 was first perfused with 50 mL of EGTA followed by 50 mL collagenase type I (0.075% in 1X
153 HBSS) perfusion solution. After perfusion, the liver was triturated and further digested with a
154 collagenase type I digestion solution (0.015%) for 10-20 min at 37°C on a shaker (90 rpm). The
155 obtained suspension was then filtered through a 70 µm nylon mesh and centrifuged for 5 min at
156 50 g. The supernatant containing the non-parenchymal cells was centrifuged at 500 g for 10 min.
157 The cell pellet was then resuspended in 8 mL of 40% Percoll, topped with 4 mL of HBSS and
158 then centrifuged at 1150 g for 17 min at 4°C. The interphase containing the non-parenchymal
159 cells was collected, washed with 1x HBSS and pelleted by centrifugation for 10 min at 500 g.
160 The obtained cell pellet was further processed by magnetic cell sorting (MACS) (endothelial cell
161 marker CD146 MicroBeads, Miltenyi) to remove sinusoidal endothelial cells as described by the
162 supplier's instructions. The CD146 negative cell fraction was seeded in 6-well plates and

163 cultured for 1 hour in RPMI supplemented with FBS (10%), penicillin (100 U/mL) and
164 streptomycin (100 µg/mL). Non-adherent cells were removed by washing, and the adherent cells
165 represented purified KC (the KC purity reached approximately 80%).

166

167 ***Cell culture***

168 Freshly isolated KC and mouse macrophage cell line RAW cells were cultivated in RPMI +10%
169 FBS and deprived for proliferation assays. The inhibitors used in this study were: EX-527
170 (SIRT-1) at 200 nM, SB203580 (P38/AKT) at 20 nM, PD98059 (MAPK/ERK) at 100 nM, and
171 SP600125 (JNK) at 100 nM, (Selleck Chemicals Llc, Houston, TX). When indicated, cells were
172 stimulated by adding rIL-6 (100 ng/ml) to the medium.

173

174 ***SIRT1 activity assay***

175 RAW cell nuclei were extracted using the NE-PER nuclear and cytoplasmic extraction kit
176 (Thermo Scientific, Waltham, MA), and were further processed to collect nuclear SIRT1 and to
177 assess enzyme activity using the SIRT1 activity assay kit (Abcam, Cambridge, UK) according to
178 manufacturer protocol.

179

180 ***Immunofluorescent staining***

181 Livers were collected after mouse euthanasia and were then placed in formalin for fixation. The
182 tissues were dehydrated in ethanol baths then embedded in paraffin. Tissues were sectioned one
183 day prior to staining and dried at 37°C. Deparaffinization and rehydration of the microsections
184 were realized using xylene and ethanol baths with decreasing concentrations. Tissue sections
185 were exposed to primary antibodies overnight at 4°C and secondary antibodies were applied for

186 1 hour at room temperature the following day after three washes of PBS. Antibodies: IBA1
187 (Abcam, Cambridge, UK), CLEC4F (Cell Signaling, Danvers, MA), F4/80 (Cell Signaling,
188 Danvers, MA), anti-rabbit Alexa fluor 488 #4412, anti-rat Alexa fluor 555 #4417 (Cell
189 Signaling), and streptavidin-conjugated 555 #S21381 (ThermoFisher, Waltham, MA).

190

191 BrdU staining was performed using the BrdU In-Situ Detection Kit #551321 (BD Pharmingen,
192 San Jose, CA). Biotinylated anti-BrdU primary antibodies were applied overnight at 4° after a
193 blocking step with goat serum for 1h. The following day, liver tissue sections were washed and
194 incubated with streptavidin coupled secondary antibodies for an hour.

195

196 ***ELISA assay***

197 Blood was collected retro-orbitally from mice at the indicated times post-PHx. Serum was
198 separated by centrifugation. Mouse IL-6 ELISA kit (M6000B) from R&D systems (Minneapolis,
199 MN) was used to quantify serum IL-6 levels and ELISA was performed following
200 manufacturer's instructions.

201

202 ***Mouse genotyping***

203 For genotyping purposes, pieces of ear were collected and digested using the DirectPCR Lysis
204 Reagent (Ear) kit (Viagen Biotech, Los Angeles, CA). The genotyping protocol information is
205 described on the Jax website. For *Il6^{fllox}* mice, DNA was amplified using the following primers:
206 *Il6^{fllox}* forward CCCACCAAGAACGATAGTCA and reverse GGT ATC CTC TGT GAA GTC
207 CTC.

208

209 ***RNA extraction and quantitative reverse transcription PCR (RT-qPCR)***

210 For gene expression and RNA extraction, snap frozen liver samples or freshly isolated KC and
211 RAW cell lines were placed in TRIzol reagent. Liver tissues were homogenized with beads in a
212 TissueLyser and collected in TRIzol. RNA was further extracted according to Qiagen RNEasy
213 Mini kit protocol and transcribed into cDNA. The primers used in this study were, for *Il6*:
214 forward 5'-TCCATCCAGTTGCCTTCTTG-3' and reverse 3'-
215 TTCCACGATTTCCCAGAGAAC-5'; *Il4*: forward 5'-GGTCTCAACCCCCAGCTAGT-3' and
216 reverse 3'-GCCGATGATCTCTCTCAAGTGAT-5'; *Csf2*: forward 5'-
217 GGCCTTGGAAGCATGTAGAGG-3' and reverse 3'-GGAGAACTCGTTAGAGACGACTT-
218 5'.

219

220 ***Statistical analysis***

221 Results are expressed as mean \pm SEM, and statistical significance was determined by a two-
222 tailed Student t test or one- or two-way analysis of variance as appropriate, using PRISM 9.0
223 software. Significance between multiple groups was determined by ANOVA tests. All $P < 0.05$
224 values were considered significant.

225

226

227

228 **RESULTS**

229

230 **Liver KC restoration after PHx is mainly driven by local KC proliferation independently**
231 **of circulating monocytes**

232 To determine the kinetics of hepatocyte and macrophage proliferation, liver tissues were
233 collected from 0 to 72 hours after PHx and Bromodeoxyuridine (BrdU) incorporation was
234 analyzed by immunofluorescence (Figure 1A). Hepatocyte proliferation peaked at 40h after PHx
235 (Figure 1A, B) where approximately 30% of hepatocytes were BrdU⁺. Next, proliferating
236 macrophages were identified by a double immunofluorescence staining for both IBA1 (a pan-
237 macrophage marker) and BrdU (a proliferation marker), which revealed that liver macrophage
238 proliferation peaked at 48h after PHx (Figure 1A, C). At the peak, approximately 22% of total
239 macrophages were proliferating (Figure 1C).

240

241 To address the question whether restoration of the pool of liver macrophages following PHx
242 resulted from recruitment of circulating monocytes or from resident KC proliferation, we
243 performed double immunostaining with IBA1 and CLEC4F antibodies. IBA1 is expressed by
244 both KC and infiltrating monocytes, while CLEC4F is specifically expressed in KC.^{13,14} At 48h
245 after surgery, immunohistochemistry analyses of livers from sham or PHx mice revealed that
246 more than 97% of total IBA1⁺ macrophages in the liver were found to also express CLEC4F
247 (Figure 1D, E), suggesting that macrophages found in the liver at the peak of proliferation after
248 PHx express KC specific marker CLEC4F, and very few CLEC4F⁻ IBA1⁺ infiltrating
249 macrophages were observed.

250 To further support the above conclusion, we used a murine model in which the green fluorescent
251 protein (GFP) gene was inserted under the control of *Cx3cr1* gene promotor, to track the flow of
252 circulating monocytes. The GFP immunohistochemical staining (Figure 1F) on liver tissue
253 sections revealed that the number of GFP⁺ infiltrating macrophages after PHx was low and
254 similar to that of sham mice (Figure 1G), suggesting that no significant monocyte infiltration
255 occurs after PHx. Furthermore, we investigated whether an impairment of circulating monocyte
256 infiltration affects macrophage restoration after PHx. To address this question, *Ccr2* KO mice, in
257 which *Ccr2* gene that encodes the key monocyte recruitment chemokine receptor CCR2, is
258 deleted, were subjected to PHx. Immunofluorescence analysis of liver tissue sections revealed
259 that both WT and *Ccr2* KO mice had approximately 30% of IBA1⁺ BrdU⁺ liver macrophages
260 40h and 48h after PHx, there were no differences between these two groups (Figure 1H, I),
261 suggesting that the peak of liver macrophage proliferation is not impacted when monocyte
262 chemotaxis is disrupted.

263

264 **Both IL-4 and colony-stimulating factor 2 (CSF2) are not required for the peak of KC** 265 **proliferation following PHx**

266 Both IL-4 and CSF-2 (also known as granulocyte-macrophage colony-stimulating factor: GM-
267 CSF) have been suggested to play an important role in macrophage proliferation and KC
268 renewal,^{45,46} therefore we first tested whether IL-4 contributes to KC proliferation after PHx. As
269 illustrated in Figure 2A, hepatic expression of *Il4* as detected by RT-qPCR was comparable in
270 sham and PHx mice. *Il4* KO mice displayed a trend with lower KC proliferation 40h and 48h
271 after PHx compared to WT mice, but the difference was not statistically significant (Figure 2B,
272 C). Similarly, hepatic expression of *Csf2* as detected by RT-qPCR was also comparable in sham

273 and PHx mice (Figure 2D). Deletion of the *Csf2* gene in *Csf2* KO mice did not affect KC
274 proliferation post-PHx (Figure 2E, F).

275

276 **IL-6 is required for the peak of KC proliferation following PHx**

277 IL-6 has been shown to contribute to hepatocyte proliferation after PHx,⁴⁷ we then proposed to
278 evaluate the potential impact of IL-6 on KC proliferation. Hepatic *Il6* mRNA expression levels
279 were upregulated in both sham and PHx groups with much higher levels in the latter group
280 (Figure 3A). To investigate the role of IL-6 in hepatocyte and KC repopulation after PHx, WT
281 and *Il6* KO mice were subjected to PHx, and hepatocyte and KC proliferation was assessed by
282 immunofluorescence staining (Figure 3B). All the WT mice survived 48h after PHx while the
283 survival rate in *Il6* KO group was 77%. The results showed that at 48h approximately 30% of
284 hepatocytes were BrdU⁺ in WT mice while proliferating hepatocytes did not exceed 10% in *Il6*
285 KO mice (Figure 3B, C). Moreover, intravenous injection of recombinant IL-6 (rIL-6) in PHx-
286 operated *Il6* KO mice partially restored hepatocyte proliferation (Figure 3C), suggesting that IL-6
287 plays an important role in promoting hepatocyte proliferation. Next, we examined KC
288 proliferation and found that 20% of IBA1⁺ cells were BrdU⁺ in WT mice, but they only
289 accounted for 6% in *Il6* KO mice (Figure 3D). Intravenous injection of rIL-6 fully restored the
290 peak of macrophage proliferation in PHx-operated *Il6* KO mice (Figure 3D).

291

292 **Both hepatocytes and KC are major sources of IL-6 after PHx**

293 To determine whether IL-6 is mainly produced by hepatocytes or myeloid cells, *Il6*^{Hep} KO and
294 *Il6*^{Mye} KO were subjected to PHx. Effective deletion of *Il-6* in hepatocytes in *Il6*^{Hep} KO mice was
295 reported previously.⁴¹ In addition, *LyzCre* has been used to effectively delete the interest genes

296 in KC by many labs including ours.⁴⁸ Here we further confirmed the efficacy of *Il6* deletion in
297 KC, which was assessed by isolating KC from *Il6*^{f/f} and *Il6*^{Mye} KO mice injected with LPS along
298 with control *Il6*^{f/f} mice injected with phosphate buffered saline (PBS). As LPS is a powerful
299 inducer of *Il6* expression, we showed that *Il6* mRNA levels were highly induced in KC isolated
300 from *Il6*^{f/f} mice 3h after LPS injection compared to the PBS control group, while there was no
301 induction of *Il6* mRNA levels in the *Il6*^{Mye} KO mice injected with LPS (Figure 4A). Sera were
302 collected 3h and 6h following surgery and were subjected to ELISA analysis of IL-6 levels. As
303 illustrated in Figure 4B, serum IL-6 concentrations were approximately 600 pg/mL in the *Il6*^{f/f}
304 control mice, which were significantly reduced to approximately 200 pg/mL in both *Il6*^{Hep} KO
305 and *Il6*^{Mye} KO mice. In addition, more than 20% of KC were proliferating (BrdU⁺) in *Il6*^{f/f} control
306 mice 48h after PHx, while only ~15% of KC were proliferating in *Il6*^{Hep} KO or *Il6*^{Mye} KO mice
307 (Figure 4C, D). Collectively these data showed that both hepatocytes and KC represent major
308 sources of IL-6 that contributes to KC proliferation.

309

310 **Disruption of IL-6 signaling in KC impairs their proliferation without triggering their** 311 **apoptosis after PHx**

312 To determine whether IL-6 leads to KC proliferation by direct or indirect effects, mice with
313 myeloid-specific *Il6r* deletion (*Il6r*^{Mye} KO) were subjected to PHx. In the WT group, 100% of
314 the mice survived 48h post-PHx, while the survival rate was reduced to 85% in the *Il6r*^{Mye} KO
315 group (n=7/group), however no significant difference in the liver to body weight ratio was found
316 between the two groups (Figure 5A). Livers from PHx-operated *Il6r*^{f/f} and *Il6r*^{Mye} KO mice were
317 collected and subjected to immunofluorescence analysis to study hepatocyte and KC
318 proliferation. As illustrated in Figure 5B-D, hepatocyte proliferation as detected by counting

319 BrdU⁺ hepatocytes was comparable between *Il6r^{f/f}* and *Il6r^{Mye}* KO mice, while KC proliferation
320 as detected by counting IBA⁺BrdU⁺ cells was significantly lower in *Il6r^{Mye}* KO mice than in
321 *Il6r^{f/f}* control mice 48h after PHx. To determine whether this reduced number of accumulating
322 KC was due to increased apoptosis, we performed TUNEL staining on liver tissue sections and
323 found few TUNEL⁺IBA1⁺ macrophages in both *Il6r^{f/f}* and *Il6r^{Mye}* KO mic 48h and 72h post-
324 PHx (Figure 5E), suggesting that the reduced number of proliferating KC in *Il6r^{Mye}* KO mice was
325 not due to enhanced macrophage apoptosis but rather to an impairment of their proliferative
326 capacities.

327

328 **IL-6 stimulates KC proliferation *in vivo* and *in vitro***

329 The above data suggest that IL-6 signaling in KC promotes KC proliferation after PHx. Next, we
330 asked whether IL-6 directly stimulates KC proliferation *in vivo* without PHx. To answer this
331 question, WT mice were treated with vehicle (PBS) or rIL-6. As illustrated in Figure 6A, B, rIL-
332 6 injection induced a significant increase of macrophage proliferation in the liver of WT mice,
333 without PHx, and no proliferating cells were detected after PBS injection. In addition, the
334 immunofluorescence analysis revealed that intravenous injection of rIL-6 led preferentially to an
335 induction of IBA1⁺ macrophage proliferation rather than hepatocyte proliferation. To define
336 whether IL-6 signaling on KC is required for IL-6 stimulation of KC proliferation *in vivo* without
337 PHx, *Il6r^{f/f}* mice and *Il6r^{Mye}* KO mice were treated with rIL-6, without PHx, and we found that
338 macrophages in proliferation reached 10% in *Il6r^{f/f}* mouse livers while this was reduced to 3% in
339 *Il6r^{Mye}* KO mice (Figure 6C, D), suggesting that IL-6 directly stimulates KC proliferation *in vivo*
340 by targeting IL-6R on KC even under normal conditions without PHx.

341

342 To further decipher the direct impact of IL-6 on macrophage proliferation, RAW macrophages
343 and freshly isolated KC were stimulated with rIL-6 *in vitro*. The immunocytochemistry analysis
344 revealed a basal level of 22% of BrdU⁺ RAW cells after 48h of culture in the control condition
345 (vehicle), which was significantly increased to 35% under rIL-6 stimulation (Figure 6E, F).
346 Similarly, on purified KC, rIL-6 was able to significantly increase their proliferation from 6% to
347 15% (Figure 6G, H). These results reveal the existence of a direct proliferative effect of IL-6 on
348 KC *in vivo* and *in vitro*.

349

350 **SIRT1 is involved in IL-6-mediated KC proliferation**

351 To further investigate the underlying factors involved in IL-6 signaling pathway leading to KC
352 proliferation, several inhibitors of downstream signaling pathways including SIRT1, p38/Akt,
353 MAPK/ERK and JNK were used (Figure 7A). As expected, rIL-6 induced RAW cell
354 proliferation when compared to the vehicle-treated cells. RAW cells exposed to both rIL-6 and
355 SIRT1 inhibitor showed a significantly reduced proliferation compared to RAW cells exposed to
356 rIL-6 alone, after 6h of culture (Figure 7A). No significant difference was reported with the other
357 inhibitors at both 3h and 6h time points. Next, we measured SIRT1 activity on RAW cells
358 exposed to rIL-6 and found that RAW macrophages stimulated with rIL-6 displayed a
359 significantly higher SIRT1 activity when compared to the controls (Figure 7B). These results
360 strongly suggest that IL-6 mediates KC proliferation in a SIRT1-dependent manner. To further
361 confirm these results, mice with myeloid cell-specific deletion of *Sirt1* gene (*Sirt1*^{Mye} KO) were
362 subjected to PHx. The analysis of liver weights at the time of sacrifice revealed that liver to body
363 weight ratios of *Sirt1*^{fl/fl} control mice were approximately 2.8, which were significantly reduced to
364 2.1 in *Sirt1*^{Mye} KO mice, 48h post-PHx (Figure 7C). Additionally, liver regeneration was further

365 analyzed by immunofluorescence and the results revealed that 48h post-PHx, hepatocyte
366 proliferation rate reached 20% in *Sirt1*^{fl/fl} mic, which was slightly but significantly reduced to
367 17% in *Sirt1*^{Mye} KO mice (Figure 7D,E). Interestingly, while over 20% of KC were BrdU⁺ in
368 *Sirt1*^{fl/fl} mice 48h after surgery, this proliferation rate significantly dropped to less than 5% in
369 *Sirt1*^{Mye} KO mice (Figure 7D, F). Altogether these results suggest that SIRT1 is required for
370 proper KC proliferation mediated by IL-6 after PHx.

371
372
373
374
375

376 **DISCUSSION**
377

378 In response to tissue damage, the liver has the unique ability to undergo a regenerative process
379 finely orchestrated by KC to maintain its mass and functions^{1,2}. As the total number of KC is
380 dramatically reduced following liver resection or partial liver transplantation, it is vital to restore
381 their initial pool. In the present study, we brought new insights shedding lights on the origin of
382 hepatic macrophages during liver regeneration after PHx, and on the underlying mechanisms of
383 their restoration.

384

385 ***Liver KC restoration after PHx is predominantly driven by local KC proliferation with minor***
386 ***contribution from circulating macrophages***

387 In this study we showed that macrophage proliferation peaked at 48h post-PHx, a few hours after
388 that of hepatocytes occurring at 40h. Whether new macrophages are derived from circulating
389 monocytes or resident KC after PHx was not clear. In fact, the origin of repopulating hepatic
390 macrophages has remained controversial as recent studies have provided conflicting data about
391 the capacity of monocytes and KC to give rise to a fully regenerated pool of liver macrophages
392 during liver injury.^{7,8} These conflicting data might result from the different models used to
393 investigate the origin of hepatic macrophages. In a study where KC were completely depleted in
394 a healthy liver without PHx, KC restoration was achieved from bone-marrow derived monocyte
395 recruitment and differentiation into the liver.⁴⁹ In another study where all immune cells including
396 KC in mice were depleted before PHx by non-lethal 5 Gy irradiation, the authors suggest that
397 monocytes were recruited into partially hepatectomized livers and play a pivotal role in
398 accelerating liver regeneration.²¹ However, under conditions where residual KC are preserved in
399 the remaining part of the liver after PHx, we provided several lines of evidence suggesting that

400 circulating monocytes are minor components contributing to restore the initial pool of KC. First,
401 after PHx, few CX3CR1 labelled monocytes were recruited into regenerating livers. Second,
402 *Ccr2* deficiency in mice, which is a key chemokine receptor for monocyte recruitment, had
403 normal KC repopulation after PHx. Third, most of macrophages found in the liver 48h post-PHx,
404 at the peak of liver macrophage proliferation, were IBA⁺CLEC4F⁺ KC, and few IBA⁺CLEC4F⁻
405 infiltrating monocytes were detected in regenerating liver after PHx. Lastly, CLEC4F⁺ KC were
406 capable of self-proliferation following PHx. In the current study, we have mainly examined the
407 peak of KC proliferation and have not traced KC at the later time points post PHx, so we cannot
408 rule out the contribution of infiltrating macrophages to liver macrophage restoration in this
409 model; however, we believe the infiltrating macrophage contribution at later time points post
410 PHx is still minor because partially hepatectomized liver is associated with little inflammation
411 and monocyte infiltration at later time points.

412

413 ***IL-6 plays an important role in promoting KC proliferation after PHx in autocrine and***
414 ***paracrine manners***

415 Although PHx is not characterized by a strong inflammatory response, several cytokines that are
416 involved in macrophage proliferation such as IL-6 are elevated post PHx.^{2,50} In the current
417 study, we demonstrated that after PHx, KC proliferation was impaired in *Il6* KO mice but not in
418 *Il4* KO and *Csf2* KO mice. Administration of rIL-6 injection partially increased hepatocyte
419 proliferation and interestingly, fully restored KC proliferation in *Il6* KO mice after PHx.
420 Collectively, our data suggest that IL-6 but not IL-4 or CSF-2 plays a critical role in promoting
421 KC proliferation after PHx.

422

423 Although the elevation of IL-6 after PHx has been well documented, the source of this cytokine
424 during liver regeneration remains obscure. Previous studies suggest that PHx induces an increase
425 of gut-derived LPS in the blood,⁵¹ which likely contributes to IL-6 elevation after PHx because
426 LPS is well known to stimulate macrophages to produce IL-6. In addition, one study suggests
427 that LPS can also stimulate hepatocytes to produce IL-6.⁵² However, the exact sources of IL-6
428 after PHx remain unclear. In the current study, we demonstrated that serum levels of IL-6 were
429 reduced by approximately 50% in myeloid- and hepatocyte-specific *Il6* KO mice, respectively,
430 compared to WT mice after PHx. Thus, our data suggest that after PHx not only hepatocytes
431 represent a significant source of IL-6 as a paracrine manner to promote KC proliferation, but KC
432 could also be considered as an important autocrine source of IL-6. Because KC and hepatocyte
433 proliferation were significantly impaired in both *Il6*^{Mye} KO and *Il6*^{Hep} KO mice, it is plausible to
434 predict that KC and hepatocyte proliferation in double mutant mice with *Il6* deletion in both
435 hepatocytes and KC will be further decreased compared to those in single KO mice.

436

437 ***IL-6 promotes KC proliferation without affecting KC survival after PHx by enhancing SIRT1***
438 ***activity***

439 In the current study, we performed double immunofluorescence staining that can clearly detect *in*
440 *situ* KC and macrophage proliferation. By using this method, we demonstrated that KC
441 proliferation is reduced in *Il6* KO, hepatocyte- or myeloid-specific *Il6* KO mice, myeloid-
442 specific *Il6r* KO, and that IL-6 stimulates KC and macrophage proliferation *in vitro*, clearly
443 supporting a direct stimulatory effect of IL-6 on KC proliferation *in vivo* and *in vitro*. The flow
444 cytometry experiment is an alternative method to detect KC proliferation, which could be also
445 performed to examine and confirm the role of IL-6 on KC proliferation in the future.

446

447 To explore the molecular mechanisms by which IL-6 stimulates KC proliferation, we used
448 several inhibitors to block IL-6 downstream signaling pathways. Interestingly, among these
449 inhibitors, the SIRT1 inhibitor showed the strongest inhibition to block IL-6 stimulation of KC
450 proliferation *in vitro*. Furthermore, we demonstrated that genetic deletion of *Sirt1* in myeloid
451 cells including KC markedly reduced KC proliferation *in vivo* after PHx, and impaired liver
452 regeneration, as shown by the reduction of liver to body weight ratio and hepatocyte proliferation
453 in *Sirt1*^{Mye} KO mice. In addition, IL-6 treatment directly increased SIRT1 activity in
454 macrophages, suggesting that SIRT1 contributes to IL-6 promotion of KC proliferation during
455 liver regeneration after PHx. A recent study also reported that SIRT1 plays a role in stimulating
456 macrophage proliferation as demonstrated by the findings that SIRT1 overexpression via
457 transfection of *Sirt1* into bone-marrow derived macrophages was associated with an increased
458 macrophage proliferation *in vitro*; whereas SIRT1 blockade by CRISPR/Cas9 gene editing or by
459 nicotinamide injection in mice impaired respectively alveolar and peritoneal macrophage self-
460 renewal capacities.⁵³ Interestingly, previous studies have reported in the PHx model that age-
461 related SIRT1 reduction and SIRT1 inhibition by short-interfering RNA (siRNA) were
462 associated with a less efficient liver regeneration (hepatocyte proliferation) after PHx.⁵⁴
463 Collectively, SIRT1 not only promotes KC renewal but also stimulates hepatocyte proliferation
464 after PHx.

465

466 In addition to promoting macrophage proliferation, IL-6 signaling also plays an important role in
467 enhancing macrophage survival.⁵⁵ However, in the current study, no enhanced KC apoptosis was
468 observed in myeloid cell-specific *Il6r* knockout mice compared to WT mice, suggesting that IL-6

469 is not required for KC survival after PHx or, alternatively, that IL-6 trans-signaling might be
470 contributing. Indeed, IL-6 receptor (IL-6R) exists in two forms: a transmembrane receptor (mIL-
471 6R) and a soluble receptor (sIL-6R). By binding to mIL-6R, IL-6 activates the canonical
472 signaling pathway and subsequently predominantly triggers anti-inflammatory responses. On the
473 other hand, in cells that do not express mIL-6R, IL-6 can activate the trans-signaling pathway via
474 binding to sIL-6R.⁵⁵ Interestingly, our recent studies demonstrated that IL-6 signaling is required
475 for infiltrating macrophage survival but not KC survival in the liver of high-fat diet-fed mice.³⁹
476 Taken together, IL-6 is required for KC proliferation but not for KC survival after PHx, which is
477 probably because long-lived KC do not need IL-6 signaling for survival.

478

479 In conclusion, our findings brought new insights into the origin of KC in regenerating liver after
480 PHx, showing local proliferation of remaining KC independently of circulating monocytes. In
481 this process, KC proliferation is partly controlled by IL-6 produced by both hepatocytes and KC,
482 in regenerating livers, and IL-6 stimulates KC proliferation by increasing SIRT1 activity. Future
483 studies on the interaction between IL-6 and other cytokines and growth factors such as
484 hepatocyte growth factor which is known to be involved in hepatocyte proliferation after PHx
485 could provide additional insights into the mechanisms implicated in KC proliferation.

486 **Acknowledgments**

487 Yeni Ait Ahmed was a participant in the NIH Graduate Partnerships Program and a graduate
488 student in the Université Paris-Est-Créteil, France, and is affiliated with the Université Paris-Est-
489 Créteil (UPEC) and the NIH Graduate Partnerships Program. The work was supported by the
490 intramural program of the NIAAA (Bin Gao), the Institut Universitaire de France (Fouad Lafdil),
491 and the Ministerio de Economía y Competitividad and European Regional Development Fund
492 RTI2018-101105-B-100 RTI2018-101105-B-100 (Juan Hidalgo).

493

494

495 **Author contributions**

496 YAA designed and performed surgical procedures and experimental work and wrote the paper.
497 YF, RMR, YH, YG, AG, RR, DF helped with PHx surgery, cell isolation, protocol optimization,
498 and other experiments. JH and CJ helped analyze the data and edited the paper. FL and BG
499 designed and supervised the study and wrote the manuscript.

500

501 **Conflict of Interest**

502 The authors declare no conflict of interest.

503

504

505

506 **REFERENCES**

507

- 508 1 Dong Z, Wei H, Sun R, Tian Z. The roles of innate immune cells in liver injury and
509 regeneration. *Cell Mol Immunol* 2007; **4**: 241–252.
- 510 2 Markose D, Kirkland P, Ramachandran P, Henderson NC. Immune cell regulation of liver
511 regeneration and repair. *J Immunol Regen Med* 2018; **2**: 1–10.
- 512 3 Gao B, Jeong W-I, Tian Z. Liver: An organ with predominant innate immunity.
513 *Hepatology* 2008; **47**: 729–736.
- 514 4 Heymann F, Tacke F. Immunology in the liver — from homeostasis to disease. *Nat Rev*
515 *Gastroenterol Hepatol* 2016; **13**: 88–110.
- 516 5 Merlin S, Bhargava KK, Ranaldo G, Zanolini D, Palestro CJ, Santambrogio L *et al.*
517 Kupffer Cell Transplantation in Mice for Elucidating Monocyte/Macrophage Biology and
518 for Potential in Cell or Gene Therapy. *Am J Pathol* 2016; **186**: 539–551.
- 519 6 Nguyen-Lefebvre AT, Horuzsko A. Kupffer Cell Metabolism and Function. *J Enzymol*
520 *Metab* 2015; **1**: 101.
- 521 7 Wen Y, Lambrecht J, Ju C, Tacke F. Hepatic macrophages in liver homeostasis and
522 diseases-diversity, plasticity and therapeutic opportunities. *Cell Mol Immunol* 2021; **18**:
523 45–56.
- 524 8 Krenkel O, Tacke F. Liver macrophages in tissue homeostasis and disease. *Nat Rev*
525 *Immunol* 2017; **17**: 306–321.
- 526 9 Cai J, Zhang X-J, Li H. The Role of Innate Immune Cells in Nonalcoholic Steatohepatitis.
527 *Hepatology* 2019; **70**: 1026–1037.
- 528 10 Wang H, Mehal W, Nagy LE, Rotman Y. Immunological mechanisms and therapeutic
529 targets of fatty liver diseases. *Cell Mol Immunol* 2021; **18**: 73–91.

- 530 11 Tacke F, Zimmermann HW. Macrophage heterogeneity in liver injury and fibrosis. *J*
531 *Hepatol* 2014; **60**: 1090–1096.
- 532 12 Guillot A, Buch C, Jourdan T. Kupffer Cell and Monocyte-Derived Macrophage
533 Identification by Immunofluorescence on Formalin-Fixed, Paraffin-Embedded (FFPE)
534 Mouse Liver Sections. In: Aouadi M, Azzimato V (eds). *Kupffer Cells: Methods and*
535 *Protocols*. Springer US: New York, NY, 2020, pp 45–53.
- 536 13 Hsieh S-LE, Yang C-Y. CLEC4F, A Kupffer Cells Specific Marker, Is Critical for
537 Presentation of Alfa-Galactoceromide to NKT Cells. *J Immunol* 2009; **182**: 78.
- 538 14 Yang C-Y, Chen J-B, Tsai T-F, Tsai Y-C, Tsai C-Y, Liang P-H *et al*. CLEC4F is an
539 inducible C-type lectin in F4/80-positive cells and is involved in alpha-galactosylceramide
540 presentation in liver. *PLoS One* 2013; **8**: e65070–e65070.
- 541 15 Yona S, Kim K-W, Wolf Y, Mildner A, Varol D, Breker M *et al*. Fate Mapping Reveals
542 Origins and Dynamics of Monocytes and Tissue Macrophages under Homeostasis.
543 *Immunity* 2013; **38**: 79–91.
- 544 16 Borst K, Frenz T, Spanier J, Tegtmeyer P-K, Chhatbar C, Skerra J *et al*. Type I interferon
545 receptor signaling delays Kupffer cell replenishment during acute fulminant viral
546 hepatitis. *J Hepatol* 2018; **68**: 682–690.
- 547 17 Blériot C, Dupuis T, Jouvion G, Eberl G, Disson O, Lecuit M. Liver-Resident
548 Macrophage Necroptosis Orchestrates Type 1 Microbicidal Inflammation and Type-2-
549 Mediated Tissue Repair during Bacterial Infection. *Immunity* 2015; **42**: 145–158.
- 550 18 Devisscher L, Scott CL, Lefere S, Raevens S, Bogaerts E, Paridaens A *et al*. Non-
551 alcoholic steatohepatitis induces transient changes within the liver macrophage pool. *Cell*
552 *Immunol* 2017; **322**: 74–83.

- 553 19 Lefere S, Degroote H, Van Vlierberghe H, Devisscher L. Unveiling the depletion of
554 Kupffer cells in experimental hepatocarcinogenesis through liver macrophage subtype-
555 specific markers. *J Hepatol* 2019; **71**: 631–633.
- 556 20 Zigmund E, Samia-Grinberg S, Pasmanik-Chor M, Brazowski E, Shibolet O, Halpern Z *et al.* Infiltrating Monocyte-Derived Macrophages and Resident Kupffer Cells Display
557 Different Ontogeny and Functions in Acute Liver Injury. *J Immunol* 2014; **193**: 344–353.
- 558
559 21 Nishiyama K, Nakashima H, Ikarashi M, Kinoshita M, Nakashima M, Aosasa S *et al.*
560 Mouse CD11b+Kupffer Cells Recruited from Bone Marrow Accelerate Liver
561 Regeneration after Partial Hepatectomy. *PLoS One* 2015; **10**: e0136774.
- 562 22 Reid DT, Reyes JL, McDonald BA, Vo T, Reimer RA, Eksteen B. Kupffer Cells Undergo
563 Fundamental Changes during the Development of Experimental NASH and Are Critical in
564 Initiating Liver Damage and Inflammation. *PLoS One* 2016; **11**: e0159524.
- 565 23 Tran S, Baba I, Poupel L, Dussaud S, Moreau M, Gélinau A *et al.* Impaired Kupffer Cell
566 Self-Renewal Alters the Liver Response to Lipid Overload during Non-alcoholic
567 Steatohepatitis. *Immunity* 2020; **53**: 627–640.
- 568 24 Elchaninov A V, Fatkhudinov TK, Usman NY, Kananykhina EY, Arutyunyan I V,
569 Makarov A V *et al.* Dynamics of macrophage populations of the liver after subtotal
570 hepatectomy in rats. *BMC Immunol* 2018; **19**: 23.
- 571 25 Fausto N, Campbell JS, Riehle KJ. Liver regeneration. *Hepatology* 2006; **43**: S45–S53.
- 572 26 Ichikawa T, Zhang Y-Q, Kogure K, Hasegawa Y, Takagi H, Mori M *et al.* Transforming
573 growth factor β and activin tonically inhibit DNA synthesis in the rat liver. *Hepatology*
574 2001; **34**: 918–925.
- 575 27 Weglarz TC, Sandgren EP. Timing of hepatocyte entry into DNA synthesis after partial

576 hepatectomy is cell autonomous. *Proc Natl Acad Sci* 2000; **97**: 12595–12600.

577 28 Melgar-Lesmes P, Edelman ER. Monocyte-endothelial cell interactions in the regulation
578 of vascular sprouting and liver regeneration in mouse. *J Hepatol* 2015; **63**: 917–925.

579 29 Wen Y, Feng D, Wu H, Liu W, Li H, Wang F *et al*. Defective Initiation of Liver
580 Regeneration in Osteopontin-Deficient Mice after Partial Hepatectomy due to Insufficient
581 Activation of IL-6/Stat3 Pathway. *Int J Biol Sci* 2015; **11**: 1236–1247.

582 30 Shan Z, Ju C. Hepatic Macrophages in Liver Injury. *Front. Immunol.* 2020; **11**: 322.

583 31 Abshagen K, Eipel C, Kalff JC, Menger MD, Vollmar B. Loss of NF- κ B activation in
584 Kupffer cell-depleted mice impairs liver regeneration after partial hepatectomy. *Am J*
585 *Physiol Liver Physiol* 2007; **292**: 1570–1577.

586 32 Meijer C, Wiezer MJ, Diehl AM, Yang S-Q, Schouten HJ, Meijer S *et al*. Kupffer cell
587 depletion by CI2MDP-liposomes alters hepatic cytokine expression and delays liver
588 regeneration after partial hepatectomy. *Liver* 2000; **20**: 66–77.

589 33 Böhm F, Köhler UA, Speicher T, Werner S. Regulation of liver regeneration by growth
590 factors and cytokines. *EMBO Mol Med* 2010; **2**: 294–305.

591 34 Blindenbacher A, Wang X, Langer I, Savino R, Terracciano L, Heim MH. Interleukin 6 is
592 important for survival after partial hepatectomy in mice. *Hepatology* 2003; **38**: 674–682.

593 35 Schmidt-Arras D, Rose-John S. IL-6 pathway in the liver: From physiopathology to
594 therapy. *J Hepatol* 2016; **64**: 1403–1415.

595 36 He Y, Hwang S, Ahmed YA, Feng D, Li N, Ribeiro M *et al*. Immunopathobiology and
596 therapeutic targets related to cytokines in liver diseases. *Cell Mol Immunol* 2021; **18**: 18–
597 37.

598 37 Garbers C, Aparicio-Siegmund S, Rose-John S. The IL-6/gp130/STAT3 signaling axis:

599 recent advances towards specific inhibition. *Curr Opin Immunol* 2015; **34**: 75–82.

600 38 Fazel Modares N, Polz R, Haghghi F, Lamertz L, Behnke K, Zhuang Y *et al.* IL-6 Trans-
601 signaling Controls Liver Regeneration After Partial Hepatectomy. *Hepatology* 2019; **70**:
602 2075–2091.

603 39 Hou X, Yin S, Ren R, Liu S, Yong L, Liu Y *et al.* Myeloid cell-specific IL-6 signaling
604 promotes miR-223-enriched exosome production to attenuate NAFLD-associated fibrosis.
605 *Hepatology* 2020; **n/a**. doi:<https://doi.org/10.1002/hep.31658>.

606 40 Quintana A, Erta M, Ferrer B, Comes G, Giralt M, Hidalgo J. Astrocyte-specific
607 deficiency of interleukin-6 and its receptor reveal specific roles in survival, body weight
608 and behavior. *Brain Behav Immun* 2013; **27**: 162–173.

609 41 He Y, Feng D, Hwang S, Mackowiak B, Wang X, Xiang X *et al.* Interleukin-20
610 exacerbates acute hepatitis and bacterial infection by downregulating Inhibitor of kappa B
611 zeta; target genes in hepatocytes. *J Hepatol* 2021. doi:10.1016/j.jhep.2021.02.004.

612 42 Schug TT, Xu Q, Gao H, Peres-da-Silva A, Draper DW, Fessler MB *et al.* Myeloid
613 deletion of SIRT1 induces inflammatory signaling in response to environmental stress.
614 *Mol Cell Biol* 2010; **30**: 4712–4721.

615 43 Sun Z, Klein AS, Radaeva S, Hong F, El-Assal O, Pan H *et al.* In vitro interleukin-6
616 treatment prevents mortality associated with fatty liver transplants in rats.
617 *Gastroenterology* 2003; **125**: 202–215.

618 44 Aparicio-Vergara M, Tencerova M, Morgantini C, Barreby E, Aouadi M. Isolation of
619 Kupffer Cells and Hepatocytes from a Single Mouse Liver BT - Alpha-1 Antitrypsin
620 Deficiency : Methods and Protocols. In: Borel F, Mueller C (eds). . Springer New York:
621 New York, NY, 2017, pp 161–171.

622 45 Jenkins SJ, Ruckerl D, Cook PC, Jones LH, Finkelman FD, van Rooijen N *et al.* Local
623 macrophage proliferation, rather than recruitment from the blood, is a signature of TH2
624 inflammation. *Science* 2011; **332**: 1284–1288.

625 46 Wynn AA, Miyakawa K, Miyata E, Dranoff G, Takeya M, Takahashi K. Role of
626 Granulocyte/Macrophage Colony-Stimulating Factor in Zymocel-Induced Hepatic
627 Granuloma Formation. *Am J Pathol* 2001; **158**: 131–145.

628 47 Kim AR, Il Park J, Oh HT, Kim KM, Hwang J-H, Jeong MG *et al.* TAZ stimulates liver
629 regeneration through interleukin-6–induced hepatocyte proliferation and inhibition of cell
630 death after liver injury. *FASEB J* 2019; **33**: 5914–5923.

631 48 Feng D, Dai S, Liu F, Ohtake Y, Zhou Z, Wang H *et al.* Cre-inducible human CD59
632 mediates rapid cell ablation after intermedilysin administration. *J Clin Invest* 2016; **126**:
633 2321–2333.

634 49 Scott CL, Zheng F, De Baetselier P, Martens L, Saeys Y, De Prijck S *et al.* Bone marrow-
635 derived monocytes give rise to self-renewing and fully differentiated Kupffer cells. *Nat*
636 *Commun* 2016; **7**: 10321.

637 50 Vassiliou I, Lolis E, Nastos C, Tympa A, Theodosopoulos T, Dafnios N *et al.* The
638 combined effect of erythropoietin and granulocyte macrophage colony stimulating factor
639 on liver regeneration after major hepatectomy in rats. *World J Surg Oncol* 2010; **8**: 57.

640 51 Liu H-X, Keane R, Sheng L, Wan Y-JY. Implications of microbiota and bile acid in liver
641 injury and regeneration. *J Hepatol* 2015; **63**: 1502–1510.

642 52 Norris CA, He M, Kang L-I, Ding MQ, Radder JE, Haynes MM *et al.* Synthesis of IL-6
643 by Hepatocytes Is a Normal Response to Common Hepatic Stimuli. *PLoS One* 2014; **9**:
644 e96053.

645 53 Imperatore F, Maurizio J, Vargas Aguilar S, Busch CJ, Favret J, Kowenz-Leutz E *et al.*
646 SIRT1 regulates macrophage self-renewal. *EMBO J* 2017; **36**: 2353–2372.

647 54 Jin J, Iakova P, Jiang Y, Medrano EE, Timchenko NA. The reduction of SIRT1 in livers
648 of old mice leads to impaired body homeostasis and to inhibition of liver proliferation.
649 *Hepatology* 2011; **54**: 989–998.

650 55 Hunter CA, Jones SA. IL-6 as a keystone cytokine in health and disease. *Nat Immunol*
651 2015; **16**: 448–457.

652

653

654

655

656 **FIGURE LEGENDS**

657

658 **Figure 1: Liver macrophage restoration after PHx is mainly driven by local KC**

659 **proliferation.** (A-C) Immunofluorescence on liver tissue sections from sham and PHx mice

660 (n=5-6/group), 32h to 72h after surgery and stained with antibodies against IBA1 (green) and

661 BrdU (red). Hepatocytes are identified by their large round shape nuclei and macrophages are

662 identified by IBA1 staining. Proliferating macrophages are highlighted by the arrowheads.

663 Quantification of hepatocyte and macrophage proliferation at the indicated time points is shown

664 in panels B-C. (D-E) IBA1 (green) and CLEC4F (red) immunofluorescence staining on liver

665 tissue sections from sham and PHx mice 48h after surgery (n=6/group). Quantification of

666 CLEC4F⁺ and CLEC4F⁻ cells among IBA1⁺ cells in sham and PHx mice at 48h is shown in panel

667 E. (F-G) GFP immunohistochemistry staining on liver tissue sections from *Cx3cr1*^{GFP/-} mice

668 collected 48h after surgery (n=6/group). The number of CX3CR1^{GFP+} cells was counted and is

669 shown in panel G. Arrowheads represent CX3CR1^{GFP+} infiltrating monocytes. (H-I)

670 Immunofluorescence on liver tissue sections from WT and *Ccr2* KO mice collected 40h and 48h

671 after PHx (n=5-6/group) and stained with antibodies against IBA1 (green) and BrdU (red).

672 Arrowheads represent proliferating macrophages. Quantification of BrdU⁺ IBA1⁺ proliferating

673 macrophages is shown in panel I. BrdU was injected two hours before sacrifice in panels A, H.

674 Values are expressed as mean ± SEM. * *P*<0.05, ** *P*<0.01, *** *P*<0.001 in comparison to

675 corresponding sham groups in panels B-C, and to CLEC4F⁻ cells in panel E.

676

677 **Figure 2: IL-4 and CSF-2 are not required for the peak of KC proliferation after PHx.** (A)

678 Kinetics of *Il4* mRNA expression in liver homogenates by RT-qPCR from WT and *Il4* KO after

679 PHx. (B-C) Immunofluorescence on liver tissue sections from WT and *Il4* KO mice collected

680 48h after PHx (n=6/group) and stained with antibodies against IBA1 (green) and BrdU (red).
681 Arrowheads represent proliferating KC. Quantification of KC proliferation in WT and *Il4* KO
682 mice at various time points is shown in panel B. (D) Kinetics of *Csf2* mRNA expression in liver
683 homogenates by RT-qPCR from WT and *Csf2* KO mice after PHx. (E-F) Immunofluorescence
684 on liver tissue sections from WT and *Csf2* KO mice collected 48h after PHx (n=6/group) and
685 stained with antibodies against IBA1 (green) and BrdU (red). Arrowheads represent proliferating
686 KC. Quantification of KC proliferation in WT and *Csf2* KO mice at various time points is shown
687 in panel D. Values are expressed as mean \pm SEM. BrdU was injected two hours before sacrifice
688 in panels B and E.

689

690 **Figure 3: IL-6 is required for a proper KC proliferation after PHx.** (A) Kinetics of *Il6*
691 mRNA expression in liver homogenates from mice subjected to sham or PHx collected at
692 indicated time points and analyzed by RT-qPCR. (B-D) Immunofluorescence staining on liver
693 tissue sections from WT, *Il6* KO mice, and *Il6* KO mice with intravenous injection of rIL-6,
694 collected 48h after PHx (n=6-7/group). IBA1⁺ (green) and BrdU⁺ (red) cells depict proliferating
695 KC. BrdU was injected two hours before sacrifice in panel B. Quantification of proliferating
696 hepatocytes and KC 48h post PHx is shown in panels C and D, respectively. Values are
697 expressed as mean \pm SEM. * $P < 0.05$, ** $P < 0.01$, *** $P < 0.001$.

698

699 **Figure 4: Hepatocytes and KC are important sources of IL-6 after PHx.** (A) RT-qPCR
700 confirms *Il6* deletion in KC from *Il6*^{Mye} KO mice. *Il6* mRNA expression in KC isolated from
701 control *Il6*^{f/f} mice injected with PBS or LPS, and *Il6*^{Mye} KO mice injected with LPS (3h
702 injection). (B) Serum IL-6 levels from *Il6*^{f/f}, *Il6*^{Hep} KO and *Il6*^{Mye} KO mice 3h after PHx

703 (n=6/group). (C-D) Immunofluorescence on liver tissue sections from *Il6^{ff}*, *Il6^{Hep}* KO and *Il6^{Mye}*
704 KO mice collected 48h after PHx (n=6/group) and stained with anti-IBA1 (green) and BrdU
705 (red) antibodies. BrdU was injected two hours before sacrifice in panel C. Arrowheads represent
706 proliferating KC. Quantification of macrophage proliferation in the liver 48h after PHx is shown
707 in panel D. Values are expressed as mean \pm SEM. * $P < 0.05$, ** $P < 0.01$.

708

709 **Figure 5: Liver macrophage proliferation is impaired in *Il6^{Mye}* KO mice after PHx.** (A)

710 Liver to body weight ratios of *Il6^{ff}* and *Il6^{Mye}* KO mice post-PHx. (B) Immunofluorescence on
711 liver tissue sections from *Il6^{ff}* and *Il6^{Mye}* KO mice subjected to PHx (n=6/group). Liver tissues
712 were collected 40h, 48h and 72h after PHx and stained with antibodies targeting IBA1 (green)
713 and BrdU (red). BrdU was injected two hours before sacrifice. Arrowheads represent
714 proliferating KC. Quantification of hepatocyte and KC proliferation from panel B is shown in
715 panels C and D. (E) Immunofluorescence on liver tissue sections from *Il6^{ff}* and *Il6^{Mye}* KO mice
716 48h and 72h after PHx stained with anti-F4/80 and TUNEL antibodies. Values are expressed as
717 mean \pm SEM. * $P < 0.05$.

718

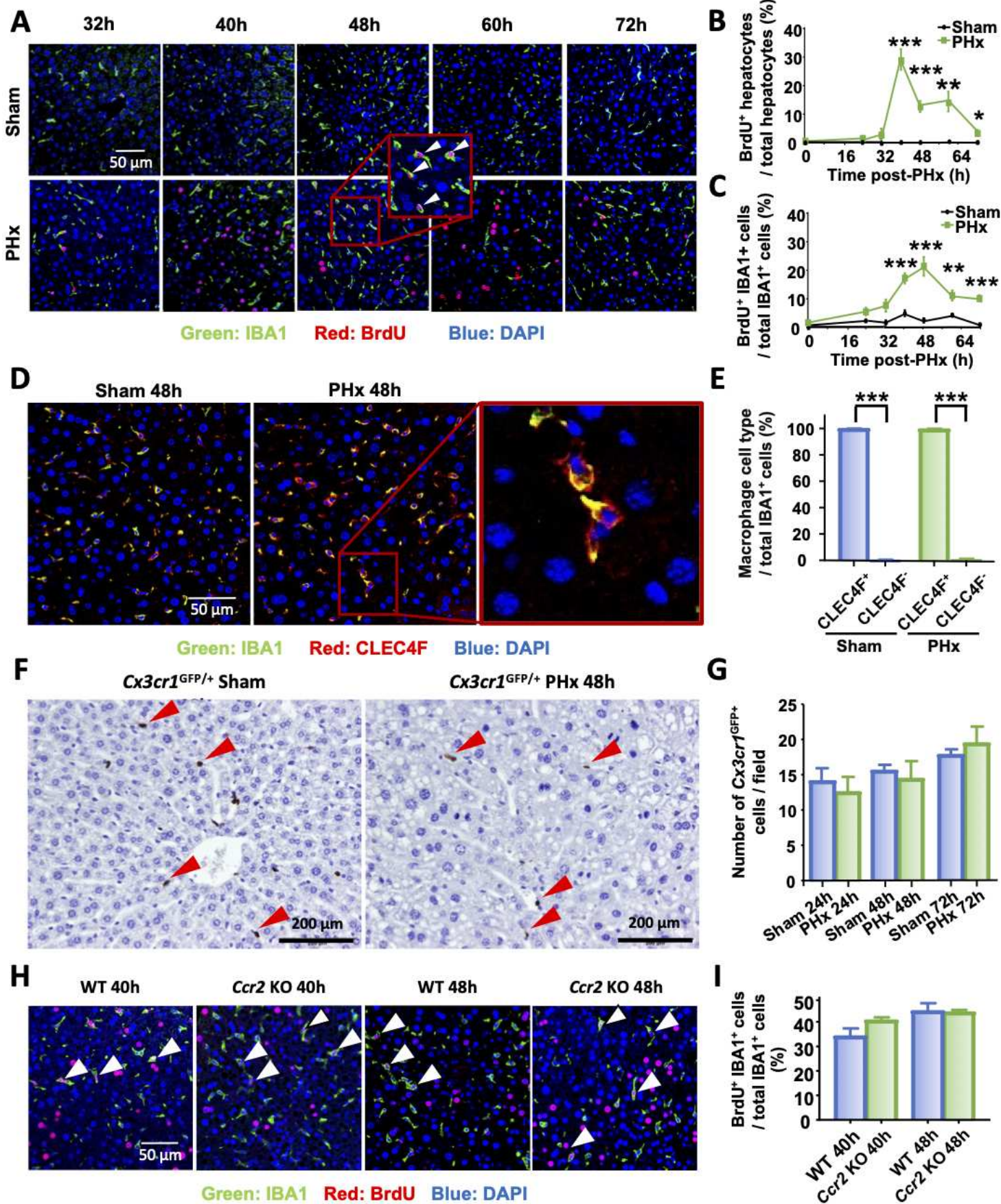
719 **Figure 6: IL-6 stimulates macrophage proliferation *in vivo* and *in vitro*.** (A-B) Naïve wild-

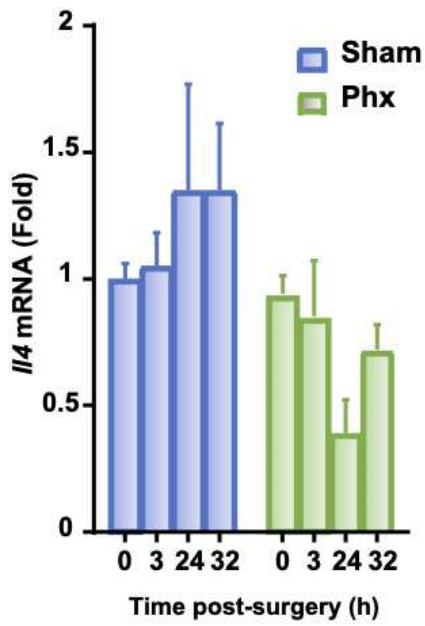
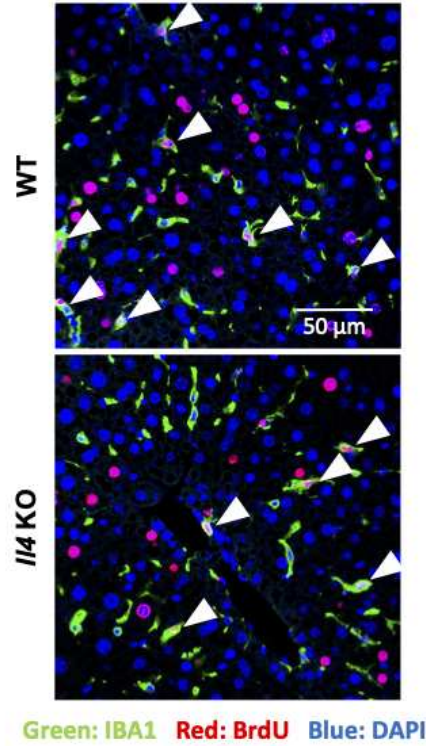
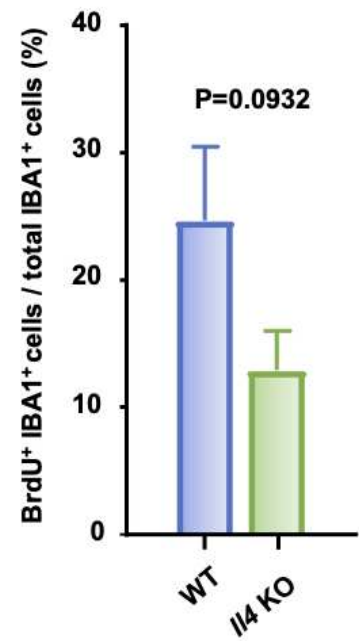
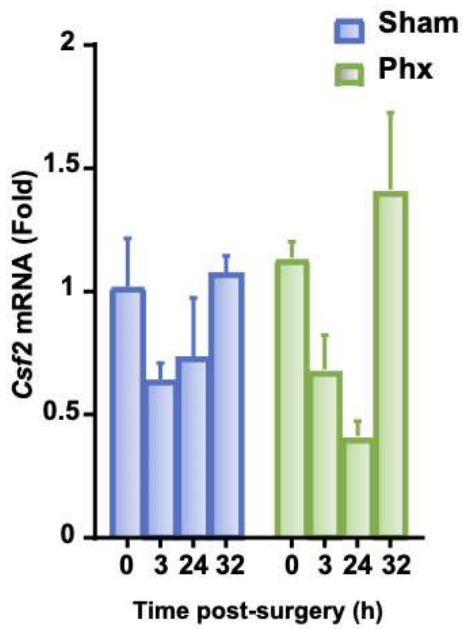
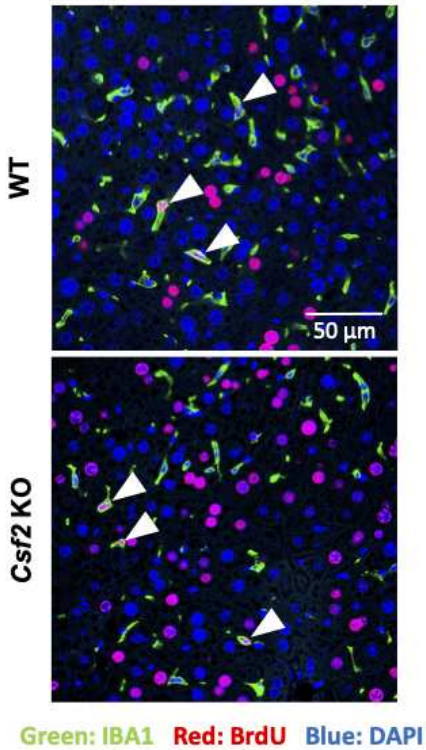
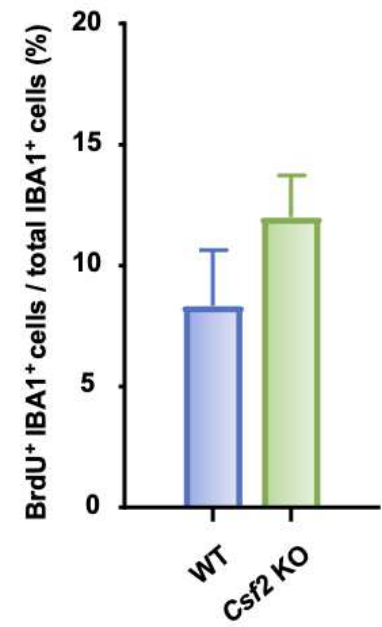
720 type mice (without PHx) were intravenously injected with PBS (control) or rIL-6, liver tissues
721 were collected 48h post injection (n=7/group) and were subjected to immunofluorescence
722 staining by using antibodies against IBA1 (green) and BrdU (red). Arrowheads represent
723 proliferating KC. Quantifications of BrdU⁺ hepatocytes and BrdU⁺ IBA1⁺ cells are shown in
724 panel B. ND: not detected. (C-D) *Il6^{ff}* and *Il6^{Mye}* KO mice without PHx were intravenously
725 injected with rIL-6 (n=7/group), liver tissues were collected 48h post injection and were

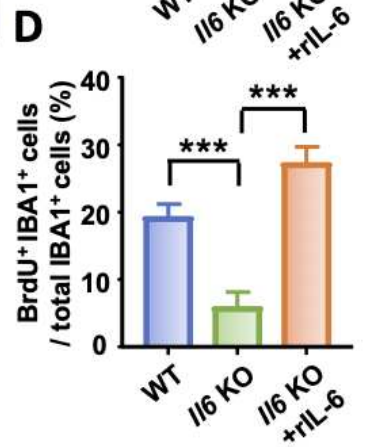
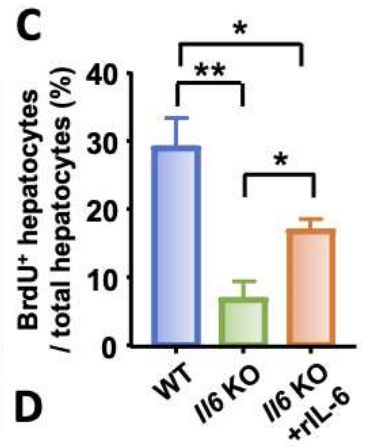
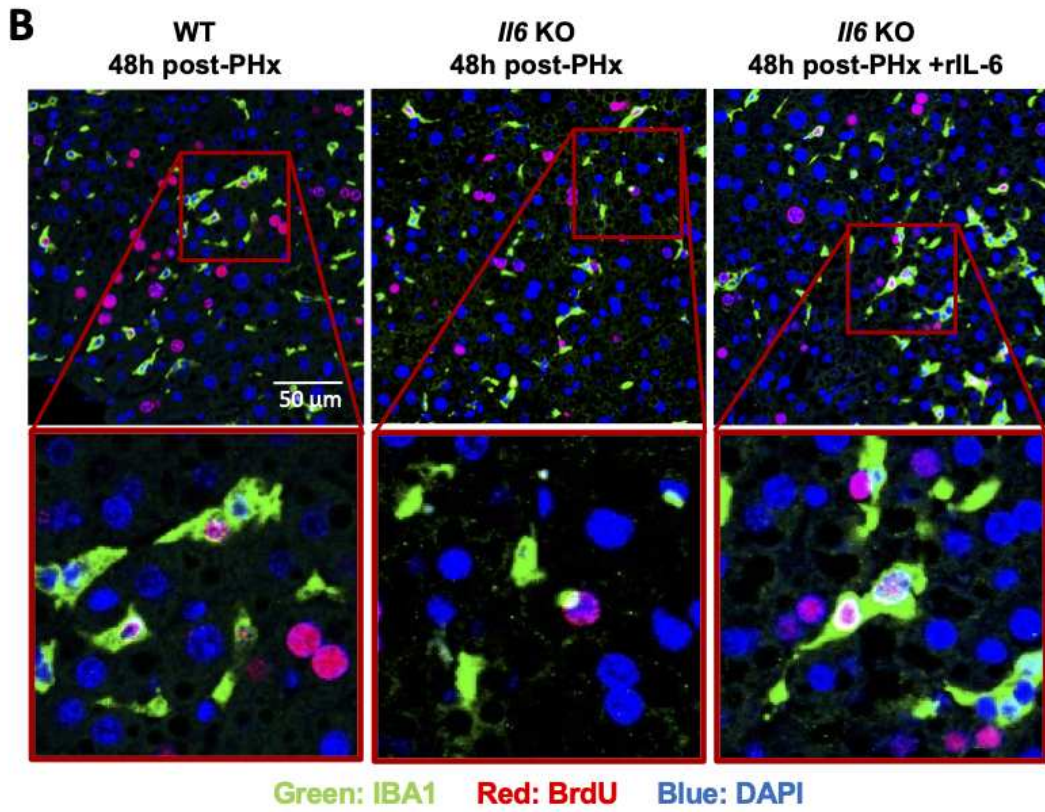
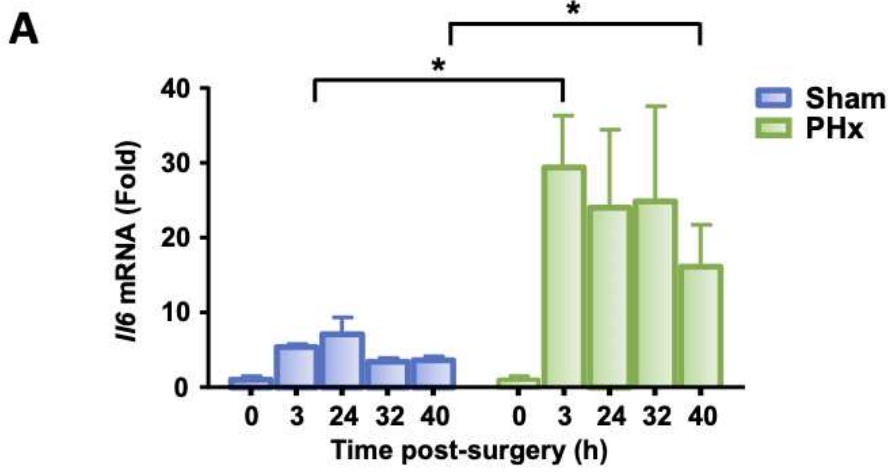
726 subjected to immunofluorescence staining by using antibodies against IBA1 (green) and BrdU
727 (red). Arrowheads represent proliferating KC. Quantification of proliferating KC in livers from
728 *Il6r^{f/f}* and *Il6r^{Mye}* KO mice 48h after intravenous injection of rIL-6 is shown in panel D. (E-F)
729 Immunofluorescence staining of RAW cells 48h after exposure to rIL-6 or control medium
730 (vehicle), stained with antibodies against BrdU (green). Proliferating RAW cells are identified by
731 the arrowheads. Quantification of proliferating RAW cells is shown in panel F. (G-H)
732 Immunofluorescence staining of freshly isolated KC 48h after exposure to rIL-6 or control
733 medium (vehicle), stained with antibodies against IBA1 (green) and BrdU (red). The arrowheads
734 represent proliferating KC. Quantification of KC proliferation is shown in panel H. BrdU was
735 injected two hours before sacrifice in panels A and C, and added in the culture medium two hours
736 before collecting the cells in panels E and G. Values are expressed as mean \pm SEM. ***
737 $P < 0.001$.

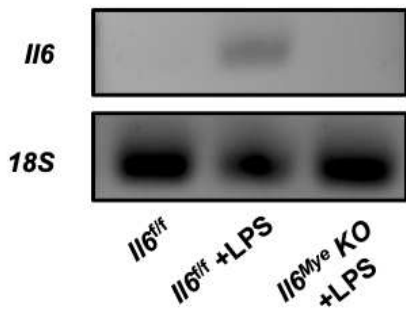
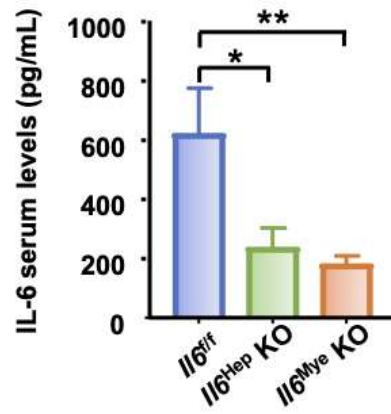
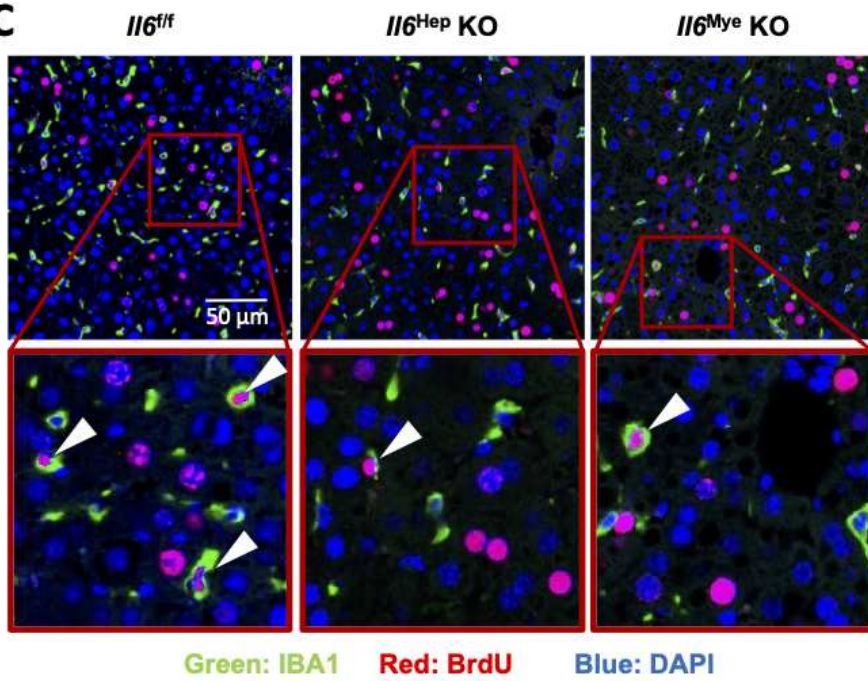
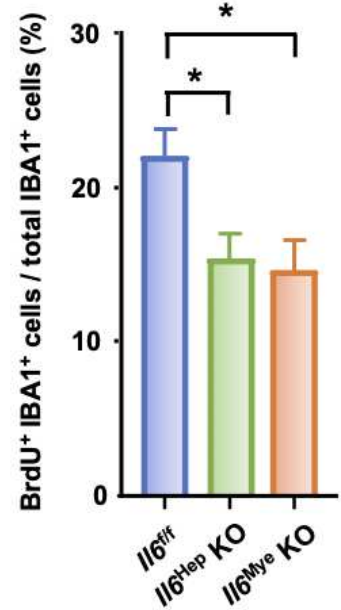
738

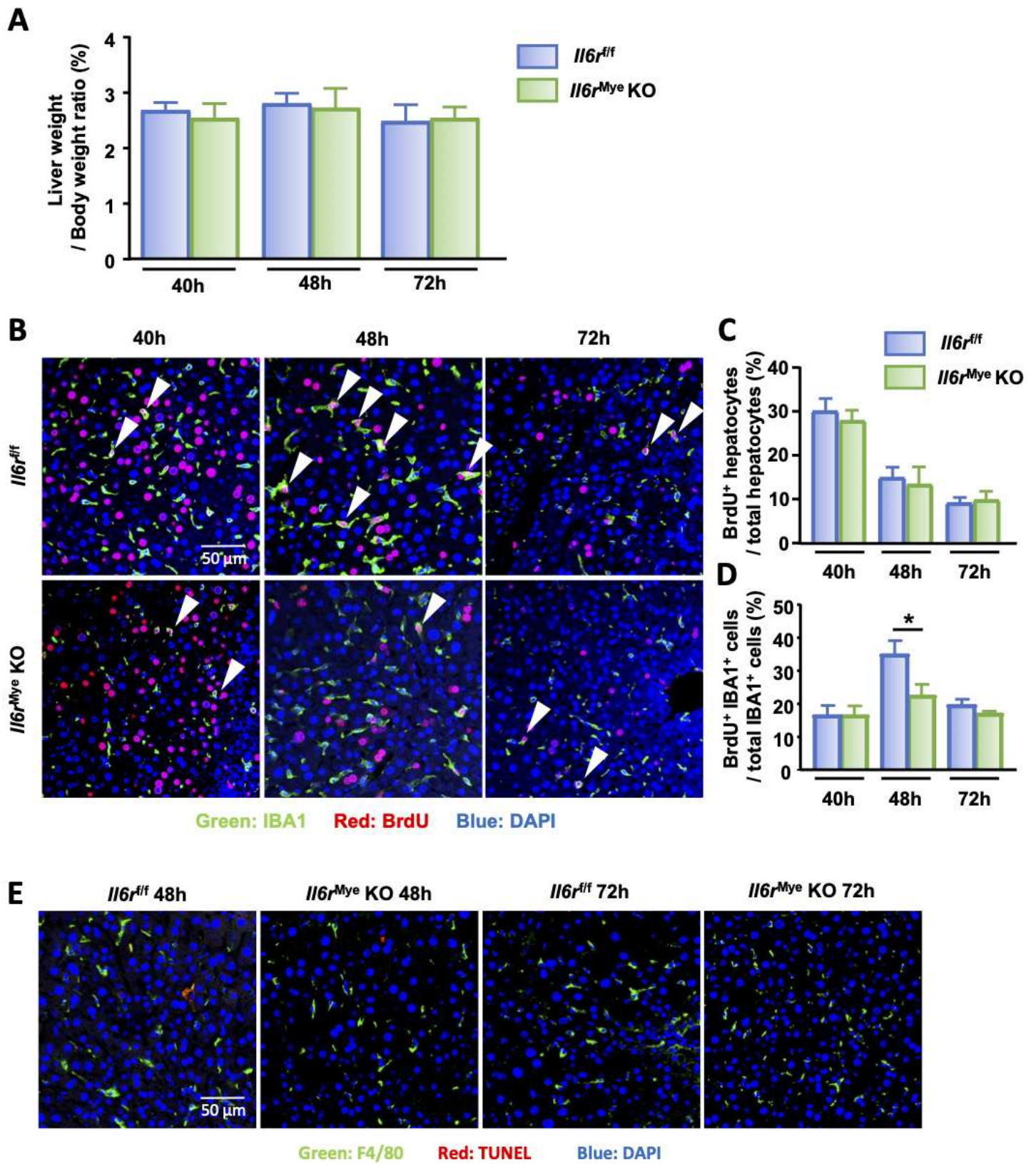
739 **Figure 7: IL-6 stimulates KC proliferation by inducing SIRT1 intracellular mechanisms**
740 **following PHx.** (A) RAW cell proliferation analysis by MTT assay 3h and 6h after exposure to
741 recombinant IL-6 (rIL-6) and the indicated inhibitors, or the vehicle control. (B) SIRT1
742 enzymatic activity in RAW cells after exposure to rIL-6 or control medium, recombinant SIRT1
743 (rSIRT1) activity is included as a positive control. (C) Liver to body weight ratios of *Sirt1^{f/f}* and
744 *Sirt1^{Mye}* KO mice sacrificed 48h post-PHx. (D) Immunofluorescence staining on liver tissue
745 sections from *Sirt1^{f/f}* and *Sirt1^{Mye}* KO mice 48h after PHx (n=6/group), stained with antibodies
746 against IBA1⁺ (green) and BrdU⁺ (red). Arrowheads represent proliferating KC. Quantification
747 of proliferating hepatocytes and KC from panel D is shown in panels E and F. Values are
748 expressed as mean \pm SEM. * $P < 0.05$, ** $P < 0.01$, *** $P < 0.001$.

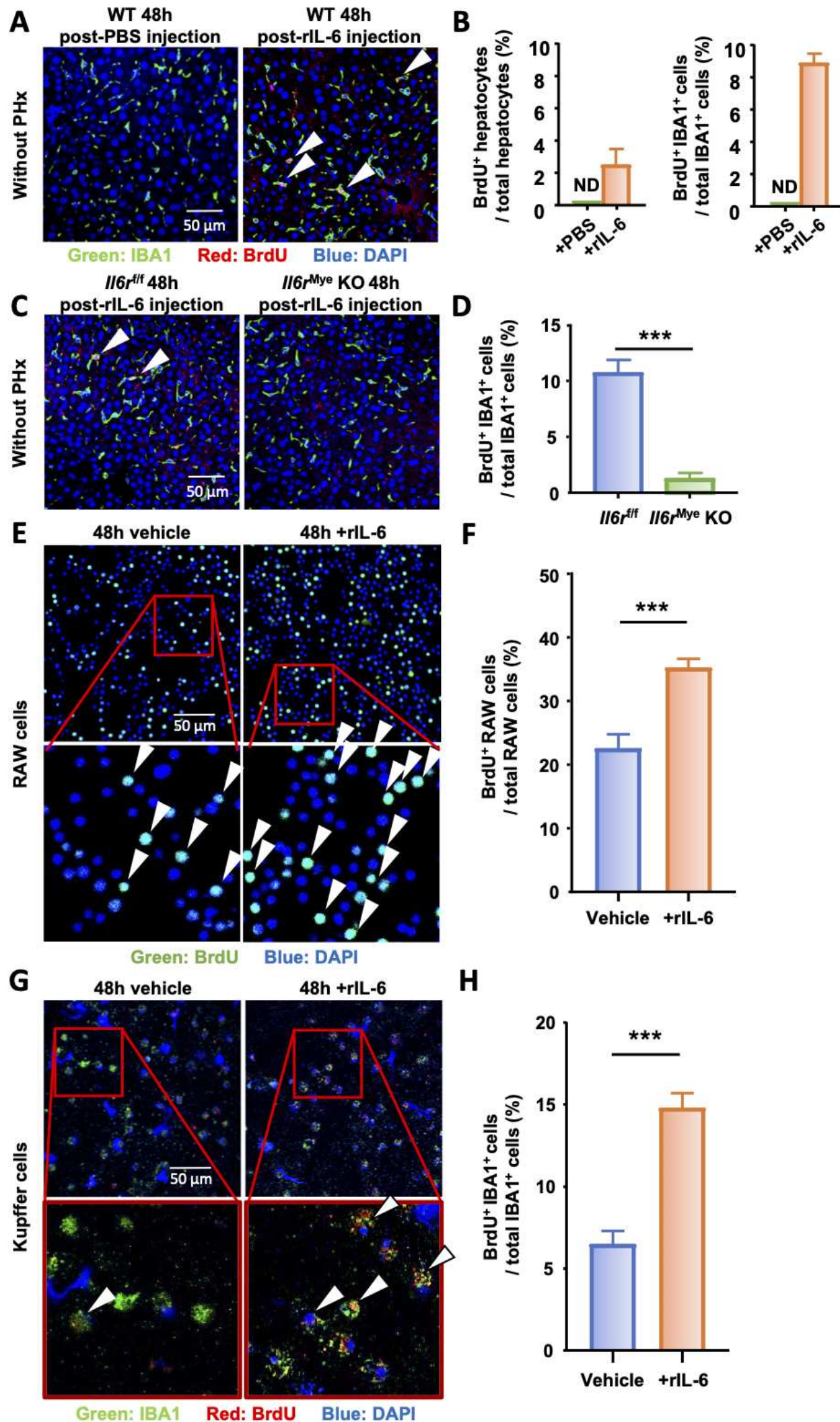


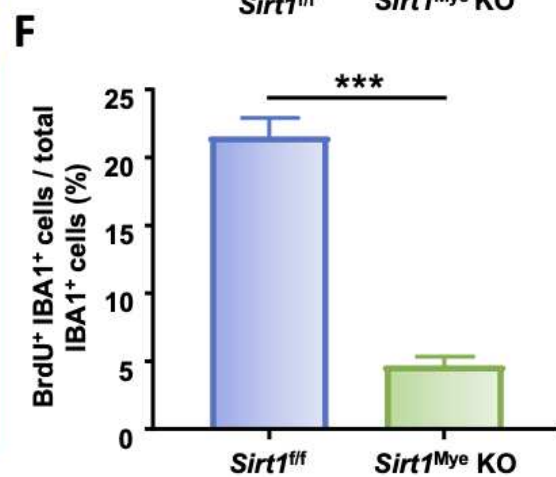
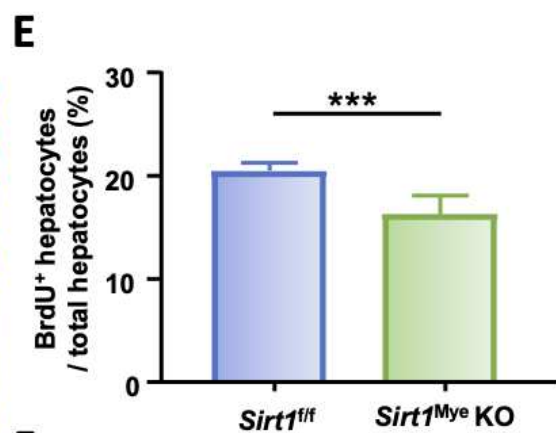
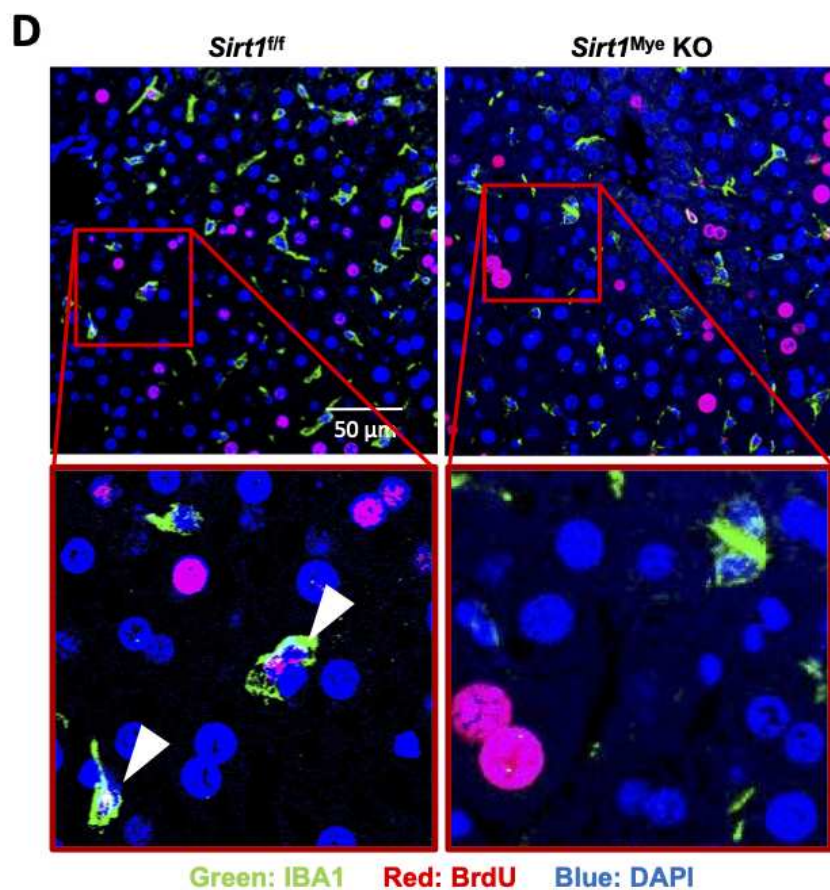
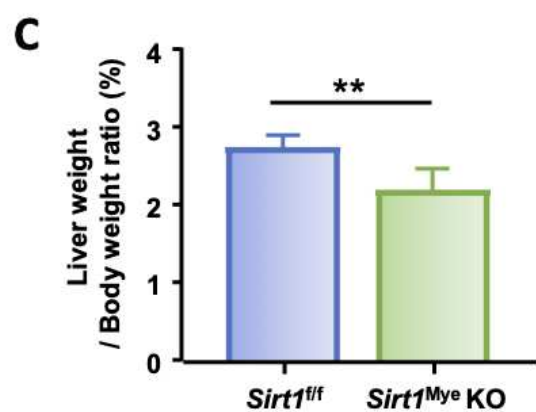
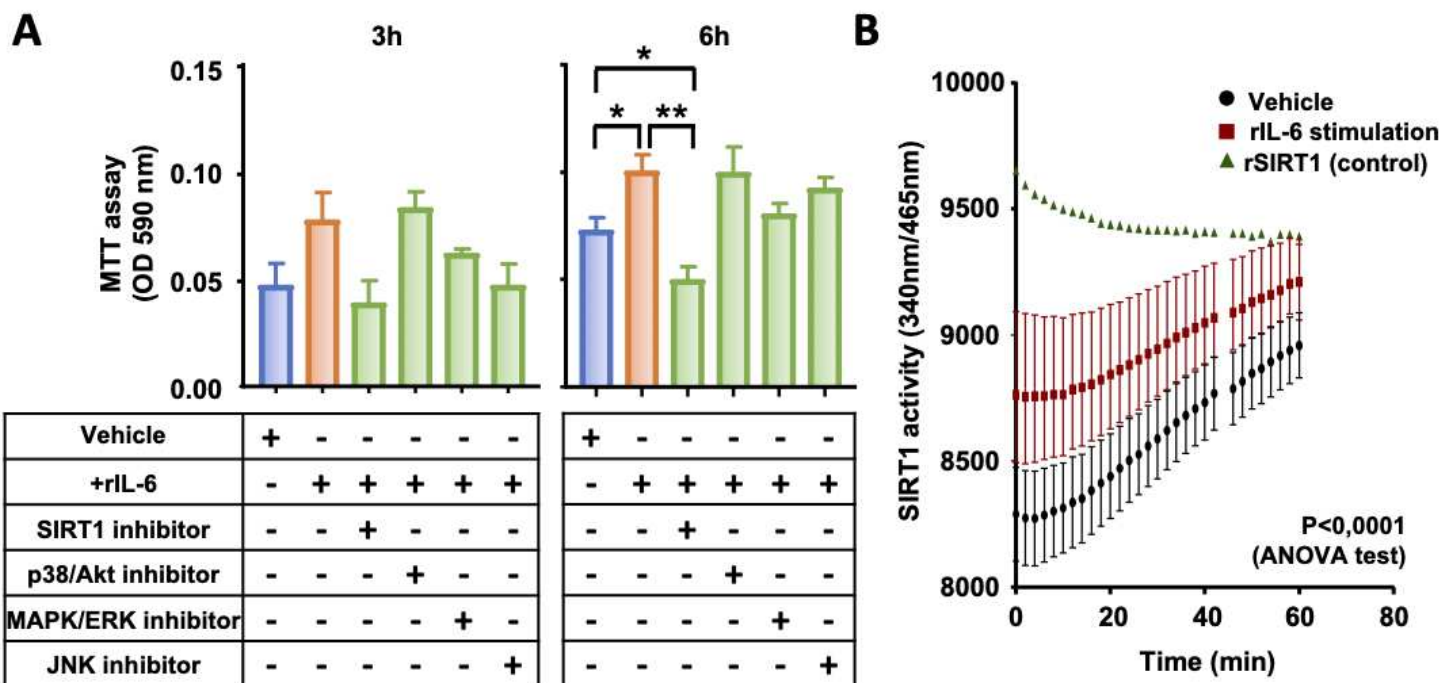
A**B****C****D****E****F**



A**B****C****D**







RESPONSE TO REVIEWERS' COMMENTS

Dear Editors,

We would like to thank you for your letter about our manuscript (CMI-2021-0054), received on February 8, 2021 and the insightful and constructive comments on our work by expert reviewers. We have improved the manuscript according to these suggestions.

Please find below a detailed point by point follow-up of all the comments (shown in blue), to address the editors' and the reviewers' concerns. We updated the changes in the manuscript in response to the reviewers' comments, which appear highlighted in yellow .

Reviewer #1:

The data presented are convincing but I have one main concern. The authors use Lyz-Cre and Alb-Cre mice but these mouse models have been shown to not be fully efficient in some macrophages (Lyz-CRE) and be leaky (Alb-CRE). Could the authors sort the Kupffer cells and the hepatocytes of both the Lyz-Cre x IL6-fl/fl and the Alb-Cre x IL6-fl/fl mice and check the expression of IL6 by qPCR? This should validate the efficiency and specificity of these genetic models.

Could the authors also sort any monocytes found during hepatectomy and check their IL6 expression by qPCR and check whether this IL6 is comparable to the IL6 in hepatocytes and Kupffer cells. Could the authors check whether the IL6 expression in Monocytes drops in the Lyz-Cre x IL6-fl/fl or the Alb-Cre x IL6-fl/fl mice?

In practice the authors need to sort monocytes, Kupffer cells and hepatocytes from the Lyz-Cre x IL6-fl/fl and the Alb-Cre x IL6-fl/fl mice and their littermate controls and check the expression of IL6 by qPCR in the steady-state and during hepatectomy.

Answer: We thank the reviewer for pointing out this important question. Serum IL-6 levels were dropped by more than 50% in AlbCreIL-6 KO or LyzCre IL-6KO, suggesting the *Il6*

gene is effectively deleted in these KO mice (Fig. 4B). To further verify that Kupffer cells of *Il6^{Mye}* KO mice do not express *Il6* as suggested by this reviewer, we have now performed RT-PCR on isolated Kupffer cells from *Il6^{f/f}* injected with PBS or LPS and *Il6^{Mye}* KO injected with LPS (see new Fig. 4A). In this new figure, we confirmed that *Il6* expression is highly induced in Kupffer cells at 3h following LPS injection compared to the control exposed to PBS, while there is no induction of *Il6* expression in Kupffer cells isolated from *Il6^{Mye}* KO mice injected with LPS (Figure 4A). This demonstrates the efficacy of the *Lyz^{Cre}* model to specifically deplete *Il6* gene in KC.

We did not isolate Kupffer cells from hepatectomized mice because of the small number of remaining KC after PHx, and we only had a very limited KO mice available due to partial shutdown of our animal facility during the current pandemic.

Reviewer #2:

Kupffer cells (KCs) self-renew at the steady to maintain themselves on the long term independently from monocytes. However, in some contexts, monocytes can participate to the KC pool. To date, the mechanisms controlling KC numbers after partial hepatectomy (PHx) remains ill defined. In their manuscript entitled “Kupffer cell restoration after partial hepatectomy is driven by their local cell proliferation in autocrine and paracrine IL-6-dependent manners”, Ait Ahmed and colleagues addressed this question. The authors argue that Kupffer cells increased their proliferate rate following PHx and thus did not rely on monocyte input to increase their numbers. In addition, the authors report IL-6 and SIRT1 drives KC proliferation during PHx.

These results are interesting but need to be complemented by flow cytometry data, especially since the immunostaining pictures provided to the reader are too low in quality to support the authors conclusions.

Answer: First, we would like to thank the reviewer for the interesting remarks and suggestions to improve our manuscript. The quality of the pictures was reduced for the initial submission to meet CMI file size requirements. However, following your request, the pictures are now reuploaded with higher definition.

We did not perform flow cytometry analyses from hepatectomized mice because of the small number of remaining KC and limited amount of tissue after PHx, leading us to prefer alternative exploratory methods such as IHC. Additionally, we only had a very limited KO mice available due to partial shutdown of our animal facility during this pandemic.

In addition, it would interesting to have information regarding how the liver regenerates in mice in which PHx-mediated KC proliferation is blunted (mice lacking Il6ra or Sirt1 in myeloid cells).

Answer: We agree with the reviewer, to address the impact of Il6ra and Sirt1 deletion on liver regeneration, we have now measured liver regeneration by quantifying hepatocyte proliferation post-PHx by immunofluorescence along with the liver to body weight ratio of those mice (See new Fig. 5A,C and 7C,E).

Specific comments:

1. The materials & methods section is largely incomplete and sketchy. It is important to provide the reader with the technical information necessary to understand and gauge the experiments carried out by the authors.

Answer: We appreciate the reviewer pointing out these elements. We incorporated the missing information to the manuscript.

Here is a non-exhaustive list of the information missing:

-Ccr2 KO mice are not mentioned in the materials & methods section.

Answer: Ccr2 KO mice are now mentioned in the animal section of the materials and methods section.

-The source of Il6 flox/flox and IL6ra flox/flox is not provided.

Answer: Il6 flox/flox mice are now described with a reference explaining how we obtained them. Similarly, IL-6ra flox/flox are now described with the reference regarding their origin.

-The BrdU staining protocol (used throughout the study) is not described in the method section.

Answer: We have now included the protocol regarding BrdU staining:

“BrdU staining was performed using the BrdU In-Situ Detection Kit 551321 (BD Pharmingen, San Jose, CA). Biotinylated anti-BrdU primary antibody was applied overnight at 4° after a blocking step with goat serum for 1h. The following day, liver tissue sections were rinsed in PBS and incubated with streptavidin coupled secondary antibody for an hour.”

-The KC isolation section does not mention the purity of the preparation. It is impossible to isolate KC with high purity only by doing percoll gradient and centrifugations. This should be acknowledged.

Answer: Indeed, this is an interesting point. KC are challenging to isolate as they are tightly bound to endothelial cells and are very sensitive to *in vitro* culture. Based on the literature^{1,2} and our experience in the laboratory, we developed and designed this protocol of KC isolation (described in the material and methods section) that optimizes purity without compromising cell viability. We have used magnetic cell sorting (MACS) (endothelial cell marker CD146 MicroBeads, Miltenyi) to remove sinusoidal endothelial cells as recommended by the supplier’s instructions. KC purity was assessed by immunofluorescence on the basis of F4/80 expression showed that in our settings KC purity was 76%. It is very hard to go beyond 80% when isolating KC. However, to exclude potential implications of undesired cell types in our primary cell culture experiments, we also confirmed the results obtained on freshly isolated KC with a murine macrophage cell line (RAW cells). **We have now mentioned this in the revised manuscript.**

-The immunofluorescence staining section is incomplete. The secondary antibodies used (source and fluorochromes) were not mentioned.

Answer: We thank the reviewer for pointing this out. The references of the secondary antibodies have been added (anti-rabbit Alexa fluor 488 #4412, anti-rat Alexa fluor 555 #4417, Cell Signaling, Danvers, Massachusetts, and streptavidin-conjugated 555 S21381, ThermoFisher, Waltham, Massachusetts).

2. There are several statements made in the introduction section that are not clear or even sometimes inaccurate.

Lines 65-67: the authors stated “The liver contains at least two macrophage populations that include resident KC and monocyte-derived macrophages”

This is inaccurate as there are no monocyte-derived macrophages in the steady state liver. Or maybe the authors were making reference to the recently described liver capsular macrophages. Please specify.

Answer: We appreciate this suggestion from the reviewer. In fact, alongside KC that represent the main population of hepatic macrophages, bone-marrow derived monocytes circulate through the hepatic vascular network at steady state as patrolling cells,^{3,4} and infiltrate the liver in many contexts of injury. This is indeed a relevant nuance to add to the manuscript. **We have now mentioned this in the revised manuscript.**

Along these lines the authors stated later “Contrastingly, CX3CR1, the G-protein coupled fractalkine receptor, is known to be expressed by monocytes and absent from KC”. It is important to note that liver capsular macrophages are CX3CR1 positive.

Answer: We agree with the reviewer, capsular macrophages are CX3CR1 high. To avoid any confusion, we modified the sentence as follow:

“Contrastingly, CX3CR1, the G-protein coupled fractalkine receptor, is known to be expressed by monocytes and capsular macrophages and absent from KC”.

Lines 77-78: the authors stated “while at steady state most macrophages present in the liver are identified as KC, following tissue damage and inflammation, which causes loss of KC, circulating monocytes infiltrate the hepatic parenchyma”

It looks like the authors assume that liver inflammation is always associated with KC loss, but this is not true. They should clearly specify the context during which KC loss has been reported.

Answer: This is indeed an interesting point. **We have now modified this in the revised manuscript.**

“For example, a loss and decrease of liver KC has been reported in several contexts fulminant hepatitis including infection with murine cytomegalovirus¹⁶ or the bacterium *Listeria monocytogenes*,¹⁷ and in models of methionine/choline-deficient (MCD) diet-induced nonalcoholic steatohepatitis (NASH)¹⁸ and hepatocellular carcinoma (HCC).¹⁹”

3. Overall, there is no mention regarding the number of mice used for each experiment. This should be added in the figure legends.

Answer: We have added the number of mice used for each experiment in the figure legend as requested.

4. Figure 1.

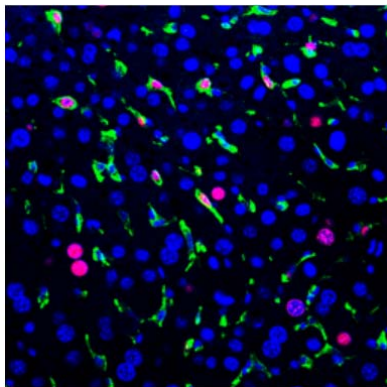
The definition of the pictures provided by the authors is extremely low. Pictures in panel A and B are blurry. It is thus impossible for the reader to appreciate if there is any colocalization between BrdU staining and IBA1+ cells. There is a similar problem with panel 1D, 1F and 1H (all blurry).

First, the authors need to provided pictures with higher quality.

Then, KC proliferation data should be supported by the analysis of Ki-67+ KCs using flow cytometry.

Answer: We agree with the reviewer, the quality of the pictures was reduced for the initial submission to meet CMI requirements of file size. However, following your request, the pictures are now reuploaded with higher definition.

Because the BrdU+IBA+ double positive cells are very clear and easy to identify and count (see a representative photo below, BrdU red, IBA green), the lab is still partially shutdown due to pandemic, and we do not have enough genetically modified mice that are ready for experiments, so we did not perform flow cytometry analyses.



5. Figure 2.

The pictures provided in panel A are not equivalent in term of quality. Only the WT 48h picture meets publication standard. The other pictures are blurry.

Answer: The pictures have now been uploaded with a better resolution.

The authors report in panel B a 2-fold decrease in proliferating macrophages 48h post PHx in IL-4 deficient mice. The authors mentioned a trend in the text but it seems more important than just a trend. What is the P value? How many mice were used in that experiment? Is it a power issue?

Answer: This is an interesting comment. Nine mice per group were used. The P value is 0.0932. We have now included this P value in the figure.

qPCR analysis of Il4 and Csf2 mRNA expression (as done for Il6 in Figure 3A) should be provided.

Answer: Thank you for pointing this out. We have now included a RT-qPCR analysis of Il4 and Csf2 in Sham and PHx mice (Figure 2A and D, respectively).

6. Figure 3.

KC proliferation data obtained by flow cytometry are needed to further support the role of IL-6 in KC proliferation.

Answer: This is a good suggestion. Unfortunately, we only had a very limited number of KO mice in the lab now due to the partial shutdown of our animal facility during pandemic. To breed a large number of these KO mice and perform new experiments will need at least 5-6 months. However, we have several lines of evidence that strongly support a stimulatory effect of IL-6 on KC proliferation, such as IL-6 stimulation of KC proliferation in vitro and in vivo, suppressed KC proliferation in IL6KO, hepatocyte- or myeloid-specific Il-6KO mice, myeloid-specific Il-6R KO. In addition, the BrdU+IBA+ double positive cells are very clear and easy to identify and count (a representative photo is shown above). **We have now included this in the discussion.**

7. Figure 4.

As mentioned in point 5, the authors reported an almost 2-fold decrease in IBA+ BrdU+ cells in IL-4 deficient animals (Figure 2A), but qualified it as a trend.

In Figure 4B, the impact of IL-6 deficiency in hepatocytes or myeloid cells is more modest but was statistically different. Could the authors comment on that point?

Answer: We thank the reviewer for that interesting question. Indeed, the data show a 2-fold decrease of IBA+ BrdU+ cells in IL-4 deficient animals, but this difference did not reach significance due to group heterogeneity. The reduction of both BrdU+ IBA1+ cells and

BrdU+ hepatocytes was greater and more homogeneous in *Il6* deficient animals (Figure 3B), than in hepatocyte or myeloid-specific *Il-6*KO mice (figure 4B). This is probably because in these cell-specific *Il-6*KO, *IL-6* may still derive from alternative cell sources, as opposed to global *Il6*KO mice in which *IL-6* is absent.

Also, the authors should generate mice lacking *IL-6* in both myeloid cells and hepatocytes to assess whether these two cell types are the main drivers of the phenotype observed in *IL-6* whole body knockout.

Answer: This is a great point. However, we did not generate double mutant mice with *IL-6* deletion in myeloid cells and hepatocytes. Currently, our lab at the NIH is still partially shutdown due to pandemic and to re-generate these mice will take 5-6 months or even longer. Because our data demonstrated that KC and hepatocyte proliferation were significantly impaired in both *IL-6* Mye KO and *IL-6* Hep KO mice, it is plausible to predict that KC and hepatocyte proliferation in double mutant mice will be further decreased compared to those in single KO mice.

we have now included this discussion in revised manuscript.

8. Figure 6 and Figure 7.

Again, all the pictures are blurry.

Answer: We agree with the reviewer, as indicated below, the pictures are now reuploaded with higher definition.

9. The authors provided evidence that *Il6ra* and *Sirt1* in myeloid cells are necessary for KC proliferation during PHx. However, information is missing regarding whether a defect in KC proliferation impacts on liver regeneration.

Using *LysM-cre* x *Il6ra* flox/flox or *LysM-cre* x *Sirt1* flox/flox, can the authors report any defect in liver regeneration following PHx?

Answer: We agree with the reviewer, to determine whether the defect of KC mediated by *Il6ra* and *Sirt1* deletion had an impact on liver regeneration, we have now included a quantification of proliferating hepatocytes in *Il6r^{Mye}* KO (Figure 5C) and *Sirt1^{Mye}* KO (Figure 7E) by immunofluorescence following PHx in the revised manuscript.

Minor comments:

- The authors mentioned that KCs would represent “80% of all macrophages in the human body”. This is a quite old assumption we can find on the internet but what is the basis of such calculation?

The intestinal tract is rich in macrophages and might contain even more of these cells than the liver as the whole intestine is 8 to 10 meters long.

Answer: This is an interesting point of view. This percentage is cited in many references. However, to be more cautious we rephrased the sentence as follow: KC represent one of the largest macrophage populations in the human body.

- In the material and methods section, the strains genotypes are not well presented.

First, mice expressing the cre recombinase under the Lysozyme M promoter (Lyz-cre) were labelled Lyz-Cre^{+/+}. However, the ^{+/+} nomenclature usually means wild-type. Please use the classical nomenclature.

Cx3cr1 knock-in mice should be marked as Cx3cr1 ^{gfp/gfp} and Cx3cr1 ^{gfp/+}.

Il6Mye KO and Il6Hep KO would be better than Il6Mye ^{-/-} and Il6Hep ^{-/-}.

Answer: We thank the reviewer for this suggestion, as requested the names have been updated.

- Line 168: RAW 264.7 cell instead of “RAW cell”

Answer: This has been changed.

Reviewer #3:

In this manuscript, the question how Kupffer cells are restored upon liver regeneration after partial hepatectomy. The authors analyze circulating macrophages and liver resident macrophages after partial hepatectomy. Using several strains of genetically modified mice together with immunohistochemical analysis, the authors demonstrate that locally proliferating Kupffer cell rather circulating monocytes are responsible for the restoration. The proliferation of Kupffer cell was dependent on IL-6 but not on IL-4 or CSF-2. IL-6 from hepatocytes and Kupffer cells was important for the proliferation response. Finally, the authors were able to demonstrate that sirtuin 1 contributed to IL-6 mediated proliferation of

Kupffer cells in vitro. This was confirmed using sirtuin 1 knock-out mice, which showed impaired Kupffer cell proliferation after partial hepatectomy.

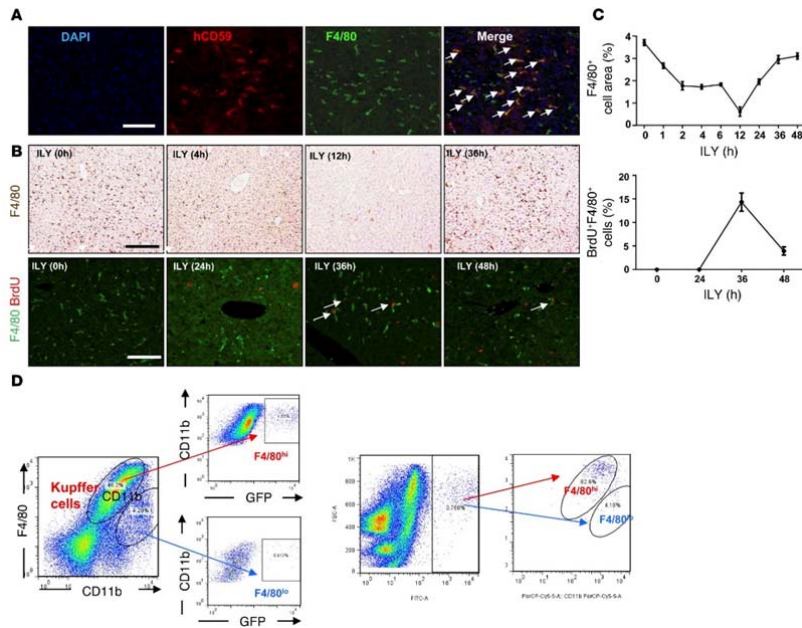
This is a very interesting and important study, which addresses a longstanding open question. There are some points, the authors might want to address.

Major points:

1. A central point of the manuscript is the efficacy of gene deletion in Kupffer cells. There is a long debate in the field ranging from data that Lyz-Cre mice cannot be used for gene deletion in Kupffer cells (see Maeda et al, Cell 2005; Fig. S6) to data, which demonstrate that Lyz-Cre mice can be used for gene deletion in Kupffer cells (see Lanaya et al, Nat Cell Biol 2014; Fig. 3c). Therefore it should be demonstrated that breeding with Lyz-Cre mice indeed leads to efficient gene deletion in Kupffer cells.

Answer: This is an interesting question. Actually, the data in Maeda et al Cell 2005 was wrong (many results from this lab cannot be reproduced by others). LyzCre has been shown to delete genes in Kupffer cells by many labs including ours. **We have now stated this and cited several references.**

Below is an image from our previous publication (Feng et al. J Clin Invest. 2016;126:2321-2333). In this paper, we developed Cre-inducible hCD59 mice, and crossed this line with LyzCre mice, LyzCre deleted flox-stop-fox and subsequently induced hCD59 expression in Kupffer cells (hCD59 staining in panel A). Injection of ILY toxin efficiently depleted hCD59+ Kupffer cells in panel B.



Additionally, we included in the revised manuscript and figures, a quantification by RT-qPCR of *Il6* expression in isolated Kupffer cells from *Il6^{f/f}* injected with PBS or LPS and *Il6^{Mye}* KO injected with LPS. We confirmed that *Il6* expression is highly induced in Kupffer cells at 3h following LPS injection compared to the control exposed to PBS, while there is no induction of *Il6* expression in Kupffer cells isolated from *Il6^{Mye}* KO mice injected with LPS (Figure 4A). This demonstrates the efficacy of the *Lyz^{Cre}* model to specifically deplete genes in macrophages.

2. The authors describe hepatectomy experiments with *IL-6^{-/-}* mice. They should shortly state how many of the mice survived as compared to wt mice. How was survival of the *IL6RMye^{-/-}* mice?

Answer: We thank the reviewer for pointing this out. 100% of the WT mice survived after PHx and the survival rate was reduced to 77% in *IL-6* KO mice and 85% in *IL6RMye^{-/-}* mice, at 48h post-PHx.

3. It has been described that *IL-6* after hepatectomy cooperates with hepatocyte growth factor to stimulate hepatocyte proliferation. Is hepatocyte growth factor also involved in the proliferation of Kupffer cells?

Answer: This is a very interesting point. *C-met*, known as HGF receptor is also expressed on KC. HGF might be involved in the proliferation of KC. However we do not have data about

the effect of HGF on KC proliferation following PHx. We have now discussed this in the revised manuscript and proposed this as future studies.

Minor points:

1. In myeloid targeted (Mye^{-/-}) mice, did the authors use heterozygous or homozygous Lys-Cre mice?

Answer: In this study, we used heterozygous Mye^{+/-} mice.

2. Did the authors quantitate the recombination efficacy in IL6Hep^{-/-} mice? This should be shown.

Answer: IL6Hep^{-/-} mice were generated via the several steps of crossing AlbCre mice (the Jax) and Il-6 flox/flox mice, and this AlbCre line has been widely used to delete interest genes in hepatocytes. We have previously used AlbCreIL-6 Hep^{-/-} mice, and demonstrated serum IL-6 levels were markedly reduced in the KO mice, suggesting that Il-6 in hepatocytes is effectively deleted (He et al. J Hepatol. 2021 Feb PMID: 33610678). We have now mentioned this in the revised manuscript.

3. On p20, the authors mention IL-6 trans-signaling. This should be shortly explained.

Answer: This is indeed an interesting point. IL-6 receptor (IL-6R) exists in two forms: a transmembrane receptor (mIL-6R) and a soluble receptor (sIL-6R). By binding to mIL-6R, IL-6 activates the canonical signaling pathway and subsequently predominantly triggers anti-inflammatory responses. On the other hand, in cells that do not express mIL-6R, IL-6 can activate the trans-signaling pathway via binding to sIL-6R. We have now included this in the revised manuscript.

We believe that by addressing the editor's and reviewers' comments, our manuscript has been significantly improved, and we hope that the revised manuscript will be acceptable for publication.

Thank you so much for your attention.

Bin Gao, MD PhD, FAASLD
Chief, Laboratory of Liver Diseases

NIAAA, NIH

Fouad Lafdil, PhD

Professor, Université Paris-Est-Créteil

INSERM U955, Team 18, Institut Mondor de Recherche Biomédicale

Créteil, France;

PUBLICATION 2

**Interleukins-17 and 27 promote liver
regeneration by sequentially inducing
progenitor cell expansion and differentiation**

Interleukins-17 and 27 Promote Liver Regeneration by Sequentially Inducing Progenitor Cell Expansion and Differentiation

Adrien Guillot,^{1,2,6} Imène Gasmî,^{1,2} Arthur Brouillet,^{1,2} Yeni Ait-Ahmed,^{1,2} Julien Calderaro ,^{1,2,5} Isaac Ruiz,^{1,2,4} Bin Gao,⁶ Sophie Lotersztajn,^{1,2} Jean-Michel Pawlotsky,^{1,2} and Fouad Lafdil¹⁻³

Liver progenitor cells (LPCs)/ductular reactions (DRs) are associated with inflammation and implicated in the pathogenesis of chronic liver diseases. However, how inflammation regulates LPCs/DRs remains largely unknown. Identification of inflammatory processes that involve LPC activation and expansion represent a key step in understanding the pathogenesis of liver diseases. In the current study, we found that diverse types of chronic liver diseases are associated with elevation of infiltrated interleukin (IL)-17-positive (+) cells and cytokeratin 19 (CK19)⁺ LPCs, and both cell types colocalized and their numbers positively correlated with each other. The role of IL-17 in the induction of LPCs was examined in a mouse model fed a choline-deficient and ethionine-supplemented (CDE) diet. Feeding of wild-type mice with the CDE diet markedly elevated CK19⁺Ki67⁺ proliferating LPCs and hepatic inflammation. Disruption of the IL-17 gene or IL-27 receptor, alpha subunit (WSX-1) gene abolished CDE diet-induced LPC expansion and inflammation. *In vitro* treatment with IL-17 promoted proliferation of bipotential murine oval liver cells (a liver progenitor cell line) and markedly up-regulated IL-27 expression in macrophages. Treatment with IL-27 favored the differentiation of bipotential murine oval liver cells and freshly isolated LPCs into hepatocytes. **Conclusion:** The current data provide evidence for a collaborative role between IL-17 and IL-27 in promoting LPC expansion and differentiation, respectively, thereby contributing to liver regeneration. (*Hepatology Communications* 2018;2:329-343)

Introduction

After liver injury, normally quiescent hepatocytes are capable of self-renewal by entering the cell cycle until restoring the liver parenchyma and initial functions. However, when the liver is subjected to severe or chronic injury, hepatocyte-driven liver regeneration is altered or insufficient, and an alternative regenerative process involving the liver progenitor cell (LPC) compartment is then engaged.⁽¹⁾

In virtually all human liver diseases, LPC proliferation is frequently observed within proliferative ductular cells and is referred to as ductular reaction (DR), with an important histologic and mechanistic heterogeneity.^(2,3) DR is defined as the proliferation of apparent ductules that accompany leukocyte infiltration in response to liver injury.⁽⁴⁾ In humans, the expansion of biliary-like cells or LPCs is associated with severity of chronic liver disease, regardless of the etiology.⁽⁵⁻⁷⁾ While LPCs are reported as key cells promoting liver

Abbreviations: Alb, albumin; BMOL, bipotential murine oval liver; CDE, choline-deficient and ethionine-supplemented; CK19, cytokeratin 19; DR, ductular reaction; HNF, hepatocyte nuclear factor; IL, interleukin; LPC, liver progenitor cell; Mcp1, monocyte chemoattractant protein 1; MELD, Model for End-Stage Liver Disease; mRNA, messenger RNA; TAT, tyrosine aminotransferase; Th, T helper; TNF, tumor necrosis factor; WSX-1, interleukin-27 receptor, alpha subunit; WT, wild-type.

Received July 24, 2017; accepted December 6, 2017.

Additional Supporting Information may be found at <http://onlinelibrary.wiley.com/doi/10.1002/hep4.1145/full>.

Supported by the Institut National de la Santé et de la Recherche Médicale, by Université Paris-Est-Créteil grants for young investigators (to F.L.), from the Agence Nationale de la Recherche ANR-09-RPDOC-016-01 HEPATICEL (Retour Postdoctorants 2009-2013 to F.L.), and the Institut Universitaire de France (Promotion 2016). A.G. was the recipient of a fellowship from the French Ministry of Education and Research (2011-2014).

Present address for Sophie Lotersztajn is INSERM-U1149, CNRS-ERL8252, Centre de Recherche sur l'Inflammation, Paris, France, and Sorbonne Paris Cité, Laboratoire d'Excellence Inflamex, Faculté de Médecine, Site Xavier Bichat, Université Paris Diderot, Paris, France.

regeneration, in certain circumstances their presence is also correlated with progressive fibrogenesis^(8,9) and could contribute to hepatocellular carcinoma initiation.⁽¹⁰⁾ Therefore, determination of the mechanisms leading to LPC activation and controlling their expansion represent a key step in understanding liver pathogenesis development and may help to propose novel therapeutic strategies.

The origin of LPCs is still subject to debate. However, most recent publications converge toward the likelihood of LPC emergence from a stem/progenitor cell niche located in the portal region around the canals of Hering. LPCs can differentiate toward functional hepatocytes and mature cholangiocytes *in vitro*. Numerous murine lineage-tracing models have suggested that LPCs do not contribute to hepatocyte regeneration in several experimental models of liver injury, including 2/3 partial hepatectomy, bile duct ligation, carbon tetrachloride intoxication, and a 3,5-diethoxycarbonyl-1,4-dihydrocollidine diet. However, after severe hepatocyte loss, biliary-like or liver progenitor cells can differentiate toward functional hepatocytes and mature cholangiocytes *in vivo* in zebrafish and in mouse models.⁽¹¹⁻¹³⁾ Furthermore, in another murine model using a choline-deficient and ethionine-supplemented diet (CDE), Español-Suñer et al.⁽¹⁴⁾ and Rodrigo-Torres et al.⁽¹⁵⁾ found that LPCs contribute to hepatic regeneration with up to 2% of newly generated hepatocytes arising from LPCs. It has recently been demonstrated that differentiated cells from such progenitors yield functional hepatocytes characterized by hepatocyte-specific marker

expressions, such as hepatocyte nuclear factor (HNF)4 α .⁽¹⁶⁾ A contribution of LPCs to the restoration of the parenchymal architecture and liver function has been assumed in humans, and a recent study reported long-term expansion of LPCs from human liver and their conversion into functional hepatocytes *in vitro* and with transplantation *in vivo*.⁽¹⁷⁾

Activation of the LPC compartment is a complex process that is not fully understood. The LPC response can be divided into four steps: activation, proliferation, migration, and differentiation.⁽¹⁸⁾ The induction and progression of the LPC-driven regenerative process is highly influenced by the microenvironment and the cytokines released by immune cells during inflammation.⁽¹⁹⁾ For instance, a recent study reported the association between portal inflammation and DR in nonalcoholic fatty liver disease.⁽²⁰⁾ Both innate and adaptive immune cells recruited during the inflammatory process are critical for the modulation of LPC-driven liver regeneration, as demonstrated by numerous studies using the CDE model. Van Hul et al.⁽²¹⁾ have reported that macrophage depletion by clodronate injections attenuates fibrogenesis and LPC parenchymal invasion. Furthermore, it has been shown that in mice lacking T cells, the LPC response was drastically weakened and mice succumbed to acute liver failure.⁽²²⁾ The LPC compartment is also highly activated during T-cell-mediated hepatitis induced by concanavalin A.⁽²³⁾ Numerous cytokines constitute key links between inflammation and LPC proliferation, such as tumor necrosis factor (TNF)- α , TNF-like weak inducer of apoptosis (TWEAK), interferon-gamma

Copyright © 2018 The Authors. *Hepatology Communications* published by Wiley Periodicals, Inc., on behalf of the American Association for the Study of Liver Diseases. This is an open access article under the terms of the [Creative Commons Attribution-NonCommercial-NoDerivs License](#), which permits use and distribution in any medium, provided the original work is properly cited, the use is non-commercial and no modifications or adaptations are made.

View this article online at wileyonlinelibrary.com.

DOI 10.1002/hep4.1145

Potential conflict of interest: Nothing to report.

ARTICLE INFORMATION:

From the ¹Université Paris-Est, UMR-S955, Créteil, France; ²Institut National de la Santé et de la Recherche Médicale (INSERM) U955, Institut Mondor de Recherche Biomédicale, Créteil, France; ³Institut Universitaire de France, Paris, France; ⁴Département d'Hépatologie, and ⁵Département de Pathologie, Hôpital Henri Mondor, Université Paris-Est, Créteil, France; ⁶Laboratory of Liver Diseases, National Institute on Alcohol Abuse and Alcoholism, National Institutes of Health, Bethesda, MD.

ADDRESS CORRESPONDENCE AND REPRINT REQUESTS TO:

Fouad Lafdil, Ph.D.
INSERM U955
Institut Mondor de Recherche Biomédicale, Hôpital Henri Mondor

94010 Créteil, France
E-mail: fouad.lafdil@inserm.fr
Tel: +33-(0)1-4981-3538

(IFN- γ), interleukin-6 (IL-6), IL-22, and lymphotoxin β .⁽²⁴⁻²⁸⁾

Among the key players in modulating liver inflammation, T helper (Th)17 lymphocytes have been implicated in several types of liver diseases through the effects of IL-17A (IL-17) and IL-22.^(29,30) While IL-22 has been reported as hepatoprotective,⁽³¹⁾ anti-fibrotic,⁽³²⁾ and promoting liver regeneration from LPCs,⁽²⁸⁾ the potential role of IL-17, notably in regeneration, has not been fully investigated. IL-17 is a proinflammatory cytokine known to contribute to the crosstalk between innate and adaptive immunity. Recently, we and others reported direct and indirect profibrogenic and proinflammatory effects of IL-17 by stimulating both myofibroblasts and macrophages.^(33,34) Furthermore, it has been shown that IL-17-producing gamma delta T ($\gamma\delta$ T) cells were recruited during hepatocyte-driven liver regeneration induced by partial hepatectomy.⁽³⁵⁾ The authors showed that IL-17-induced IL-6 production by macrophages and dendritic cells, favored hepatocyte proliferation, and could also be involved in LPC-driven liver regeneration. To achieve hepatic regeneration from LPCs, those cells need to proliferate but also to undergo cell differentiation into mature cells. Interestingly, several groups demonstrated that IL-27, a cytokine mainly produced by macrophages, has been shown to directly favor stem/progenitor cell differentiation in different organs.⁽³⁶⁻³⁹⁾ IL-27 is a pleiotropic cytokine belonging to the IL-12 family that signals through its heterodimeric receptor composed of gp130 and IL-27 receptor alpha (WSX-1) subunits, mainly expressed by immune and epithelial cells, including hepatocytes.⁽⁴⁰⁾ We therefore hypothesized that communication between adaptive and innate immune cells through IL-17 and IL-27 production, respectively, could contribute to the achievement of liver regeneration from LPCs.

In biopsies obtained from patients with various types of liver diseases, IL-17⁺ cells were identified in close association with liver ductular cells, and their infiltration positively correlated with the degree of DR in our study. To address the role of IL-17 and IL-27 in LPC activation, proliferation, and differentiation into mature hepatocytes, IL-17-deficient (IL-17^{-/-}) and WSX-1-deficient (WSX-1^{-/-}) mice were fed a CDE diet, and murine liver progenitor cells were used. Our results showed complementary roles of IL-17 and IL-27 in achieving the regenerative process of the liver by inducing LPC proliferation and by favoring differentiation, respectively.

Materials and Methods

HUMAN SAMPLES

Forty-three liver samples from patients with diverse chronic liver diseases were analyzed. The study conformed to the ethical guidelines of the 1975 Declaration of Helsinki. As required by French legislation, the study was approved by the local ethics committee Ile de France I (Institutional Review Board 2017-A01215-48). Blocks of formalin-fixed paraffin-embedded samples from explanted livers were obtained from the Department of Pathology of Henri Mondor University Hospital (Creteil, France). For the assessment of cytokeratin 19 (CK19)⁺ and IL-17⁺ cell density, a training set of 20 slides was first reviewed by two evaluators, including a pathologist specialized in liver diseases. The whole cohort was then analyzed independently by the two evaluators using a semiquantitative score, and patients were dichotomized into high versus low density of stained cells for each labeling.

ANIMALS

We used 6-8-week-old male mice on a C57BL/6 background in this study. IL-17^{-/-} mice were generously provided by Professor Yoichiro Iwakura (Japan). WSX-1^{-/-} mice were purchased from the Jackson Laboratory. Mice were fed a control (choline-sufficient) or choline-deficient diet (MP Biomedicals, Illkirch, France), and drinking water was supplemented with DL-ethionine (0.15% weight/volume) (Sigma-Aldrich, Lyon, France) in the CDE-fed group. Animals were killed at indicated time points, blood was collected for serum extraction, and the liver was either fixed in buffered formalin or snap frozen in liquid nitrogen. Experiments were performed on at least four animals per group and per time point. All animals were housed and fed *ad libitum* in a pathogen-free animal facility and used in accordance with protocols approved by the French ethical committee (COMETH, Authorization N°12-079) and under the supervision of authorized investigators.

STATISTICAL ANALYSIS

Results are expressed as mean \pm SEM, and statistical significance was determined by a two-tailed Student *t* test or one- or two-way analysis of variance as appropriate, using PRISM 4.0 software. Data were considered significantly different for $P < 0.05$. Contingency between CK19 and IL-17 staining and Model

for End-Stage Liver Disease (MELD) scores were assessed by Fisher's exact test and Child-Pugh scores by the chi-square test.

Results

DR CORRELATES WITH IL-17-PRODUCING CELL INFILTRATION IN HUMAN DISEASED LIVERS

DR with LPCs is frequently observed in several types of liver diseases and is often associated with the inflammatory process.^(3,20) In addition, IL-17⁺ cells were found in the livers of patients with chronic liver diseases.^(29,30) To determine whether the proliferative LPCs correlate with the number of infiltrating IL-17-producing cells, a cohort of 43 patients with chronic liver diseases from various etiologies was analyzed. Most of the patients presented with mild inflammatory activity (86.1%, METAVIR score A1–A2) with severe fibrosis (93.0% METAVIR F4) (Supporting Table S1). On paraffin-embedded liver tissues from these patients, we revealed an infiltration of IL-17-producing cells surrounding CK19⁺ LPCs with a close interaction, regardless of the etiology (Fig. 1). A score was defined

semiquantitatively, and patients were classified into two groups with a low and high degree of DR (Fig. 2A). Similarly, IL-17⁺ cells infiltrating the livers were scored and classified into two groups with a low and high degree of IL-17-expressing cells. A positive correlation was found between the densities of these two cell types ($P < 0.001$) (Fig. 2B), with a majority of CK19^{high} patients having a high density of infiltrating IL-17⁺ cells in the liver. In addition, patients with low CK19 and IL-17 scores were predominantly Child-Pugh class A with a MELD score ≤ 15 , whereas most patients who were CK19^{high} IL-17^{high} were Child-Pugh class B or C with a MELD score > 15 (Fig. 2C,D; Supporting Table S1). Collectively, these data showed that increased IL-17⁺ cell infiltration is associated with CK19⁺ LPC accumulation in human DR and with a less optimistic prognosis. These clinical observations led us to hypothesize that IL-17 could promote LPC accumulation in diseased livers.

DISRUPTION OF THE IL-17 GENE IMPAIRS LPC ACTIVATION IN REGENERATING LIVER

To determine the role of IL-17 in LPC-compartment activation in regenerating livers, wild-

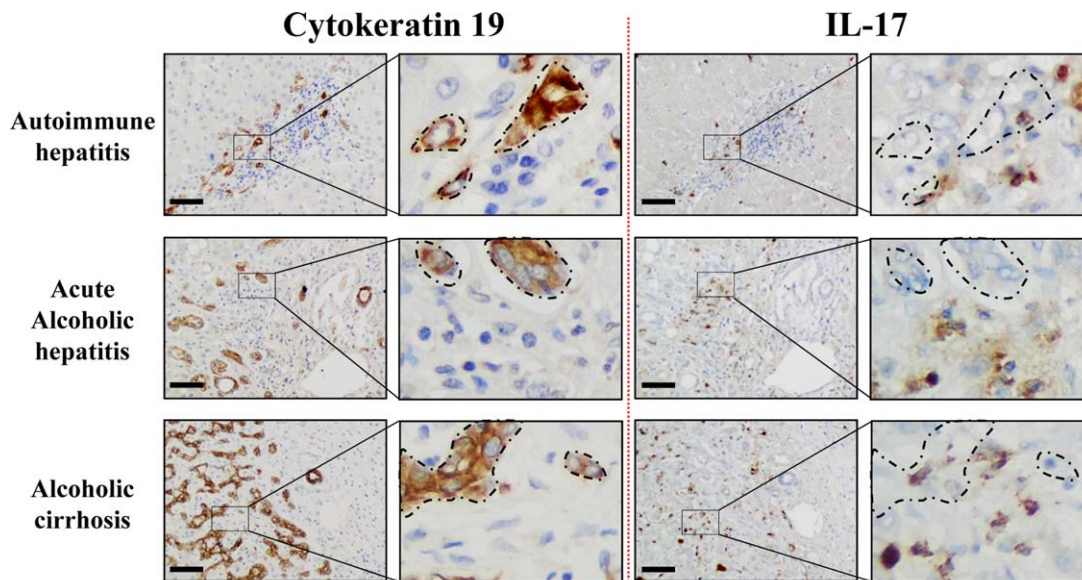


FIG. 1. IL-17-expressing cells and CK19⁺ cells are localized in similar areas in diseased livers. Representative CK19 and IL-17 (brown color) immunostaining on human serial liver sections from diverse etiologies with an enlargement magnification field. Areas where CK19⁺ cells accumulate are delimited with dotted lines on serial sections to highlight their proximity with IL-17⁺-infiltrating cells. Scale bar, 100 μ m.

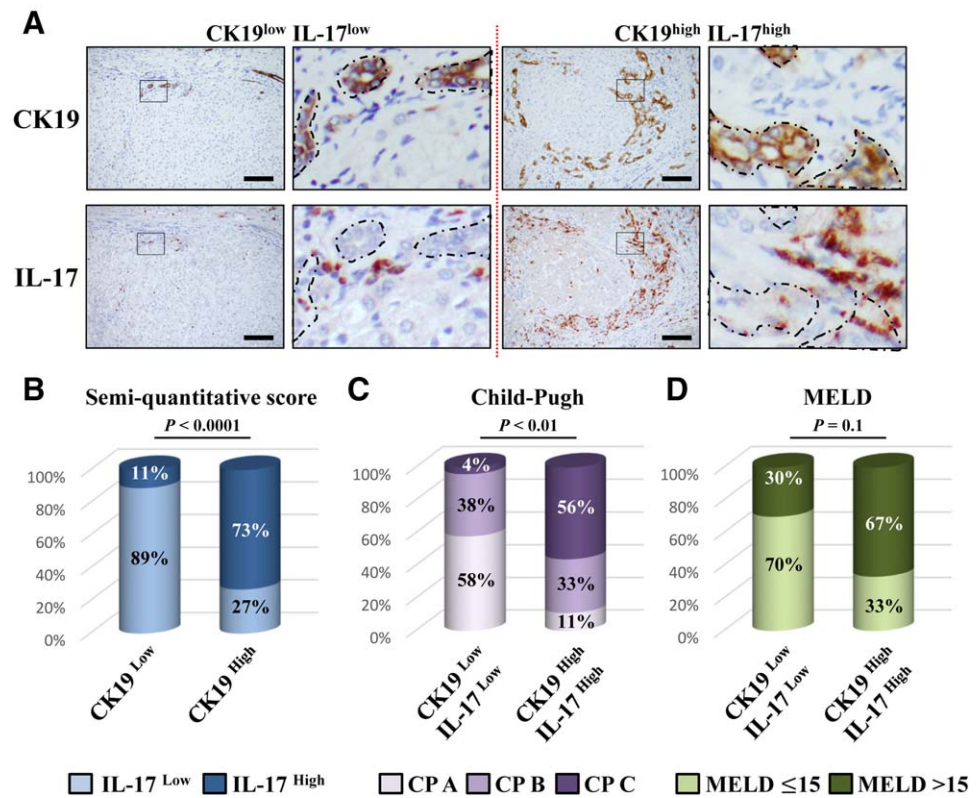


FIG. 2. Ductular reaction correlates with IL-17-producing cell infiltration in human diseased livers. (A) Representative liver sections from patients with CK19^{low} IL-17^{low} (left) and CK19^{high} IL-17^{high} (right) immunolabeling. Scale bar, 100 μ m. (B) Relative CK19 and IL-17 quantification was realized. (C) Child-Pugh score class A (5 to 6), B (7 to 9), and C (10 to 15) in CK19^{low} IL-17^{low} and CK19^{high} IL-17^{high} patients. (D) Percentage of patients with a MELD score ≤ 15 or > 15 in both groups. Abbreviation: CP, Child-Pugh.

type (WT) and IL-17^{-/-} mice were subjected to the CDE diet for 3, 10, or 21 days. In this model, expression of several inflammatory genes inducing Th17 cell differentiation (IL-6, transforming growth factor β) and specific markers, including IL-23 receptor (IL-23R) and retinoic acid receptor-related orphan receptor alpha (ROR- α) but not ROR γ t, were up-regulated as early as 3 days and were maintained along with the diet in WT animals (Supporting Fig. S1). LPC accumulation was evaluated on liver tissue sections of both WT and IL-17^{-/-} CDE-fed mice with CK19 immunostaining (Fig. 3A). WT mice showed a significant increase in CK19⁺ cells from day 3, with a progressive accumulation along with the CDE diet. In contrast, IL-17 deficiency was sufficient to significantly prevent LPC accumulation as early as 3 days after the CDE diet (Fig. 3A). This result has been confirmed in another model of DR in a cholestatic environment induced by bile duct ligation and section (Supporting Fig. S2). Along the same line of evidence, messenger RNA (mRNA) expression of LPC response-associated markers (alpha-fetoprotein [AFP], M2-pyruvate kinase), with the exception of the hematopoietic Thy-1 cell surface antigen (Thy1) marker, were induced in

the liver from WT mice in the CDE model, reaching a peak at day 3; such inductions were markedly reduced in IL-17^{-/-} mice (Fig. 3B). Double-stained CK19⁺Ki67⁺ cells revealed proliferative LPCs reaching 15% of the total CK19⁺ counted cells in WT mice, whereas no proliferating LPCs were detected in IL-17^{-/-} mice after 21 days of the CDE diet (Fig. 3C,D). This reduced-LPC activation in IL-17^{-/-} mice was not attributable to a difference in liver injury as serum transaminases (alanine aminotransferase, aspartate aminotransferase) and alkaline phosphatase activities were similarly increased in WT and IL-17^{-/-} animals at earlier time points (Fig. 3E). No difference was observed on histologic analysis on hematoxylin and eosin-stained liver tissue sections (Supporting Fig. S3). In addition, food intake was assessed in both groups and did not show any difference (Supporting Fig. S4). Finally, despite a slight increase in fibrogenesis-related gene expressions in livers of WT CDE-fed mice, no obvious increase in sirius red staining was observed in those mice (Supporting Fig. S5A-C). Taken together, these data showed that IL-17 deficiency is associated with reduced LPC accumulation.

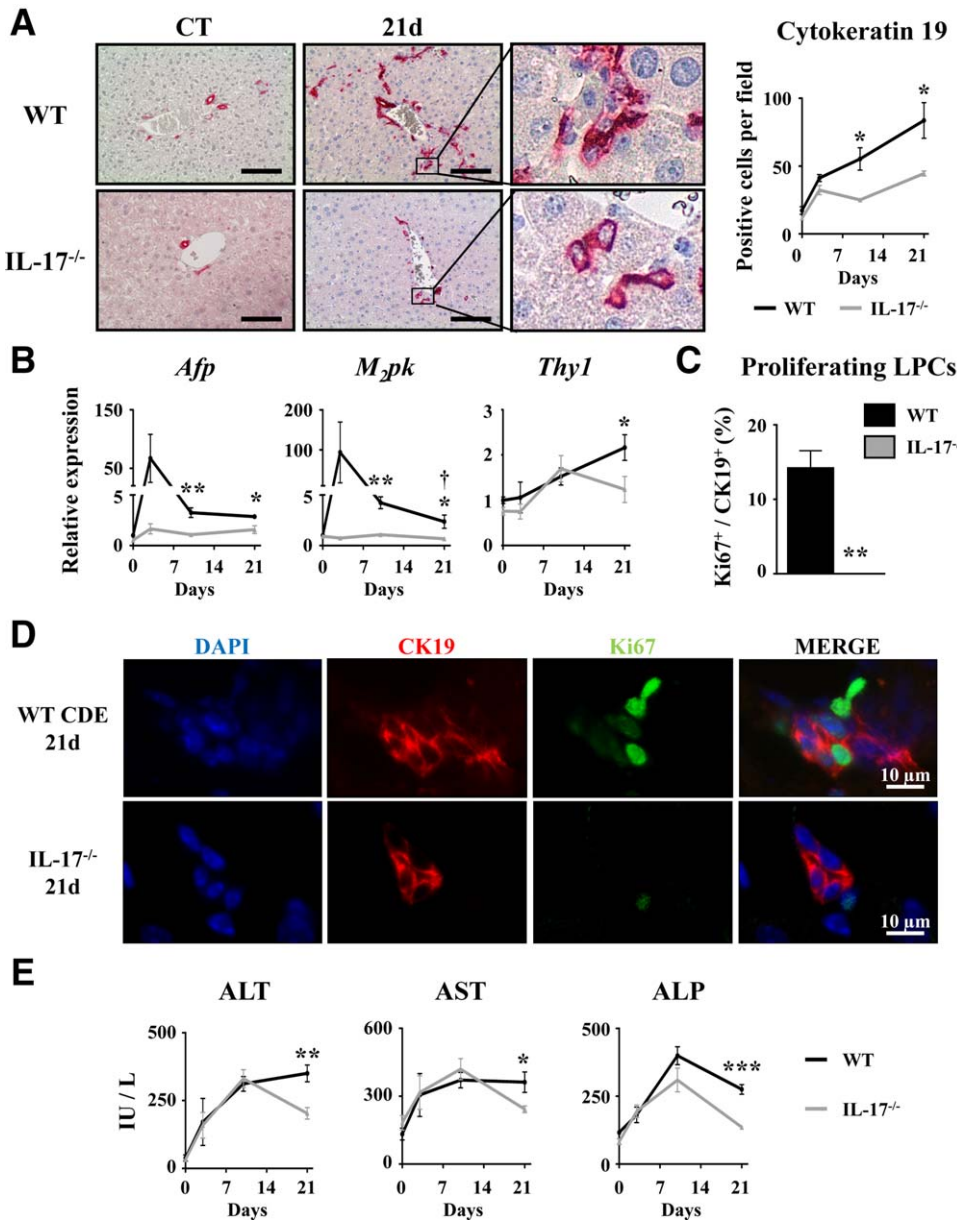


FIG. 3. Disruption of the IL-17 gene impairs liver progenitor cell activation in regenerating liver. Wild-type and IL-17^{-/-} mice were fed a CDE diet and killed at the indicated time points. (A) Liver tissue sections were stained for CK19, and positive cell number quantification was realized. (B) Hepatic mRNA expression of LPC-associated genes *Afp*, *M₂pk*, and *Thy1* was analyzed by qRT-PCR and expressed as fold change over control diet-fed WT mice. (C,D) Liver tissue sections were immunolabeled with antibodies directed against CK19 (red) and Ki67 (green), and the percentage of proliferating CK19⁺ cells was determined. (E) Serum ALT, AST, and ALP activities were measured. **P* < 0.05, ***P* < 0.01, ****P* < 0.005, WT versus IL-17^{-/-} mice; each group n = 4-7 animals. Data represent mean ± SEM. Abbreviations: ALP, alkaline phosphatase; ALT, alanine aminotransferase; AST, aspartate aminotransferase; CT, control; d, day; DAPI, 4',6-diamidino-2-phenylindole; *M₂pk*, type 2 muscle pyruvate kinase; qRT-PCR, quantitative reverse-transcription polymerase chain reaction.

IL-17 DEFICIENCY REPRESSES LIVER INFLAMMATION, INCLUDING IL-27 PRODUCTION

It is well established that the liver inflammatory response triggered by macrophage recruitment and activation tightly controls LPC expansion. To further determine whether defective LPC accumulation, identified in IL-17^{-/-} animals, could result from the reduced liver inflammatory response, we evaluated macrophage recruitment and the expression of their

secreted inflammatory mediators. While monocyte chemoattractant protein 1 (*Mcp1*) and *F4/80* mRNA expressions were induced with a peak reached at 3 days in WT, such induction was not observed in IL-17^{-/-} mice (Fig. 4A). Furthermore, F4/80 immunostaining in WT mice showed a 3-fold increase in macrophage cell numbers infiltrating the livers 3 days after the CDE diet; such infiltration was significantly lower in IL-17^{-/-} mice (Fig. 4B). Expressions of several macrophage-associated inflammatory cytokines were also assessed; in WT animals under the CDE diet, the

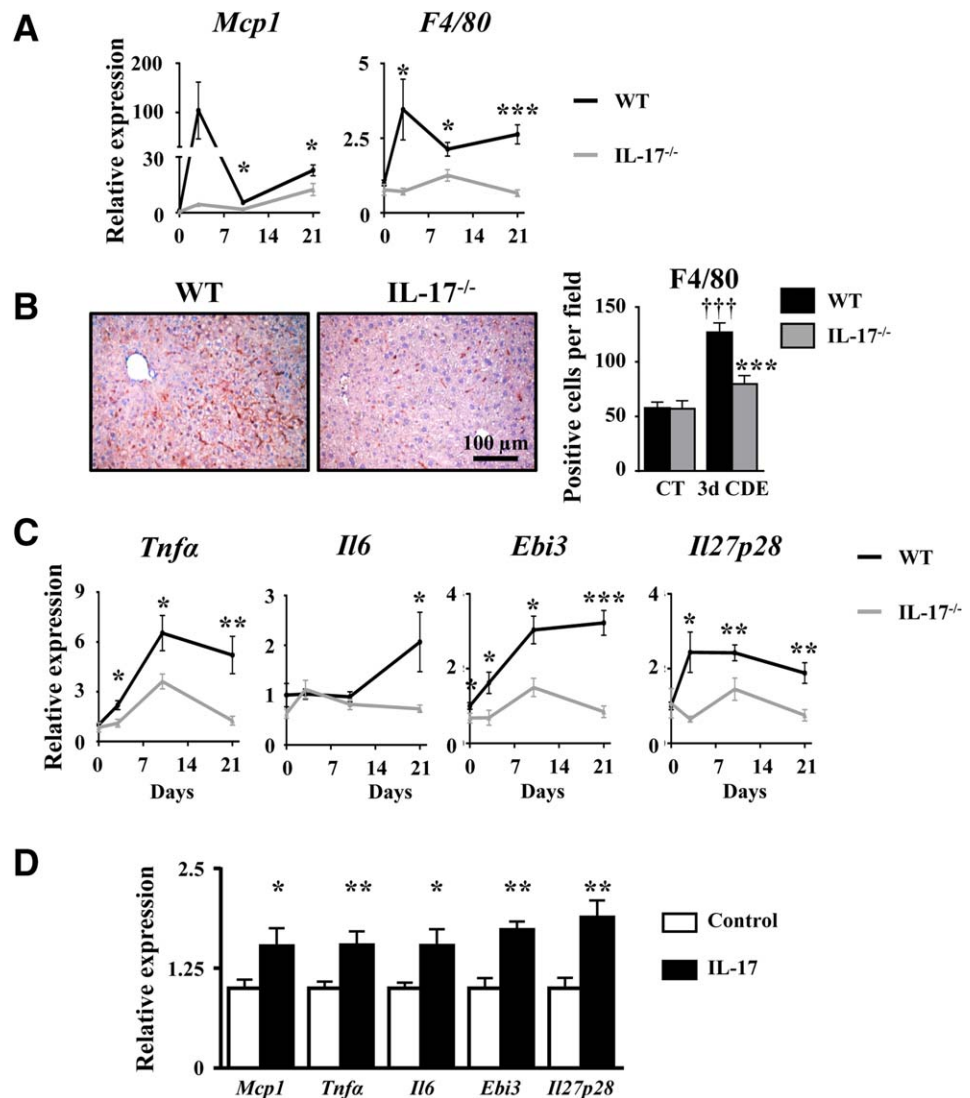


FIG. 4. IL-17 deficiency represses liver inflammation, including IL-27 production. (A) mRNA expression of MCP1 and F4/80 were quantified by qRT-PCR. (B) Liver macrophage infiltration was analyzed by F4/80 immunostaining and counting. (C) TNF- α , IL-6, and IL-27 (Ebi3 and IL-27p28 subunits) mRNA expressions were quantified by qRT-PCR in WT and IL-17^{-/-} mice after 3, 10, or 21 days of the CDE diet. * $P < 0.05$, ** $P < 0.01$, *** $P < 0.005$, WT versus IL-17^{-/-} mice. (D) Inflammatory gene expressions were quantified by qRT-PCR in the IL-17-treated RAW264.7 macrophage cell line. Data represent mean \pm SEM. Abbreviations: CT, control; d, day; qRT-PCR, quantitative reverse-transcription polymerase chain reaction.

data revealed an up-regulated hepatic expression of *Tnfa*, *Il6*, and of Epstein-Barr virus-induced 3 (*Ebi3*) and *Il27p28*, two subunits constituting the heterodimeric IL-27 cytokine (Fig. 4C). In contrast, the expressions of those genes were not up-regulated in mice lacking IL-17 expression (Fig. 4C). In addition, treatment of RAW264.7 macrophages with recombinant IL-17 significantly induced proinflammatory chemokine/cytokine mRNA expressions, including *Mcp1*, *Tnfa*, *Il6*, and *Ebi3* and *Il27p28* (Fig. 4D). Altogether, these data showed a key role of IL-17 in triggering the well-described hepatic inflammatory response necessary for LPC activation (e.g., *Mcp1*, *Tnfa*, *Il6*) and revealed an induced expression of IL-27 with a putative role in LPC-driven liver regeneration.

WSX-1 DEFICIENCY REPRESSES LPC-DRIVEN LIVER REGENERATION

IL-27 is a cytokine with a well-known modulatory function in progenitor cell-mediated tissue repair in other organs.^(41,42) To address the potential role of the IL-27-WSX-1 axis in LPC accumulation, WT and WSX-1^{-/-} mice were subjected to CDE-diet feeding. CK19 immunostaining on liver tissue sections showed a strong inhibition of LPC accumulation in WSX-1^{-/-} animals when compared with their WT counterpart from day 3 after the CDE diet (Fig. 5A). In agreement with these CK19 immunostaining data, mRNA

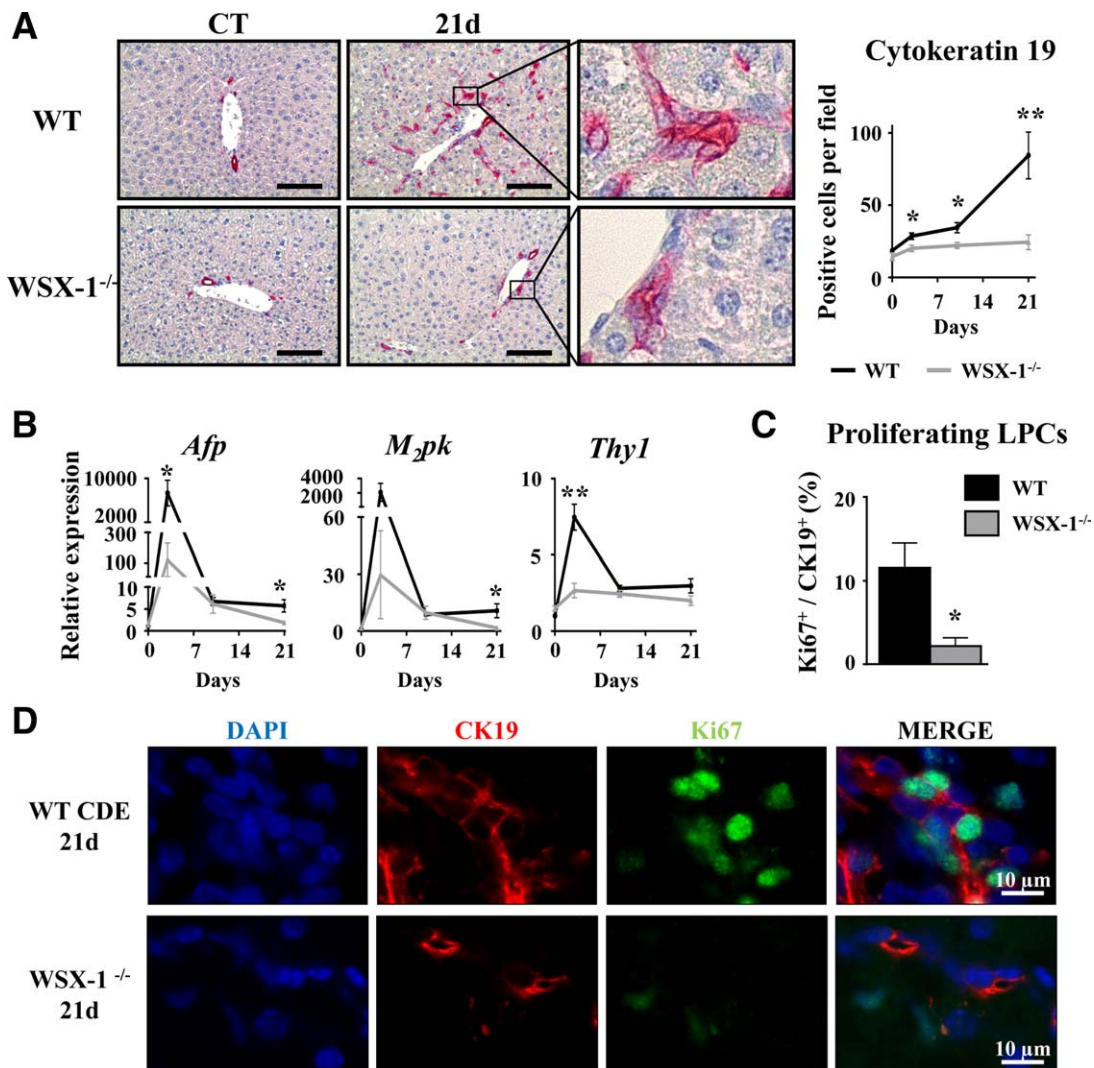


FIG. 5. WSX-1-deficiency represses LPC-driven liver regeneration. Wild-type and WSX-1^{-/-} mice were fed a CDE diet, and samples were collected at the indicated time points. (A) CK19⁺ cells were stained and counted. Scale bar, 100 μ m. (B) Hepatic mRNA expressions of LPC-associated genes were measured by qRT-PCR. (C,D) CK19 (red) and Ki67 (green) staining and counting after 21 days of the CDE diet. * $P < 0.05$, ** $P < 0.01$, WT versus WSX-1^{-/-} mice; each group $n = 4-7$ animals. Data represent mean \pm SEM. Abbreviations: CT, control; d, day; DAPI, 4',6-diamidino-2-phenylindole; *M₂pk*, type 2 muscle pyruvate kinase; qRT-PCR, quantitative reverse-transcription polymerase chain reaction.

expressions of LPC activation-related genes (*Afp*, *Thy1*) were not induced in WSX-1^{-/-} mice (Fig. 5B). Interestingly, proliferating CK19⁺ cells identified by CK19 and Ki67 double staining revealed that 12% of CK19⁺ LPCs were proliferating 21 days after the CDE diet in WT mice, while only 2.5% of proliferating CK19⁺ cells were counted in WSX-1^{-/-} mice (Fig. 5C,D). This strongly suggests an essential involvement of the IL-27-WSX-1 axis in the LPC activation process.

CDE DIET-INDUCED LIVER INFLAMMATION IS REDUCED IN WSX-1^{-/-} MICE

A disrupted IL-27 signaling pathway is associated with reduced LPC accumulation after a CDE diet. To better characterize the mechanisms that could explain this observation, we evaluated liver injury and inflammation. Serum transaminases and hematoxylin and eosin staining on liver tissue sections showed similar

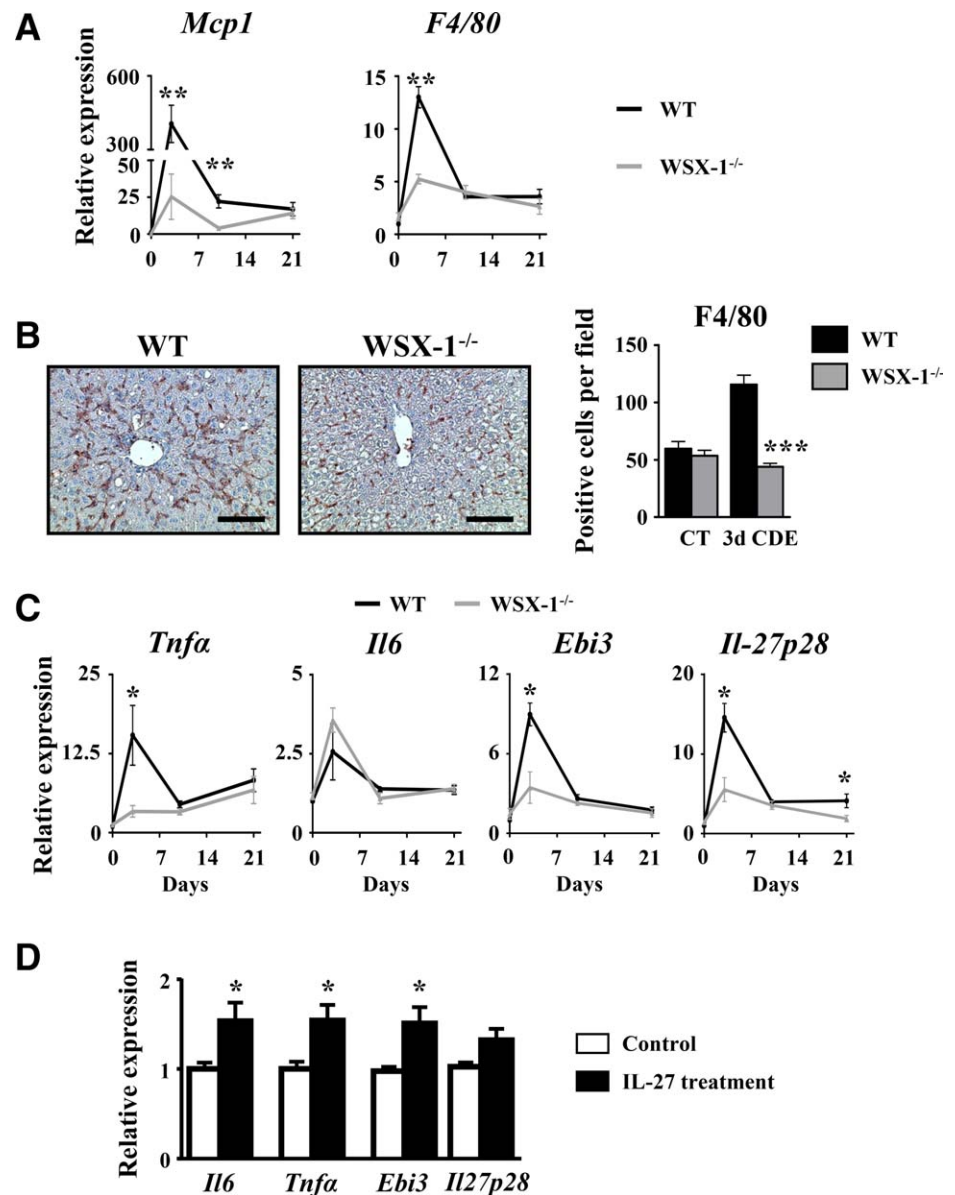


FIG. 6. CDE diet-induced liver inflammation is reduced in WSX-1^{-/-}. Wild-type and WSX-1^{-/-} mice were subjected to the CDE model. (A) Hepatic mRNA expression of macrophage-related genes was assessed by qRT-PCR. (B) Immunostaining of F4/80 was performed on WT and WSX-1^{-/-} mice, and positive cells were counted after 3 days of the CDE diet. Scale bar, 100 μ m. (C) Hepatic mRNA expressions of inflammation-related genes were quantified by qRT-PCR; each group n = 4-7 animals. * P < 0.05, ** P < 0.01, *** P < 0.005, WT versus WSX-1^{-/-} mice. (D) RAW264.7 cells were cultured in the presence of 50 ng/mL IL-27, and mRNA expressions of IL-6, TNF- α , and IL-27 subunits were analyzed by qRT-PCR. * P < 0.05, control versus IL-27-treated cells. Data represent mean \pm SEM. Abbreviations: CT, control; d, day; qRT-PCR, quantitative reverse-transcription polymerase chain reaction.

injury in WT and WSX-1^{-/-} mice (Supporting Figs. S6A and S4B). In addition, food intake was assessed in both types of mice and did not show any difference (Supporting Fig. S6C). Liver macrophages infiltrating the liver after the CDE diet were quantified in WT and WSX-1^{-/-} mice. *Mcp1* and *F4/80* mRNA expressions were significantly induced and peaked 3 days after the CDE diet in WT animals but not in WSX-1^{-/-} mice (Fig. 6A). In addition, F4/80 immunostaining of liver samples confirmed a 3-fold increase in the number of macrophages infiltrating the livers of

CDE-treated WT mice, but such increase was completely abolished in livers of CDE-treated WSX-1^{-/-} animals (Fig. 6B). Analysis of inflammatory cytokines revealed an increase in mRNA expression of *Tnfa*, *Il6*, *Ebi3*, and *Il27p28* in WT mice but not in WSX-1^{-/-} animals. Moreover, IL-27-treated RAW cells showed increased *Il6*, *Tnfa*, and *Ebi3* but not *Il27p28* mRNA expressions (Fig. 6D). Lastly, CDE-induced Th1, Th2, and Th17 marker gene expressions were significantly lowered in WSX-1^{-/-} compared to WT mice (Supporting Fig. S7). This strongly suggests

that the IL-27–WSX-1 axis is required to promote the inflammatory response required for supporting the LPC compartment.

IL-17 FAVORS LPC PROLIFERATION WHEREAS IL-27 INDUCES EXPRESSION OF HEPATOCYTE DIFFERENTIATION MARKERS

As LPC accumulation was strongly altered in both IL-17^{-/-} and IL-27^{-/-} animals under the CDE diet, we further deciphered the direct role of IL-17 and IL-27 on LPCs *in vitro*. Bipotential murine oval liver (BMOL) cells, a well characterized LPC cell line, were cultured in the absence or presence of either IL-27 or IL-17. Cell viability and proliferation were evaluated by the 3-(4,5-dimethylthiazol-2-yl)-5-(3-carboxymethoxyphenyl)-2-(4-sulfophenyl)-2H-tetrazolium assay and showed that IL-17 potentiated BMOL cell growth along with a 5-day culture while IL-27 had no effect (Fig. 7A). To evaluate the potent role of IL-17 and IL-27 in LPC differentiation, hepatocytic cell differentiation marker mRNA expressions, including albumin (*Alb*), tyrosine aminotransferase (*Tat*), and *Hnf4α* were also assessed (Fig. 7B). Our data revealed that IL-17 did not increase but instead decreased some of those markers, including *Alb* and *Tat* expressions. In contrast, BMOL treatment with IL-27 increased *Alb* and *Hnf4α* mRNA expressions (Fig. 7B). Similarly, hepatocytic cell markers analyzed at protein levels by western blot showed an increased expression of Alb, TAT, and HNF4α in the presence of IL-27 (Fig. 7C,D). IL-27 did not potentiate the effects of the hepatocyte-differentiation culture medium (Supporting Fig. S8). However, IL-17 treatment in similar conditions reduced hepatocytic differentiating markers consistently with results obtained in normal culture conditions (Fig. 7B). To confirm the putative role of IL-27 in differentiating LPCs into hepatocytes, freshly isolated LPCs from mouse livers after a 21-day CDE diet were cultured in the absence or presence of IL-27 or IL-17. The purity of freshly isolated LPCs was assessed by flow cytometry and showed 94.8% epithelial cell adhesion molecule (EpCAM)⁺ CD45⁻ isolated cells (Supporting Fig. S9). IL-27 treatment strongly induced *Alb*, *Tat*, and *Hnf4α* mRNA expressions when compared to nontreated controls. IL-17 treatment did not induce any of those hepatocytic markers but diminished *Hnf4α* mRNA expression

(Fig. 7E). Similarly, HNF4α immunostaining on freshly isolated LPCs showed a weak basal level in control cells (Fig. 7F) while IL-27 treatment significantly induced HNF4α expression. In contrast, IL-17 treatment completely abolished HNF4α expression. Compared to BMOL cells that have been immortalized, freshly isolated LPCs do not show significant proliferation *in vitro* in our basal culture conditions. Therefore, no significant effect of IL-17 or IL-27 treatment was obtained on proliferation assays (data not shown). Taken together, these data demonstrate a direct role of IL-17 in mediating LPC accumulation while IL-27 plays a complementary role by favoring LPC differentiation toward a hepatocytic phenotype.

Discussion

A large spectrum of growth factors and cytokines has been reported to contribute to LPC niche activation, and some of these have been described as dispensable due to redundant functions. In the present study, we report a correlation between IL-17-producing cell recruitment and the severity of the DR, and we identify IL-17 as a cytokine with a central role in triggering LPC compartment activation and proliferation. We also reveal that IL-17 is responsible for macrophage-induced IL-27 expression that favors LPC differentiation into hepatocytes. We therefore highlight collaborative work between IL-17 and IL-27 that is required to properly achieve liver regeneration from progenitor cells (Fig. 8).

ASSOCIATION OF DR WITH INFLAMMATORY CELLS

In virtually all types of chronic liver diseases, biliary and liver progenitor cell accumulation, referred to as DR, is frequently observed.⁽³⁾ In humans, LPC accumulation is an important prognostic marker in advanced liver diseases and is often associated with a less optimistic outcome.⁽⁴³⁾ In our study, comparison of CK19^{low} with CK19^{high} groups of patients revealed a higher Child-Pugh and MELD score severity associated with increased LPC expansion. DR is accompanied by recruitment of immune cells nearby, and compelling findings in both animal and human studies emphasize the pivotal role of inflammatory cytokines in the LPC-driven regenerative process.^(19,20,23-25)

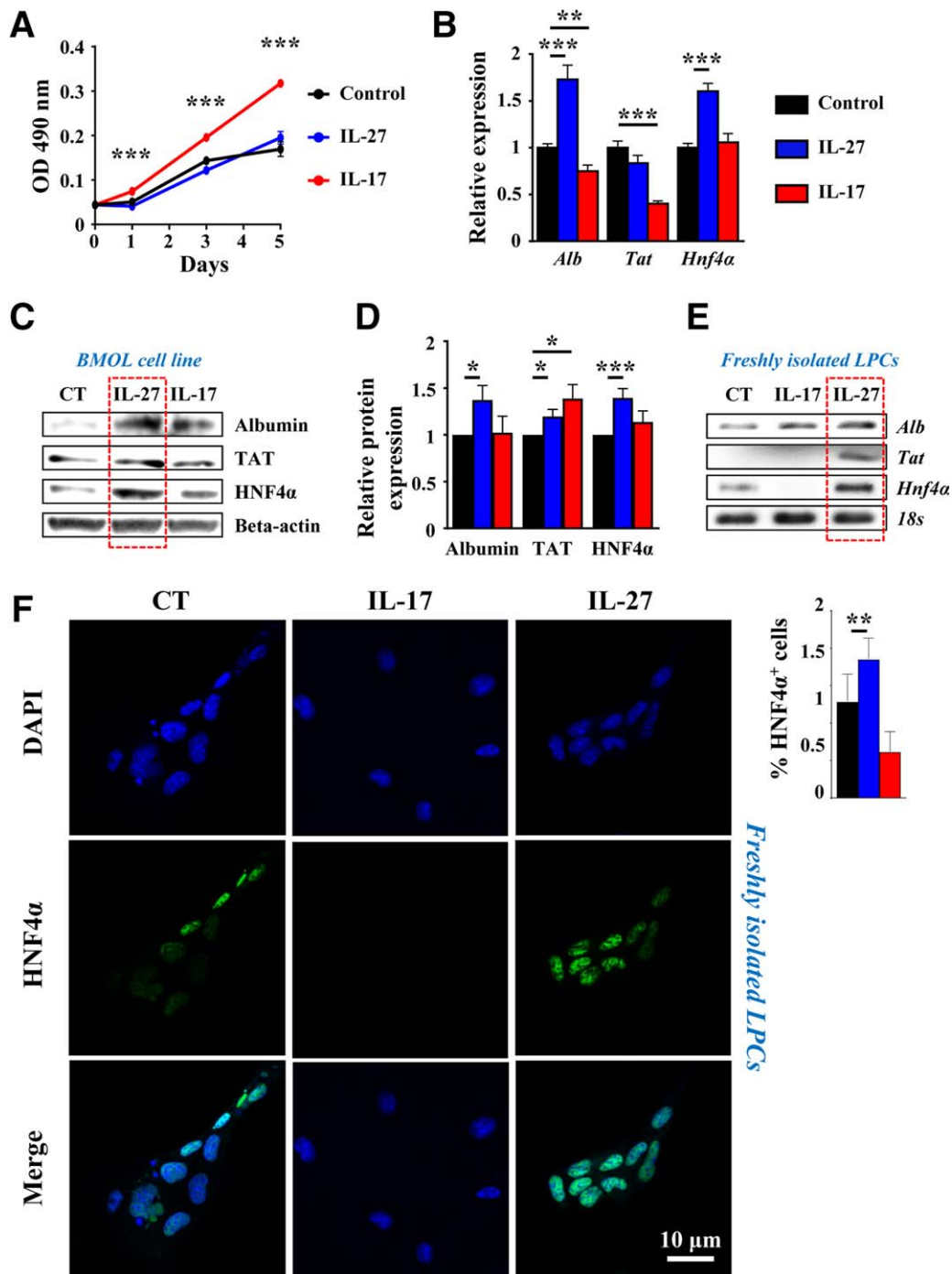


FIG. 7. IL-17 favors LPC proliferation whereas IL-27 induces their differentiation. BMOL cells were treated with 50 ng/mL recombinant IL-27 or IL-17, and (A) proliferation was assessed by optical density using an MTS assay. Hepatocyte differentiation marker expression was analyzed by (B) qRT-PCR after 6 hours or (C) by western blot after 24 hours of treatment. (D) Western blot quantification ($n = 6-8$ independent experiments). Results are expressed as fold change over untreated cells. $*P < 0.05$, $**P < 0.01$, $***P < 0.005$. (D,E) Primary LPCs were cultured in the presence of 50 ng/mL recombinant IL-17 or IL-27 for 24 hours. Hepatocyte differentiation marker expressions were analyzed by (E) qRT-PCR and (F) immunocytochemistry using an anti-HNF4 α antibody. HNF4 α ⁺ cells were counted in each condition. Data represent mean \pm SEM. Abbreviations: CT, control; DAPI, 4',6-diamidino-2-phenylindole; MTS, 3-(4,5-dimethylthiazol-2-yl)-5-(3-carboxymethoxyphenyl)-2-(4-sulfophenyl)-2H-tetrazolium; OD, optical density; qRT-PCR, quantitative reverse-transcription polymerase chain reaction.

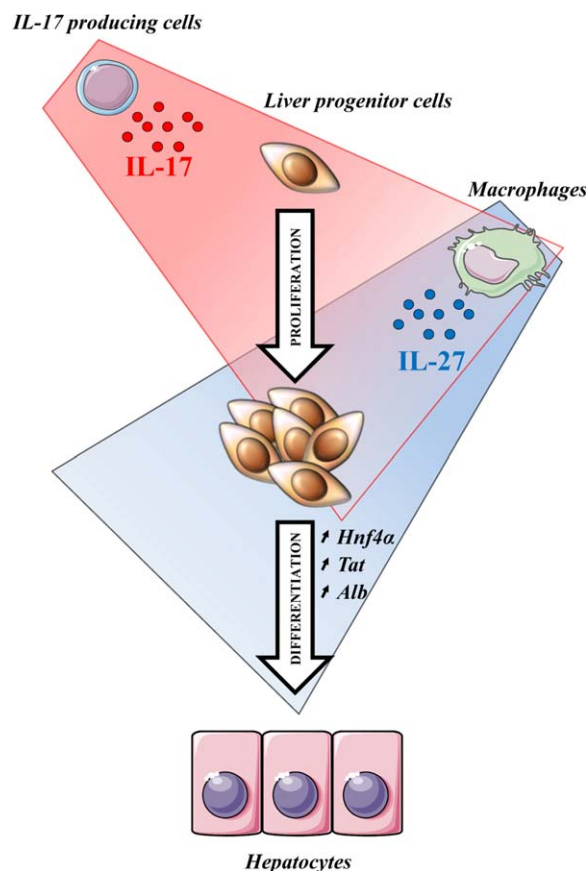


FIG. 8. IL-17 induces liver progenitor cell proliferation while IL-27 favors their differentiation toward a hepatocytic phenotype. Taken together, these data provide evidence of a collaborative role of IL-17 and IL-27 in promoting liver regeneration. IL-17 directly acts on LPCs to favor their proliferation. IL-17 also induces macrophage IL-27 production, which enhances LPC differentiation toward hepatocytes.

IL-17 IN LPC ACTIVATION AND PROLIFERATION

Based on the clinical study of chronic liver diseases, regardless of etiology, we report a positive correlation between the degree of DR and the number of IL-17-producing cells infiltrating the liver. The proximity between IL-17⁺ cells and LPCs led us to hypothesize that IL-17 could be associated with LPC activation and proliferation. Moreover, increased IL-17⁺ cells infiltrating the liver of CK19^{high} patients aggravate their Child-Pugh and MELD scores (Supporting Table S1). Mixed phenotypes CK19^{high} IL-17^{low} and CK19^{low} IL-17^{high} were found in few patients. The source of IL-17-producing cells reported in human livers is heterogeneous and mainly includes Th17

lymphocytes, $\gamma\delta$ T cells, and neutrophils.^(20,29,30,33) In mouse, we cannot exclude a different profiling of IL-17-producing cell types, depending on the experimental model, when compared to human liver diseases. However, in the murine model of CDE-diet-induced liver regeneration from LPCs, we revealed an induced expression of Th17-associated genes as early as 3 days after a CDE diet in WT animals. Such induced expressions were maintained along with the protocol (Supporting Fig. S1), although IL-17 levels in the serum or liver were not detectable by using currently available kits (data not shown). In keeping with results obtained in a previous work,⁽²²⁾ our data strongly support the participation of Th17 cells in the hepatic production of IL-17. Interestingly, we showed that in mice lacking IL-17 expression and subjected to a CDE diet, the capacity of LPCs to accumulate is dramatically altered when compared to WT animals. Along the same lines of evidence, LPC treatment with IL-17 promoted LPC expansion *in vitro*. Furthermore, we previously reported a role of IL-17 in polarizing macrophages toward a proinflammatory M1 phenotype.⁽³⁴⁾ In this study, we show that IL-17 deficiency causes impairment of macrophage cell recruitment in CDE-diet-induced liver regeneration, resulting in reduced hepatic inflammation. This reduced inflammatory response may explain the reduced liver injury observed at later time points in IL-17^{-/-} animals. These results are consistent with previous reports showing that macrophage depletion by clodronate injections abrogates LPC accumulation and subsequent liver regeneration during a CDE diet.⁽²¹⁾ The results obtained *in vivo* clearly provide evidence that IL-17 deficiency alters LPC expansion, which fits with *in vitro* data. However, neither IL-17 deficiency (Fig. 3A) nor macrophage depletion⁽⁴⁴⁾ were sufficient to completely abolish DR. This suggests that IL-17 could contribute to LPC expansion by i) directly promoting LPC proliferation and ii) indirectly through M1-macrophage-induced production of required factors, e.g., TNF- α and IL-6, which support LPC accumulation.^(19,45) IL-17 has been detected in several types of chronic liver diseases^(29,30) and was associated with increased liver injury and fibrosis^(33,34) and hepatocellular carcinoma.^(46,47) Our data highlight that a sustained IL-17 inflammatory response lacking a differentiating process may be responsible for incomplete hepatic regeneration, with uncontrolled accumulation of progenitor cells susceptible to undergo genetic and epigenetic alterations and to initiate carcinogenic processes.

LPC-MEDIATED DIFFERENTIATION THROUGH THE IL-27-WSX-1 AXIS

In addition to its function in triggering LPC activation in regenerating livers, we demonstrated that IL-17 also induced IL-27 cytokine production by macrophages. IL-27 is also described as an IFN- γ -like cytokine that favors hematopoietic and neural precursor differentiation through signal transducer and activator of transcription 1^(41,42); this is in addition to its proinflammatory⁽⁴⁸⁾ or anti-inflammatory⁽⁴⁹⁾ role according to the pathogenesis. Numerous studies revealed antitumor properties of IL-27 through the complex regulation of immune response, and this cytokine has also been reported to exert antiproliferative and anti-angiogenic effects by directly acting on cancer cells.⁽⁵⁰⁾ IL-27 has also been shown to directly favor cardiac progenitor cell differentiation,⁽³⁷⁾ expansion and differentiation of hematopoietic stem cells,^(38,39) and could support retinal progenitor cell differentiation.⁽³⁶⁾ In this model, we showed that disruption of IL-27 receptor signaling also prevented LPC accumulation. Alternatively, we showed a direct role of IL-27 on LPCs by favoring their differentiation into a hepatocytic phenotype *in vitro* without a direct mitogenic effect. Additional experiments, such as lineage tracing in several models, including CDE, or hepatocyte-specific MDM2 proto-oncogene (Mdm2)-deficient mice, are required to conclude on the role of IL-27 effects on LPC differentiation *in vivo*.⁽¹¹⁻¹³⁾ Reduced LPC accumulation in WSX-1^{-/-} mice was associated with a significant decrease in recruitment of macrophages, which are reported as crucial actors in supporting LPC expansion.⁽⁴⁴⁾ We also showed a direct effect of IL-27 on promoting proinflammatory cytokine gene expressions in macrophages. These data suggest that IL-27 may indirectly enhance LPC proliferation through favoring macrophage activation and cytokine production.

Taken together, in this present work we provide evidence of a dual role of IL-17 in regenerating livers from progenitors. IL-17 not only targets LPCs and stimulates their proliferation but also promotes IL-27-induced expression from macrophages, which contribute to LPC differentiation into a hepatocytic phenotype. These data shed light on the fact that both proliferative and differentiating processes of LPCs are essential to achieve liver regeneration. Our data also suggest that lack of a differentiating process may lead to immature LPC accumulation that is susceptible to cell transformation into cancer cells.

Acknowledgment: We thank Professor Yoichiro Iwakura (Japan) for providing IL-17-deficient mice and Professor George Yeoh (Australia) for providing the BMOL cell line. We are grateful to Gilles Carpentier from the CRRET laboratory at the University of Paris-Est for his kind help in confocal microscopy analysis.

REFERENCES

- 1) Williams MJ, Clouston AD, Forbes SJ. Links between hepatic fibrosis, ductular reaction, and progenitor cell expansion. *Gastroenterology* 2014;146:349-356.
- 2) Desmet VJ. Ductal plates in hepatic ductular reactions. Hypothesis and implications. I. Types of ductular reaction reconsidered. *Virchows Arch* 2011;458:251-259.
- 3) Gouw AS, Clouston AD, Theise ND. Ductular reactions in human liver: diversity at the interface. *Hepatology* 2011;54:1853-1863.
- 4) Roskams TA, Libbrecht L, Desmet VJ. Progenitor cells in diseased human liver. *Semin Liver Dis* 2003;23:385-396.
- 5) Clouston AD, Powell EE, Walsh MJ, Richardson MM, Demetris AJ, Jonsson JR. Fibrosis correlates with a ductular reaction in hepatitis C: roles of impaired replication, progenitor cells and steatosis. *Hepatology* 2005;41:809-818.
- 6) Richardson MM, Jonsson JR, Powell EE, Brunt EM, Neuschwander-Tetri BA, Bhatnagar PS, et al. Progressive fibrosis in nonalcoholic steatohepatitis: association with altered regeneration and a ductular reaction. *Gastroenterology* 2007;133:80-90.
- 7) Sancho-Bru P, Altamirano J, Rodrigo-Torres D, Coll M, Millan C, Jose Lozano J, et al. Liver progenitor cell markers correlate with liver damage and predict short-term mortality in patients with alcoholic hepatitis. *Hepatology* 2012;55:1931-1941.
- 8) Ruddell RG, Knight B, Tirnitz-Parker JE, Akhurst B, Summerville L, Subramaniam VN, et al. Lymphotoxin-beta receptor signaling regulates hepatic stellate cell function and wound healing in a murine model of chronic liver injury. *Hepatology* 2009;49:227-239.
- 9) Van Hul NK, Abarca-Quinones J, Sempoux C, Horsmans Y, Leclercq IA. Relation between liver progenitor cell expansion and extracellular matrix deposition in a CDE-induced murine model of chronic liver injury. *Hepatology* 2009;49:1625-1635.
- 10) Wu K, Ding J, Chen C, Sun W, Ning BF, Wen W, et al. Hepatic transforming growth factor beta gives rise to tumor-initiating cells and promotes liver cancer development. *Hepatology* 2012;56:2255-2267.
- 11) Choi TY, Ninov N, Stainier DY, Shin D. Extensive conversion of hepatic biliary epithelial cells to hepatocytes after near total loss of hepatocytes in zebrafish. *Gastroenterology* 2014;146:776-788.
- 12) He J, Lu H, Zou Q, Luo L. Regeneration of liver after extreme hepatocyte loss occurs mainly via biliary transdifferentiation in zebrafish. *Gastroenterology* 2014;146:789-800.e788.
- 13) Lu WY, Bird TG, Boulter L, Tsuchiya A, Cole AM, Hay T, et al. Hepatic progenitor cells of biliary origin with liver repopulation capacity. *Nat Cell Biol* 2015;17:971-983.

- 14) Español-Suñer R, Carpentier R, Van Hul N, Legry V, Achouri Y, Cordi S, et al. Liver progenitor cells yield functional hepatocytes in response to chronic liver injury in mice. *Gastroenterology* 2012;143:1564-1575.e1567.
- 15) Rodrigo-Torres D, Affo S, Coll M, Morales-Ibanez O, Millan C, Blaya D, et al. The biliary epithelium gives rise to liver progenitor cells. *Hepatology* 2014;60:1367-1377.
- 16) Sackett SD, Li Z, Hurtt R, Gao Y, Wells RG, Brondell K, et al. Foxl1 is a marker of bipotential hepatic progenitor cells in mice. *Hepatology* 2009;49:920-929.
- 17) Huch M, Gehart H, van Boxtel R, Hamer K, Blokzijl F, Verstegen MM, et al. Long-term culture of genome-stable bipotent stem cells from adult human liver. *Cell* 2015;160:299-312.
- 18) Erker L, Grompe M. Signaling networks in hepatic oval cell activation. *Stem Cell Res* 2007;1:90-102.
- 19) **Knight B, Matthews VB**, Akhurst B, Croager EJ, Klinken E, Abraham LJ, et al. Liver inflammation and cytokine production, but not acute phase protein synthesis, accompany the adult liver progenitor (oval) cell response to chronic liver injury. *Immunol Cell Biol* 2005;83:364-374.
- 20) Gadd VL, Skoien R, Powell EE, Fagan KJ, Winterford C, Horsfall L, et al. The portal inflammatory infiltrate and ductular reaction in human nonalcoholic fatty liver disease. *Hepatology* 2014;59:1393-1405.
- 21) **Van Hul N, Lanthier N**, Espanol Suner R, Abarca Quinones J, van Rooijen N, Leclercq I. Kupffer cells influence parenchymal invasion and phenotypic orientation, but not the proliferation, of liver progenitor cells in a murine model of liver injury. *Am J Pathol* 2011;179:1839-1850.
- 22) Strick-Marchand H, Masse GX, Weiss MC, Di Santo JP. Lymphocytes support oval cell-dependent liver regeneration. *J Immunol* 2008;181:2764-2771.
- 23) Hines IN, Kremer M, Isayama F, Perry AW, Milton RJ, Black AL, et al. Impaired liver regeneration and increased oval cell numbers following T cell-mediated hepatitis. *Hepatology* 2007;46:229-241.
- 24) **Knight B, Lim R**, Yeoh GC, Olynyk JK. Interferon-gamma exacerbates liver damage, the hepatic progenitor cell response and fibrosis in a mouse model of chronic liver injury. *J Hepatol* 2007;47:826-833.
- 25) **Nguyen LN, Furuya MH**, Wolfrain LA, Nguyen AP, Holdren MS, Campbell JS, et al. Transforming growth factor-beta differentially regulates oval cell and hepatocyte proliferation. *Hepatology* 2007;45:31-41.
- 26) Tirnitz-Parker JE, Viebahn CS, Jakubowski A, Klopčič BR, Olynyk JK, Yeoh GC, et al. Tumor necrosis factor-like weak inducer of apoptosis is a mitogen for liver progenitor cells. *Hepatology* 2010;52:291-302.
- 27) Subrata LS, Voon DC, Yeoh GC, Ulgiati D, Quail EA, Abraham LJ. TNF-inducible expression of lymphotoxin-beta in hepatic cells: an essential role for NF-kappaB and Ets1 transcription factors. *Cytokine* 2012;60:498-504.
- 28) Feng D, Kong X, Weng H, Park O, Wang H, Dooley S, et al. Interleukin-22 promotes proliferation of liver stem/progenitor cells in mice and patients with chronic hepatitis B virus infection. *Gastroenterology* 2012;143:188-198.e187.
- 29) Hammerich L, Bangen JM, Govaere O, Zimmermann HW, Gassler N, Huss S, et al. Chemokine receptor CCR6-dependent accumulation of gammadelta T cells in injured liver restricts hepatic inflammation and fibrosis. *Hepatology* 2014;59:630-642.
- 30) Lafdil F, Miller AM, Ki SH, Gao B. Th17 cells and their associated cytokines in liver diseases. *Cell Mol Immunol* 2010;7:250-254.
- 31) Radaeva S, Sun R, Pan HN, Hong F, Gao B. Interleukin 22 (IL-22) plays a protective role in T cell-mediated murine hepatitis: IL-22 is a survival factor for hepatocytes via STAT3 activation. *Hepatology* 2004;39:1332-1342.
- 32) Kong X, Feng D, Wang H, Hong F, Bertola A, Wang FS, et al. Interleukin-22 induces hepatic stellate cell senescence and restricts liver fibrosis in mice. *Hepatology* 2012;56:1150-1159.
- 33) Meng F, Wang K, Aoyama T, Grivennikov SI, Paik Y, Scholten D, et al. Interleukin-17 signaling in inflammatory, Kupffer cells, and hepatic stellate cells exacerbates liver fibrosis in mice. *Gastroenterology* 2012;143:765-776.e763.
- 34) Guillot A, Hamdaoui N, Bizy A, Zoltani K, Souktani R, Zafrani ES, et al. Cannabinoid receptor 2 counteracts interleukin-17-induced immune and fibrogenic responses in mouse liver. *Hepatology* 2014;59:296-306.
- 35) **Rao R, Graffeo CS, Gulati R**, Jamal M, Narayan S, Zambirinis CP, et al. Interleukin 17-producing gammadeltaT cells promote hepatic regeneration in mice. *Gastroenterology* 2014;147:473-484.e472.
- 36) Xu Y, Balasubramanian B, Copland DA, Liu J, Armitage MJ, Dick AD. Activated adult microglia influence retinal progenitor cell proliferation and differentiation toward recoverin-expressing neuron-like cells in a co-culture model. *Graefes Arch Clin Exp Ophthalmol* 2015;253:1085-1096.
- 37) **Tanaka T, Obana M**, Mohri T, Ebara M, Otani Y, Maeda M, et al. Interleukin-27 induces the endothelial differentiation in Sca-1 + cardiac resident stem cells. *Cytokine* 2015;75:365-372.
- 38) Hoyt TR, Dobrinen E, Kochetkova I, Meissner N. B cells modulate systemic responses to *Pneumocystis murina* lung infection and protect on-demand hematopoiesis via T cell-independent innate mechanisms when type I interferon signaling is absent. *Infect Immun* 2015;83:743-758.
- 39) Furusawa J, Mizoguchi I, Chiba Y, Hisada M, Kobayashi F, Yoshida H, et al. Promotion of expansion and differentiation of hematopoietic stem cells by interleukin-27 into myeloid progenitors to control infection in emergency myelopoiesis. *PLoS Pathog* 2016;12:e1005507.
- 40) **Bender H, Wiesinger MY**, Nordhoff C, Schoenherr C, Haan C, Ludwig S, et al. Interleukin-27 displays interferon-gamma-like functions in human hepatoma cells and hepatocytes. *Hepatology* 2009;50:585-591.
- 41) Seita J, Asakawa M, Oochara J, Takayanagi S, Morita Y, Watanabe N, et al. Interleukin-27 directly induces differentiation in hematopoietic stem cells. *Blood* 2008;111:1903-1912.
- 42) Koch M, May U, Kuhns S, Drechsler H, Adam N, Hattermann K, et al. Interleukin 27 induces differentiation of neural C6-precursor cells into astrocytes. *Biochem Biophys Res Commun* 2007;364:483-487.
- 43) Lowes KN, Brennan BA, Yeoh GC, Olynyk JK. Oval cell numbers in human chronic liver diseases are directly related to disease severity. *Am J Pathol* 1999;154:537-541.
- 44) Elsegood CL, Chan CW, Degli-Esposti MA, Wikstrom ME, Domenichini A, Lazarus K, et al. Kupffer cell-monocyte communication is essential for initiating murine liver progenitor cell-mediated liver regeneration. *Hepatology* 2015;62:1272-1284.
- 45) Jakubowski A, Ambrose C, Parr M, Lincecum JM, Wang MZ, Zheng TS, et al. TWEAK induces liver progenitor cell proliferation. *J Clin Invest* 2005;115:2330-2340.
- 46) **Liao R, Sun J**, Wu H, Yi Y, Wang JX, He HW, et al. High expression of IL-17 and IL-17RE associate with poor

- prognosis of hepatocellular carcinoma. *J Exp Clin Cancer Res* 2013;32:3.
- 47) Lukacs-Kornek V, Lammert F. The progenitor cell dilemma: cellular and functional heterogeneity in assistance or escalation of liver injury. *J Hepatol* 2017;66:619-630.
- 48) Siebler J, Wirtz S, Frenzel C, Schuchmann M, Lohse AW, Galle PR, et al. Cutting edge: a key pathogenic role of IL-27 in T cell-mediated hepatitis. *J Immunol* 2008;180:30-33.
- 49) **Hirahara K, Ghoreschi K**, Yang XP, Takahashi H, Laurence A, Vahedi G, et al. Interleukin-27 priming of T cells controls IL-17 production in trans via induction of the ligand PD-L1. *Immunity* 2012;36:1017-1030.
- 50) Hasegawa H, Mizoguchi I, Chiba Y, Ohashi M, Xu M, Yoshimoto T. Expanding diversity in molecular structures and functions of the IL-6/IL-12 heterodimeric cytokine family. *Front Immunol* 2016;7:479.

Author names in bold designate shared co-first authorship.

Supporting Information

Additional Supporting Information may be found at <http://onlinelibrary.wiley.com/doi/10.1002/hep4.1145/full>.

PUBLICATION 3

Bile acid-activated macrophages promote biliary epithelial cell proliferation through integrin $\alpha v \beta 6$ upregulation following liver injury

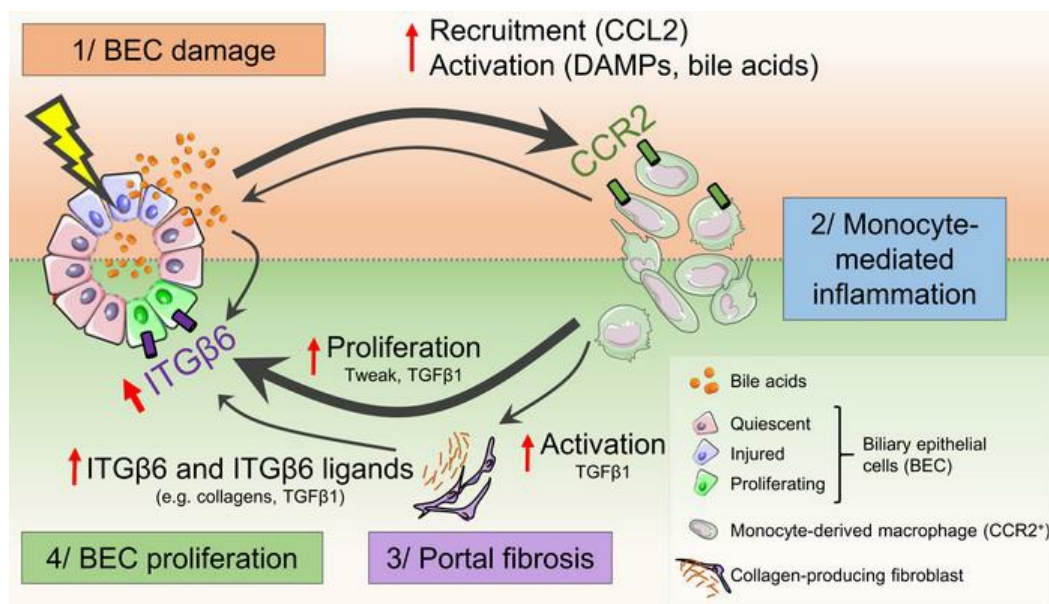
Bile acid–activated macrophages promote biliary epithelial cell proliferation through integrin $\alpha\beta6$ upregulation following liver injury

Adrien Guillot, ... , Frank Tacke, Bin Gao

J Clin Invest. 2021;131(9):e132305. <https://doi.org/10.1172/JCI132305>.

Research Article Hepatology

Graphical abstract



Find the latest version:

<https://jci.me/132305/pdf>



Bile acid-activated macrophages promote biliary epithelial cell proliferation through integrin $\alpha\beta6$ upregulation following liver injury

Adrien Guillot,^{1,2} Lucia Guerri,³ Dechun Feng,¹ Seung-Jin Kim,¹ Yeni Ait Ahmed,¹ Janos Palocz,⁴ Yong He,¹ Kornel Schuebel,³ Shen Dai,⁵ Fengming Liu,⁵ Pal Pacher,⁴ Tatiana Kisseleva,⁶ Xuebin Qin,⁵ David Goldman,³ Frank Tacke,² and Bin Gao¹

¹Laboratory of Liver Diseases, National Institute on Alcohol Abuse and Alcoholism (NIAAA), NIH, Bethesda, Maryland, USA. ²Department of Hepatology and Gastroenterology, Charité University Medicine Berlin, Berlin, Germany. ³Laboratory of Neurogenetics and ⁴Laboratory of Cardiovascular Physiology and Tissue Injury, NIAAA, NIH, Bethesda, Maryland, USA. ⁵Division of Comparative Pathology, Tulane National Primate Research Center, Covington, Louisiana, USA. ⁶Department of Surgery, UCSD, San Diego, California, USA.

Cholangiopathies caused by biliary epithelial cell (BEC) injury represent a leading cause of liver failure. No effective pharmacologic therapies exist, and the underlying mechanisms remain obscure. We aimed to explore the mechanisms of bile duct repair after targeted BEC injury. Injection of intermedilysin into BEC-specific human CD59 (hCD59) transgenic mice induced acute and specific BEC death, representing a model to study the early signals that drive bile duct repair. Acute BEC injury induced cholestasis followed by CCR2⁺ monocyte recruitment and BEC proliferation. Using microdissection and next-generation RNA-Seq, we identified 5 genes, including *Mapk8ip2*, *Cdkn1a*, *Itgb6*, *Rgs4*, and *Ccl2*, that were most upregulated in proliferating BECs after acute injury. Immunohistochemical analyses confirmed robust upregulation of integrin $\alpha\beta6$ (ITG $\beta6$) expression in this BEC injury model, after bile duct ligation, and in patients with chronic cholangiopathies. Deletion of the *Itgb6* gene attenuated BEC proliferation after acute bile duct injury. Macrophage depletion or *Ccr2* deficiency impaired ITG $\beta6$ expression and BEC proliferation. In vitro experiments revealed that bile acid-activated monocytes promoted BEC proliferation through ITG $\beta6$. Our data suggest that BEC injury induces cholestasis, monocyte recruitment, and induction of ITG $\beta6$, which work together to promote BEC proliferation and therefore represent potential therapeutic targets for cholangiopathies.

Introduction

The biliary tree occupies a substantial space in the liver and has crucial functions such as the transport and maturation of bile (1). Cholangiopathies led to approximately 16% of liver transplantations in the USA between 1988 and 2014 (2) and include primary sclerosing cholangitis (PSC), primary biliary cholangitis (PBC), biliary atresia, cholangiocarcinoma, sclerosing cholangitis of critically ill patients (SC-CIPs), and coronavirus disease 2019 (COVID-19) cholangiopathy (1, 3). Classical clinical presentations for these disorders include cholestasis and portal inflammation, fibrosis, as well as portal hypertension and disturbances of the liver microcirculation (4). Ductular reaction, which involves biliary epithelial or liver progenitor cell proliferation as well as portal inflammation and portal fibrosis, is observed in numerous hepatopathies and is notably associated with a poor outcome in chronic liver diseases of various etiologies (5, 6). Although several studies reported a potent role for immune cells in promoting the ductular reaction (5, 7–9), the precise mechanisms underlying bile duct injury and regeneration have not been identified because of the lack of a specific biliary epithelial cell (BEC) injury model.

Several models have been used to study BEC injury, but they are associated with chronic injury and inflammation and are not specific for BEC injury (10). For example, multidrug resistance gene 2-deficient (*Mdr2*-deficient) mice spontaneously develop severe biliary fibrosis and have been extensively used to mimic PSC progression, but the chronicity of this model impedes the study of mechanisms that promote BEC repair (11). Extrahepatic bile duct obstruction has also been induced by injection of bili-atresone (12). More recently, a novel model of sclerosing cholangitis has been described, consisting of intrabiliary injection of BV6, an antagonist of the inhibitors of apoptosis (IAP), and leading to TRAIL toxicity and BEC damage (13). Using this model, Guicciardi et al. showed that BEC damage is followed by CCL2-dependent proinflammatory monocyte recruitment, which was prevented by genetic deletion of the *Ccr2* gene or using the CCR2/CCR5 antagonist cenicriviroc (13). Impairment of CCL2-dependent monocyte recruitment reduced liver injury and fibrosis in the BV6 model, however, bile duct regeneration has not been characterized in this model. Moreover, it has been shown that conditional deletion of the murine double minute 2 (*Mdm2*) gene in bile ducts caused BEC senescence, a classic feature in PBC and PSC, and subsequently increased macrophage activation and fibrogenesis (14). These findings further argue in favor of a role for injured cholangiocytes to recruit immune and fibrogenic cells. Bile duct ligation (BDL) surgery is another model widely used to explore cholangiopathies. In this model, cholestasis is induced by ligation and

Conflict of interest: The authors have declared that no conflict of interest exists.

Copyright: © 2021, American Society for Clinical Investigation.

Submitted: August 2, 2019; **Accepted:** March 11, 2021; **Published:** May 3, 2021.

Reference information: *J Clin Invest.* 2021;131(9):e132305.

<https://doi.org/10.1172/JCI132305>.

sectioning of the common bile duct. This procedure is associated with intense hepatocyte death and large necrotic areas in the liver, potent inflammation, and peribiliary fibrosis (10, 11, 15). All these models suffer from the lack of specific BEC damage or lead to irreversible liver injury that may prevent or obscure BEC-specific tissue responses during bile duct regeneration.

To better understand the consequences attributable to a sole BEC injury and to unravel the mechanisms underlying bile duct repair through BEC proliferation after acute injury, we developed a mouse model of inducible BEC death by overexpressing human CD59 (hCD59) on BECs (biliary-specific hCD59-transgenic mice, referred to hereafter as *ihCD59^{BEC-TG}* mice). *ihCD59^{BEC-TG}* mice were generated by breeding floxed hCD59-knockin mice (*ihCD59*) with *Sox9CreERT⁺* mice that express Cre recombinase under the regulation of the *Sox9* promoter following tamoxifen injection. Injection of these mice with intermedilysin (ILY), a pore-forming toxin that lyses hCD59-expressing cells exclusively by binding to hCD59 but not mouse CD59, resulted in the acute, selective death of BECs (16). ILY has a large pharmacological window with no known off-target effects. Thus, *ihCD59^{BEC-TG}* mice represent an innovative, biliary cell-specific model for studying BEC injury and regeneration after specific cell-targeted acute death. Using this model, we demonstrate here that acute and targeted BEC death was sufficient to induce rapid monocyte recruitment, cholestasis, and liver blood microcirculation impairment. Additionally, bile acid accumulation in the portal area directly drove these recruited monocytes to a regenerative phenotype, enabling these cells to support BEC proliferation through integrin $\alpha\text{v}\beta6$.

Results

ihCD59^{BEC-TG} mice: a model of rapid and specific BEC injury and of bile duct repair. In order to decipher the immunological mechanisms implicated in bile duct injury and repair, and because most mouse liver injury models are associated with strong injury to both hepatocytes and BECs, we took advantage of our recently developed model of targeted acute BEC injury in ILY-treated, BEC-specific (*ihCD59^{BEC-TG}*) mice (16) and characterized bile duct repair after acute injury. As illustrated by H&E staining in Figure 1A, ILY injection into *ihCD59^{BEC-TG}* mice rapidly induced mononuclear cell accumulation in the portal areas. In addition, TUNEL staining revealed very localized and specific BEC damage, as early as 3 hours after ILY injection. Neither necrotic areas nor TUNEL⁺ hepatocytes were observed in the parenchyma (Figure 1A), whereas alanine aminotransferase (ALT) and alkaline phosphatase (ALP) serum levels only showed a limited increase that was possibly attributable to a surrounding hepatocyte stress response (Figure 1B). Acute BEC death led to a potent elevation of the total bilirubin (TBIL) serum concentration, which peaked between 6 and 9 hours after ILY injection (Figure 1C). Interestingly, TUNEL staining and TBIL returned to normal levels 24 hours after the initial injury, thus demonstrating that this procedure yields a model of acute intrahepatic BEC injury (Figures 1, A–C). Cholestasis was also evidenced by an increase in bile acid concentrations in liver homogenates (Figure 1C), and a dysregulation of bile acid metabolism-related gene (*Fxr*, *Gpbar1*, *Cyp7a1*, *Cyp8b1*) expression (Figure 1D and Supplemental Figure 1A; supplemental material available online with this article; <https://doi.org/10.1172/>

JCI132305DS1). Moreover, portal hypertension and liver ischemia are hallmarks of chronic liver diseases, cholestatic disorders, and arterial thrombosis leading to liver failure (4). Here, we show that acute BEC injury, per se, induced hypoxia-associated *Hif1a* and *Angpt2* mRNA expression (Supplemental Figure 1B), decreased liver microcirculation, and increased portal vein pressure (Figure 1E and Supplemental Figure 1C). Of note, we did not observe persistent liver microcirculation impairment at later time points (data not shown), which is in line with *Hif1a* and *Angpt2* mRNA expression and the rapid liver microcirculation recovery that occurred after acute BEC injury. Moreover, there was a potent and rapid elevation of the inflammation-related cytokines *Il6*, *Tnfa*, *Il1b*, and *Ccl2*, which peaked 3 hours after ILY injection, indicating an early and intense inflammatory response to acute BEC injury (Figure 1F). All these parameters remained unchanged in control *ihCD59* mice injected with ILY (data not shown).

Acute BEC injury alone triggers bile duct repair, i.e., portal fibrogenesis and BEC proliferation. In our model of BEC injury, we demonstrated that acute and targeted BEC injury is sufficient to induce portal fibrogenesis after 48 hours. This was notably shown by the increased Picrosirius red and α -smooth muscle actin (α -SMA) staining (Figure 2, A–C) and the increased expression of fibrogenesis-related genes (Figure 2D and Supplemental Figure 2). Furthermore, we found that hepatic expression of liver regeneration-associated genes including *Afp*, *Pkm2*, *Cd133*, and *Tweek* (5) was upregulated 48 hours after BEC injury (Figure 2E). Moreover, we examined BEC proliferation by measuring BrdU incorporation into BECs. As illustrated in Figure 2, F and G, BrdU incorporation into pan-cytokeratin⁺ (panCK⁺) cells peaked 48 hours after ILY injection. BrdU incorporation into other cells, such as hepatocytes, was very rare (data not shown). To summarize these data, our model of acute BEC death displays the classical histopathology observed in patients with cholangiopathies, including portal inflammation, fibrosis, and BEC proliferation, as well as cholestasis and portal hypertension, and represents what we believe to be a good model to study the early signals that drive bile duct repair.

Microdissection and RNA-Seq identify integrin $\alpha\text{v}\beta6$ as one of the most upregulated genes in proliferating BECs after acute BEC injury, which is also observed in patients with cholangiopathies. To identify potential mechanisms implicated in bile duct repair after acute cholangiocyte damage, we performed next-generation sequencing and untargeted transcriptome RNA-Seq of purified regenerating BECs 48 hours after ILY-induced injury. We adapted an innovative staining protocol that allowed for next-generation sequencing of the purified BEC's transcriptome captured by expression microdissection (xMD) (Figure 3A and Supplemental Figure 3). Although the differential gene expression and pathway enrichment analysis revealed significant differences and notably potent induction in organ regeneration and cell-cycle genes, we also observed a clear increase in the expression of extracellular matrix component and adhesion molecule genes (Figure 3, B and C, and Supplemental Table 2). The 5 genes that were most upregulated in proliferating BECs after acute injury included *Mapk8ip2*, *Cdkn1a*, *Itgb6*, *Rgs4*, and *Ccl2* (Figure 3D and Table 1). *Ccl2* upregulation, which is in line with data obtained using the BV6 model (13), could have contributed to monocyte recruitment in our model. *Cdkn1a*, which encodes p21, inhibits cell proliferation and is implicated in cellular

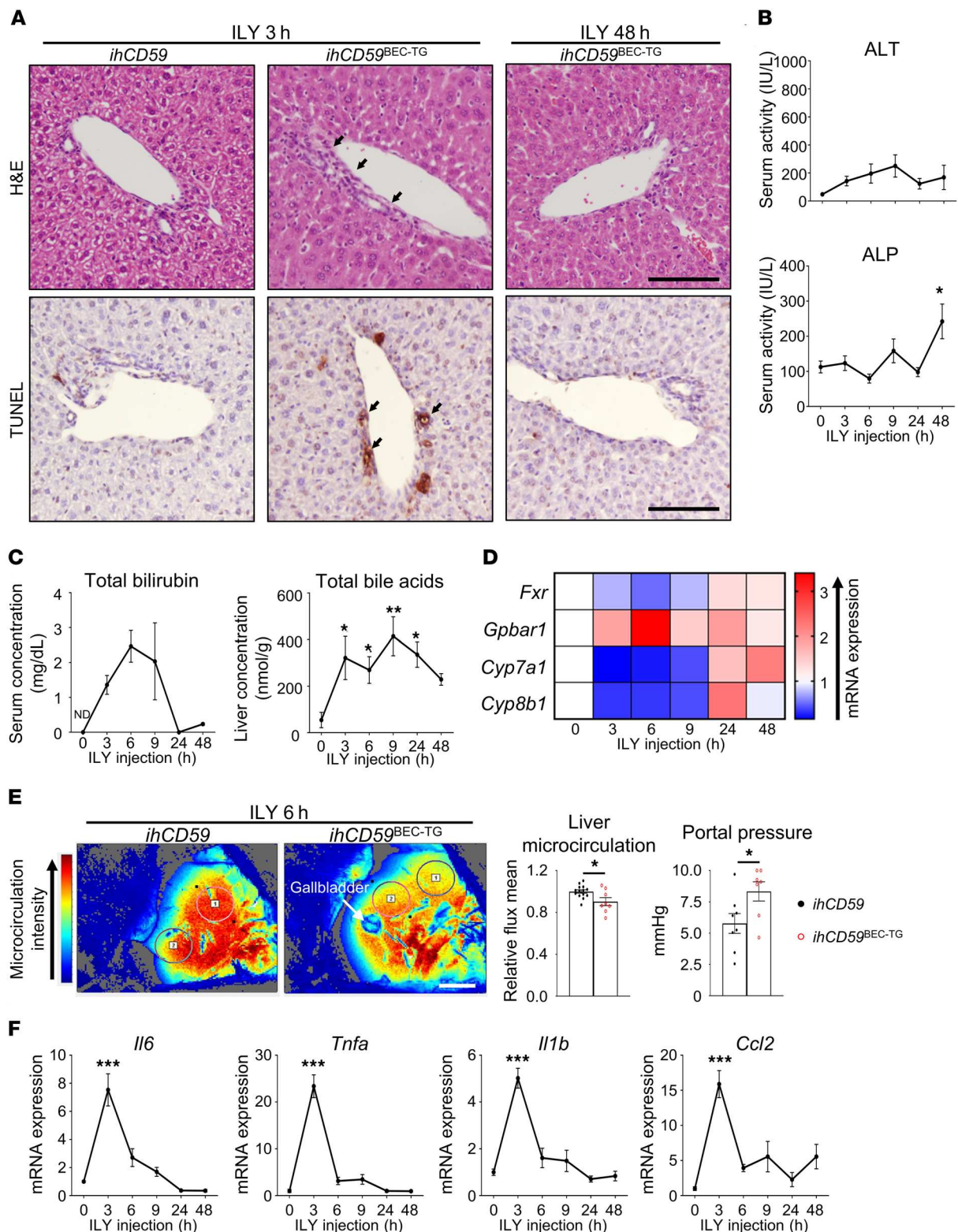


Figure 1. ILY injection triggers a specific and rapid hCD59⁺ BEC injury leading to liver blood microcirculation impairment and inflammation in *ihCD59^{BEC-TG}* mice. *ihCD59* (control group) and *ihCD59^{BEC-TG}* (injured) mice were injected intravenously with ILY (140 μg/kg). Mice were euthanized, and samples were collected at the indicated time points after injection. **(A)** H&E and TUNEL staining was performed. Black arrows indicate injured bile ducts. Scale bars: 50 μm. **(B)** ALT and ALP serum levels were measured (*n* = 3–4 per group). **(C)** TBIL serum levels and liver bile acid concentrations were measured (*n* = 3–6 per group). **(D)** Relative expression of cholestasis-associated genes from snap-frozen liver homogenates (statistical analyses are shown in Supplemental Figure 1A). **(E)** Liver blood microcirculation from circled areas labeled 1 and 2 and portal vein pressure were measured 6 hours after ILY injection (*n* = 7–14 per group). Scale bar: 5 mm. **(F)** Relative expression of inflammation-associated genes from liver homogenates (*n* = 3–7 per group). Data represent the mean ± SEM. **P* < 0.05, ***P* < 0.01, and ****P* < 0.005, compared with control *ihCD59* mice, by 1-way ANOVA (**B**, **C**, and **F**) and unpaired Student's *t* test (**E**). ND, nondetectable.

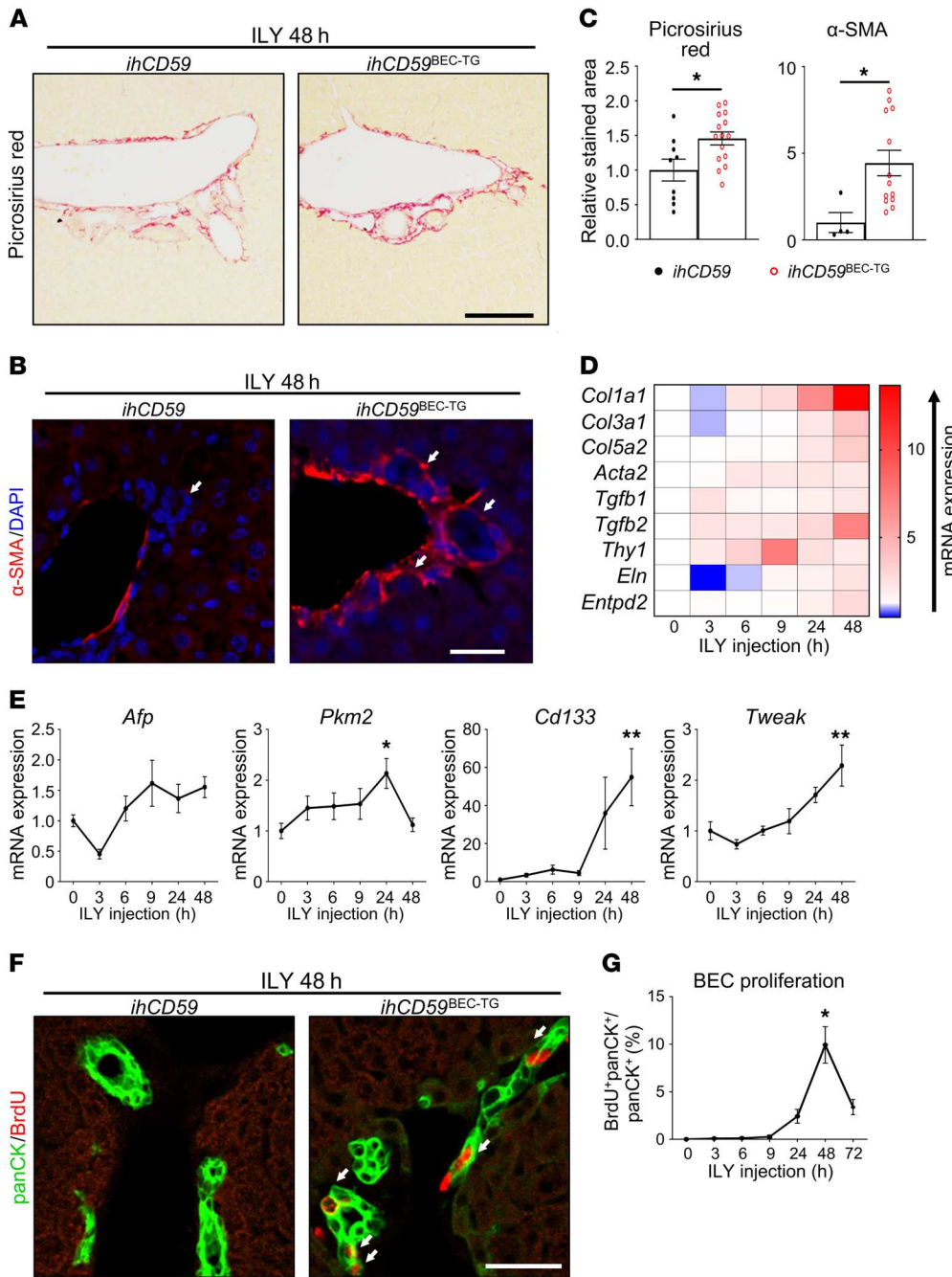


Figure 2. Acute BEC-specific injury alone triggers portal fibrogenesis and BEC proliferation. *ihCD59* and *ihCD59^{BEC-TG}* mice were injected intravenously with ILY and euthanized at the indicated time points. Forty-eight hours after ILY injection, (A) Picrosirius red (scale bar: 100 μ m) and (B) α -SMA (red) staining was performed. White arrows in the left panel indicate bile ducts, white arrows in the right panel indicate bile ducts surrounded by α -SMA. Scale bar: 20 μ m. (C) Picrosirius red- and α -SMA-stained areas were quantified ($n = 4$ –15 per group). (D) Expression of fibrogenesis-related genes was assessed in liver homogenates at the indicated time points after ILY administration ($n = 3$ –7 per group). Statistical analysis is shown in Supplemental Figure 2. (E) Hepatic expression of liver regeneration-associated genes was assessed by qRT-PCR ($n = 3$ –7 per group). (F) Mice were injected with BrdU 2 hours prior to euthanization, and panCK (green) and BrdU (red) staining was performed. White arrows indicate proliferating BECs that incorporated BrdU. (G) BrdU⁺panCK⁺ cells were quantified ($n = 9$ –18 per group). Scale bar: 20 μ m. Data represent the mean \pm SEM. * $P < 0.05$ and ** $P < 0.01$, compared with control *ihCD59* mice, by 1-way ANOVA (E and G) and an unpaired Student's *t* test (C).

senescence, a known phenomenon implicated in the pathogenesis of hepatobiliary diseases (17). The effects of *Mapk8ip2* and *Rgs4* on cell proliferation have not been reported. In contrast, *Itgb6* encodes ITG β 6 protein, which has been suggested to be a prognostic marker in cholangiocarcinoma and to promote BEC and liver progenitor cell proliferation in cholestasis and liver regeneration models (8, 18–21). Using quantitative reverse transcription PCR (qRT-PCR), we confirmed that mRNA expression of *Itgb6* was highly elevated in liver homogenates of ILY-injured animals (Figure 4A). Furthermore, ITG β 6 immunostaining revealed very localized ITG β 6 protein expression in BECs 48 hours after ILY injection (Figure 4B). mRNA expression of the adhesion molecule fibronectin 1 (*Fn1*) (18), an ITG β 6 cognate binding partner, was also increased, whereas

other integrins did not show a significant change at 48 hours (Figure 4C). Furthermore, immunohistochemical analyses revealed that ITG β 6 protein was strongly induced in ductular cells in patients with a variety of chronic liver diseases (Figure 4D and Supplemental Figure 4). Finally, we investigated whether macrophage and ductular cell accumulation, hallmarks of chronic liver disease, correlated with ITG β 6 expression in liver sections from patients with cholangiopathies (PBC and PSC). These studies revealed colocalization of macrophages and ITG β 6 staining in CK19⁺ cells in livers from these patients (Figure 4, D and E).

Integrin α v β 6 is critical for BEC proliferation in 2 mouse models of bile duct injury induced by ILY-targeted *hCD59* or BDL. Because *Itgb6* induction was so strong in our model of acute BEC inju-

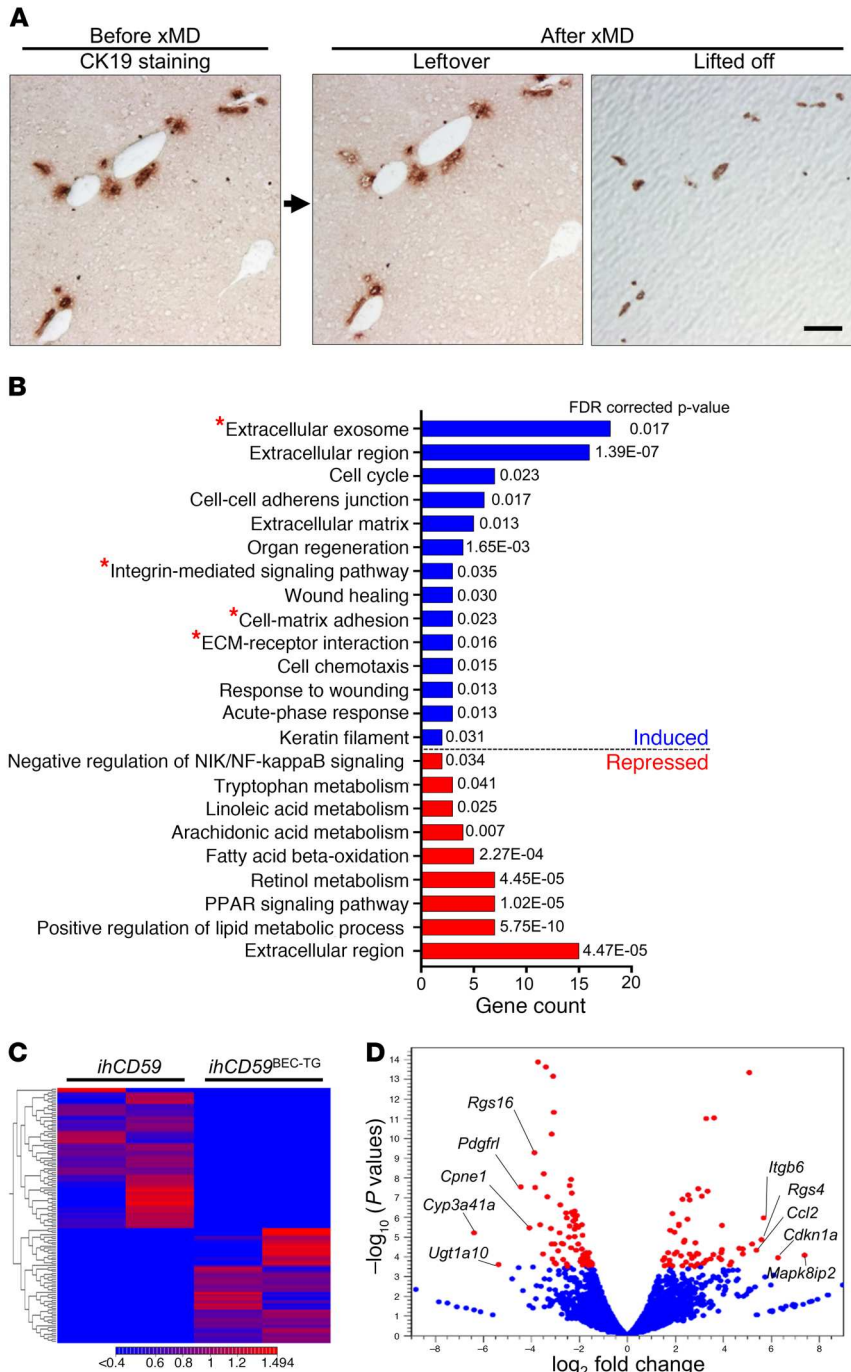


Figure 3. xMD and RNA-Seq identify ITGβ6 as one of the most upregulated genes in BECs after acute, targeted BEC death. *ihCD59* and *ihCD59^{BEC-TG}* mice were injected intravenously with ILY. (A) Fresh-frozen liver tissue sections collected 48 hours after ILY injection were stained with a CK19 antibody using an RNA-friendly staining protocol, followed by purification of CK19⁺ biliary cells by xMD and transcriptome RNA-Seq analysis ($n = 2$ in each group, as detailed in Supplemental Figure 3). Representative CK19 immunostaining on frozen liver sections and leftover versus lifted-off samples are shown. Only purified BECs (lifted off) were used for RNA-Seq and analysis. Scale bar: 100 μm. (B) GO term enrichment analysis of differentially expressed genes between the control and injured groups. GO terms comprising integrin $\alpha\beta 6$ (*Itgb6*) are shown with a red star. (C) Heatmap of differentially expressed genes between the injured and control groups. (D) Volcano plot of expressed genes (RPKM ≥ 0.05). Differentially expressed genes (FDR ≤ 0.05) between the injured and control groups are shown in red.

ry, we aimed to evaluate its functional role in BEC proliferation by deleting the *Itgb6* gene in *ihCD59^{BEC-TG}* mice. Surprisingly, we failed to generate *ihCD59^{BEC-TG} Itgb6^{KO}* mice (*ihCD59^{BEC-TG} Itgb6^{KO}*) for unknown reasons, so, instead, we generated *ihCD59^{LIV-TG} Itgb6^{KO}* mice, in which ILY injection induced both BEC and hepatocyte death, as revealed by necrotic areas and mononuclear cell infiltrates in the liver parenchyma (Supplemental Figure 5 and ref. 16). Despite a previous study describing the potential of ITGβ6 as a target to prevent chronic liver fibrosis (19), our data showed that α -SMA staining and fibrogenesis-related gene expression remained unchanged in *ihCD59^{LIV-TG} Itgb6^{KO}* mice compared with *ihCD59^{LIV-TG}* mice (Figure 5, A and B). Similarly, there was no influence of *Itgb6* deficiency on macrophage recruitment in the portal areas (Figure 5C). In contrast, BEC proliferation was markedly suppressed, as evidenced by a striking reduction of BrdU⁺panCK⁺ cells in *ihCD59^{LIV-TG} Itgb6^{KO}* mice compared with *ihCD59^{LIV-TG}* mice (Figure 5D).

We further assessed the role of ITGβ6 in another well-established model of cholestatic disorders by performing BDL in WT and *Itgb6^{KO}* mice with multiplex fluorescence immunostaining. We observed no differences in tissue injury, monocyte recruitment, liver blood microcirculation and portal pressure, or early fibrosis (Figure 5E and Supplemental Figures 6 and 7). However, *Itgb6* deficiency led to reduced BEC proliferation in the BDL model (Figure 5E and Supplemental Figure 7).

Myofibroblast activation is strongly associated with bile duct repair and favors ITGβ6 expression in BECs. The above data revealed that acute BEC injury leads to myofibroblast activation. Interestingly, we also observed colocalization of fibrogenic cells and macrophages in the liver upon BEC injury and proliferation, as demonstrated by immunostaining with desmin (hepatic stellate cell marker) and IBA1 (Figure 6A and Supplemental Figure 8A). To further examine the colocalization of fibrogenic cells and macrophages, we crossed *Coll1^{GFP}* mice, in which collagen-producing cells are labeled with GFP protein (17), with *ihCD59^{BEC-TG}* mice to generate *ihCD59^{BEC-TG} Coll1^{GFP}* double-mutant mice. As illustrated in Figure 6, B and C, and Supplemental Figure 8, B and C, we observed colocalization of IBA1⁺ macrophages and collagen or α -SMA-expressing fibrogenic cells in our acute BEC injury model. Additionally, α -SMA⁺ and IBA1⁺ cell clusters were identified and quantified in sev-

Table 1. Top-five induced and repressed transcripts in microdissected BECs from the *ihCD59^{BEC-TG}* mouse model, 48 hours after ILY injection

	Name	Identifier	Fold change	log fold change	P value	FDR P value
Induced	<i>Mapk8ip</i>	ZENSMUSG00000022619	169.27	7.4	8.79×10^{-5}	0.02
	<i>Cdkn1a</i>	ENSMUSG00000023067	77.89	6.28	1.12×10^{-4}	0.03
	<i>Itgb6</i>	ENSMUSG00000026971	51.49	5.69	1.09×10^{-6}	7.71×10^{-4}
	<i>Rgs4</i>	ENSMUSG00000038530	48.64	5.6	1.43×10^{-5}	5.82×10^{-3}
	<i>Ccl2</i>	ENSMUSG00000035385	41.89	5.39	4.91×10^{-5}	0.02
Repressed	<i>Rgs16</i>	ENSMUSG00000026475	-14.67	-3.87	5.59×10^{-10}	1.36×10^{-6}
	<i>Cpne1</i>	ENSMUSG00000074643	-16.71	-4.06	3.59×10^{-6}	1.83×10^{-3}
	<i>Pdgfr1</i>	ENSMUSG00000031595	-21.69	-4.44	2.93×10^{-8}	4.94×10^{-5}
	<i>Ugt1a10</i>	ENSMUSG00000090165	-41.1	-5.36	2.60×10^{-4}	0.05
	<i>Cyp3a41a</i>	ENSMUSG00000075551	-82.55	-6.37	6.38×10^{-6}	2.84×10^{-3}

eral models of liver injury and in patients with various liver diseases (Figure 6D and Supplemental Figures 9 and 10), which suggests that these inflammatory and fibrogenic cell clusters were more prominent in models or diseases that specifically target BECs rather than hepatocytes.

To decipher the potential role of myofibroblasts in inducing BEC proliferation, we obtained collagen-producing myofibroblasts (MFBs) (CD45⁺GFP⁺ cells) from carbon tetrachloride-injected (CCl₄-injected) *Coll1^{GFP}* mice and performed cell sorting (Supplemental Figure 11A). We then cocultured BECs with these primary MFBs for 24 hours and found that coculturing with MFBs did not affect BEC proliferation (Ki67 staining) but increased *Itgb6* expression in BECs (Figure 6, E–G). Intriguingly, 48 hours after injection of ILY into *ihCD59^{BEC-TG}* *Coll1^{GFP}* mice, we also found the presence of GFP⁺ (collagen⁺) cells expressing monocyte-derived macrophage (MoMF) markers such as CD45, CD11b, F4/80, and CCR2 (Supplemental Figure 11, B–D). This GFP⁺ (collagen⁺) macrophage population needs to be further characterized.

Macrophage depletion abrogates bile duct repair and ITGβ6 expression in BECs. Monocyte/macrophage recruitment is a direct consequence of tissue injury and is known to play crucial roles in cell debris clearance as well as in the initiation of tissue regeneration and fibrosis in a classical immune response (22). To explore the role of macrophages in BEC injury and bile duct repair, we injected *ihCD59^{BEC-TG}* and control mice with clodronate-loaded liposomes to deplete monocytes and macrophages and evaluated the tissue response to acute BEC death. We studied the effects of macrophage depletion on BEC injury and repair 6 and 48 hours after ILY injection, as we identified these time points to be the peaks of bile duct injury and BEC proliferation, respectively. Macrophage depletion was verified by the absence of F4/80 and IBA1 staining and reduced mRNA expression of the inflammation-related genes *Il6*, *Tnfa*, and *Il1b* (Supplemental Figure 12). Macrophage depletion did not influence liver or BEC injury, as shown by similar TUNEL staining in panCK⁺ BECs and similar ALT activity in the serum (Figure 7A and Supplemental Figure 13, A and B). However, and interestingly, serum TBIL levels were lowered after macrophage depletion, as was total bile acid accumulation in the liver of *ihCD59^{BEC-TG}* mice (Figure 7B). Further, macrophage depletion reversed the downregulation of *Fxr*,

Cyp7a1, and *Cyp8b1* and the upregulation of *Gpbar1* (Figure 7C and Supplemental Figure 13C). These data indicate that macrophages did not participate in the initial injury caused by the ILY toxin, but on the other hand may have exacerbated cholestasis. Clodronate-mediated macrophage depletion led to significantly reduced Picrosirius red and α-SMA staining 48 hours after ILY injection (Figure 7D). Accordingly, fibrogenesis-related gene expression was dramatically reduced in the clodronate-treated mice (Figure 7E and Supplemental Figure 13D). Most important, our results revealed that macrophage depletion dramatically decreased proliferation of the remaining BECs in our specific BEC injury model (Figure 7F). As illustrated in Figure 7, G and H, clodronate-loaded liposome injection drastically reduced ITGβ6 staining and mRNA expression. Interestingly, when macrophage depletion was performed 8 hours after injury, BEC proliferation and fibrogenesis were reduced to a similar extent at 48 hours, showing that the initial inflammation response was not solely responsible for inducing portal regeneration, but that the extended presence of macrophages was required for proper bile duct repair (Supplemental Figure 14). Altogether, these data revealed a role for macrophages in mediating ITGβ6 upregulation in BECs.

Circulating CCR2⁺ monocytes and not Kupffer cells are rapidly recruited around damaged bile ducts, promoting BEC proliferation and hepatic *Itgb6* expression. Liver macrophages are composed of resident Kupffer cells and MoMFs (23). To further characterize the monocyte/macrophage population recruited around injured bile ducts, we performed immunostaining for CLEC4F, which is used to identify Kupffer cells, and IBA1, a pan-macrophage marker of both Kupffer cells and infiltrating monocytes/macrophages (24–28). Here, we showed that as early as 3 hours after acute injury, IBA1⁺CLEC4F⁻ circulating monocytes were recruited around damaged bile ducts, whereas IBA1⁺CLEC4F⁺ Kupffer cells did not migrate toward the injured area (Figure 8A and Supplemental Figure 15). IBA1, panCK, and TUNEL costaining further showed that there was a significant increase in direct contact between monocytes and BECs following acute injury (Figure 8B and Supplemental Figure 16). Moreover, MoMF numbers were increased in the liver, as assessed by flow cytometry, whereas T cell and neutrophil numbers remained constant, and these cells did not accumulate in portal areas, demonstrating a potent role of

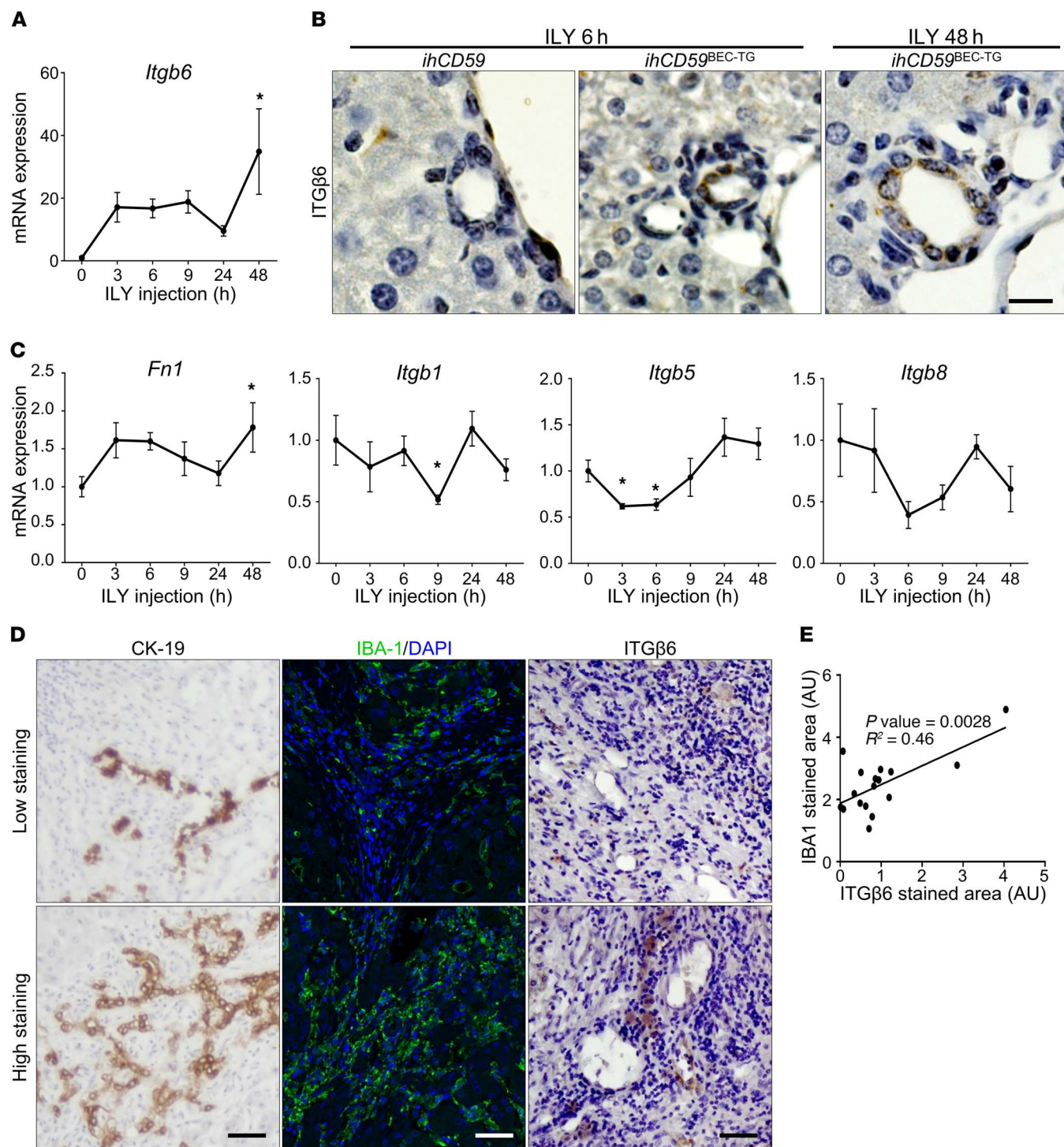


Figure 4. Increased ITGβ6 levels correlate with the ductular reaction in the ILY-*ihCD59^{BEC-TG}* model and in human chronic liver diseases. (A–C) *ihCD59* and *ihCD59^{BEC-TG}* mice were injected intravenously with ILY. **(A)** qRT-PCR analysis of relative expression of the *Itgb6* gene in liver homogenates ($n = 3$ –7 per group). **(B)** ITGβ6 immunostaining of BECs from ILY-treated *ihCD59^{BEC-TG}* mice. Scale bar: 12.5 μm. **(C)** qRT-PCR analysis of relative gene expression of *Fn1*, *Itgb1*, *Itgb5*, and *Itgb8* in liver homogenates ($n = 3$ –7 per group). Data represent the mean ± SEM. * $P < 0.05$ compared with control *ihCD59* mice, by 1-way ANOVA. **(D)** Representative immunostaining images from 17 livers of patients with cholangiopathies (PBC and PSC), showing a correlation between CK19, IBA1, and ITGβ6 staining. Scale bars: 50 μm. **(E)** ITGβ6 and IBA1 staining was quantified, and a correlation was established using Pearson's r .

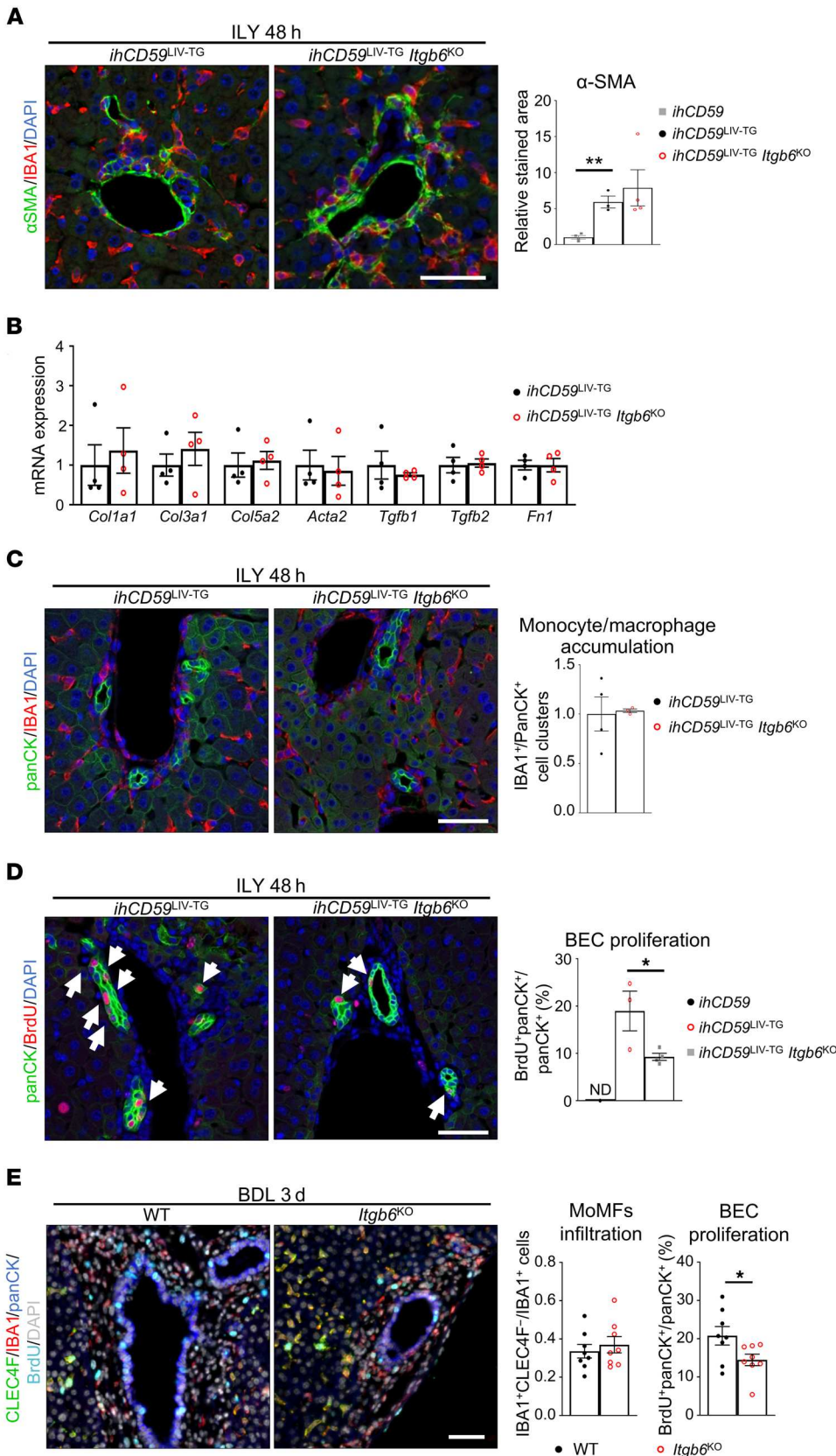


Figure 5. ITGβ6 deficiency impairs BEC proliferation but not early portal fibrosis or inflammation in 2 models of bile duct injury. (A–D) *ihCD59^{LIV-TG}* and *ihCD59^{LIV-TG} Itgb6^{KO}* mice were injected intravenously with ILY, and samples were collected at the indicated time points after ILY injection. (A) IBA1 (red) and α-SMA (green) staining and quantitation were performed ($n = 3-4$ per group). (B) Liver mRNA expression of fibrogenesis-related genes was assessed by qRT-PCR ($n = 4$ per group). (C) panCK (green) and IBA1 (red) staining was performed, and cell clusters were quantified ($n = 3-4$ per group). (D) panCK (green) and BrdU (red) staining and quantitation were performed ($n = 3-4$ per group). White arrows indicate BrdU⁺ BECs. (E) WT and *Itgb6^{KO}* mice were euthanized 3 days after BDL. Immunostaining was performed on IFPE liver sections (single-channel images are shown in Supplemental Figure 7), and then monocyte-derived IBA1⁺CLEC4F⁻ macrophages and proliferating BrdU⁺panCK⁺ BECs were quantified ($n = 8$ per group). Data represent the mean ± SEM. * $P < 0.05$ and ** $P < 0.01$, by unpaired Student's *t* test (A, C, and E) and 1-way ANOVA (B and D). Scale bars: 50 μm.

monocytic cells in the early immune response (Supplemental Figures 17 and 18). These recruited cells accumulating around injured bile ducts also expressed the CX3CR1 and CCR2 chemokine receptors, as demonstrated in *ihCD59^{BEC-TG} Cx3cr1^{GFP}* and *ihCD59^{BEC-TG} Ccr2^{RFP}* reporter mice, respectively (Figure 8, C and D), and were F4/80^{lo} (data not shown), further arguing for monocyte recruitment rather than Kupffer cell migration.

We also noticed that CX3CR1^{GFP+} and CCR2^{RFP+} cells were still present around regenerating bile ducts 48 hours after ILY injection (Supplemental Figure 19). To elucidate the function of these monocytic cells, we first performed qRT-PCR analyses of primary MoMFs isolated from *ihCD59^{BEC-TG}* mice 48 hours after ILY injection and found that, compared with macrophages isolated from control livers, the activated MoMFs had a proregenerative phenotype, as characterized by increased expression of the *Tweak* gene, a known mitogen for BECs (29), and a ten-

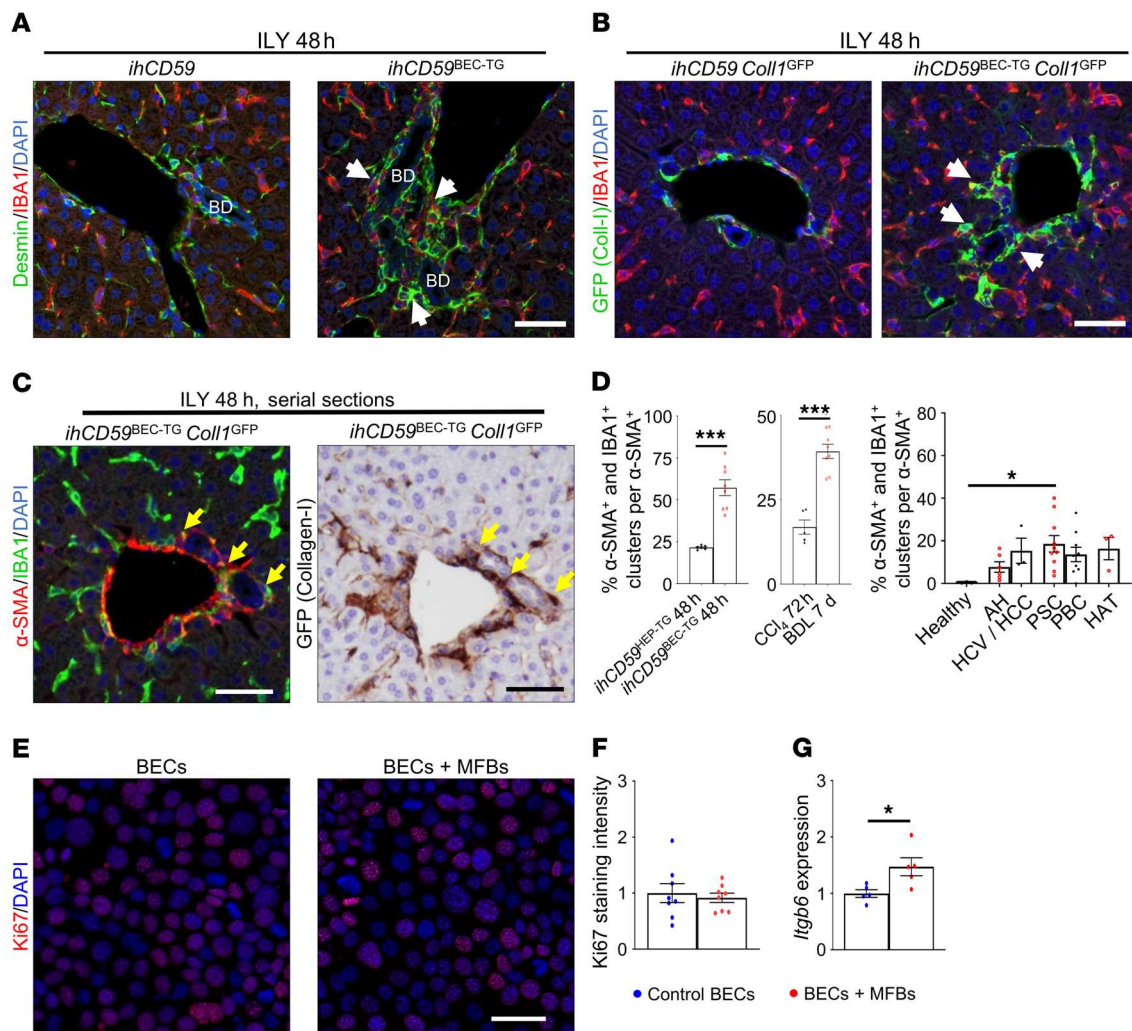


Figure 6. Myofibroblast activation is closely related to macrophage accumulation and BEC proliferation and increases *Itgb6* expression after acute BEC injury. (A) *ihCD59* and *ihCD59^{BEC-TG}* mice were injected with ILY, and desmin (green) and IBA1 (red) staining was performed on liver sections. White arrows show close localization of IBA1⁺ and desmin⁺ cells. Scale bar: 50 μ m. BD, bile duct. (B) *ihCD59Coll1^{GFP}* and *ihCD59^{BEC-TG} Coll1^{GFP}* mice were injected with ILY, and GFP (green) and IBA1 (red) staining was performed. White arrows indicate stained cell clusters. Scale bar: 50 μ m. (C) α -SMA (red) and IBA1 (green) or collagen GFP (brown) immunostaining on serial liver sections. Arrows indicate cell clusters. Scale bars: 50 μ m. (D) α -SMA and IBA1 staining was performed, and stained cell clusters were quantitated in the indicated models of liver injury or in liver sections from patients with chronic liver disease ($n = 3$ –10 per group). ILY-treated *ihCD59^{HEP-TG}* and ILY-treated *ihCD59^{BEC-TG}* mice represent hepatocyte and BEC injury models, respectively. Data represent the mean \pm SEM. AH, alcoholic hepatitis; HCV/HCC, HCV infection and hepatocellular carcinoma; HAT, hepatic artery thrombosis. (E) Collagen I-producing (GFP⁺) CD45⁻ MFBs were sorted from CCl₄-injected *Coll1^{GFP}* mouse livers, placed in Transwells, and cocultured with SV40-transformed murine BECs. Ki67 staining was performed in BECs after 24 hours (representative images are shown). Scale bar: 40 μ m. (F) Ki67 staining was quantified ($n = 4$ –8 per group). (G) *Itgb6* mRNA expression analysis was performed on BECs cultured with primary myofibroblasts ($n = 4$ –8 per group). Data represent the mean \pm SEM. * $P < 0.05$ and *** $P < 0.005$, by unpaired Student's *t* test (F and G) and 1-way ANOVA (D).

gency toward increased expression of *Tgfb1*, a potent profibrogenic cytokine (Figure 8E and Supplemental Figure 20). Interestingly, those macrophages also overexpressed G protein-coupled bile acid receptor 1 (*Gpbar1*), showing an increased sensitivity to bile acid-mediated signals (Figure 8E and Supplemental Figure 20). We next aimed to better elucidate the role of MoMFs in bile duct repair after targeted and acute BEC damage. We performed an additional deletion of the *Cx3cr1* or *Ccr2* gene in *ihCD59^{BEC-TG}* mice by generating *ihCD59^{BEC-TG} Cx3cr1^{KO}* or *ihCD59^{BEC-TG} Ccr2^{KO}* double-mutant mice. Interestingly, the *Ccr2*-deficient mice had reduced Picosirius red staining and a tendency toward reduced α -SMA staining (Figure 8F and Supplemental Figure 21A).

Moreover, fibrogenesis-related gene expression was reduced in *ihCD59^{BEC-TG} Ccr2^{KO}* mice (Figure 8G and Supplemental Figure 21B). Strikingly and as shown in Figure 8, H–J, *ihCD59^{BEC-TG} Ccr2^{KO}* mice displayed reduced BEC proliferation and reduced hepatic *Itgb6* expression 48 hours after ILY injection. However, we observed no difference in BEC proliferation between *ihCD59^{BEC-TG}* and *ihCD59^{BEC-TG} Cx3cr1^{KO}* mice (data not shown).

In response to bile acids, infiltrating CCR2⁺ macrophages promote BEC proliferation via the upregulation of ITG β 6 expression. Our data showed that CCR2⁺ monocytes played an important role in promoting BEC proliferation in vivo and that macrophage depletion abrogated BEC ITG β 6 expression in response to acute

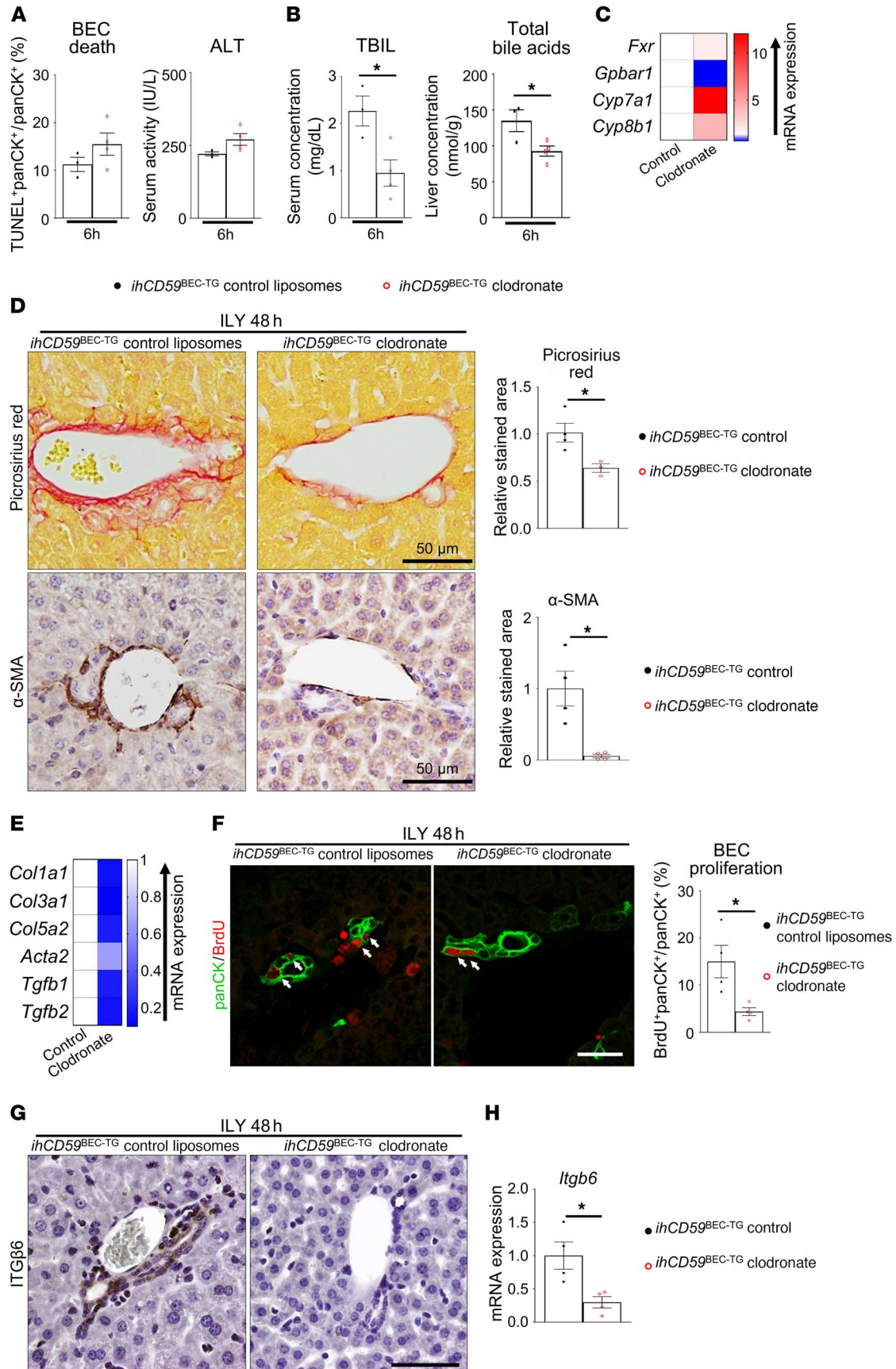


Figure 7. Macrophage depletion reduces cholestasis, fibrogenesis, BEC proliferation and ITGβ6 expression after acute BEC injury. Macrophages were depleted in *ihCD59^{BEC-TG}* mice by clodronate-loaded liposome injection (liposomes were injected as controls) 24 hours prior to ILY injection. (A) Six hours after ILY treatment, TUNEL and panCK staining was performed on paraffin-embedded liver sections, panCK⁺TUNEL⁺ cells were quantified ($n = 3-4$ in each group), and serum ALT activity was measured. Representative images are shown in Supplemental Figure 14B. (B) TBIL and total intrahepatic bile acid concentrations were assessed. (C) Hepatic bile acid metabolism-related gene expression was assessed by qRT-PCR 6 hours after ILY injection ($n = 3-4$ per group). Statistical analysis is shown in Supplemental Figure 14C. (D) Picrosirius red and α -SMA staining was performed, and stained areas were quantified ($n = 3-4$ per group). Scale bars: 50 μ m. (E) Fibrogenesis-related gene expression was assessed by qRT-PCR. Statistical analysis is shown in Supplemental Figure 14D. (F) panCK and BrdU immunostaining was performed and quantified in livers from clodronate-loaded liposome-injected *ihCD59^{BEC-TG}* mice and in *ihCD59^{BEC-TG} Ccr2^{KO}* mice, 48 hours after ILY injection ($n = 4$ per group). White arrows indicate BrdU⁺ BECs. Scale bar: 30 μ m. (G) Macrophages were depleted in *hCD59^{BEC-TG}* mice by clodronate-loaded liposomes, followed by ILY injection. ITGβ6 immunostaining (brown) was then performed on mouse liver sections. Scale bar: 50 μ m. (H) Liver *Itgb6* mRNA expression from clodronate-injected *hCD59^{BEC-TG}* mice ($n = 4$ in each group). Data represent the mean \pm SEM. * $P < 0.05$, by unpaired Student's *t* test.

BEC injury. To understand the mechanisms involved and whether macrophages directly stimulate BEC proliferation, we isolated primary CCR2⁺ MoMFs from ILY-treated *ihCD59^{BEC-TG}* mouse livers and cocultured them with BECs, followed by the measurement of BEC proliferation. The data in Figure 9, A and B, revealed that coculturing with CCR2⁺ MoMFs markedly enhanced BEC proliferation, as demonstrated by increased Ki67 staining, and thus showed that CCR2⁺ macrophages from bile duct-injured livers can directly stimulate BEC proliferation. One of the characteristics of bile duct injury is cholestasis, defined as the accumulation of bile acids in the liver due to impaired bile export, which was also demonstrated in our model (shown in Figure 1C). Notably, bile acids have been shown to direct macrophages toward a proregenerative phenotype by targeting the farnesoid X receptor (FXR) and the G protein-coupled bile acid receptor 1 (GPBAR1, also known as TGR5) (30, 31). Thus, we asked whether macrophages respond to bile acids to favor increased expression of *Itgb6* in BECs. To answer this question, we treated murine bone marrow monocytes with tauroithochoic acid (TLCA), a potent GPBAR1 agonist. The conditioned culture medium of these cells was then transferred to BEC cultures, followed by evaluation of BEC *Itgb6* expression and proliferation. As illustrated in Figure 9, C and D, and Supplemental Figure 22, TLCA alone increased *Itgb6* expression but did not induce BEC proliferation, whereas conditioned media from TLCA-treated monocytes increased both BEC *Itgb6* expression and proliferation. Similarly, conditioned media from TLCA-treated RAW264.7 macrophages increased BEC proliferation, as measured by an MTS absorbance assay (Figure 9E). Furthermore, incubation with an ITGβ6-blocking antibody prevented the induction of BEC proliferation by conditioned media from TLCA-treated RAW264.7 macrophages (Figure 9F). These data demonstrate that after bile acid stimulation, MoMFs promote BEC proliferation via the induction of ITGβ6 (Figure 9G).

Discussion

In the current study, we demonstrated that the ILY/*ihCD59^{BEC-TG}* BEC-specific death-inducing method (16) represents a model of acute BEC injury, followed by bile duct repair. Unlike chronic injury models, this method allowed us to characterize 2 stages of tissue response to specific and targeted acute bile duct injury, consisting of (a) an injury response stage including BEC death, liver microcirculation impairment, and monocyte recruitment and (b) a regenerative stage in which the remaining BECs proliferate concurrently with portal fibrogenesis. This BEC proliferation in the regenerative stage is dependent on the recruitment of circulating MoMFs and a potent elevation in ITGβ6 expression. In addition, we demonstrated that bile acids play a role in promoting macrophage polarization toward a regenerative phenotype and in inducing cholangiocyte ITGβ6 expression. We have integrated all of these findings into a model representing how acute BEC injury triggers the early tissue response that induces BEC proliferation via the interaction of bile acids, macrophages, and ITGβ6 (Figure 9G).

Upon chronic or severe injury, liver progenitor cells or activated cholangiocytes proliferate and accumulate in the liver. This phenomenon, known as the ductular reaction, coincides with intense and localized inflammation and fibrogenesis as part of the tissue response to chronic or severe injury, in an attempt to repair or regenerate the bile ducts and liver architecture. Repair mechanism dysregulation and exacerbation may lead to chronic inflammation, fibrosis, and cirrhosis and may ultimately serve as a soil for liver cancer and organ failure. Although the ductular reaction is widespread in virtually any chronic liver disease, and BECs represent a crucial cell type implicated in liver function and architecture, there is a paucity of data on their regeneration and interaction with other cell populations in liver disease, given the lack of targeted BEC injury models.

Acute BEC injury rapidly leads to recruitment of monocytes to the injured area, which interact with myofibroblasts. Inflammatory monocytes are among the first responders after injury, clearing pathogens and cell debris and initiating tissue regeneration. A recent study reported that macrophages play a crucial role in inducing the ductular reaction, portal area fibrosis, and monocyte-driven inflammation in a chronic (*Mdr2^{-/-}* mice) mouse model of sclerosing cholangitis (13). An interesting finding in the current study was that monocytes were rapidly recruited in response to sudden BEC death, as early as 3 hours after injury, and this recruitment may have been induced by a number of factors, including the release of damage-associated molecular patterns (DAMPs) and/or the production of chemokines (e.g., CCL2) by surrounding cells including BECs and Kupffer cells (32). Indeed, as shown in the current study, *Ccl2*, which encodes the key CCL2 chemokine, was 1 of the top 5 genes that were most strongly upregulated in regenerating BECs. Notably, we observed that recruited monocytes expressed CCR2 (the CCL2 receptor) and the chemokine receptor CX3CR1. However, an additional deletion of either *Ccr2* or *Cx3cr1* did not dramatically affect monocyte recruitment in ILY-treated *ihCD59^{BEC-TG}* mice (data not shown), suggesting that monocyte recruitment after acute BEC injury may be dependent on additional factors. Another possibility that we have not excluded is that because of the redundancy of both receptors, deletion of 1 of them was insufficient to affect monocyte recruitment. Despite

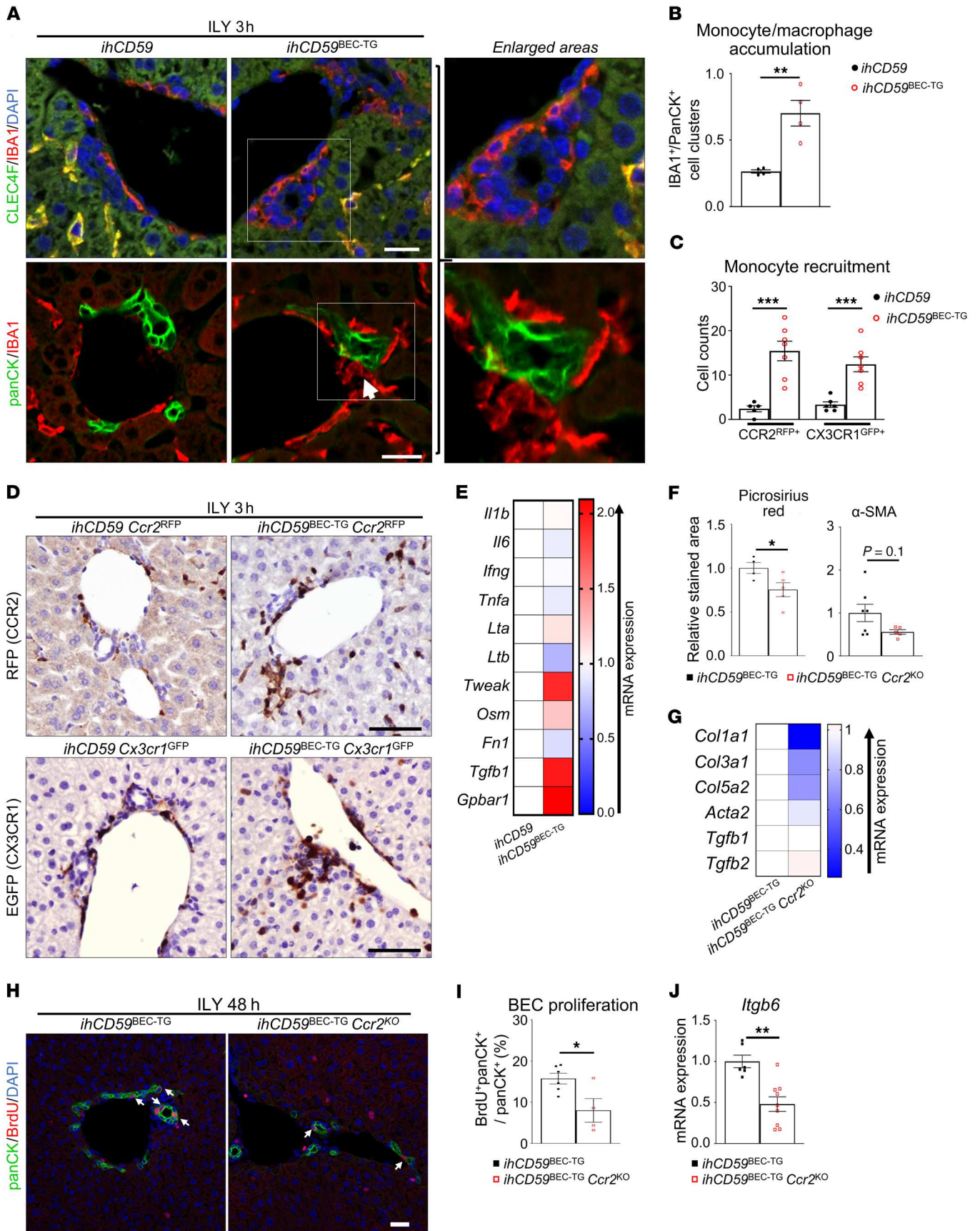


Figure 8. Monocyte-derived CCR2⁺ macrophages accumulate around injured bile ducts after acute BEC injury, promoting BEC proliferation and *Itgb6* expression. (A and B) *ihCD59* and *ihCD59^{BEC-TG}* mice were injected intravenously with ILY for 3 hours. Liver tissues were collected for immunofluorescence staining with IBA1 (red) and CLEC4F (green) or with anti-panCK (green) and anti-IBA1 (red) antibodies. Double-stained IBA1⁺CLEC4F⁺ Kupffer cells appear in yellow, whereas IBA1⁺CLEC4F⁻ MoMFs appear in red in the upper panel of A. Double staining of anti-panCK (green) and anti-IBA1 (red) antibodies on liver sections as shown in lower panel A. The white arrow indicates an IBA1⁺ monocyte in contact with a panCK⁺ BEC. Single-channel images are provided in Supplemental Figure 15. Scale bars: 20 μ m. panCK⁺ and IBA1⁺ cell clusters from A were counted ($n = 4$ per group) as shown in B. (C) CCR2⁺ and CX3CR1⁺ recruited monocytes from ILY-treated *ihCD59^{BEC-TG} Ccr2^{RFP}* or *ihCD59^{BEC-TG} Cx3cr1^{GFP}* reporter mice were counted as indicated ($n = 5$ –7 per group). (D) Representative images of RFP and GFP staining in liver tissues from *ihCD59^{BEC-TG} Ccr2^{RFP}* and *ihCD59^{BEC-TG} Cx3cr1^{GFP}* reporter mice, respectively. Scale bars: 30 μ m. (E) Liver MoMFs (CD45⁺CD11b⁺CCR2^{hi}GR-1^{int}) were isolated from *ihCD59* and *ihCD59^{BEC-TG}* mice 48 hours after ILY injection, and gene expression was analyzed by qRT-PCR. Statistical analysis is shown in Supplemental Figure 20. (F) Picosirius red and α -SMA staining was performed on liver tissues from ILY-treated *ihCD59^{BEC-TG}* and *ihCD59^{BEC-TG} Ccr2^{KO}* mice, and stained areas were quantified ($n = 4$ –7 per group). Representative images are shown in Supplemental Figure 21A. (G) Fibrogenesis-related gene expression was examined by qRT-PCR. Statistical analysis is shown in Supplemental Figure 21B. (H) panCK and BrdU immunostaining was performed on *ihCD59^{BEC-TG}* and *ihCD59^{BEC-TG} Ccr2^{KO}* mouse livers 48 hours after ILY injection ($n = 4$ –6 per group). Scale bar: 30 μ m. (I) panCK⁺BrdU⁺ BECs were counted. (J) *Itgb6* mRNA expression in livers from ILY-treated *ihCD59^{BEC-TG}* and *ihCD59^{BEC-TG} Ccr2^{KO}* mice ($n = 6$ –9 in each group). Data represent the mean \pm SEM. * $P < 0.05$, ** $P < 0.01$, and *** $P < 0.005$, by unpaired Student's t test.

this, *Ccr2*-deficient mice displayed reduced BEC proliferation, suggesting that CCL2 signaling polarized recruited monocytes toward a regenerative phenotype. As evidenced by our data, acute BEC injury did not lead to the accumulation of neutrophils around damaged bile ducts. This was quite different from chronic liver injury-induced classical wound responses that are associated with significant neutrophil infiltration (9). Indeed, it was proposed very recently that during alcoholic hepatitis, recruited neutrophils aggravate cholangiocyte injury through the binding of BEC integrin $\beta 1$ (ITG $\beta 1$) with neutrophil membrane proteins, leading to a loss of the type 3 inositol 1,4,5-trisphosphate receptor (ITPR3) and increased cholestasis (33). On the other hand, our data suggest that the moderate and localized BEC injury in ILY-treated *ihCD59^{BEC-TG}* mice preferably leads to a monocyte-driven response, highlighting the required and beneficial roles of monocyte recruitment without the induction of potentially detrimental neutrophilic activation during bile duct repair.

Another important finding from the current study was that the recruited monocytes after BEC injury were intimately interacting with collagen-producing cells in ILY-treated *ihCD59^{BEC-TG}* mice in vivo. First, liver macrophages isolated from *ihCD59^{BEC-TG}* mice during BEC regeneration tended to have increased *Tgfb1* gene expression. Second, by performing immunohistochemical analyses in 2 strains of *ihCD59^{BEC-TG} Cx3cr1^{GFP}* and *ihCD59^{BEC-TG} Coll1^{GFP}* double-mutant mice, we demonstrated that IBA⁺ macrophages near damaged bile ducts were in close contact with α -SMA⁺ and collagen-expressing fibroblasts. Macrophages and fibrogenic cells were so intimately colocalized that confocal microscopy led to a partial staining overlap, raising doubts about the possibility that

some cells may coexpress IBA1 and α -SMA or GFP (collagen I). Intriguingly, flow cytometric analyses revealed that numerous collagen-producing cells expressed macrophage markers such as CD45, CD11b, and F4/80 in ILY-treated *ihCD59^{BEC-TG} Coll1^{GFP}* double-mutant mice. Using the BDL model and *Mdr2^{-/-}* mice, Kisseleva's group implicated portal fibroblasts as well as circulating fibrocytes in the development of portal fibrosis (34, 35). Fibrocytes are defined as bone marrow-derived CD45⁺ circulating cells that can infiltrate tissues and produce collagen and have notably been observed in wound healing and fibrosis in multiple organs including the liver (34–36). The origin of fibrocytes is still subject to debate. Monocyte-derived, collagen-producing cells have been implicated in the wound-healing response or fibrosis in several organs, including skin, lung, kidney, and liver, and although their characterization varies among studies, they are commonly identified as CD45⁺CD11b⁺collagen I⁺ (37). In the liver, this phenotype may not only contribute to fibrogenesis but may also support BEC regeneration by providing mitogens and by participating in extracellular matrix (ECM) deposition, a known requirement for cholangiocyte regeneration (12, 38–40). However, more studies are needed to confirm and characterize these potential monocyte-derived, collagen-producing cells in our models.

Monocyte-derived CCR2⁺ macrophages enhance BEC repair through ITG $\beta 6$: a potential role of bile acid. In the current study, we demonstrated that macrophage depletion or *Ccr2* deficiency reduced BEC proliferation in *ihCD59^{BEC-TG}* mice, indicating that the recruited monocyte-derived CCR2⁺ macrophages promote bile duct repair. Macrophages are known partners of tissue regeneration through their extensive production of mitogens. Indeed, our data showed that liver macrophages isolated at the peak of BEC proliferation overexpressed *Tweak*, a known mitogen for BECs and liver progenitor cells (29, 41, 42). Although fibrogenesis may lead to fibrosis, it provides crucial signals for bile ducts to regenerate and should thus be regarded as a part of normal bile duct regeneration, if it does not become excessive. This could partly explain why our data indicated that macrophage depletion, which reduced both inflammation and fibrogenesis, also impaired BEC proliferation, although the initial cell injury was identical. Furthermore, using the approach of RNA-friendly xMD, we were able to perform next-generation transcriptome sequencing specifically on regenerating BECs and identified 5 genes, namely *Mapk8ip2*, *Cdkn1a*, *Itgb6*, *Rgs4*, and *Ccl2*, that were most upregulated in proliferating BECs after acute injury. Given the small proportion of BECs in the liver, these important gene expression changes would not have been detectable using whole-tissue transcriptomics. Among these, ITG $\beta 6$ has been implicated in promoting BEC- and liver progenitor-mediated liver regeneration (8, 18, 19, 21). Furthermore, it was previously proposed in a chronic mouse model of congenital hepatic fibrosis that macrophages are implicated in ITG $\beta 6$ induction in chronically injured BECs (43). For these reasons, we further focused on the role of ITG $\beta 6$ in BEC proliferation in our ILY/*ihCD59^{BEC-TG}* acute BEC-specific death model. Immunohistochemical analyses confirmed a robust upregulation of ITG $\beta 6$ expression in this BEC injury model as well as in patients with chronic cholangiopathies, correlating with intense monocyte-derived macrophage recruitment in the portal area. Deletion of the *Itgb6* gene attenuated BEC regeneration after acute BEC

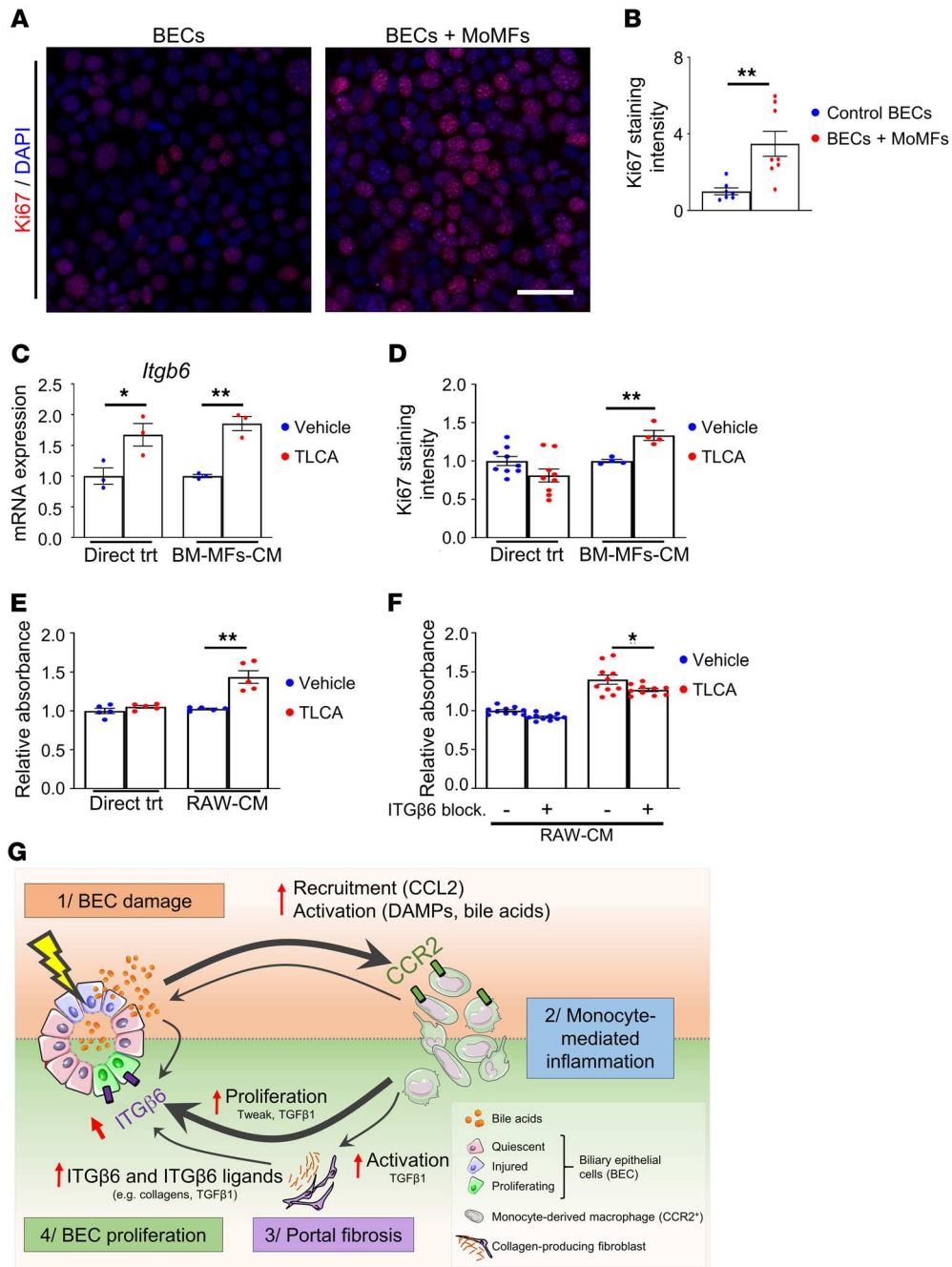


Figure 9. Monocyte-derived CCR2⁺ macrophages promote BEC proliferation through ITGB6 in vitro. (A) Sorted primary MoMFs (CD45⁺CD11b⁺CCR2^{hi}GR-1^{int}) isolated from 48-hour ILY-treated *ihCD59^{BEC-TG}* mouse livers were cocultured with BECs for 24 hours. BECs were then fixed in 4% paraformaldehyde, and Ki67 staining was performed (representative images are shown). Scale bar: 40 μ m. (B) Ki67⁺ BECs cultured with primary MoMFs were counted ($n = 4-8$ per group). (C and D) Bone marrow–derived macrophages (BM-MFs) were isolated and stimulated with TLCA (20 μ M). Conditioned media (CM) were then transferred to BECs. BECs were also directly treated with TLCA (20 μ M). *Itgb6* mRNA expression in BECs was assessed in C; Ki67 staining of BECs was analyzed in D. (E) RAW264.7 murine macrophages (RAW) were similarly treated with TLCA, and conditioned media were transferred to BECs, or BECs were directly treated (Direct trt) with TLCA (20 μ M). BEC numbers were assessed by an MTS [3-(4,5-dimethylthiazol-2-yl)-5-(3-carboxymethoxyphenyl)-2-(4-sulfophenyl)-2H-tetrazolium] absorbance assay ($n = 5$ per group). (F) RAW264.7 conditioned media were added to BEC culture with or without an ITGB6-blocking antibody, followed by measurement of BEC proliferation ($n = 10$ per group). Data represent the mean \pm SEM. * $P < 0.05$ and ** $P < 0.01$, by unpaired Student's *t* test for B–E, compared with the TLCA vehicle condition, and for F, compared with the ITGB6-blocking antibody control condition. (G) Proposed mechanisms by which BEC injury alone triggers the early signals that induce BEC proliferation via the interaction of bile acids, macrophages, and ITGB6. BEC injury leads to the release of chemoattractants (e.g., CCL2) and DAMPs, which rapidly recruit and activate circulating CCR2⁺ monocytes to the injured area. Macrophages induce portal fibrogenesis and further increase bile acid release. Macrophages, myofibroblasts, and bile acids upregulate ITGB6 expression in BECs, which contributes to BEC proliferation. The illustration in G was created using Servier Medical Art templates, which are licensed under a Creative Commons Attribution 3.0 Unported License; <https://smart.servier.com>.

injury and BDL. Macrophage depletion or CCR2 deficiency impaired ITG β 6 expression and BEC regeneration. In addition, incubation with an ITG β 6-blocking antibody reduced the BEC proliferation in vitro that was induced by conditioned media from TLCA-treated macrophages. Together, these in vivo and in vitro findings highlight an important role of macrophages in promoting BEC regeneration through ITG β 6. In addition, in our model, hepatic expression of fibronectin 1, a potent ITG β 6 agonist (18) that is mainly produced by hepatocytes and activated macrophages, was upregulated after acute BEC injury. Thus, it is likely that activated macrophages promote BEC regeneration by expressing fibronectin, which interacts with ITG β 6 on BECs.

A hallmark of bile duct injury is cholestasis, which leads to accumulation of bile acids. In the current study, we demonstrated that TLCA treatment directly upregulated ITG β 6 expression on BECs without affecting BEC proliferation, whereas conditioned media from TLCA-treated macrophages enhanced BEC proliferation in an ITG β 6-dependent manner. These data suggest that bile acids can direct monocytes toward a regenerative phenotype, which stimulates BEC proliferation via ITG β 6. However, how bile acid-activated macrophages promote BEC proliferation via ITG β 6 remains unknown. It has been shown that activated macrophages produce fibronectin 1 (18), but we did not detect *Fn1* upregulation in TLCA-treated macrophages (data not shown), although we observed *Fn1* upregulation in the liver after acute BEC injury. Therefore, it is possible that other unknown ITG β 6 ligands are involved in BEC proliferation induced by TLCA-treated macrophages. Programmed death ligand 1 (PD-L1) is a potential candidate, since it has been shown to promote bladder cancer cell proliferation through ITG β 6 (44). PD-L1 expression has been detected on macrophages (45). We observed the presence of PD-L1-expressing cells in both normal and regenerating conditions and demonstrated the presence of PD-L1⁺IBA1⁺ macrophages in close contact with BECs, 48 hours after acute BEC injury and 3 days after BDL surgery (Supplemental Figure 23). The Hippo pathway, notably implicating YAP and TAZ, and c-Met have been reported to be critical in controlling the ductular reaction (46–49). However, we did not observe a reduction in those 3 pathways in *Itgb6*^{KO} mice compared with WT mice after acute BEC injury (Supplemental Figure 24). Collectively, but tentatively, our data suggest that PD-L1, but not YAP/TAZ or c-Met, may contribute to macrophage-mediated promotion of BEC proliferation through the upregulation of ITG β 6.

Conclusions and potential therapeutic implications. By taking advantage of a BEC-targeted and specific, acute injury model, we identified the early signals from recruited monocyte-derived CCR2⁺ macrophages to promote bile duct reparative processes through the induction of ITG β 6-mediated BEC proliferation. These findings complement previous studies demonstrating the relevance of ITG β 6 in chronic biliary injury models and highlight the role of ITG β 6 in early and acute bile duct injury. Our results underline the potent role of BEC injury in generating immune responses that dysregulate liver microcirculation. Portal hypertension remains a challenging and major complication of liver cirrhosis and has been associated with potent bile duct injury, e.g., after liver transplantation (4). Our findings suggest that BEC

injury, per se, can lead to liver microcirculation dysregulation and increased portal vein pressure. We observed the impairment of liver microcirculation at early time points but not in the later reparative phase, suggesting that the proinflammatory immune reaction without fibrosis may be sufficient for portal hypertension. Additional studies will be required to unravel potential new therapeutic targets to modulate the immune response, potentially ameliorating cholestatic liver damage and enhancing graft survival. Finally, bile duct damage may accompany virtually any liver injury. As shown by our data, further attention should be drawn to bile duct-related injury and repair mechanisms not only in cholestatic disorders, but also in other liver diseases.

Methods

Mice. Two- to 4-month-old male and female mice were used in this study. We generated BEC-specific *hCD59*-transgenic (*ihCD59*^{BEC-TG}) mice as previously described (16). Tamoxifen was prepared in corn oil and injected intraperitoneally (50 mg/kg) into *ihCD59*^{BEC-TG} mice every 2 days for a total of 3 injections to induce BEC *hCD59* expression. ILY was administered once by tail vein injection (140 μ g/kg) after a 1-week tamoxifen washout period. Liver-specific *hCD59*-transgenic (*ihCD59*^{LIV-TG}) mice, in which *hCD59* is expressed on both hepatocytes and BECs, were generated by crossing *ihCD59* mice with albumin-Cre-transgenic mice (The Jackson Laboratory). *ihCD59* mice were generated on a C57BL/6 background, and littermate control mice were used for *ihCD59*^{BEC-TG} and *ihCD59*^{LIV-TG} mice. Integrin α β 6-deficient (*Itgb6*^{KO}) mice on a C57BL/6 background were provided by Dean Sheppard's laboratory (UCSF, San Francisco, California, USA) (50). *ihCD59*^{LIV-TG} *Itgb6*^{KO} double-mutant mice were generated via several steps of crossing of *ihCD59*^{LIV-TG} mice with *Itgb6*^{KO} mice. *Itgb6*^{KO} (with Cre-*ihCD59*) littermates were used as controls for the *ihCD59*^{LIV-TG} *Itgb6*^{KO} double-mutant mice. Hepatocyte-specific *hCD59*-transgenic (*ihCD59*^{HEP-TG}) mice were generated by injecting 5×10^{10} genome copies per *ihCD59* mouse of AAV8-TBG-PI-Cre-rBG (Perelman School of Medicine at the University of Pennsylvania, Philadelphia, Pennsylvania, USA) (16). Hepatocyte injury in these mice was induced by 3 daily ILY tail vein injections (140 μ g/kg). Mice were euthanized 48 hours after the last injection. The *Sox9CreERT⁺*, *Cx3cr1*^{GFP}, *Ccr2*^{RFP} mouse strains that express tamoxifen-inducible Cre, GFP, or RFP under the *Sox9*, *Cx3cr1*, or *Ccr2* promoters, respectively, were purchased from The Jackson Laboratory. Homozygous *Ccr2*^{RFP} mice were used as *Ccr2*-KO animals, and heterozygous *Ccr2*^{RFP} mice were used as CCR2 reporter mice. *Cx3cr1*^{GFP} and *Ccr2*^{RFP} mice were on a C57BL/6J background as described on The Jackson Laboratory's website. *Coll1*^{GFP} mice expressing GFP under the *Coll1* promoter were described previously in the C3H/C57B1 strain (51). All mouse strains used in this study were backcrossed for at least 5 generations on a C57BL/6J background. Tamoxifen- and ILY-injected *ihCD59* littermates were used as negative controls.

Other mouse liver injury models included carbon tetrachloride (CCl₄) injection and BDL. CCl₄ was injected once (1 mL/kg, diluted 10% v/v in corn oil), and samples were collected 72 hours later. BDL and sectioning was performed as previously described (52), and tissues were collected 3 or 7 days after surgery.

Macrophage depletion was performed by intravenous injection of 70 mg/kg clodronate disodium-loaded liposomes (FormuMax).

Mice were injected with 30 µg/g BrdU (MilliporeSigma) 2 hours before euthanasia to assess cell proliferation.

Monocyte cell culture. Primary monocytes were isolated from bone marrow as previously described, using the mouse Monocyte Isolation Kit (BM) (Miltenyi Biotec, Bergisch Gladbach). RAW264.7 murine macrophages were obtained from the American Type Culture Collection (ATCC). Cells were treated with TLCA at a final concentration of 20 µM or with vehicle (0.5% dimethyl sulfoxide, MilliporeSigma).

Liver myofibroblast sorting. *Coll1*^{GFP} mice were intraperitoneally injected with CCl₄ (1 injection of 0.5 mL/kg diluted 25% v/v in corn oil, every 3 days) to induce liver myofibroblast accumulation. Twenty-four hours after the last injection, livers were perfused with GBSS containing 0.5 g/L collagenase IV (Millipore Sigma), collected and minced with scissors, and further digested for 20 minutes at 37°C under agitation in GBSS containing 0.5 g/L collagenase IV and 0.5 g/L pronase (MilliporeSigma). Cells were then passed through a 70 µm cell strainer, and hepatocytes were removed after 3 consecutive low-speed centrifugations (60g for 5 minutes). Red blood cells were lysed using ACK Lysing Buffer (Thermo Fisher Scientific). CD45⁻ (Coll1) GFP⁺ cells were sorted. The antibodies used for flow cytometry are listed in Supplemental Table 1. Myofibroblasts were then transferred onto Transwell plates and incubated with preattached BECs overnight.

MoMFs. Monocyte-derived CCR2⁺ macrophages (CD45⁺CD-11b⁺CCR2^{hi}GR-1^{int}) were isolated from *ihCD59*^{BEC-TG} mouse livers 48 hours after ILY injection.

BEC culture and proliferation assay. SV40-transformed BECs were provided by Gianfranco Alpini's group (Indiana University School of Medicine, Indianapolis, Indiana, USA) (53). Cell culture supernatant from activated monocytes or RAW264.7 cells were collected, centrifuged to remove potential cell debris, supplemented with 2% heat-inactivated FBS and blocking ITGβ6 antibody (Abcam) as indicated, and then added to the BEC culture. Following treatments, the cells were fixed in 4% paraformaldehyde for 15 minutes and then incubated with an anti-Ki67 antibody (Dako, Agilent Technologies) in 5% normal goat serum and 0.3% Triton X-100. Cell proliferation was assessed using a colorimetric MTS Assay Kit (Cell Proliferation, Abcam).

Immunohistochemical and multiplex immunofluorescence staining. Formalin-fixed, paraffin-embedded liver samples were sectioned and stained as described in the Supplemental Methods. For BDL samples, multiplex immunostaining was performed as previously described (27).

Staining and microdissection of BECs. BECs were stained for microdissection using a modified immunohistochemistry protocol that preserves RNA integrity for further next-generation sequencing. Briefly, *ihCD59*^{BEC-TG} and *ihCD59* (control) mice were intravenously injected with ILY, and the liver was dissected 48 hours later, immediately mounted with O.C.T. and frozen on dry ice and then stored at -80°C. Fresh-frozen liver sections (12 µm thick) were used, and a solution containing 1 mg/mL BSA and 0.1% Tween-20 was used for blocking and permeabilization. BECs were stained with the monoclonal anti-cytokeratin-19 antibody (TROMA-III, Developmental Studies Hybridoma Bank) and revealed with an HRP-conjugated, anti-rat secondary antibody and DAB substrate (both from Vector Laboratories). Every step was performed at 4°C, except for the DAB reaction and dehydration, which were performed at room temperature. Blocking and antibody mixes contained 0.5 U/L RNase Inhibitor (Applied Biosystems). Incubation durations were kept short: 30 minutes for blocking and permeabilization, 1 hour for the primary antibody, and

30 minutes for the secondary antibody. The capture was achieved by xMD, as previously described (54). Laser irradiation consisted of 5 discharges at intensity level 5, against a white background with a SensEpil lamp (Home Skinovations).

BEC RNA purification, amplification, and next-generation sequencing. Total RNA was purified using a PicoPure RNA Isolation Kit (Thermo Fisher Scientific), including DNase treatment. Preferential mRNA amplification was performed using the Ovation RNA-seq System V2 (NuGEN). The amplified material was quantified and its quality assessed using Qubit (dsDNA HS Assay Kit, Thermo Fisher Scientific) and Bioanalyzer (High Sensitivity DNA Kit, Agilent Technologies), respectively. The amplified material was sheared to approximately 150 bp fragments using Covaris microtubes and a sonicator (Covaris S2). Sequencing libraries were made using the Ion Plus Fragment Library Kit and Ion Xpress Barcode Adapters (IonTorrent, Thermo Fisher Scientific). Quantification and quality were assessed as in the previous step, as well as with the Ion Library TaqMan Quantitation Kit (IonTorrent, Thermo Fisher Scientific). Sequencing was performed using Ion P1 Hi-Q kits and the Ion P1 Chip Kit, version 3 in an Ion Torrent Proton sequencer.

RNA-Seq bioinformatics analysis. CLC Genomics Workbench (QIAGEN Bioinformatics, version 10) was used to map sequencing reads to the mouse reference genome (Mm10) and for subsequent analysis. All steps were run using default settings for RNA-Seq analysis. Only protein-coding genes (21,950 genes) with an expression value of reads per kilobase per million mapped reads (RPKM) of 0.5 or higher were considered for the analysis (8483 genes). Filtering on a FDR-corrected *P* value of 0.05 or lower and a fold change greater than 2 resulted in 135 genes. Pathway and Gene Ontology (GO) term enrichment analysis was performed using DAVID (55). RNA-Seq data are available in the NCBI's GenBank via BioProject (accession number PRJNA510784).

Liver microcirculation and portal vein pressure. Hepatic microcirculation was assessed by the laser speckle contrast approach as described previously (52). To measure mean portal pressure, a polyethylene cannula (PE-8) connected to a fluid-filled pressure catheter (ADInstruments) was introduced into the portal vein. After stabilization, pressure signal was recorded using the PowerLab data acquisition system and analyzed by LabChart 7 Software (ADInstruments).

Statistics. Results are expressed as the mean ± SEM (*n* = 3-10 per group as indicated), and statistical significance was determined by a 2-tailed, unpaired Student's *t* test or 1-way ANOVA as appropriate (GraphPad Prism, GraphPad Software). Results were considered significantly different for *P* values of less than 0.05. For RNA-Seq data analysis, a FDR-corrected *P* value was used. Correlations were calculated using Pearson's *r*.

Study approval. Mice were cared for in accordance with NIH guidelines. The study was approved by the IACUC of the NIAAA. Normal human liver samples and chronic liver disease tissues were obtained from donor livers or recipient livers during liver transplantation from the Liver Tissue Procurement and Distribution System at the University of Minnesota (Minneapolis, Minnesota, USA), with the patients' written informed consent (supported by the NIH contract HHSN276201200017C).

Author contributions

AG, LG, DF, SJK, YH, YAA, JP, and KS were involved in the acquisition, analysis, statistical analysis, and interpretation of the data.

SD, FL, and XQ provided the ILY and were involved in data analysis. PP, TK, XQ, DG, and FT provided relevant intellectual input and edited the manuscript. AG and BG designed the study and wrote the manuscript. BG obtained funding and supervised the study. All authors approved the final manuscript.

Acknowledgment

This work was supported by the intramural program of the NIAAA, NIH (to BG). AG was a visiting postdoctoral fellow supported by the intramural program of the NIAAA, NIH during 2015–2019 and is currently a recipient of a Humboldt Research Fellowship for Postdoctoral Researchers (Alexander von Humboldt Foundation). We thank Gianfranco Alpini (Indiana University School of Medicine) for providing the biliary epithelial cell line, Dean Sheppard (UCSF) for providing the *Itgb6*^{KO} mice, and Martha Kirby (National Human

Genome Research Institute [HGRI], NIH) for her assistance with myofibroblast cell sorting.

Address correspondence to: Bin Gao, Laboratory of Liver Diseases, NIAAA, NIH, 5625 Fishers Lane, Bethesda, Maryland 20892, USA. Phone: 301.443.3998; Fax: Email: bgao@mail.nih.gov.

SJK's present address is: Department of Biochemistry, College of Natural Sciences, and Kangwon Institute of Inclusive Technology, Kangwon National University, Chuncheon, Korea.

KS's present address is: Experimental and Computational Genomics Core, CRB 2, Sidney Kimmel Comprehensive Cancer Center, The Johns Hopkins University School of Medicine, Baltimore, Maryland, USA.

- Cheung AC, et al. Pathobiology of biliary epithelia. *Biochim Biophys Acta Mol Basis Dis.* 2018;1864(4 Pt B):1220–1231.
- Lazaridis KN, LaRusso NF. The cholangiopathies. *Mayo Clin Proc.* 2015;90(6):791–800.
- Edwards K, et al. Secondary sclerosing cholangitis in critically ill patients: a rare disease precipitated by severe SARS-CoV-2 infection. *BMJ Case Rep.* 2020;13(11):e237984.
- Baker TB, et al. Biliary reconstructive techniques and associated anatomic variants in adult living donor liver transplantations: The adult-to-adult living donor liver transplantation cohort study experience. *Liver Transpl.* 2017;23(12):1519–1530.
- Guillot A, et al. Interleukins-17 and 27 promote liver regeneration by sequentially inducing progenitor cell expansion and differentiation. *Hepatology.* 2018;2(3):329–343.
- Sancho-Bru P, et al. Liver progenitor cell markers correlate with liver damage and predict short-term mortality in patients with alcoholic hepatitis. *Hepatology.* 2012;55(6):1931–1941.
- Knight B, et al. Liver inflammation and cytokine production, but not acute phase protein synthesis, accompany the adult liver progenitor (oval) cell response to chronic liver injury. *Immunol Cell Biol.* 2005;83(4):364–374.
- Fabris L, et al. Emerging concepts in biliary repair and fibrosis. *Am J Physiol Gastrointest Liver Physiol.* 2017;313(2):G102–G116.
- Banales JM, et al. Cholangiocyte pathobiology. *Nat Rev Gastroenterol Hepatol.* 2019;16(5):269–281.
- Mariotti V, et al. Animal models of cholestasis: an update on inflammatory cholangiopathies. *Biochim Biophys Acta Mol Basis Dis.* 2019;1865(5):954–964.
- Liu Y, et al. Animal models of chronic liver diseases. *Am J Physiol Gastrointest Liver Physiol.* 2013;304(5):G449–G468.
- Waisbourd-Zinman O, et al. The toxin bilitresone causes mouse extrahepatic cholangiocyte damage and fibrosis through decreased glutathione and SOX17. *Hepatology.* 2016;64(3):880–893.
- Guicciardi ME, et al. Macrophages contribute to the pathogenesis of sclerosing cholangitis in mice. *J Hepatol.* 2018;69(3):676–686.
- Ferreira-Gonzalez S, et al. Paracrine cellular senescence exacerbates biliary injury and impairs regeneration. *Nat Commun.* 2018;9(1):1020.
- Guillot A, et al. Cannabinoid receptor 2 counteracts interleukin-17-induced immune and fibrogenic responses in mouse liver. *Hepatology.* 2014;59(1):296–306.
- Feng D, et al. Cre-inducible human CD59 mediates rapid cell ablation after intermediate-dose administration. *J Clin Invest.* 2016;126(6):2321–2333.
- Meng L, et al. Functional role of cellular senescence in biliary injury. *Am J Pathol.* 2015;185(3):602–609.
- Patsenker E, et al. Inhibition of integrin α 6 on cholangiocytes blocks transforming growth factor- β activation and retards biliary fibrosis progression. *Gastroenterology.* 2008;135(2):660–670.
- Peng ZW, et al. Integrin α 6 critically regulates hepatic progenitor cell function and promotes ductular reaction, fibrosis, and tumorigenesis. *Hepatology.* 2016;63(1):217–232.
- Patsenker E, et al. The α 6 integrin is a highly specific immunohistochemical marker for cholangiocarcinoma. *J Hepatol.* 2010;52(3):362–369.
- Pi L, et al. Connective tissue growth factor and integrin α 6: a new pair of regulators critical for ductular reaction and biliary fibrosis in mice. *Hepatology.* 2015;61(2):678–691.
- Wen Y, et al. Hepatic macrophages in liver homeostasis and diseases—diversity, plasticity and therapeutic opportunities. *Cell Mol Immunol.* 2021;18(1):45–56.
- Guillot A, Tacke F. Liver macrophages: old dogmas and new insights. *Hepatology.* 2019;3(6):730–743.
- Lavin Y, et al. Tissue-resident macrophage enhancer landscapes are shaped by the local microenvironment. *Cell.* 2014;159(6):1312–1326.
- Kim SJ, et al. Adipocyte death preferentially induces liver injury and inflammation through the activation of chemokine (C-C Motif) receptor 2-positive macrophages and lipolysis. *Hepatology.* 2019;69(5):1965–1982.
- Reh JE, et al. The utility of immunohistochemistry for the identification of hematopoietic and lymphoid cells in normal tissues and interpretation of proliferative and inflammatory lesions of mice and rats. *Toxicol Pathol.* 2012;40(2):345–374.
- Guillot A, et al. Deciphering the immune microenvironment on a single archival formalin-fixed paraffin-embedded tissue section by an immediately implementable multiplex fluorescence immunostaining protocol. *Cancers (Basel).* 2020;12(9):E2449.
- Guillot A, et al. Kupffer cell and monocyte-derived macrophage identification by immunofluorescence on formalin-fixed, paraffin-embedded (FFPE) mouse liver sections. *Methods Mol Biol.* 2020;2164:45–53.
- Tirnitz-Parker JE, et al. Tumor necrosis factor-like weak inducer of apoptosis is a mitogen for liver progenitor cells. *Hepatology.* 2010;52(1):291–302.
- Hogenauer K, et al. G-protein-coupled bile acid receptor 1 (GPBAR1, TGR5) agonists reduce the production of proinflammatory cytokines and stabilize the alternative macrophage phenotype. *J Med Chem.* 2014;57(24):10343–10354.
- Biagioli M, et al. The bile acid receptor GPBAR1 regulates the M1/M2 phenotype of intestinal macrophages and activation of GPBAR1 rescues mice from murine colitis. *J Immunol.* 2017;199(2):718–733.
- Tacke F. Targeting hepatic macrophages to treat liver diseases. *J Hepatol.* 2017;66(6):1300–1312.
- Takeuchi M, et al. Neutrophils interact with cholangiocytes to cause cholestatic changes in alcoholic hepatitis. *Gut.* 2021;70(2):342–356.
- Kisseleva T, et al. Bone marrow-derived fibrocytes participate in pathogenesis of liver fibrosis. *J Hepatol.* 2006;45(3):429–438.
- Scholten D, et al. Migration of fibrocytes in fibrogenic liver injury. *Am J Pathol.* 2011;179(1):189–198.
- Weiskirchen R, et al. Organ and tissue fibrosis: Molecular signals, cellular mechanisms and translational implications. *Mol Aspects Med.* 2019;65:2–15.
- Xu J, et al. Contribution of bone marrow-derived fibrocytes to liver fibrosis. *Hepatobiliary Surg Nutr.* 2015;4(1):34–47.
- Hall C, et al. Regulators of cholangiocyte proliferation. *Gene Expr.* 2017;17(2):155–171.
- Tanimizu N, et al. Liver progenitor cells develop cholangiocyte-type epithelial polarity in three-dimensional culture. *Mol Biol Cell.* 2007;18(4):1472–1479.

40. He Y, et al. Interaction of CD44 and hyaluronic acid enhances biliary epithelial proliferation in cholestatic livers. *Am J Physiol Gastrointest Liver Physiol*. 2008;295(2):G305–G312.
41. Jakubowski A, et al. TWEAK induces liver progenitor cell proliferation. *J Clin Invest*. 2005;115(9):2330–2340.
42. Karaca G, et al. TWEAK/Fn14 signaling is required for liver regeneration after partial hepatectomy in mice. *PLoS One*. 2014;9(1):e83987.
43. Locatelli L, et al. Macrophage recruitment by fibrocystin-defective biliary epithelial cells promotes portal fibrosis in congenital hepatic fibrosis. *Hepatology*. 2016;63(3):965–982.
44. Cao D, et al. Retinoic acid-related orphan receptor C regulates proliferation, glycolysis, and chemoresistance via the PD-L1/ITGB6/STAT3 signaling axis in bladder cancer. *Cancer Res*. 2019;79(10):2604–2618.
45. Lu D, et al. Beyond T cells: understanding the role of PD-1/PD-L1 in tumor-associated macrophages. *J Immunol Res*. 2019;2019:1919082.
46. Lu L, et al. Hippo pathway coactivators Yap and Taz are required to coordinate mammalian liver regeneration. *Exp Mol Med*. 2018;50(1):e423.
47. Lee DH, et al. LATS-YAP/TAZ controls lineage specification by regulating TGF β signaling and Hnf4a expression during liver development. *Nat Commun*. 2016;7:11961.
48. Planas-Paz L, et al. YAP, but not RSPO-LGR4/5, signaling in biliary epithelial cells promotes a ductular reaction in response to liver injury. *Cell Stem Cell*. 2019;25(1):39–53.
49. Ishikawa T, et al. Hepatocyte growth factor/c-met signaling is required for stem-cell-mediated liver regeneration in mice. *Hepatology*. 2012;55(4):1215–1226.
50. Huang XZ, et al. Inactivation of the integrin beta 6 subunit gene reveals a role of epithelial integrins in regulating inflammation in the lung and skin. *J Cell Biol*. 1996;133(4):921–928.
51. Yata Y, et al. DNase I-hypersensitive sites enhance alpha1(I) collagen gene expression in hepatic stellate cells. *Hepatology*. 2003;37(2):267–276.
52. Varga ZV, et al. Disruption of renal arginine metabolism promotes kidney injury in hepatorenal syndrome in mice. *Hepatology*. 2018;68(4):1519–1533.
53. Glaser S, et al. Differential transcriptional characteristics of small and large biliary epithelial cells derived from small and large bile ducts. *Am J Physiol Gastrointest Liver Physiol*. 2010;299(3):G769–G777.
54. Rosenberg AZ, et al. High-throughput microdissection for next-generation sequencing. *PLoS One*. 2016;11(3):e0151775.
55. Huang da W, et al. Systematic and integrative analysis of large gene lists using DAVID bioinformatics resources. *Nat Protoc*. 2009;4(1):44–57.